

# Parameters for Properly Designed and Operated Flares

Report for Flare Review Panel  
April 2012

Prepared by  
U.S. EPA Office of Air Quality Planning and Standards (OAQPS)

*This information is distributed solely for the purpose of pre-dissemination peer review under applicable information quality guidelines. It has not been formally disseminated by EPA. It does not represent and should not be construed to represent any Agency determination or policy.*

## ACRONYMS

<b>Acronym</b>	<b>Definition</b>
AFTIR	Active Fourier Transform Infrared
API	American Petroleum Institute
ARI	Aerodyne Research, Inc.
BTU	British Thermal Units
CZ	Combustion Zone Gas
C <sub>CZ</sub>	Fraction of Combustibles in the Combustion Zone Gas
CFR	Code of Federal Regulations
DCS	Distributed Control System
EPA	U.S. Environmental Protection Agency
FHR	Flint Hills Resources
FHR AU	Flint Hills Resources - Aromatics Unit
FHR LOU	Flint Hills Resources - Light Olefins Unit
FLIR	Forward Looking Infrared
FTIR	Fourier Transform Infrared Technology
IMACC	Industrial Monitor and Control Corporation
INEOS	INEOS ABS (USA) Corporation
ISO	International Standards Organization
LFL	Lower Flammability Limit
LFL <sub>CZ</sub>	Lower Flammability Limit of the Combustion Zone Gas
LFL <sub>VG</sub>	Lower Flammability Limit of the Flare Vent Gas
LHV	Lower Heating Value
LFL <sub>VG, C</sub>	Lower Flammability Limit of the Combustible Portion of the Flare Vent Gas
MFR	Momentum Flux Ratio
MPC	Marathon Petroleum Company, LP
MPC Detroit	Marathon Petroleum Company, LP Detroit Refinery
MPC TX	Marathon Petroleum Company, LP Texas City Refinery
NESHAP	National Emission Standards for Hazardous Air Pollutants
NHV	Net Heating Value
NHV <sub>CZ</sub>	Net Heating Value of the Combustion Zone Gas
NHV <sub>LFL</sub>	Net Heating Value of the Flare Vent Gas if Diluted to the Lower Flammability Limit
NHV <sub>VG</sub>	Net Heating Value of the Flare Vent Gas
NHV <sub>VG-LFL</sub>	Net Heating Value of the Flare Vent Gas if Diluted to the Lower Flammability Limit
NSPS	New Source Performance Standards
OAQPS	Office of Air Quality Planning and Standards
PFTIR	Passive Fourier Transform Infrared Technology
SCF	Standard Cubic Feet
SDP	Shell Deer Park Refinery
SDP GF	Shell Deer Park Refinery Ground Flare
SDP EPF	Shell Deer Park Refinery East Property Flare
SR	Stoichiometric Air Ratio
TCEQ	Texas Commission on Environmental Quality

*This information is distributed solely for the purpose of pre-dissemination peer review under applicable information quality guidelines. It has not been formally disseminated by EPA. It does not represent and should not be construed to represent any Agency determination or policy.*

<b>Acronym</b>	<b>Definition</b>
UFL	Upper Flammability Limit
$V_{\max}$	Maximum Flare Tip Velocity Including, if Applicable, Center Steam at Which Flame Lift Off is Not Expected to Occur

## TABLE OF CONTENTS

1.0	INTRODUCTION.....	1-1
2.0	AVAILABLE FLARE TEST DATA.....	2-1
2.1	Flare Performance Studies and Test Reports.....	2-1
2.2	Flare Vent Gas Constituents.....	2-3
2.3	Steam Injection Rates and Tip Design for Available Flare Test Data....	2-5
2.4	Air Injection Rates and Tip Design for Available Flare Test Data.....	2-6
2.5	Flare Test Methods.....	2-7
2.6	Combining All Available Test Run Data.....	2-9
2.7	Data Removed After Being Considered.....	2-10
2.8	Determination of Combustion Efficiency Representing Good Flare Performance.....	2-11
3.0	STEAM AND FLARE PERFORMANCE.....	3-1
3.1	Lower Flammability Limit of Combustion Zone Gas for Steam-Assisted Flares.....	3-1
3.1.1	Flare Test Data and $LFL_{CZ}$ .....	3-5
3.1.2	The Le Chatelier Principle.....	3-7
3.1.3	Specific Test Data Not Fitting the Trend.....	3-11
3.1.4	Data Points with Good Combustion and High $LFL_{CZ}$ .....	3-20
3.1.5	Excluding Pilot Gas.....	3-26
3.2	Combustible Gas Concentration in the Combustion Zone.....	3-27
3.3	Heat Content Based Limit for Steam-Assisted Flares.....	3-28
3.4	Other Operating Parameters Considered for Steam-Assisted Flares....	3-31
3.4.1	Net Heating Value.....	3-31
3.4.2	Steam Ratios.....	3-34
4.0	AIR AND FLARE PERFORMANCE.....	4-1
4.1	Stoichiometric Air Ratio.....	4-1
4.2	TCEQ Test Data.....	4-3
4.3	Other Test Data.....	4-4
4.4	Analysis of Stoichiometric Air Ratio.....	4-4
4.5	Considering $LFL_{VG}$ for Air-Assisted Flares.....	4-7
5.0	WIND AND FLARE PERFORMANCE.....	5-1
5.1	Introduction.....	5-2
5.2	Flare Flow Mixing Regimes.....	5-2
5.3	Efficiency Studies.....	5-4
5.4	Test Data Analysis.....	5-10
6.0	FLARE FLAME LIFT OFF.....	6-1
6.1	Literature Review and $V_{max}$ Calculation.....	6-1
6.2	Test Data Analysis.....	6-2
6.3	Other Operating Parameters Considered for Flame Lift Off.....	6-6

7.0	OTHER FLARE TYPE DESIGNS TO CONSIDER.....	7-1
7.1	Non-Assisted Flares.....	7-1
7.2	Pressure-Assisted Flares and Other Flare Designs.....	7-2
8.0	MONITORING CONSIDERATIONS .....	8-1
8.1	LFL <sub>CZ</sub> , LFL <sub>VG</sub> , and LFL <sub>VG,C</sub> .....	8-1
8.2	Ratio of NHV <sub>CZ</sub> to NHV <sub>VG-LFL</sub> .....	8-2
8.3	C <sub>CZ</sub> .....	8-2
8.4	SR .....	8-3
8.5	MFR.....	8-3
8.6	V <sub>max</sub> .....	8-4
9.0	REFERENCES.....	9-1

## TECHNICAL APPENDICES

- Appendix A. Brief Review Summary of Each Flare Performance Study and Test Report.
- Appendix B. Excel Workbook That Combines All Data Sets.
- Appendix C. Test Report Nomenclature Matrix.
- Appendix D. Detailed Calculation Methodologies For The Specific Parameters.
- Appendix E. Type and Amount of Components in Each Test Run by Test Report.
- Appendix F. Charts of Calculated and Measured LFL for Various Combustible Gases in Nitrogen and Carbon Dioxide.
- Appendix G. Details About Inerts and Further Explanation for Including an Equivalency Adjustment to Correct For Different Inert Behavior.
- Appendix H. Effect of Nitrogen and Carbon Dioxide on the LFL of Various Components: A Comparison of Le Chatelier Equation to Experimental LFL Values.
- Appendix I. Methodology for Calculating Unobstructed Cross Sectional Area of Several Flare Tip Designs.

## **LIST OF TABLES**

<b>Tables</b>	<b>Page</b>
Table 2-1. Flare Performance Test Reports.....	2-2
Table 2-2. Flare Vent Gas Constituents by Test Report .....	2-3
Table 2-3. Minimum, Maximum, and Average Volume Percents of Primary Constituents in Flare Vent Gas.....	2-4
Table 2-4. Steam-Assisted Flare Tip Design Detail .....	2-5
Table 2-5. Air-Assisted Flare Tip Design Detail.....	2-7
Table 2-6. Criteria To Exclude Data Points .....	2-12
Table 3-1. Recommended Values of Coefficient of Nitrogen Equivalency for Water and Carbon Dioxide Relative to Nitrogen.....	3-10
Table 3-2. Test Run Detail for 11 Data Points with $LFL_{CZ} < 15.3\%$ but Combustion Efficiency $< 96.5\%$ .....	3-12
Table 3-3. Olefin and Hydrogen Approximately Equal.....	3-15
Table 3-4. High Hydrogen and Low Olefin .....	3-16
Table 3-5. Higher Olefin and Low Hydrogen .....	3-18
Table 3-6. Breakdown Of Steam Use For The 66 Test Runs <sup>a</sup> .....	3-21
Table 3-7. Potential $LFL_{CZ}$ Thresholds based on $LFL_{VG,C}$ .....	3-23

## LIST OF FIGURES

<b>Figures</b>	<b>Page</b>
Figure 3-1. Zabetakis Nose Plot For Methane And Inert In Air.....	3-3
Figure 3-2. Time Sequence of Flare Vent Gas Volume Moving Through Flammability Region Source: (Adapted from Evans and Roesler, 2011) .....	3-4
Figure 3-3. Combustion Efficiency vs. $LFL_{CZ}$ .....	3-7
Figure 3-4. Combustion Efficiency vs. $LFL_{CZ}$ Adjusted for Nitrogen Equivalency .....	3-11
Figure 3-5. Combustion Efficiency vs. $LFL_{CZ}$ for Category A Test Runs (see Table 3-7).....	3-23
Figure 3-6. Combustion Efficiency vs. $LFL_{CZ}$ for Category B Test Runs (see Table 3-7).....	3-24
Figure 3-7. Combustion Efficiency vs. $LFL_{CZ}$ for Category C Test Runs (see Table 3-7).....	3-24
Figure 3-8. Combustion Efficiency vs. $LFL_{CZ}$ for Category D Test Runs (see Table 3-7).....	3-25
Figure 3-9. Combustion Efficiency vs. $C_{CZ}$ .....	3-28
Figure 3-10. Combustion Efficiency vs. Ratio of $NHV_{CZ}$ to $NHV_{VG-LFL}$ .....	3-29
Figure 3-11. $LFL_{CZ}$ vs. Ratio of $NHV_{CZ}$ to $NHV_{VG-LFL}$ .....	3-30
Figure 3-12. Combustion Efficiency vs. $NHV_{VG}$ .....	3-32
Figure 3-13. Combustion Efficiency vs. $NHV_{CZ}$ .....	3-33
Figure 3-14. $NHV_{VG}$ vs. $LFL_{VG}$ .....	3-34
Figure 3-15. Combustion Efficiency vs. S/VG by weight .....	3-35
Figure 3-16. Combustion Efficiency vs. S/VG by volume .....	3-36
Figure 3-17. Combustion Efficiency vs. S/HC by volume.....	3-37
Figure 4-1. Combustion Efficiency vs. SR (using TCEQ data) .....	4-3
Figure 4-2. Combustion Efficiency vs. SR (using EPA-600/2-85-106 data).....	4-4
Figure 4-3. Combustion Efficiency vs. SR (combined TCEQ and EPA-600/2-85-106 data).....	4-5
Figure 4-4. Combustion Efficiency vs. SR, zoomed (using TCEQ data) .....	4-6
Figure 5-1. Air Egression Into Flare Stack Source: (Smoot et al., 2009) .....	5-2
Figure 5-2. Images of Flow Mixing Regimes Source: (Seebold et al., 2004).....	5-3

Figure 5-3. Fuel Detection Downwind of Wake-Dominated Flare Source: (Johnston et. al, 2001)5-4

Figure 5-4. Flame Images Relating to Momentum Flux Ratio and Combustion Efficiency Source: (Johnson and Kostiuk, 2000) ..... 5-6

Figure 5-5. Combustion Efficiency vs. Momentum Flux Ratio, Seebold Data Source: (Seebold et al., 2004)..... 5-7

Figure 5-6. Combustion Efficiency vs. Momentum Flux Ratio .....5-12

Figure 5-7. Combustion Efficiency vs. Momentum Flux Ratio, zoomed (MFR < 3.0; wake-dominated mixing regime) .....5-13

Figure 5-8. Combustion Efficiency vs. Momentum Flux Ratio, further zoomed (MFR < 0.1) .5-14

Figure 5-9. Combustion Efficiency vs. Power Factor.....5-16

Figure 6-1. Conditions for Stable Flare Flame ..... 6-4

## 1.0 INTRODUCTION

Based on a series of flare performance studies conducted in the early 1980s, the EPA concluded that properly designed and operated flares achieve good combustion efficiency (e.g., greater than 98 percent conversion of organic compounds to carbon dioxide). It was observed, however, that flares operating outside “their stable flame envelope” produced flames that were not stable or would rapidly destabilize, causing a decrease in both combustion and destruction efficiency (Pohl and Soelberg, 1985). To define the stable flame envelope of operating conditions, the resulting regulations for flares (i.e., 40 CFR 60.18 and 40 CFR 63.11(b)), promulgated in their current form in 1998, included both minimum flare vent gas net heating value requirements and a limit on velocity as a function of net heating value.

Flares are often used at chemical plants and petroleum refineries as a control device for regulated vent streams as well as to handle non-routine emissions (e.g., leaks, purges, emergency releases); and since the development of the current flare regulations, industry has significantly reduced the amount of waste gas being routed to flares. Generally this reduction has affected the base load to flares and many are now receiving a small fraction of what the flare was originally designed to receive with only periodic releases of episodic or emergency waste gas that may use up to the full capacity of the flare. Many flare vent gas streams that are regulated by NESHAP and NSPS are often continuous streams that contribute to the base load of a flare; therefore, it is critical for flares to achieve good combustion efficiency at all levels of utilization.

Available data suggest that there are numerous factors that should be considered in order to be confident that a flare is operated properly to achieve good combustion efficiency. Factors that can reduce the destruction efficiency capabilities of the flare include:

Over Steaming. Using too much steam in a flare can reduce flare performance. Given that many steam-assisted flares are designed to have a minimum steam flow rate in order to protect the flare tip, over steaming has resulted, especially during base load conditions. In addition, operators acting cautiously to avoid non-compliance with the visible emissions standards for flares have liberally used steaming to control any potential visible emissions, also resulting in over steaming in some cases.

Excess Aeration. Using too much air in a flare can reduce flare performance. Air-assisted flares operate similarly to steam-assisted flares; however, air is used as the assist-media instead of steam.

High Winds. A high crosswind velocity can have a strong effect on the flare flame dimensions and shape, causing the flame to be wake-dominated (i.e., the flame is bent over on the downwind side of a flare and imbedded in the wake of the flare tip). This type of flame can reduce flare performance; and potentially damage the flare tip.

Flame Lift Off. A condition in which a flame separates from the tip of the flare and there is space between the flare tip and the bottom of the flame due to excessive air induction as a result of the flare gas and center steam exit velocities. This type of flame can reduce flare performance; and can progress to a condition where the flame becomes completely extinguished.

The observations presented in this report are a result of the analysis of several experimental flare efficiency studies and flare performance test reports. Section 2.0 summarizes these data and reports. In addition, scientific information from peer-reviewed studies and other technical assessments about flammability, wind, and flame lift off were used in this report. Sections 3.0 through 8.0 describe the development of our observations. Section 9.0 provides a list of documents referenced in this report. The primary observations are as follows:

- To identify over steaming situations that may occur on steam-assisted flares, the data suggest that the lower flammability limit of combustion zone gas ( $LFL_{CZ}$ ) is the most appropriate operating parameter. Specifically, the data suggest that, in order to maintain good combustion efficiency, the  $LFL_{CZ}$  must be 15.3 percent by volume or less for a steam-assisted flare. As an alternative to  $LFL_{CZ}$ , the data suggest that the ratio of the net heating value of the combustion zone gas ( $NHV_{CZ}$ ) to the net heating value of the flare vent gas if diluted to the lower flammability limit ( $NHV_{LFL}$ ) must be greater than 6.54. Section 3.0 documents the analysis supporting these observations.
- To identify excess aeration situations that may occur on air-assisted flares, the data suggest that the stoichiometric air ratio (SR) (the actual mass flow of assist air to the theoretical stoichiometric mass flow of air needed to combust the flare vent gas) is the most appropriate operating parameter. Specifically, the data suggest that, in order to maintain good combustion efficiency, the SR must be 7 or less for an air-assisted flare. Furthermore, the data suggest that the lower flammability limit of the flare vent gas ( $LFL_{VG}$ ) should be 15.3 percent by volume or less to ensure the flare vent gas being sent to the air-assisted flare is capable of adequately burning when introduced to enough air. Section 4.0 documents the analysis supporting these observations.

- The data suggest that flare performance is not significantly affected by crosswind velocities up to 22 miles per hour (mph). There are limited data for flares in winds greater than 22 mph. However, a wake-dominated flame in winds greater than 22 mph may affect flare performance. The data available indicate that the wake-dominated region begins at a momentum flux ratio (MFR) of 3 or greater. The MFR considers whether there is enough flare vent gas and center steam (if applicable) exit velocity (momentum) to offset crosswind velocity. Because wake-dominated flames can be identified visually, observations could be conducted to identify wake-dominated flames during crosswind velocities greater than 22 mph at the flare tip. Section 5.0 documents the analysis supporting these observations.
- To avoid flame lift off, the data suggest that the actual flare tip velocity (i.e., actual flare vent gas velocity plus center steam velocity, if applicable) should be less than an established maximum allowable flare tip velocity calculated using an equation that is dependent on combustion zone gas composition, the flare tip diameter, density of the flare vent gas, and density of air. Section 6.0 documents the analysis supporting this observation.
- $LFL_{CZ}$  could apply to non-assisted flares (i.e., the  $LFL_{CZ}$  must be 15.3 percent by volume or less in order to maintain good combustion efficiency). Also, the same operating conditions that were observed to reduce poor flare performance associated with high crosswind velocity and flame lift off could apply to non-assisted flares. Finally, because of lack of performance test data on pressure-assisted flare designs and other flare design technologies, it seems likely that the parameters important for good flare performance for non-assisted, steam-assisted, and air-assisted flares cannot be applied to pressure-assisted, or other flare designs without further information. Section 7.0 documents the analysis supporting these observations.

For purposes of this report, flare vent gas shall mean all gas found in the flare just prior to the gas reaching the flare tip. This gas includes all flare waste gas, flare sweep gas, flare purge gas, and flare supplemental gas, but does not include pilot gas, assist steam, or assist air. Also, combustion zone gas, a term only used for steam-assisted flares, shall mean all gases and vapors found just after a flare tip. Combustion zone gas includes all flare vent gas and total steam.

## **2.0 AVAILABLE FLARE TEST DATA**

This section identifies the data and reports that were used to support our investigation on the effects of flare performance with varying levels of steam (for steam-assisted flares); or air (for air-assisted flares); and high wind and flame lift off (for both types of flares).

### **2.1 Flare Performance Studies and Test Reports**

Specific test run data were extracted from the experimental flare efficiency studies and flare performance test reports identified in Table 2-1. A brief summary of each study or report is provided in Appendix A.

Data sets A through C in Table 2-1 are based on experimental data conducted on pilot-scale test flares with tip sizes ranging from 3 to 12 inches (for steam-assisted flare designs); and 1.5 inches (for the air-assisted flare design tested in data set C). Although data set A includes experimental data for an air-assisted flare, air flow rates and tip design were held confidential so it was not considered in our analysis (see Section 2.7); efforts to acquire this information from the authors were not successful.

Data sets D through I in Table 2-1 are from steam-assisted flares located at various chemical and refinery facilities for which EPA Office of Enforcement and Compliance Assurance either requested studies pursuant to section 114 of the Clean Air Act, or required the study pursuant to a consent decree. With the exception of data set I (and the exception of data sets A through C), flare tip sizes (in terms of the effective diameter of the flare tip) for these data sets range from 16 to 54 inches (for steam-assisted flare designs). Data set I includes test data for a unique flare design and was not considered in our analysis (see Section 2.7). Data set J is based on experimental data from a 36-inch steam-assisted flare tip; and a 24-inch air-assisted flare tip.

In general, the flare test runs were conducted at a high turndown ratio, which means the actual flare vent gas flow rate is much lower than what the flare is designed to handle. Data sets D through J focus completely on high turndown operating conditions. Data sets A through C offer some test data at low turndown ratios, while also offering test data at high turndown ratios.

**Table 2-1. Flare Performance Test Reports**

<b>Data Set ID</b>	<b>Test Study (or Test Report) ID</b>	<b>Title</b>	<b>Author</b>	<b>Date Published</b>	<b>Test Method(s) Used</b>
A	EPA-600/2-83-052	Flare Efficiency Study.	McDaniel, M.	July 1983	Extractive
B	EPA-600/2-84-095	Evaluation of the Efficiency of Industrial Flares: Test Results.	Pohl, J., et al.	May 1984	Extractive
C	EPA-600/2-85-106	Evaluation of the Efficiency of Industrial Flares: Flare Head Design and Gas Composition.	Pohl, J. and N. Soelberg.	September 1985	Extractive
D	MPC TX	Performance Test of a Steam-Assisted Elevated Flare With Passive FTIR. (Conducted in Texas City, TX)	Clean Air Engineering, Inc.	May 2010	PFTIR
E	INEOS	Passive Fourier Transform Infrared Technology (FTIR) Evaluation of P001 Process Control Device at the INEOS ABS (USA) Corporation Addyston, Ohio Facility.	INEOS ABS (USA) Corporation	July 2010	PFTIR
F	MPC Detroit	Performance Test of a Steam-Assisted Elevated Flare With Passive FTIR. (Conducted in Detroit, MI)	Clean Air Engineering, Inc.	November 2010	PFTIR
G	FHR AU FHR LOU	Flint Hills Resources	Clean Air Engineering, Inc.	June 2011	PFTIR
H	SDP EPF	Shell Deer Park Refining LP Deer Park Refinery East Property Flare Test Report.	Shell Global Solutions (US) Inc.	April 2011	PFTIR
I	SDP GF	Shell Deer Park Site Deer Park Chemical Plant OP-3 Ground Flare Performance Test Report.	Shell Global Solutions (US) Inc.	May 2011	AFTIR
J	TCEQ	TCEQ 2010 Flare Study Final Report.	Allen, David T. and Vincent M. Torres.	August 2011	Extractive, AFTIR, and PFTIR

## 2.2 Flare Vent Gas Constituents

Table 2-2 identifies the components that were quantified in each experimental flare efficiency study and flare performance test report. With the exception of data set E, all test runs were based on flares burning propane, propylene, or a mixture of other refinery/petrochemical type gases (with some olefins and aromatics). In general, test runs containing only propane or propylene (with mixtures of inert) were from data sets A through C, and J; and test runs containing a mixture of combustible refinery gases and inerts were from data sets D, and F through I. Test runs associated with data set E were conducted while flaring 1,3-butadiene, in various mixtures of natural gas and nitrogen at a chemical plant.

**Table 2-2. Flare Vent Gas Constituents by Test Report**

Flare Vent Gas Constituent	A: EPA 2-83-052	B: EPA 2-84-095	C: EPA 2-85-106	D: MPC TX	E: INEOS	F: MPC Detroit	G1: FHR AU	G2: FHR LOU	H: SDP EPF	I: SDP GF	J: TCEQ
<b>-----Combustibles-----</b>											
1-Butene				Y		Y	Y		Y	Y	
1,3-Butadiene				Y	Y	Y	Y	Y		Y	
Acetylene						Y	Y		Y	Y	
Benzene							Y	Y		Y	
Carbon Monoxide				Y		Y		Y	Y	Y	
Cis-2-Butene				Y		Y	Y	Y	Y	Y	
Ethane				Y		Y	Y	Y	Y	Y	
Ethyl Benzene								Y	Y	Y	
Ethylene				Y		Y	Y	Y	Y	Y	
Hydrogen				Y		Y	Y	Y	Y	Y	
Hydrogen Sulfide									Y	Y	
Iso-Butane				Y		Y	Y	Y	Y	Y	
Iso-Butylene							Y	Y			
Methane				Y	Y	Y	Y	Y	Y	Y	Y
Methyl Acetylene							Y				
n-Butane				Y		Y	Y	Y	Y	Y	
Pentane and Heavier Alkanes				Y		Y	Y	Y	Y	Y	
Propane		Y	Y	Y		Y	Y	Y	Y	Y	Y
Propylene	Y			Y		Y	Y	Y	Y	Y	Y
Toluene								Y		Y	
Trans-2-Butene				Y		Y	Y		Y	Y	
Xylenes										Y	
<b>Total Combustibles In Flare Vent Gas</b>	<b>1</b>	<b>1</b>	<b>1</b>	<b>14</b>	<b>2</b>	<b>15</b>	<b>17</b>	<b>16</b>	<b>16</b>	<b>20</b>	<b>3<sup>(1)</sup></b>

**Table 2-2. Flare Vent Gas Constituents by Test Report (Continued)**

Flare Vent Gas Constituent	A: EPA 2-83-052	B: EPA 2-84-095	C: EPA 2-85-106	D: MPC TX	E: INEOS	F: MPC Detroit	G1: FHR AU	G2: FHR LOU	H: SDP EPF	I: SDP GF	J: TCEQ
-----Other-----											
Nitrogen	Y	Y	Y	Y	Y	Y	Y	Y	Y	Y	Y
Oxygen				Y		Y		Y	Y	Y	
Carbon Dioxide				Y		Y	Y	Y	Y	Y	
Water				Y					Y	Y	
<b>Total Other Constituents In Flare Vent Gas</b>	<b>1</b>	<b>1</b>	<b>1</b>	<b>4</b>	<b>1</b>	<b>3</b>	<b>2</b>	<b>3</b>	<b>4</b>	<b>4</b>	<b>1</b>

1 – For data set J, tests were not performed with all three combustibles; tests were either performed with propane and methane, or propylene and methane.

Data sets D, and F through I, used flare vent gas with methane and hydrogen as the primary combustibles, and data sets D and F also had significant amounts of olefins in the flare vent gas. Table 2-3 shows the range and average of methane, hydrogen, olefins, and nitrogen in the flare vent gas for each data set. More specific details regarding flare vent gas constituents are discussed in Appendix A. Also, chemical composition for each test run (by test report) used in the steam data analysis is discussed in section 3.0 of this report.

**Table 2-3. Minimum, Maximum, and Average Volume Percents of Primary Constituents in Flare Vent Gas**

Test Report	% Hydrogen (Average)	% Methane (Average)	% Total Olefins (Average)	% Total Other Combustibles (Average)	% Nitrogen (Average)
EPA-2-83-052			8.8–100 (46)		0–9 (54)
EPA-2-85-106				12–18 (15)	82–88 (85)
MPC TX	3.1–24 (14)	3.8–41 (28)	11–44 (19)	7.6–43 (17)	8.2–35 (21)
INEOS		0–61 (20)	2.4–33 (18)		36–78 (61)
MPC Detroit	7.0–55 (23)	16–46 (30)	4.5–65 (20)	4.2–24 (13)	5.7–70 (16)
FHR AU	13–47 (30)	29–75 (55)	0.018–0.47 (0.13)	3.7–12 (6.5)	3.5–16 (7.2)
FHR LOU	20–30 (27)	55–69 (63)	1.2–7.7 (3.1)	3.2–4.2 (3.7)	0.90–9.0 (2.9)
SDP EPF	37–62 (52)	8.5–31 (18)	0.010–0.49 (0.14)	11–20 (13.8)	10–27 (16)
TCEQ		0–6.9 (4.0)	0–100 (24)	0–14.8 (2.2)	0–83 (70)

## 2.3 Steam Injection Rates and Tip Design for Available Flare Test Data

A steam-assisted flare uses steam at the flare stack or flare tip for purposes including, but not limited to, protecting the design of the flare tip, promoting turbulence for mixing or inducing air into the flame. Test data are available for nine different steam-assisted flares when considering the data sets listed in Table 2-1.

There are several different ways steam can be injected into the flare waste stream. The location of steam injection on each of nine steam-assisted flares varied between the data sets. The steam-assisted flares had steam injected through either: nozzles located above the main flare tip opening (upper steam), nozzles on an external ring around the top of the flare tip (ring steam), a single nozzle located inside the flare prior to the flare tip (center steam), or internal tubes interspersed throughout the flare tip (lower steam). The location of steam injection can change the nominal flare tip diameter. An effective diameter of the flare tip considers the location of steam injection by subtracting the obstructed exit area of the flare tip (i.e., area of any stability tabs, stability rings, and steam tubes) from the total exit area of the flare tip.

Table 2-4 summarizes the design detail (including steam injection location and effective flare tip diameter) of each steam-assisted flare tip used for each data set. For most performance tests, not only were the steam injection locations different, but also the steam rate varied between test runs. For certain data sets and steam injection locations, the steam rate was held constant over all test runs. Owners and operators are limited regarding how much they can reduce steam flow to the flare tip because steam-assisted flares often have a manufacturer's minimum steam requirement in order to protect the integrity and life of the flare tip.

**Table 2-4. Steam-Assisted Flare Tip Design Detail**

Data Set ID	Flare Tip Manufacturer and Model Number	Effective Diameter <sup>1</sup> (inch)	Tip Design and Steam Injection Test Rates			
			At or Above Tip			Inside Tip
			Upper (lb/hr)	Ring (lb/hr)	Lower (lb/hr)	Center (lb/hr)
A	John Zink STF-S-8	5.86	<i>Varied</i>	None	None	None

**Table 2-4. Steam-Assisted Flare Tip Design Detail (Continued)**

Data Set ID	Flare Tip Manufacturer and Model Number	Effective Diameter <sup>1</sup> (inch)	Tip Design and Steam Injection Test Rates			
			At or Above Tip			Inside Tip
			Upper (lb/hr)	Ring (lb/hr)	Lower (lb/hr)	Center (lb/hr)
B	Energy and Environmental Research Corporation; and other manufacturer designs <sup>2</sup>	3, 6, and 12	<i>Varied</i>	None	None	None
C	Unknown Commercial Coanda (tulip) Flare Tip	12	<b>140</b>	None	None	None
D	Callidus Technologies BTZ-IS3/US-24-C	23.25	None <sup>3</sup>	None	<i>Varied</i>	<b>500</b>
E	John Zink EEF-QS-16	16	<i>Varied</i>	None	None	None
F	NAO Inc. 20" NFF-RC	16	None	<i>Varied</i>	None	<b>300</b>
G	Callidus Technologies BTZ-US-16/20-C	20	None	<i>Varied</i>	None	<b>500</b>
G	Callidus Technologies BTZ-1S3-54C	54	None	None	<i>Varied</i>	<b>2,890</b>
H	John Zink EEF-QA-36-C	36	<i>Varied</i>	None	None	<i>Varied</i>
J	John Zink EE-QSC-36"	36	<i>Varied</i>	None	None	<i>Varied</i>

1 – The effective diameter of each flare tip was either directly extracted from the test report or calculated from effective area reported in the test report. The effective diameter (or area) considers the portion of the area that is occupied by obstructions and not available for flare vent gas to flow through; it is determined by subtracting the obstructed exit area of the flare tip (i.e., area of any stability tabs, stability rings, and steam tubes) from the total exit area of the flare tip.

2 – Three simple pipe flare heads were designed and built by Energy and Environmental Research Corporation for testing. A retention ring was used on the 3-inch flare head during some testing, so the effective diameter would be less than 3 inches during those specific tests. In addition to these simple pipe flare heads, three commercial 12-inch diameter pipe flares were also tested; these flares were supplied by various flare manufacturers, but the specific design of the flare heads was held confidential.

3 – The flare tip is equipped with upper steam; however, it was not used during any test runs. (Dickens 2011)

## 2.4 Air Injection Rates and Tip Design for Available Flare Test Data

An air-assisted flare uses assist air at the flare tip for purposes including, but not limited to, protecting the design of the flare tip, promoting turbulence for mixing, and inducing air into the flame. Test data are available for three different air-assisted flares when considering the data sets listed in Table 2-1. However, the experimental data for the air-assisted flare associated with data set A were not considered in our analysis (see Section 2.7) because air flow rates and tip design were held confidential. Table 2-5 summarizes the design detail of each air-assisted flare tip used for each data set.

Air is injected into the flare waste stream through nozzles located above the main flare tip opening. Air injection rates were varied during each test run; ranges of injection rates for each air-assisted flare tip tested are provided in Table 2-5.

**Table 2-5. Air-Assisted Flare Tip Design Detail**

<b>Data Set ID</b>	<b>Flare Tip Manufacturer and Model Number</b>	<b>Effective Diameter<sup>1</sup> (inch)</b>	<b>Range of Tested Air Injection Rates (lb/hr)</b>
A	John Zink STF-LH-457-5	Unknown	Unknown
C	Unknown	1.5	8,100 to 150,000
J	John Zink LHTS-24/60	24	250 to 4,700

1 – The effective diameter of each flare tip was either directly extracted from the test report or calculated from effective area reported in the test report. The effective diameter (or area) considers the portion of the area that is occupied by obstructions and not available for flare vent gas to flow through; it is determined by subtracting the obstructed exit area of the flare tip (i.e., area of any stability tabs, stability rings, and steam tubes) from the total exit area of the flare tip.

## 2.5 Flare Test Methods

Measuring emissions from a flare can be difficult and dangerous because flares lack an enclosed combustion chamber, may be elevated, and come in many different designs and sizes. With combustion taking place at and above the tip of the flare, the combusted gases are released into the atmosphere in any direction given the meteorological conditions and flare vent gas velocity that exist at that moment. Although extractive techniques have been used to measure emissions from flares, they require placement of a hood-like structure, sampling rake with multiple sample ports, or other scheme to ensure representative collection of the flare plume. This renders the use of extraction methods for testing industrial flares impractical and relegated to research studies, usually on smaller flares.

Recent technological advances have produced remote sensing instruments capable of indicating the presence of combustion products (e.g., carbon dioxide, carbon monoxide, and select hydrocarbons) without the safety hazards introduced by physically extracting a sample of a flare plume. The remote sensing techniques that have been used on flares discussed in this report include: active Fourier transform infrared (AFTIR) and passive Fourier transform infrared (PFTIR). The main difference between AFTIR and PFTIR is that AFTIR requires the remote

sensor be aligned to an artificial light source; whereas PFTIR simply detects infrared radiation emitted as heat (i.e., PFTIR uses thermal imaging). Table 2-1 identifies whether each test report used extractive, AFTIR, or PFTIR test methods to determine the combustion efficiency of a flare. The majority of these reports used PFTIR, which involves using a spectrometer positioned on the ground to view hot gases from the flare which radiate spectra that are unique to each compound. The PFTIR tests were performed and analyzed by one company, and we are unaware of other companies currently using this technique on flares.

Although AFTIR and PFTIR remote sensing offers an attractive alternative to characterize emissions from flares, AFTIR and PFTIR are relatively expensive, new tools that currently have no approved methods for universal use on flares. Furthermore, for these remote sensing techniques, accurate fitting of measurement and reference spectra for chemical species of interest at representative flare temperatures are pivotal in accurately characterizing industrial flares. Currently, high temperature spectra are not available for all chemical species that may be found in flare vent gas.

The test report for data set J evaluated the performance of remote sensing technologies against extractive techniques. The test report for data set J concluded that the mean difference and standard deviation of the reported AFTIR and PFTIR combustion efficiency values increase as the reported extractive combustion efficiency values decrease; however, both the AFTIR and PFTIR methods actually compare very well to the extractive test results for combustion efficiencies reported as 90 percent or greater. For combustion efficiencies reported as 90 percent or greater, the test report for data set J states that the mean difference of combustion efficiency values averaged 2.5 percentage points different between extractive and AFTIR, and 2.2 percentage points different between extractive and PFTIR. Based on these conclusions, the data collected from all the reports in Table 2-1 were combined and used to support our investigation on the effects of flare performance.

## **2.6 Combining All Available Test Run Data**

All data sets identified in Table 2-1 were combined into an Excel workbook (see Appendix B) and the data were separated by flare type (i.e., steam-assisted versus air-assisted). The Excel workbook identifies each specific test run by the exact test condition and run identification used in each individual report. For data sets A through C, test run data from tables provided within the reports had to be extracted and manually entered into the Excel workbook. Raw test data in the form of Excel worksheets were available for data sets D through J, which eliminated the need to manually enter data into the Excel workbook for these sets. Each individual test run is identified in the “All Run Data” tab of the Excel workbook.

The amount of detail provided per test run varies between each data set. Also, the nomenclature used to describe a variable is different between each data set. For example, data set A uses the term “Lower Heating Value (Btu/scf)” when identifying the net heating value of the flare vent gas, and data set D uses the term “Vent Gas HV” to describe the same variable. Appendix C shows the nomenclature that each data set uses and how it is mapped to one common term used in the Excel workbook.

In some cases, a data set did not explicitly provide a variable, but it could be calculated using details from the test reports. For example, for some data sets, in order to calculate a volumetric flow rate of the flare vent gas for a specific test run, known values for the mass flow rate, molecular weight of the flare vent gas, and a conversion factor for molar volume of an ideal gas (379.48 scf/mol) were used. These cases are identified with the words “Calc Eq. D.##” in Appendix C; where “##” is the specific calculation methodology number. Each calculation methodology is described in Appendix D.

## **2.7 Data Removed After Being Considered**

A total of 582 steam-assisted test runs (118 of these runs came from tests performed on a steam-assisted flare, but no steam was used during the test) and 111 air-assisted test runs were considered in our analysis. However, 270 of the steam-assisted test runs (no steam was used during the test for 109 of these runs) and 67 of the air-assisted test runs were removed prior to any final analysis.

Data sets B and I were not used in any of our analysis. Data set B does not provide enough data to determine a flare vent gas flow rate, which is critical to calculating the various operating limits and parameters we examined. Data set I provides performance testing data for a unique flare design that did not operate in the same way as the other flares and the test data did not appear consistent. The design is a multistage steam-assisted enclosed ground flare with three different stages, which become active at successively higher flows. The flare has 92 horizontally-mounted burners (basically a refractory lined steel shell into which 92 raw flare vent gas burners discharge). Because the flare tested in data set I is so different from the flare designs in other data sets, it is not appropriate to combine and compare its results with the others.

In addition to excluding data sets B and I in their entirety, Table 2-6 identifies various reasons why an individual test run was removed prior to any final analyses described in this Report. Each individual test run removed from the analysis is identified in the “Removed Data” tab of the Excel workbook (see Appendix B). Each individual air-assisted or steam-assisted test run remaining (after removing data due to the reasons described in Table 2-6) is identified in either the “Air Data Used All Analysis” or “Steam Data Used All Analysis” tabs of the Excel workbook depending on flare tip type.

## **2.8 Determination of Combustion Efficiency Representing Good Flare Performance**

The PFTIR testing measures carbon dioxide, carbon monoxide, and hydrocarbons in the plume of the flare in order to calculate combustion efficiency. Several current regulations, including NSPS and NESHAP, require non-flare control devices to be installed and operated to achieve 98 percent destruction efficiency. Therefore, it seemed reasonable to assume that a 98 percent destruction efficiency represents good performance for flares as well. However, most of the flare data was reported in terms of combustion efficiency, making it necessary to estimate a combustion efficiency equivalent to 98 percent destruction efficiency as a means for determining which test runs (in reviewing the flare test data) demonstrated good performance.

According to the John Zink Combustion Handbook (Baukal, 2001), destruction efficiency is a measure of how much of the hydrocarbon is destroyed; and combustion efficiency is a measure of how much the hydrocarbon burns completely to yield carbon dioxide and water vapor. Baukal states that combustion efficiency will always be less than or equal to the destruction efficiency; and a flare operating with a combustion efficiency of 98 percent can achieve a destruction efficiency in excess of 99.5 percent. The relationship between destruction and combustion efficiency is not constant and changes with different compounds; however, we believe Baukal's estimation of 1.5% difference is a reasonable assumption. Extrapolating this to 98 percent destruction efficiency, and also considering the variability in results from the different test methods used in this analysis (e.g., PFTIR vs. AFTIR, vs. extractive sampling methods), it was determined that a combustion efficiency of 96.5 percent in the flare test data demonstrates good flare performance.

**Table 2-6. Criteria To Exclude Data Points**

<b>Criteria</b>	<b>Explanation</b>
Test report did not record combustion efficiency for a specific test run.	It was determined there was not enough information to be able to use the data point.
Test report recorded combustion efficiency as 0% for a specific test run.	The flare flame was completely snuffed out and the data point was not useful in determining trends. However, the data point was reviewed to determine conditions that do not provide good combustion (all data points in this category had a $LFL_{CZ}$ greater than 15.3%; see Section 3.0 of this report for an explanation on $LFL_{CZ}$ ).
Test report recorded that the extraction probe positioning for a specific test run was located in the flame.	The specific test run was considered invalid because the extraction technique did not obtain a good sample of the flare plume.
Test report recorded that the extraction probe positioning for a specific test run was uncertain.	The specific test run was considered invalid because the extraction technique may not have obtained a good sample of the flare plume.
Test report recorded a specific test run time as less than 5 minutes.	The specific test run has too much uncertainty and variability in the reported values. Note, there were four data points in data set D (i.e., runs 6-1, 8-1, 10-1, and 10-2 from condition D) that were reported as having a run time greater than 5 minutes; however, these points are included in this removal category because several of the minutes in the average of the test run either showed zero entries for the PFTIR data. These 4 runs had less than 5 minutes of data that were not zero or not affected by wind.
Test report recorded single test runs and an average of the specific single test runs; the single test runs were removed, but the average was kept.	The single test runs were considered duplicative because each run was performed at the exact same conditions.
Test report recorded a specific test run as smoking.	The specific test run was considered out of compliance because visible emissions are a violation with the current regulation, and determined that test runs that were considered out of compliance should not be used to establish operating parameters for good combustion.
Test report did not record enough information to determine the flare vent gas flow for a specific test run.	It was determined there was not enough information to be able to use the data point.
Test report recorded that the flare vent gas flow rate of a specific test run was less than 10 pounds per hour.	The specific test results for these runs are based on an extractive test method. The results showed very different CE values than other similar runs except that these runs had flare vent gas flow rates less than 10 pounds per hour. The extractive test method may not have correctly detected the waste gas compositions because flow was too low.
Specific to only data set H, the test report concluded that the "GE Panametric flow readings must be in error when nitrogen concentrations in the SDP EPF line were greater than 30v%".	The flare vent gas flow rates (above 30% $N_2$ ) for data set H are reported as not accurate. This observation is limited to ten specific test runs.
Specific to only data set C, two specific test runs were reported as achieving greater than 99% combustion efficiency, yet the fraction of combustible in the stream was less than 2%.	The specific test results for these two test runs are based on an extractive test method which may not have correctly detected the waste gas compositions. Given the flammability of the stream, it is not possible for these two test runs to have achieved greater than 99% combustion efficiency (the combustibility of the stream is too low).

### **3.0 STEAM AND FLARE PERFORMANCE**

Steam is used in some flares as a design feature to protect the flare tip. Steam injection also promotes smokeless burning in a flare. A key factor to smokeless burning is having enough waste gas momentum as it exits the flare burner so that sufficient amounts of air can mix with the waste gas and achieve complete combustion. Steam injection is the most common technique for adding momentum to low-pressure gases. In addition to adding momentum, steam also provides smoke suppression benefits of gas dilution and participates in the chemistry of the combustion process (Baukal, 2001). Steam will react with hot carbon particles in soot, removing the carbon before it can cool and form smoke. Steam will also react with intermediate combustion products to form compounds that readily burn at lower temperatures (Castiñeira, 2006). Using too much steam in a flare (over steaming) can result in a flare operating outside its stable flame envelope, reducing the destruction efficiency capabilities of the flare. Moreover, the cooling effect from use of excessive steam may actually inhibit dispersion of flared gases. In extreme cases, over steaming can actually snuff out a flame and allow waste gases to go into the atmosphere unburned (Peterson, 2007).

To identify over steaming situations that may occur on steam-assisted flares, the data suggest that the lower flammability limit of combustion zone gas ( $LFL_{CZ}$ ) is the most appropriate operating parameter. Specifically, the data suggest that, in order to maintain good combustion efficiency, the  $LFL_{CZ}$  must be 15.3 percent by volume or less for a steam-assisted flare. As an alternative to  $LFL_{CZ}$ , the data suggest that the ratio of the net heating value of the combustion zone gas ( $NHV_{CZ}$ ) to the net heating value of the flare vent gas if diluted to the lower flammability limit ( $NHV_{LFL}$ ) must be greater than 6.54. Section 3.1 documents the analysis supporting this observation. Sections 3.2 through 3.4 explain other operating conditions that we investigated for good combustion efficiency for steam-assisted flares.

#### **3.1 Lower Flammability Limit of Combustion Zone Gas for Steam-Assisted Flares**

The lower flammability limit (LFL) is an important chemical property when considering combustibility of a gas mixture. The LFL of any mixture is the lowest concentration of that mixture in air at which the mixture will burn. Mixtures with a relatively high LFL are less

flammable when released to the air than mixtures with a relatively low LFL. A gas mixture with a relatively high LFL requires a larger volume of the mixture to burn in a specific volume of air, than would a mixture of gases with a relatively low LFL being combusted in that same volume of air. The LFL of a mixture is therefore influenced by both the type and amount of chemical components (including inerts) present in the gas being burned and is a significant parameter when assessing whether a mixture being combusted with an open flame will adequately combust.

The combustion zone of a steam-assisted flare includes the gas mixture that is created by the flare vent gas and the steam that is supplied to the flare. The flare vent gas includes all waste gas, sweep gas, purge gas, and supplemental gas, but does not include pilot gas, or assist media. Therefore, the combustion zone gas includes all the gases injected into the combustion zone of the flare except the pilot gas. See Section 3.1.5 for a discussion of why pilot gas is not included in the combustion zone gas. The chemical components and their relative amounts in the combustion zone for each test run used in the data analysis for this section can be seen in Appendix E by test report. The  $LFL_{CZ}$  is the resulting LFL of the mixture that is created by combining both the flare vent gas and steam. This parameter was considered as a means to take into account the effect of steam on the capability of the flare vent gas to burn.

Figure 3-1 shows the boundaries of flammability for several different inerts in methane and air mixtures (Zabetakis, 1965). The plot is referred to as a Zabetakis plot, or “nose plot”, because of its shape and represents the concentrations of fuel (methane in this case), inert and air, and the conditions in which combustion will occur. Note that the air concentration is determined by subtracting the methane and inert concentrations from 100 percent. The line hitting the y-axis near the bottom of the figure is the LFL with no inert added (5% for methane). The upper flammability limit (UFL) is the line hitting the y-axis at a higher level (about 15%). The x-axis shows the quantity of inert added to the methane and air mixture. The curves show that the UFL falls rapidly for mixtures with increasing amounts of inert and the lowest UFL value occurs at the maximum amount of inert at which combustion can still be supported. At this amount of inert, the UFL has been reduced to be equal to the LFL and combustion can only occur at this concentration. An amount of inert above this maximum would render the mixture non-flammable, because there would not be enough air to sustain combustion.

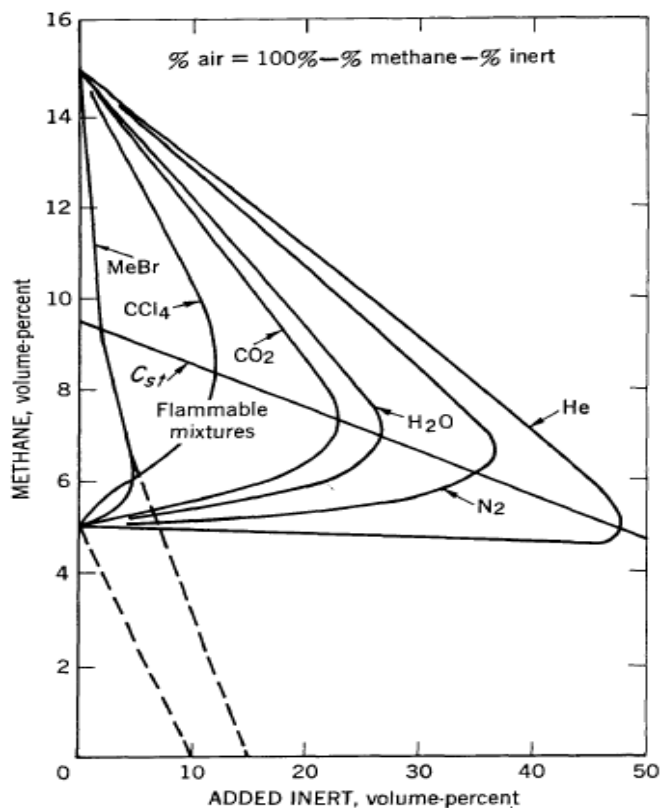


**Figure 3-1. Zabetakis Nose Plot For Methane And Inert In Air**

At the UFL, at any inert concentration, the combustible-inert-air mixture is oxygen limited; there is enough fuel to burn but just enough oxygen to sustain combustion. Any less oxygen, the mixture is not flammable. At the LFL, at any inert concentration, there is plenty of oxygen with respect to the amount of fuel available. At any combustible concentration less than the LFL, the fuel is too lean and the mixture is not flammable.

Adapted from Evans and Roesler (2011), Figure 3-2 uses a Zabetakis plot for methane in air with water as the inert in order to illustrate how a ‘pocket’ of flare vent gas and steam mixture interacts with the atmosphere as it travels from the flare tip through the combustion zone. For simplicity, Figure 3-2 assumes that the flare vent gas is methane and center steam has been added, so the flare vent gas and steam mixture is 25 volume percent methane and 75 volume percent water. Just prior to the flare vent gas and steam mixture being released from the flare tip into the combustion zone, it contains no oxygen and is therefore above the UFL (this point is not

represented on Figure 3-2 because this condition would exist off the graph). However, from the point of release at the flare tip, the flare vent gas and steam mixture is quickly diluted by the ambient air. At point A on Figure 3-2, the flare vent gas and steam mixture has mixed with air to about 15 percent methane, 45 percent water, and 40 percent air; and the gas mixture is still too rich to burn. As the gas mixture continues mixing with air it approaches the UFL (point B on Figure 3-2). For this example, the UFL of the gas mixture is 8.3 percent methane, 25 percent water, and 66.7 percent air. Just beyond point B, the gas mixture is within the UFL and LFL and will burn. While the gas mixture is burning it also continues to be diluted until the concentration of the gas mixture is just at the LFL (point C on Figure 3-2) of 5.8 percent methane, 17.5 percent water, and 76.7 percent air. Using this thought process for other mixtures, it becomes clearer that if the flare vent gas and steam mixture are already near the LFL when the gas mixture is released into air, the concentration could quickly fall below the mixture's LFL (point D on Figure 3-2) before having a chance to ignite and burn completely; and therefore, it is possible to dilute the flammable gas mixture to a mixture with no combustible characteristics.

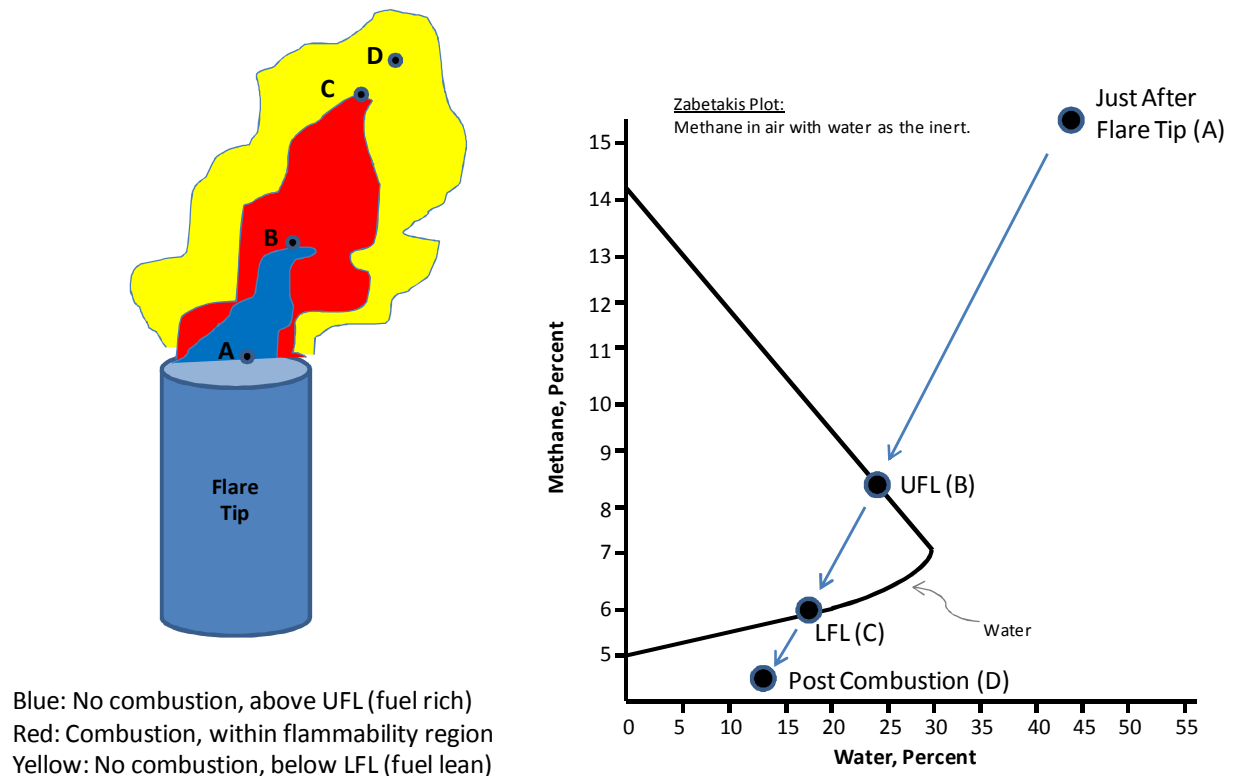


**Figure 3-2. Time Sequence of Flare Vent Gas Volume Moving Through Flammability Region**  
Source: (Adapted from Evans and Roesler, 2011)

In addition, the inerts (e.g., nitrogen, carbon dioxide, steam, etc.) of the combustion zone gas, which are either included in the flare vent gas or are added as assist steam, compete for space with the air and combustible components. The inert gases reduce the flammable range of the gas-air mixtures (increase the LFL and decrease the UFL). Some of the heat from the combustion reaction is absorbed by the inert gases (Molnarne et. al., 2005), which cools the flame and slows the propagation of combustion. This is especially a concern for mixtures with higher LFL values. The higher the inert concentration present in the combustion zone gas, the higher the  $LFL_{CZ}$ . When the higher LFL combustion zone gas mixes with air, it takes less air to dilute the gas mixture below the LFL and therefore this diluting effect can happen much more quickly. Also, because there are fewer combustible gas molecules in the combustion zone gas, more mixing is required to get the combustible components near oxygen molecules. Therefore, the higher the LFL of the combustion zone gas, the more difficult it is to achieve and maintain good combustion.

Section 3.1.1 discusses the flare test data and how these data suggest that 15.3 percent  $LFL_{CZ}$  may be an appropriate threshold (an operating condition representing good combustion). Section 3.1.2 describes the method for calculating  $LFL_{CZ}$  for mixtures using Le Chatelier's principle and the level of accuracy expected given different flare vent gas compositions. Section 3.1.3 analyzes data points that had a  $LFL_{CZ}$  less than 15.3 percent but a combustion efficiency less than 96.5 percent. Section 3.1.4 analyzes the 66 data points with good combustion efficiency and a  $LFL_{CZ}$  greater than 15.3 percent, and provides possible further categorizing of the  $LFL_{CZ}$  to provide more chemical component specificity to the  $LFL_{CZ}$  limit. Section 3.1.5 provides an explanation for excluding pilot gas in these analyses.

### **3.1.1 Flare Test Data and $LFL_{CZ}$**

The  $LFL_{CZ}$  was examined for 312 steam-assisted flare test runs to determine if there is a  $LFL_{CZ}$  threshold that would indicate whether good combustion would occur. Figure 3-3 shows that as the  $LFL_{CZ}$  increases, the combustion efficiency of a flare deteriorates. The vertical dotted line in Figure 3-3 marks the threshold where all test runs (47) at a  $LFL_{CZ}$  of less than or equal to 10.0 percent achieved a combustion efficiency of 96.5 percent or greater. However, there are several test runs with gas mixtures that have a  $LFL_{CZ}$  greater than 10.0 percent that had good

combustion efficiencies. Looking at the extent of test points both above and below 96.5 percent combustion efficiency reveals that test runs with a  $LFL_{CZ}$  of 15.3 percent or less resulted in good combustion efficiency for all runs except eleven. At a  $LFL_{CZ}$  greater than 15.3 percent, there are several test runs with good combustion efficiency, but for every run with good combustion, there is at least one run with bad combustion. For example, using test runs with a  $LFL_{CZ}$  of 20.0 percent or less, there are 30 test runs with good combustion and 33 test runs with combustion efficiency less than 96.5 percent.

The vertical solid line in Figure 3-3 shows a threshold where most test runs at a  $LFL_{CZ}$  of less than or equal to 15.3 percent achieved a combustion efficiency of 96.5 percent or greater. This level maximizes the number of test runs (105) with a combustion efficiency of 96.5 percent or greater that are below 15.3 percent  $LFL_{CZ}$  while minimizing the number of test runs (11) that have a combustion efficiency less than 96.5 percent. There are 11 test runs (highlighted in red on Figure 3-3) with a  $LFL_{CZ}$  between 10.0 and 15.3 percent that did not achieve a combustion efficiency of 96.5 percent or greater; further detail about the 11 test runs is provided in Section 3.1.3. Also evident from Figure 3-3 are several test runs that achieved good combustion but all had a  $LFL_{CZ}$  greater than 15.3 percent. There are 197 data points with a  $LFL_{CZ}$  greater than 15.3 percent and 61 of these points have a combustion efficiency of greater than 96.5 percent. These data points are discussed further in Section 3.1.4.



**Figure 3-3. Combustion Efficiency vs. LFL<sub>CZ</sub>**

### 3.1.2 The Le Chatelier Principle

Le Chatelier’s principle was used to estimate lower flammability limits of the flare combustion zone gas for each test run. Le Chatelier’s principle for determining flammability limits for mixtures uses the reciprocal of the volume weighted average over the LFL of the individual compounds for estimating the gas mixture’s LFL (Equation 3-1).

$$LFL_a = \frac{100}{\sum_{j=1}^n \left( \frac{\chi_j}{LFL_j} \right)} \quad (\text{Eq. 3-1})$$

Where:

- LFL<sub>a</sub> = Lower flammability limit of any gas mixture ‘a’, volume %.
- a = Placeholder for any gas mixture.
- n = Number of components in gas mixture ‘a’.
- j = Individual pure component in gas mixture ‘a’.

$x_j$  = Concentration of individual pure component  $j$  in gas mixture 'a', volume %.

$LFL_j$  = Lower flammability limit of individual pure component  $j$ , volume %.

Le Chatelier's equation was originally limited to binary mixtures of combustible gases (Coward et al., 1919). Coward et al. (1919) generalized the equation for mixtures containing more than two combustible gases. Coward and Jones (1952) presented a method for using Le Chatelier's equation when inert gases are included in the mixture. This method entails assigning amounts of inert gas to the combustible gases, identifying a LFL for each combustible–inert combination from previous experimental data, and then using Le Chatelier's equation to calculate the LFL for the full mixture. For example, a mixture of 50:20:30 percent nitrogen/hydrogen/methane could be broken up into two mixtures, one with 60:40 percent nitrogen/hydrogen (30% nitrogen and 20% hydrogen from original mixture, or total of 50% of the original mixture) and one with 40:60 nitrogen/methane (20% nitrogen and 30% methane from original mixture, or total of 50% of the original mixture). Experimental data of nitrogen and hydrogen, and nitrogen and methane mixtures, such as the data graphed in Appendix F, can then be used to determine each partial mixture's LFL. Looking at Appendix F, the LFL of a 60:40 percent nitrogen/hydrogen mixture is 6.5 percent; and 12.5 percent for a 40:60 percent nitrogen/methane mixture. Then using Le Chatelier's equation, a LFL of 8.6 percent is determined for the full mixture:

$$\frac{100}{\frac{50}{6.5} + \frac{50}{12.5}} = 8.6\% \quad (\text{Eq. 3-2})$$

This method is not practical for determining the LFL of flare vent gas and steam mixtures because flare vent gases can change at any moment and consist of a wide variety of chemicals. The LFL data for mixtures with nitrogen (or carbon dioxide) and a combustible is limited; and this type of information is essentially unavailable for steam. The results of the method also vary significantly depending on how the combustibles and inerts are paired together.

Karim et al. (1985) describes another way to address mixtures with inerts, which is to include the inert in Le Chatelier's equation and assume a LFL for the inert gas of infinity. This zeros out the term for the inert in the equation since one divided by infinity is zero. The  $LFL_{CZ}$  in Figure 3-3 assumes inerts have an infinite LFL (or a reciprocal of the LFL equal to zero).

However, assuming infinity for all inerts as Karim et al. (1985) suggests does not address the difference in behavior for the different inerts. Molnarne et al. (2005) describes a method for taking into account non-nitrogen inerts. This method is used in the International Standards Organization (ISO) Standard 10156 and was originally presented by Besnard (1996). In this method, a nitrogen equivalency factor is used that varies depending on both the type of inert(s) and combustible compound(s) in the mixture. Molnarne, et al. describes the possible values for nitrogen equivalency for the specific combustion gas and inert combinations. Equation 3-3 incorporates this method into Le Chatelier’s equation. More details about inerts and further explanation for including an equivalency adjustment to correct for different inert behavior are provided in Appendix G. Appendix G also provides a more detailed discussion about LFL and the accuracy of calculated LFL values with respect to varying amounts of inerts and specific combustible gases that can be contained in a mixture. Appendix G does not specifically discuss the flare test data, but includes important concepts and considerations helpful in understanding the discussions contained in Sections 3.1.3 and 3.1.4.

$$LFL_a = \frac{100}{\sum_{j=1}^n \left( \frac{\chi_j}{LFL_j} \right) - (N_{e,H_2O} - 1)(x_{H_2O}) - (N_{e,CO_2} - 1)(x_{CO_2})} \quad (\text{Eq. 3-3})$$

Where:

- LFL<sub>a</sub> = Lower flammability limit of any gas mixture ‘a’, volume %.
- a = Placeholder for any gas mixture (e.g., flare combustion zone gas, ‘cz’; flare vent gas with center steam, ‘vgcs’; or flare vent gas ‘vg’).
- n = Number of components in gas mixture ‘a’.
- j = Individual pure component in gas mixture ‘a’.
- x<sub>j</sub> = Concentration of individual pure component j in gas mixture ‘a’, volume %.
- LFL<sub>j</sub> = Lower flammability limit of individual pure component j, volume %. The LFL of individual compounds are based on experimental data and are provided in a Bureau of Mines Bulletin entitled: “Flammability Characteristics of Combustible Gases and Vapors” (Zabetakis 1965). All inerts, including nitrogen, are assumed to have an infinite lower flammability limit (e.g., LFL<sub>N2</sub> = ∞).
- N<sub>e,H2O</sub> = Coefficient of nitrogen equivalency for water relative to nitrogen, unitless. See Table 3-1.

- $x_{H_2O}$  = Concentration of water in gas mixture ‘a’, volume fraction.
- $N_{e,CO_2}$  = Coefficient of nitrogen equivalency for carbon dioxide relative to nitrogen, unitless. See Table 3-1.
- $x_{CO_2}$  = Concentration of carbon dioxide in gas mixture ‘a’, volume fraction.

**Table 3-1. Recommended Values of Coefficient of Nitrogen Equivalency for Water and Carbon Dioxide Relative to Nitrogen**

<b>Combustible Component i in Flare Vent Gas</b>	<b><math>N_{e,H_2O}</math></b>	<b><math>N_{e,CO_2}</math></b>
Methane	1.87	2.23
Ethane	1.40	1.87
Propane	1.51	1.93
Ethylene	1.68	1.84
Propylene	1.36	1.92
Hydrogen	1.35	1.51
All Other Combustibles	1.50	1.87

Source: Molnarne et al. (2005)

Figure 3-4 is the same plot as Figure 3-3, except the  $LFL_{CZ}$  has been adjusted for nitrogen equivalency. All data points have essentially shifted to the right; and the amount each test run shifted is dependent on the amount of water and carbon dioxide in the combustion zone gas. By applying this adjustment, one of the 11 test runs highlighted (in red) in Figure 3-3, is no longer between the 10.0 and 15.3 percent  $LFL_{CZ}$  region. (See Section 3.1.3 about these test runs.) The differences between Figures 3-3 and 3-4 do not appear significant; however, from the perspective of assuring that a  $LFL_{CZ}$  of 15.3 percent or less specifies a flare with good combustion, it is important as will become more evident throughout this section and Appendix G.

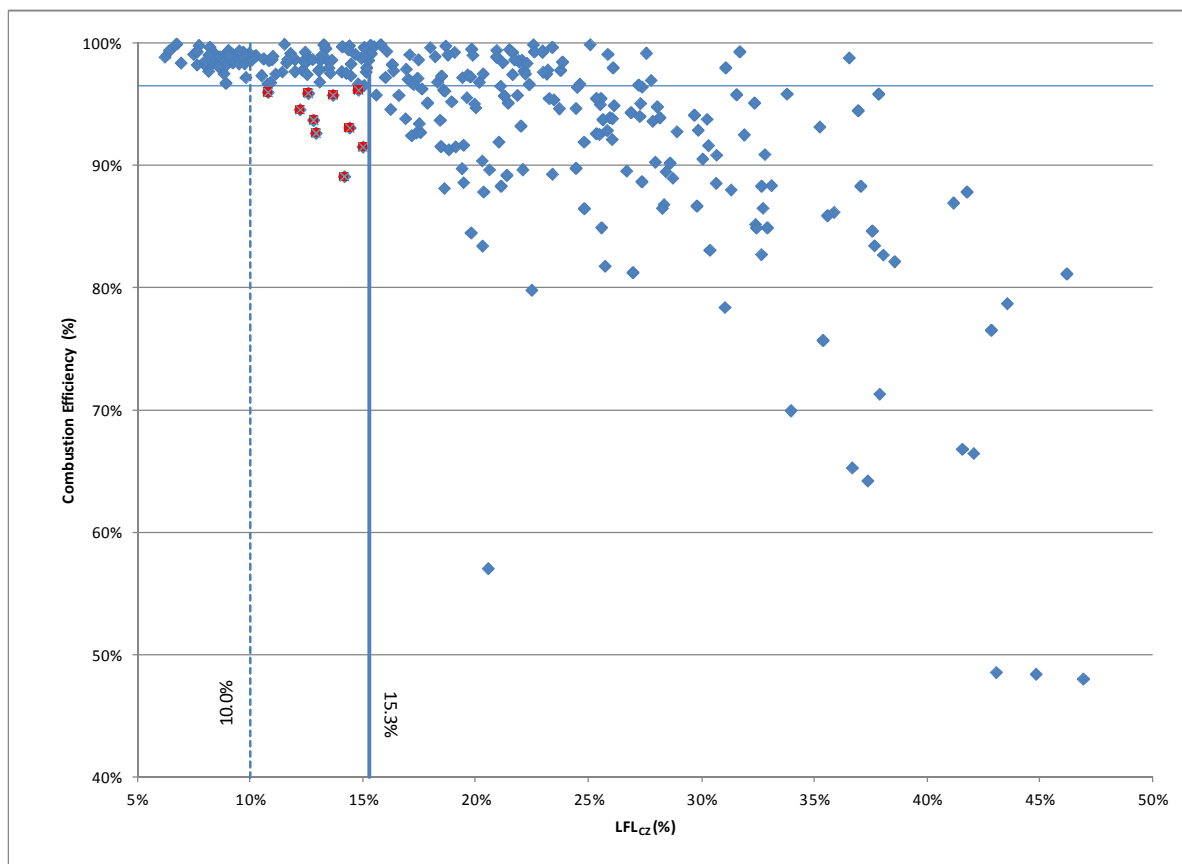


**Figure 3-4. Combustion Efficiency vs. LFL<sub>CZ</sub> Adjusted for Nitrogen Equivalency**

### 3.1.3 Specific Test Data Not Fitting the Trend

The test runs highlighted red in Figures 3-3 through 3-8 (Figures 3-5 through 3-8 are shown in Section 3.1.4) do not seem to fit the trend found for the other test runs that good combustion efficiency is achieved with a LFL<sub>CZ</sub> less than 15.3 percent depicted by the vertical blue line in each figure. These test runs have a LFL<sub>CZ</sub> of less than 15.3 percent but they did not have a combustion efficiency of greater than 96.5 percent. The specific test reports associated with these test runs were examined. These test runs could be in error or have a higher variability than other test runs, the estimate of the LFL could be incorrect, or the LFL may not be an appropriate indicator of combustion efficiency. Given the previous discussion in Sections 3.1.1 and 3.1.2, the LFL appears to be a good indicator of combustion efficiency (assuming wind and velocity of the flare vent gas are within reasonable limits as discussed in Sections 5 and 6 of this report). Therefore, this section investigates the possibility of inaccuracies in testing or calculating the LFL (the appropriateness of using Le Chatelier's equation for the mixture). Note that four of

the test runs are within the statistical uncertainty for the test method. As determined by Clean Air Engineering (2010a), the measured combustion is  $\pm 1.5\%$  at a confidence level of 99%.

These data points (Table 3-2) were scrutinized against all of the other test runs to see if they were unique results that indicated an issue with the accuracy in the test results, or whether they are indicating a previously unseen trend. Figure 3-3 presents 11 data points in red; however, Figures 3-4 through 3-8 only indicate 10 data points that do not fit the trend. The eleventh data point (Flint Hills Resources LOU-C) shown in Figure 3-3 has a  $LFL_{CZ}$  greater than 15.3 percent after the nitrogen equivalency adjustment was made. Therefore, the data point follows the trend of the majority of the data and is not discussed further in this section. Section 3.1.3.1 describes any test run specific information revealed by the review of the test reports. Section 3.1.3.2 includes observations from examining these test runs and comparing them to other test runs. Section 3.1.3.3 provides conclusions regarding these test runs.

**Table 3-2. Test Run Detail for 11 Data Points with  $LFL_{CZ} < 15.3\%$  but Combustion Efficiency  $< 96.5\%$**

Test Site	Condition ID	Run ID	Combustion Efficiency (%)	% Combustible In CZ (%)	% Inert In CZ (%)	% Olefin In CZ (%) <sup>a</sup>	% H2 In CZ (%)
MPC TX	B	8-2 <sup>b</sup>	95.8	28.0	72.0	5.06	5.72
MPC TX	B	9-2	89.1	27.0	73.0	4.89	5.56
MPC TX	D	7-2 <sup>b</sup>	96.0	20.5	79.5	8.89	1.36
MPC Detroit	B	8-1	94.6	28.0	72.0	4.20	10.5
MPC Detroit	C	4-1	92.7	21.9	78.1	14.8	1.67
MPC Detroit	C	4-2	93.7	22.3	77.7	14.5	1.83
MPC Detroit	C	5-1	93.1	19.8	80.2	13.2	1.74
MPC Detroit	C	5-2	91.6	19.4	80.6	12.3	1.70
MPC Detroit	D	8-1 <sup>b</sup>	96.2	24.8	75.2	2.75	11.6
FHR LOU	LOU-A	2.0(1) <sup>b</sup>	95.9	35.0	65.0	2.83	10.6
FHR LOU	LOU-C	3.0(2) <sup>b, c</sup>	95.8	30.8	69.2	0.50	9.03

<sup>a</sup> Olefins include: 1-Butene, 1,2-Butadiene, 1,3-Butadiene, Cis-2-Butene, Ethylene, Iso-Butylene, Propadiene, Propylene, and Trans-2-Butene.

<sup>b</sup> These test runs are within the testing uncertainty of 96.5%; they each had combustion efficiencies less than 1.5% below 96.5%.

<sup>c</sup> After making the nitrogen equivalency adjustment for this run, the  $LFL_{CZ}$  is greater than 15.3% and therefore follows the trend for the majority of the data points (see Figures 3-3 and 3-4).

### ***3.1.3.1 Review of Test Reports***

The MPC TX test report (Clean Air Engineering, Inc., 2010a) discusses a potential problem with some reported data. The report says that when the wind came from a certain direction steam may have interfered with the pilot due to a “shaping steam ring failure.” The report states that “the shaping steam ring failure caused the shaping pressure to be unbalanced, with one side of the concentric ring starved for steam. As the wind blew towards the area of unbalance, the flame sheared off of the flare tip and was extinguished.” For all of the test runs where this was noted in the raw data, the efficiency was more variable on a minute-by-minute basis during the testing than for the other runs. This could mean that the efficiencies for test runs affected by the flare steam ring failure and wind could be biased low. All of the MPC TX data points included in Table 3-2 (i.e., B 8-2, B 9-2, and D 7-2) were affected by this issue. The raw data showed that for test run B 8-2, there were 9 out of 12 minutes tested affected by this issue; for test run B 9-2, there were 10 out of 10 minutes affected; and for test run D 7-2, there were 4 out of 10 minutes affected.

The MPC Detroit test report (Clean Air Engineering, Inc., 2010b) stated that if the wind was “blowing directly away from the PFTIR at more than 5 mph,” the PFTIR view of the flare plume could be obscured causing inaccuracies in the testing. The wind was blowing in the “wrong” direction (for the PFTIR analysis) for all of the MPC Detroit Condition C runs and for the B 8-1 test run. However, the wind speeds were not excessive during these runs (average wind speed for these test runs was less than 3.6 miles per hour). The test run data revealed no issues with the MPC Detroit test run D 8-1 and the Flint Hills Resources (LOU) test run LOU-A 2.0(1).

### ***3.1.3.2 Comparison of Data Runs***

The data points listed in Table 3-2 can be divided, generally, into three groups when considering the combustion zone gas: one with olefin and hydrogen both approximately equal to 5 percent; one with high hydrogen content (9 to 11.6%) and low olefin content (0.5 to 2.8%); and the third group with relatively high olefin content (8.9 to 14.8%) and low hydrogen content (less than 2%). All of the available test data were reviewed to determine if there were any similar test runs to those in Table 3-2. The information found for each group is discussed below.

### *Olefin and Hydrogen Approximately Equal*

The test runs at MPC TX numbered B 8-2 and B 9-2 did not fit the trend, and both had olefin and hydrogen content at about 5 percent. Looking at the full set of test data, there were several other test runs with a similar composition yet had combustion efficiencies greater than 96.5 percent and a LFL<sub>CZ</sub> greater than 15.3 percent. Table 3-3 shows all the test runs where olefin and hydrogen concentrations were approximately equal; data with an olefin to hydrogen ratio from 0.81 to 1.23 were reviewed. As evident by Table 3-3, there were several data points with very similar concentrations of olefin, hydrogen, other combustibles and inerts. “Other combustibles” include primarily methane and other alkanes.

### *High Hydrogen and Low Olefin*

The test runs MPC Detroit B 8-1 and D 8-1, and Flint Hills test LOU-A 2.0(1) had a higher concentration of hydrogen than olefin by about 2.5 to 4 times. Table 3-4 provides the information for all test runs with relatively high hydrogen and low olefin concentrations (ratio of olefin to hydrogen of 0.12 to 0.55). All the test runs in Table 3-4 have less olefin than hydrogen by a factor of between 2 and 8 and there is inert content of between 49 and 88 percent. Test runs MPC Detroit D 8-1 and Flint Hills LOU-A 2.0(1) have measured combustion efficiencies that are within the statistical uncertainty of 96.5%. Also, Table 3-4 shows several other test runs that have similar conditions and all had combustion efficiencies of 96.5% or greater. These test runs do not appear to indicate a unique trend.

The MPC Detroit test run B 8-1 is similar to several test runs in Table 3-4 but it does have a relatively high inert concentration (72%) for the group. The MPC Detroit test runs A 4-2 and A 3-1 both have similar amounts of inert at 74 and 72 percent respectively. However, there is more hydrogen and olefin in the B 8-1 run than these runs.

This information is distributed solely for the purpose of pre-dissemination peer review under applicable information quality guidelines. It has not been formally disseminated by EPA. It does not represent and should not be construed to represent any Agency determination or policy.

**Table 3-3. Olefin and Hydrogen Approximately Equal**

Test Site	Condition	Run	CE	% Olefin-CZ (%)	% H <sub>2</sub> -CZ (%)	Ratio % Olefin-CZ / % H <sub>2</sub> -CZ	Other Combustibles in CZ (%)	Inert in CZ (%)	Fraction Combustible in CZ	Steam Fraction of CZ	LFL <sub>CZ</sub> Adjusted for Nitrogen Equivalency
MPC TX	A11	4-1	95.5%	2.84	3.53	0.81	9.78	83.86	0.16	0.77	25.33%
MPC TX	C	3-2	99.2%	6.34	7.82	0.81	24.33	61.51	0.38	0.55	9.93%
MPC TX	A11	12-1	61.6%	1.38	1.69	0.82	4.35	92.57	0.07	0.89	62.75%
MPC TX	LTS	2-5	99.4%	6.91	8.41	0.82	23.94	60.75	0.39	0.53	9.50%
MPC TX	LTS	2-6	97.2%	7.40	8.89	0.83	19.20	64.51	0.35	0.54	9.79%
MPC TX	A11	6-1	92.5%	2.26	2.71	0.83	8.64	86.39	0.14	0.81	31.88%
MPC TX	B	4-2	99.3%	6.89	8.09	0.85	23.59	61.44	0.39	0.54	9.66%
MPC TX	LTS	2-2	99.3%	6.88	8.07	0.85	23.56	61.49	0.39	0.54	9.68%
MPC TX	A11	2-1	95.6%	3.62	4.25	0.85	11.82	80.31	0.20	0.70	19.58%
MPC TX	LTS	2-3	99.0%	6.96	8.01	0.87	23.60	61.42	0.39	0.54	9.64%
MPC TX	B	5-2	99.0%	6.16	7.09	0.87	20.88	65.86	0.34	0.59	10.98%
MPC TX	B	10-2	96.7%	4.69	5.39	0.87	15.94	73.99	0.26	0.69	14.76%
MPC TX	B	6-1	98.4%	5.54	6.31	0.88	18.54	69.61	0.30	0.64	12.43%
MPC TX	B	6-2	98.5%	5.53	6.29	0.88	18.63	69.56	0.30	0.64	12.42%
MPC TX	B	9-2	89.1%	4.89	5.56	0.88	16.58	72.97	0.27	0.68	14.16%
MPC TX	B	7-2	97.9%	5.27	5.98	0.88	17.87	70.88	0.29	0.65	13.06%
MPC TX	B	7-1	97.8%	5.32	6.03	0.88	17.77	70.88	0.29	0.65	13.01%
MPC TX	B	8-2	95.8%	5.06	5.72	0.88	17.18	72.05	0.28	0.67	13.65%
MPC TX	B	9-1	97.6%	4.89	5.53	0.89	16.39	73.20	0.27	0.68	14.24%
MPC TX	B	8-1	97.6%	5.14	5.80	0.89	17.15	71.92	0.28	0.66	13.53%
MPC TX	B	5-1	98.7%	6.21	7.01	0.89	20.86	65.92	0.34	0.59	10.94%
MPC Detroit	LTS	8	98.7%	7.12	6.78	1.05	25.83	60.28	0.40	0.56	8.72%
MPC Detroit	LTS	7	99.3%	10.77	10.20	1.06	21.65	57.38	0.43	0.53	7.62%
MPC Detroit	LTS	5	99.1%	8.76	7.92	1.11	23.56	59.76	0.40	0.55	8.14%
MPC Detroit	LTS	4	98.9%	8.03	7.24	1.11	22.86	61.87	0.38	0.57	8.64%
MPC Detroit	LTS	1	98.9%	8.70	7.39	1.18	23.64	60.27	0.40	0.55	8.33%
MPC TX	C	3-1	98.9%	3.94	3.20	1.23	20.84	72.02	0.28	0.66	9.73%

Pink = CE less than 96.5%, and LFL<sub>CZ</sub> less than 15.3% (Test Runs from Table 3-2).

Gray = LFL<sub>CZ</sub> greater than 15.3%.

This information is distributed solely for the purpose of pre-dissemination peer review under applicable information quality guidelines. It has not been formally disseminated by EPA. It does not represent and should not be construed to represent any Agency determination or policy.

**Table 3-4. High Hydrogen and Low Olefin**

Test Site	Condition	Run	CE	% Olefin-CZ (%)	% H <sub>2</sub> -CZ (%)	Ratio % Olefin-CZ / % H <sub>2</sub> -CZ	Other Combustibles in CZ (%)	Inert in CZ (%)	Fraction Combustible in CZ	Steam Fraction of CZ	LFL <sub>CZ</sub> Adjusted for Nitrogen Equivalency
FHR LOU	LOU-B	1.0 (2)	99.4%	1.49	12.38	0.12	36.84	49.29	0.51	0.48	9.01%
MPC Detroit	D	3-1	97.5%	2.04	16.49	0.12	11.07	70.39	0.30	0.68	12.50%
FHR LOU	LOU-A	MIN (3)	98.8%	1.59	11.47	0.14	22.98	63.96	0.36	0.60	12.59%
FHR LOU	LOU-A	8.5 (1)	78.8%	0.62	3.86	0.16	7.89	87.63	0.12	0.87	43.54%
FHR LOU	LOU-A	3.0 (2)	99.1%	1.30	8.01	0.16	18.18	72.50	0.27	0.71	17.05%
FHR LOU	LOU-A	4.0 (2)	98.6%	1.06	6.41	0.17	14.57	77.95	0.22	0.77	21.87%
FHR LOU	LOU-A	5.0 (2)	96.5%	0.89	5.30	0.17	11.92	81.90	0.18	0.81	27.35%
MPC Detroit	D	5-1	91.6%	1.85	11.05	0.17	7.49	79.61	0.20	0.78	18.43%
FHR LOU	LOU-A	6.0 (1)	88.6%	0.86	5.11	0.17	10.41	83.61	0.16	0.83	30.63%
MPC Detroit	D	6-1	98.4%	3.43	20.30	0.17	13.17	63.10	0.37	0.60	9.73%
FHR LOU	LOU-A	6.0 (2)	95.1%	0.79	4.67	0.17	10.29	84.25	0.16	0.83	32.34%
FHR LOU	LOU-A	5.0 (1)	95.5%	1.01	5.93	0.17	12.13	80.94	0.19	0.80	25.53%
FHR LOU	LOU-A	2.0 (3)	98.6%	1.66	9.53	0.17	22.45	66.36	0.34	0.63	13.59%
MPC Detroit	D	4-1	88.6%	1.84	10.31	0.18	7.25	80.60	0.19	0.79	19.44%
FHR LOU	LOU-A	4.0 (1)	96.5%	1.25	6.91	0.18	14.19	77.64	0.22	0.77	21.08%
FHR LOU	LOU-A	3.0 (1)	97.2%	1.59	8.09	0.20	16.89	73.43	0.27	0.72	17.37%
FHR LOU	LOU-A	MIN (2)	99.2%	2.10	10.05	0.21	26.28	61.57	0.38	0.59	11.76%
MPC Detroit	D	9-1	98.6%	3.84	16.98	0.23	14.80	64.37	0.36	0.61	10.05%
FHR LOU	LOU-A	2.0 (2)	98.6%	1.65	7.29	0.23	25.65	65.41	0.35	0.64	13.42%
<b>MPC Detroit</b>	<b>D</b>	<b>8-1</b>	<b>96.2%</b>	<b>2.75</b>	<b>11.61</b>	<b>0.24</b>	<b>10.43</b>	<b>75.22</b>	<b>0.25</b>	<b>0.73</b>	<b>14.78%</b>
FHR LOU	LOU-A	MIN (1)	97.5%	3.01	12.04	0.25	24.27	60.67	0.39	0.59	11.10%
<b>FHR LOU</b>	<b>LOU-A</b>	<b>2.0 (1)</b>	<b>95.9%</b>	<b>2.83</b>	<b>10.57</b>	<b>0.27</b>	<b>21.56</b>	<b>65.04</b>	<b>0.35</b>	<b>0.63</b>	<b>12.55%</b>
MPC Detroit	D	7-1	83.5%	2.19	8.06	0.27	8.28	81.47	0.19	0.80	20.28%
MPC Detroit	A	3-2	98.6%	2.69	8.77	0.31	18.26	70.28	0.30	0.65	13.08%
MPC Detroit	A	2-2	98.5%	3.23	9.73	0.33	19.84	67.20	0.33	0.62	11.60%
MPC Detroit	D	10-1	81.8%	2.12	5.40	0.39	7.27	85.21	0.15	0.84	25.71%
<b>MPC Detroit</b>	<b>B</b>	<b>8-1</b>	<b>94.6%</b>	<b>4.20</b>	<b>10.46</b>	<b>0.40</b>	<b>13.30</b>	<b>72.04</b>	<b>0.28</b>	<b>0.69</b>	<b>12.19%</b>
MPC TX	LTS	2-4	98.7%	5.10	11.02	0.46	16.24	67.64	0.32	0.54	11.64%
MPC Detroit	A	1-1	99.0%	4.51	9.00	0.50	23.26	63.23	0.37	0.56	10.23%
MPC Detroit	A	7-1	95.2%	2.84	5.62	0.50	13.87	77.67	0.22	0.73	17.83%
MPC Detroit	A	8-1	92.0%	2.31	4.53	0.51	12.09	81.07	0.19	0.77	21.00%
MPC Detroit	A	4-2	97.7%	3.18	6.18	0.51	16.46	74.18	0.26	0.69	15.12%
MPC Detroit	B	1-1	98.9%	9.07	17.61	0.52	27.10	46.21	0.54	0.41	6.19%
MPC Detroit	A	3-1	98.0%	3.48	6.65	0.52	18.13	71.74	0.28	0.66	13.47%
MPC Detroit	A	9-1	81.3%	1.93	3.66	0.53	9.90	84.51	0.15	0.82	26.94%
MPC Detroit	A	6-2	96.7%	2.88	5.38	0.54	14.74	76.99	0.23	0.73	17.22%
MPC Detroit	A	2-1	97.7%	3.98	7.25	0.55	19.91	68.86	0.31	0.63	11.96%

Pink = CE less than 96.5%, and LFL<sub>CZ</sub> less than 15.3% (Test Runs from Table 3-2). Gray = LFL<sub>CZ</sub> greater than 15.3%.

### *Higher Olefin and Low Hydrogen*

There are five test runs from Table 3-2 that are in this category and they are shown in Table 3-5 in the pink rows along with all other test runs where the olefin concentration was greater than the hydrogen concentration (except for those runs where the olefin concentration was just above hydrogen which are shown in Table 3-4). Only one of the five test runs is within the statistical uncertainty of 96.5% combustion efficiency (MPC TX D 7-2). Table 3-5 shows several test runs with good combustion efficiencies that match the conditions of the five test runs. However, none of the data points had the same or higher amounts of inerts than these five test runs had. These five runs have the highest amounts of inerts (between 78 to 81%) of any of the test runs with similar compositions in Table 3-5.

#### *3.1.3.3 Conclusions on Ten Data Points*

The data points in Table 3-2 were expected to achieve good combustion efficiency because their  $LFL_{CZ}$  were determined to be less than 15.3 percent using Le Chatelier's equation and adjusting for nitrogen equivalency. However, these test runs achieved combustion efficiencies between 89.1 and 96.2 percent. These data points were reviewed to determine if these anomalies were an indication that the 15.3 percent  $LFL_{CZ}$  was incorrect and should be adjusted to better fit the data or if the points were just a few inaccurate test results in a group of over 300 test points. By comparing the compositions and results of other test runs with the tests in Table 3-2 it can be speculated whether the tests are inaccurate or a clue to something else.

For the two test runs where the olefin and hydrogen concentration are approximately equal (MPC TX B 9-2 and B 8-2), there are several examples of test runs of almost identical conditions where a combustion efficiency of greater than 96.5 percent was achieved. Also, both of these test runs had the majority of the testing time affected by the steam ring failure. It appears likely that these two test runs had inaccurate results and that their results should not impact the 15.3 percent  $LFL_{CZ}$  value.

This information is distributed solely for the purpose of pre-dissemination peer review under applicable information quality guidelines. It has not been formally disseminated by EPA. It does not represent and should not be construed to represent any Agency determination or policy.

**Table 3-5. Higher Olefin and Low Hydrogen**

Test Site	Condition	Run	CE	% Olefin-CZ (%)	% H <sub>2</sub> -CZ (%)	Ratio % Olefin-CZ / % H <sub>2</sub> -CZ	Other Combustibles in CZ (%)	Inert in CZ (%)	Fraction Combustible in CZ	Steam Fraction of CZ	LFL <sub>CZ</sub> Adjusted for Nitrogen Equivalency
MPC TX	D	4-1	98.4%	11.03	1.83	6.03	12.63	74.51	0.25	0.69	8.75%
<b>MPC TX</b>	<b>D</b>	<b>7-2</b>	<b>96.0%</b>	<b>8.89</b>	<b>1.36</b>	<b>6.54</b>	<b>10.23</b>	<b>79.51</b>	<b>0.20</b>	<b>0.76</b>	<b>10.77%</b>
MPC TX	D	4-2	98.2%	11.01	1.68	6.56	12.20	75.11	0.25	0.70	8.86%
MPC Detroit	C	3-1	96.8%	16.62	2.50	6.64	6.95	73.93	0.26	0.72	10.89%
MPC Detroit	C	2-1	98.4%	18.59	2.61	7.12	8.72	70.07	0.30	0.68	9.48%
MPC Detroit	C	2-2	99.1%	20.97	2.93	7.16	9.46	66.63	0.33	0.64	8.45%
<b>MPC Detroit</b>	<b>C</b>	<b>5-2</b>	<b>91.6%</b>	<b>12.33</b>	<b>1.70</b>	<b>7.26</b>	<b>5.37</b>	<b>80.60</b>	<b>0.19</b>	<b>0.79</b>	<b>14.98%</b>
MPC Detroit	C	1-2	99.4%	26.15	3.47	7.54	12.70	57.67	0.42	0.55	6.40%
<b>MPC Detroit</b>	<b>C</b>	<b>5-1</b>	<b>93.1%</b>	<b>13.18</b>	<b>1.74</b>	<b>7.58</b>	<b>4.93</b>	<b>80.15</b>	<b>0.20</b>	<b>0.79</b>	<b>14.39%</b>
<b>MPC Detroit</b>	<b>C</b>	<b>4-2</b>	<b>93.7%</b>	<b>14.54</b>	<b>1.83</b>	<b>7.93</b>	<b>5.89</b>	<b>77.74</b>	<b>0.22</b>	<b>0.76</b>	<b>12.79%</b>
MPC Detroit	C	3-2	97.4%	17.53	2.15	8.17	7.11	73.22	0.27	0.71	10.49%
<b>MPC Detroit</b>	<b>C</b>	<b>4-1</b>	<b>92.7%</b>	<b>14.78</b>	<b>1.67</b>	<b>8.83</b>	<b>5.48</b>	<b>78.06</b>	<b>0.22</b>	<b>0.77</b>	<b>12.90%</b>
MPC TX	E	3-3	98.3%	12.32	1.10	11.20	13.69	72.89	0.27	0.70	7.62%
MPC TX	E	5-2	97.5%	10.68	0.94	11.33	11.91	76.46	0.24	0.74	8.81%
MPC TX	E	4-3	97.7%	11.52	1.01	11.38	12.86	74.60	0.25	0.72	8.13%
MPC TX	E	5-1	96.8%	11.44	0.86	13.37	11.50	76.21	0.24	0.74	8.89%
MPC TX	E	3-1	98.6%	12.84	0.93	13.74	12.76	73.47	0.27	0.71	7.97%
MPC TX	E	4-1	98.1%	12.12	0.85	14.31	11.80	75.23	0.25	0.73	8.59%

Pink = CE less than 96.5%, and LFL<sub>CZ</sub> less than 15.3% (Test Runs from Table 3-2).

Gray = LFL<sub>CZ</sub> greater than 15.3%.

The three test runs that had relatively high hydrogen content, all about 10.5 percent, and lower olefin content [FHR LOU-A 2.0(1), MPC Detroit B 8-1 and D 8-1] were compared with other test runs. The FHR LOU-A 2.0(1) and MPC Detroit D 8-1 were both very similar test runs, and they both had combustion efficiencies within the statistical uncertainty of the method. There were also several test runs that were very close matches to these runs that all achieved good combustion. These test runs do not appear to signify a separate trend or raise doubt regarding the 15.3 percent  $LFL_{CZ}$  threshold. The MPC Detroit test run B 8-1 can be nearly matched to a few test runs, including some with more inert that still achieved greater than 96.5 percent combustion efficiency; indicating that these test runs are likely due to inaccurate test results.

The remaining test runs in Table 3-3 (MPC TX D 7-7 and MPC Detroit C 4-1, 4-2, 5-1, and 5-2) are all very similar to each other, except that the MPC TX run has a much lower olefin content and a higher amount of other combustibles (and it is the only run in this group with a combustion efficiency within the statistical uncertainty of 96.5%). There are several similar runs with good combustion efficiency shown in Table 3-5, but they all have lower amounts of inert than those runs shown in Table 3-2 — 78 to 81 percent inert for the test runs with a combustion efficiency less than 96.5 percent compared to 58 to 76 percent inert for runs achieving greater than 96.5 percent combustion efficiency. Because there are five test runs all similar in composition and results, it seems that there could be issues with one or more components acting to inhibit the combustion to some degree; thereby interfering with the accuracy of the Le Chatelier's equation. Azatyan et al. (2005a, 2005b, and 2007) showed that small amounts of propylene can react with hydrogen and form chain terminating products that inhibit some of the combustion reactions (see Appendix G for further discussion). However, these test runs have larger amounts of olefins and a small amount of hydrogen; it is unknown whether inhibition is possible with this situation. Also, the test runs contain other combustibles, such as methane and propane. Therefore, it is difficult to make any conclusion. The flare steam analysis was performed on 312 data points; all but 17 had some amount of olefin in the gas mixture, 203 test runs with at least 1 percent olefin, and 198 test runs with both hydrogen and olefin. If there are chain terminating reactions from olefins or another compound, the inhibition affected very few data points with respect to a  $LFL_{CZ}$  of 15.3 percent.

### **3.1.4 Data Points with Good Combustion and High LFL<sub>CZ</sub>**

Out of the 312 data points available for this analysis, 164 test runs achieved a combustion efficiency of 96.5 percent or greater; Figure 3-4 shows 66 of these runs (or 40%) have a LFL<sub>CZ</sub> greater than 15.3 percent and achieve greater than 96.5 percent combustion efficiency. This means that for approximately 40 percent of the test runs that achieved a combustion efficiency of 96.5 percent or greater, and if LFL<sub>CZ</sub> were being used to monitor flare performance, owners would need to reduce the amount of inert in the combustion zone (i.e., reduce the amount of assist steam being used), or add additional combustible gas in order to lower the LFL<sub>CZ</sub> below the threshold of less than 15.3 percent. The test data were scrutinized to see if there were any commonalities or trends that could explain why the 66 test points still achieved good combustion efficiency with a higher than expected LFL<sub>CZ</sub>. Approximately half (36) of the 66 test points are from INEOS, EPA, and TCEQ data sets and have only one or two flammable gases. Gas compositions for these tests included nitrogen, propane, propylene, 1,3-butadiene, and natural gas. The other 30 test points are from Shell, Marathon, and Flint Hill Resources data sets and have 10 or more combustible constituents in the flare vent gas. The primary gas components for these tests were hydrogen and methane.

Similar to the data points discussed in Section 3.1.3, the 66 data points do not fit the overall trend because the calculation of the LFL<sub>CZ</sub> is inaccurate, the combustion efficiency measurements are inaccurate, or the flammability is not an appropriate parameter to represent flare performance or it does not completely explain the performance of a flare. This section explores two explanations for the 66 data points: (1) The potential that some of the steam may not enter the combustion zone due to wind effects, and (2) The LFL<sub>CZ</sub> representing good combustion may vary with the composition of the flare vent gas.

#### ***3.1.4.1 Partial Steam Contribution***

One factor that may contribute to overestimated LFL<sub>CZ</sub> values is that the calculation methodology for LFL<sub>CZ</sub> that was used in this analysis assumes all assist steam is incorporated into the combustion zone gas. However, it is possible that some of the steam delivered from the upper and/or lower ring steam nozzles may actually not participate in mixing with the

combustion zone because wind can blow the flame away from a portion of the nozzles causing steam to be shot directly into the atmosphere without ever hitting the combustion zone. With this in mind, the LFL<sub>CZ</sub> values could be overestimated for some test runs depending on the steam injection configuration and the wind direction and velocity.

The location of steam injection on each of the steam-assisted flares varied between test data sets (see Table 2-4 in Section 2.0). Table 3-6 shows the breakdown of steam use for the 66 test runs that have a LFL<sub>CZ</sub> greater than 15.3 percent and achieve greater than 96.5 percent combustion efficiency when the LFL<sub>CZ</sub> is adjusted for nitrogen equivalency. Sixty-one out of the 66 test runs that have a LFL<sub>CZ</sub> greater than 15.3 percent (and achieve greater than 96.5% combustion efficiency), were using steam that potentially did not mix completely with the other combustion zone gases. This means that for these test runs, the LFL<sub>CZ</sub> that was calculated in this analysis may actually be too high, which would explain why these test runs achieved greater than 96.5 percent combustion efficiency but the calculation shows a LFL<sub>CZ</sub> greater than 15.3 percent.

**Table 3-6. Breakdown Of Steam Use For The 66 Test Runs<sup>a</sup>**

Steam Configuration	Test Run Count	Test Reports
Upper	18	EPA-600/2-83-052; EPA-600/2-85-106; TCEQ; and INEOS
Upper and Center	26	TCEQ and SDP EPF
Lower and Center	12	FHR LOU and MPC TX
Ring <sup>b</sup> and Center	5	MPC Detroit and FHR AU
No Steam	5	EPA-600/2-83-052

<sup>a</sup> Those test runs that have a LFL<sub>CZ</sub> greater than 15.3% and achieve greater than 96.5% combustion efficiency when the LFL<sub>CZ</sub> is adjusted for nitrogen equivalency.

<sup>b</sup> The specific test reports do not clarify whether the ring steam is located in an upper or lower position at the flare tip.

In a recent report, Marathon Petroleum Company reviewed their performance testing results against wind conditions and flare plume position to characterize how wind speed affects the amount of steam mixing with the combustion zone gas (Cade et al., 2010). The report derived a “Steam Contribution Factor” calculation methodology to predict conditions when non-mixing steam is occurring; however, the methodology is not practical to apply to all flares because it relies heavily on flare design, specific test data and flame images.

The amount of steam that mixes in the combustion zone at a given moment would depend on the wind speed and direction and would vary moment-by-moment. Because of the difficulties in determining how much upper, lower, and ring steam mixes with the combustion zone, and since the upper, lower, and ring steam is designed to be injected into the combustion zone gas; it is logical to assume that in the majority of situations complete mixing occurs and includes all the steam, regardless of where it is injected, when calculating the  $LFL_{CZ}$ . However, to estimate the possible effect of this assumption, a worst case analysis was conducted assuming no upper, lower, and ring steam participated in mixing with the combustion zone (i.e., only center steam was used in the  $LFL_{CZ}$  calculation). The  $LFL_{CZ}$  for 37 of the 66 test runs, with only center steam considered, computed to less than 15.3 percent. Therefore, even if it were known that the wind was great enough on the day of testing to remove all upper, lower, and ring steam from the combustion zone, this would only resolve just over half (56%) of the test runs with good combustion efficiency but high  $LFL_{CZ}$  (greater than 15.3%).

#### **3.1.4.2 More Specific $LFL_{CZ}$ Thresholds**

Another detail that could be considered when establishing a  $LFL_{CZ}$  threshold on the entire 312 test runs is the commonalities in composition of flare vent gas. Figures 3-5 through 3-8 are plots of the same 312 test runs shown in Figures 3-3 and 3-4; however, the test runs are divided into one of the four figures depending on the test run composition. The lower flammability limit of the combustible portion of the flare vent gas ( $LFL_{VG,C}$ ) was used to define the composition categories. This scheme was developed based on the observation that the smaller the LFL of a pure component, the greater the amount of inert that chemical can withstand and still propagate a flame (Kondo, 2006a). Therefore, to allow the greatest amount of inert (or highest  $LFL_{CZ}$ ), the data were divided into categories associated with their LFL without inert.

Four categories were developed and are shown in Table 3-7. For example, if the combustible portion of the flare vent gas for a test run consisted of 30 percent propane (and the other 70% was nitrogen), the test run would fall into category A because the  $LFL_{VG,C}$  is equal to that of propane, or 2.1 percent. Table 3-7 also shows the potential  $LFL_{CZ}$  threshold for each category based on Figures 3-5 through 3-8. The test runs that do not fit the trends in these figures, as having not achieved a combustion efficiency of 96.5 percent or greater (but are

meeting the potential  $LFL_{CZ}$  threshold), are highlighted in red and have been discussed in Section 3.1.3.

**Table 3-7. Potential  $LFL_{CZ}$  Thresholds based on  $LFL_{VG,C}$**

Category ID	$LFL_{VG,C}$ (%)	Potential Threshold for $LFL_{CZ}$ (%)
A	$\leq 2.4$	$\leq 24.0$
B	$>2.4$ and $\leq 2.8$	$\leq 18.5$
C	$>2.8$ and $\leq 3.8$	$\leq 16.0$
D	$>3.8$	$\leq 14.5$

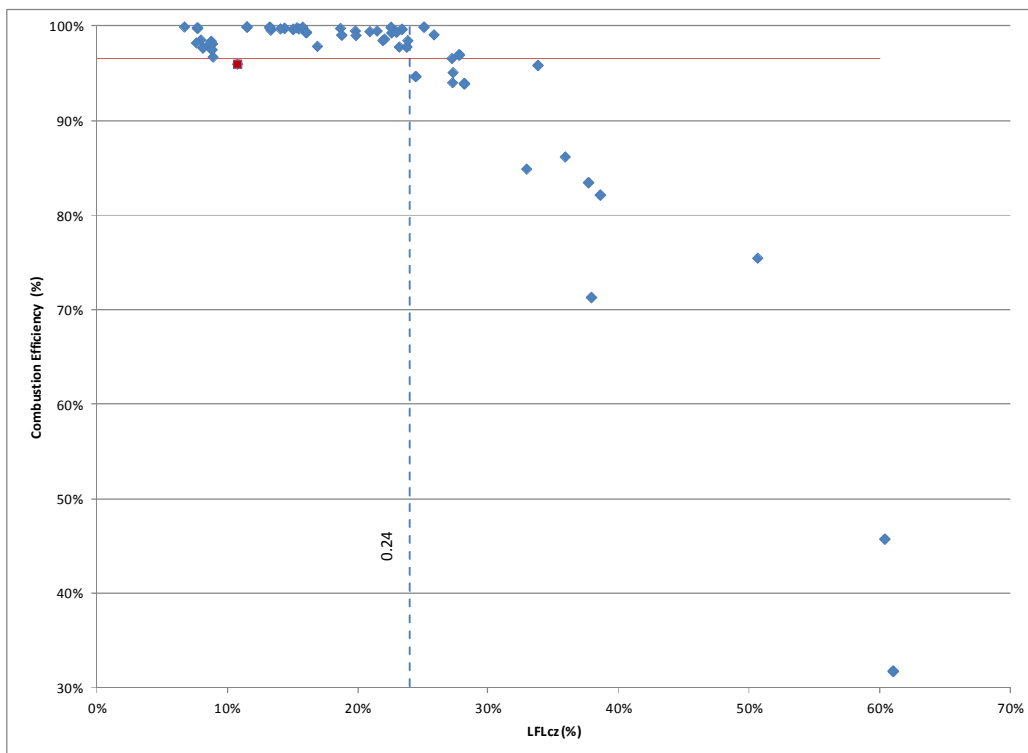


**Figure 3-5. Combustion Efficiency vs.  $LFL_{CZ}$  for Category A Test Runs (see Table 3-7)**

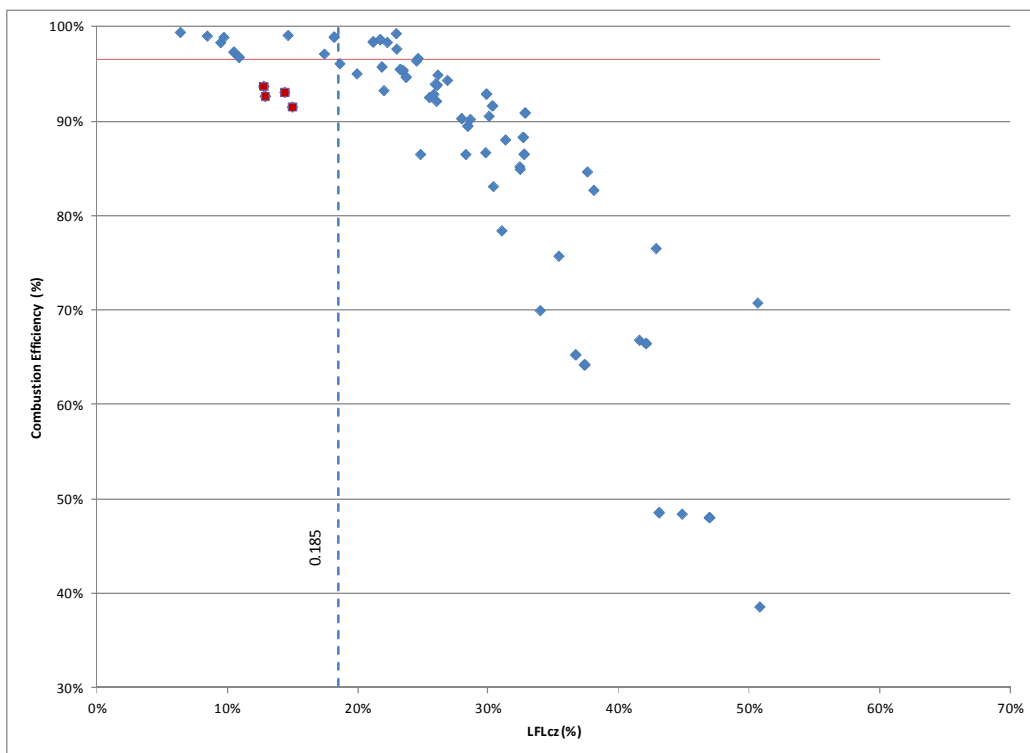


Figure 3-6. Combustion Efficiency vs. LFL<sub>Cz</sub> for Category B Test Runs (see Table 3-7)

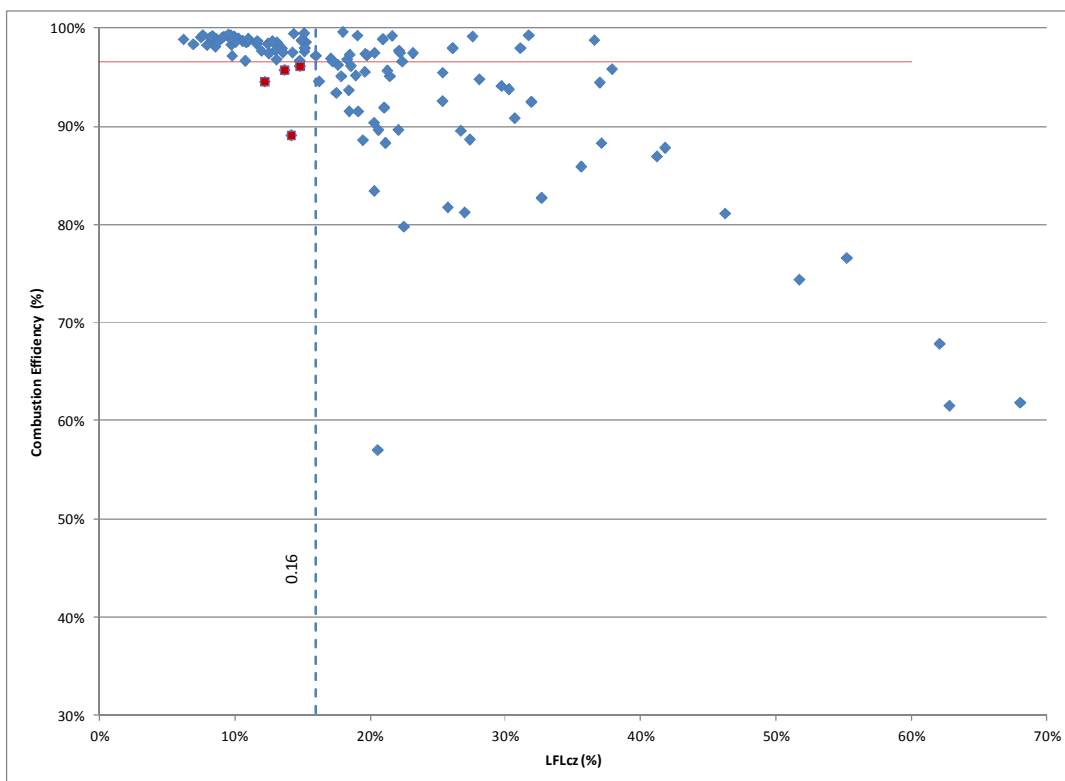
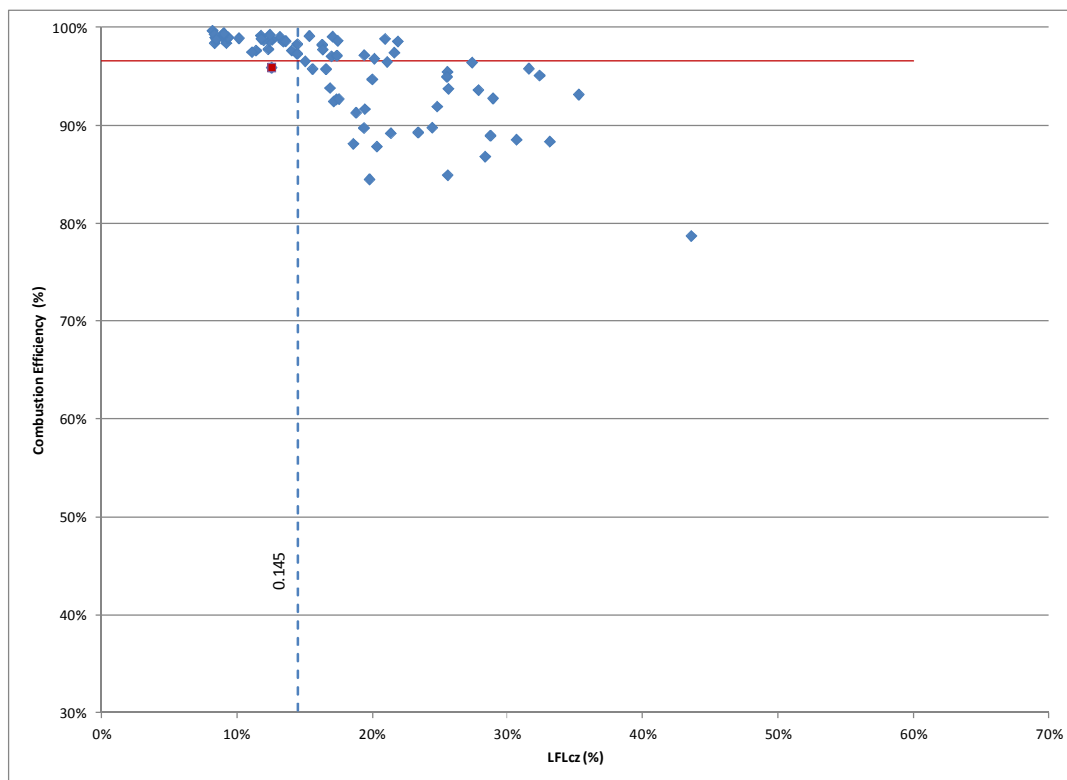


Figure 3-7. Combustion Efficiency vs. LFL<sub>Cz</sub> for Category C Test Runs (see Table 3-7)



**Figure 3-8. Combustion Efficiency vs. LFL<sub>CZ</sub> for Category D Test Runs (see Table 3-7)**

By categorizing the data into these four categories, one test run (in Category D) no longer meets the LFL<sub>CZ</sub> threshold ( $\leq 14.5\%$ ) and has a combustion efficiency of 96.5 percent or better. However, 22 test runs now meet the LFL<sub>CZ</sub> threshold (in Table 3-7), and have an efficiency of 96.5 percent or greater. This reduces the number of test runs that have good combustion efficiency, yet do not meet the LFL<sub>CZ</sub> threshold, from 66 to 45 test runs. All but two of the 22 test runs that meet the thresholds in Table 3-7 and have good combustion efficiency are in Category A. Generally, Category A includes test runs with only 1 or 2 combustible components and Categories C and D have several constituents and most include hydrogen and methane. Categorizing did not improve the results for Categories C and D. The test runs that make up a given category generally are from specific test reports. For example, SDP EPF test runs are all in Category C, while Category D is almost entirely FHR AU or FHR LOU test runs. The SDP EPF, FHR AU and FHR LOU test runs are for mixtures with higher amounts of hydrogen. Combustible mixtures that have components that enhance the combustion of other constituents would also be a reason that a mixture with a higher calculated LFL<sub>CZ</sub> could have a combustion efficiency of greater than 96.5 percent. As discussed in Appendix G, hydrogen can enhance the

combustion of methane and this enhancement is not reflected in the calculated LFL. However, an understanding of the role that other constituents play in the combustion efficiency (such as amounts of olefin, propane, etc., and better quantification of this hydrogen-methane effect) are needed before this could be considered.

Also, there could be issues with the testing of the combustion efficiencies for these runs. Information was not available to judge the accuracy for the FHR test runs. The SDP EPF test report cited the possibility of inaccurately high combustion efficiency measurements during times of unstable combustion conditions. However, the test runs were not identified in the report where this may have occurred. Without further testing it is difficult to determine why these 45 test runs had good combustion efficiencies with  $LFL_{CZ}$  greater than 15.3 percent.

### **3.1.5 Excluding Pilot Gas**

Our analyses have not included the heat value or flammability properties of the pilot gas. The pilot gas serves as a source of ignition for the combustion zone gas. The pilot gas does not significantly contribute to the combustion zone gas mixture, or the final output or operating limit value of the  $LFL_{CZ}$ . In theory, the pilot gas is already fully combusted at the combustion zone, and therefore would contribute a small amount of inert (i.e., carbon dioxide and water vapor) to the combustion zone gas mixture. However, the amount of inert that could be attributed to the pilot gas is expected to be negligible — relative to the volume of flare vent gas that would actually participate in the combustion zone gas mixture (e.g. for 304 of the 312 test runs, the pilot gas contributed less than 3% of the volumetric flow rate of the flare vent gas; and the pilot gas contributed to less than 1% for 224 of these test runs).

In addition, pilot gas is needed to maintain the pilot flame which is a requirement of current flare regulations. Including the pilot gas in the calculation of the combustion zone parameters, does not add any accuracy in identifying flares with (or without) good combustion. Also, by leaving pilot gas out of the calculations, the equations are simplified.

## **3.2 Combustible Gas Concentration in the Combustion Zone**

If there are not enough combustible components in the combustion zone, then the flare vent gas will not burn, or will burn inadequately, resulting in lower combustion efficiency. The addition of assist steam dilutes the combustible components of the flare vent gas, which can make it more difficult for the flare vent gas to burn. To simplify consideration of the operating conditions for good combustion, we looked at the minimum quantity of combustibles present in the combustion zone that would maintain good combustion for the chemical compositions tested.

Figure 3-9 shows the combustion efficiency versus the fraction of combustibles in the combustion zone gas ( $C_{CZ}$ ). The vertical dotted line in Figure 3-9 identifies the threshold where all, but one test run with a fraction of combustibles in the combustion zone gas of 0.32 or greater achieved a combustion efficiency of 96.5 percent or greater. All data sets had test runs with a fraction of combustibles in the combustion zone gas at greater and less than 0.32, except TCEQ. Therefore, this trend was observable for a variety of flare vent gas compositions and constituents. All TCEQ test runs had enough inert (either nitrogen or steam) to cause the fraction of combustibles in the combustion zone gas to be less than 0.32. Although Figure 3-9 illustrates a strong trend (because all test runs except for FHR LOU-A 2.0(1) performed with at least 32 percent combustibles in the combustion zone gas achieved greater than 96.5 percent combustion efficiency – see Section 3.1.3 for a discussion about test run FHR LOU-A 2.0(1)), there are a significant number of test runs that achieved good combustion efficiency that did not have at least 32 percent combustibles in the combustion zone gas. For these situations, a more detailed review of the operating conditions would have to be considered, such as consideration of the  $LFL_{CZ}$ .

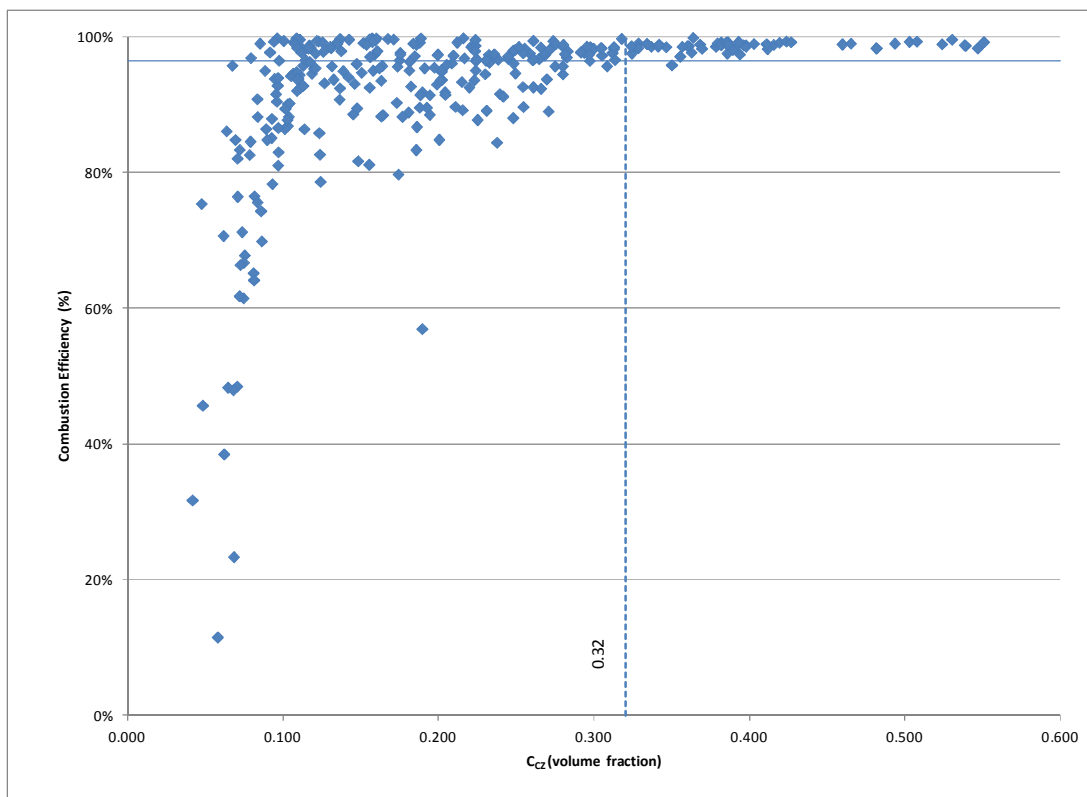


**Figure 3-9. Combustion Efficiency vs. C<sub>CZ</sub>**

### 3.3 Heat Content Based Limit for Steam-Assisted Flares

A white paper (Evans and Roesler, 2011) was reviewed that describes a method to define flare operating conditions using the net heating value and the lower flammability limit. The method is nearly identical mathematically (observations with test data reveal some differences that are discussed later in this section) to the reciprocal of the  $LFL_{CZ}$  parameter discussed in Section 3.1 (provided you apply “combustion factors” as described in the white paper); however, it may be easier for flare owners and operators to understand and implement because it uses a familiar parameter (net heating value). The white paper uses Le Chatelier’s principle and provides a methodology for determining the ratio of the net heating value of the combustion zone gas ( $NHV_{CZ}$ ) to the net heating value of the flare vent gas if diluted to the lower flammability limit ( $NHV_{VG-LFL}$ ).

Figure 3-10 shows that as the ratio of  $NHV_{CZ}$  to  $NHV_{VG-LFL}$  decreases, the combustion efficiency of a flare deteriorates. The vertical dotted line in Figure 3-10 marks the threshold

where all test runs with a ratio of  $NHV_{CZ}$  to  $NHV_{VG-LFL}$  greater than or equal to 10 achieved a combustion efficiency of 96.5 percent or greater. The vertical solid line in Figure 3-10 shows another threshold where most test runs with a ratio of  $NHV_{CZ}$  to  $NHV_{VG-LFL}$  greater than or equal to 6.5 achieved a combustion efficiency of 96.5 percent or greater. There are 12 test runs with a ratio of  $NHV_{CZ}$  to  $NHV_{VG-LFL}$  between 6.54 and 10.0 that did not achieve a combustion efficiency of 96.5 percent or greater. Eleven of these 12 runs are those listed in Table 3-2. This observation was to be expected since this ratio is mathematically equal to the inverse of the  $LFL_{CZ}$ ; however, this method has two more test runs (having a  $NHV_{CZ}$  to  $NHV_{VG-LFL}$  ratio greater than 6.54) that do not achieve a combustion efficiency of 96.5 percent or greater. Out of the 312 data points available for this analysis, 164 test runs achieved a combustion efficiency of 96.5 percent or greater; Figure 3-10 shows 61 of these runs (or 37%) have a  $NHV_{CZ}$  to  $NHV_{VG-LFL}$  ratio less than 6.54 and achieve greater than 96.5 percent combustion efficiency.

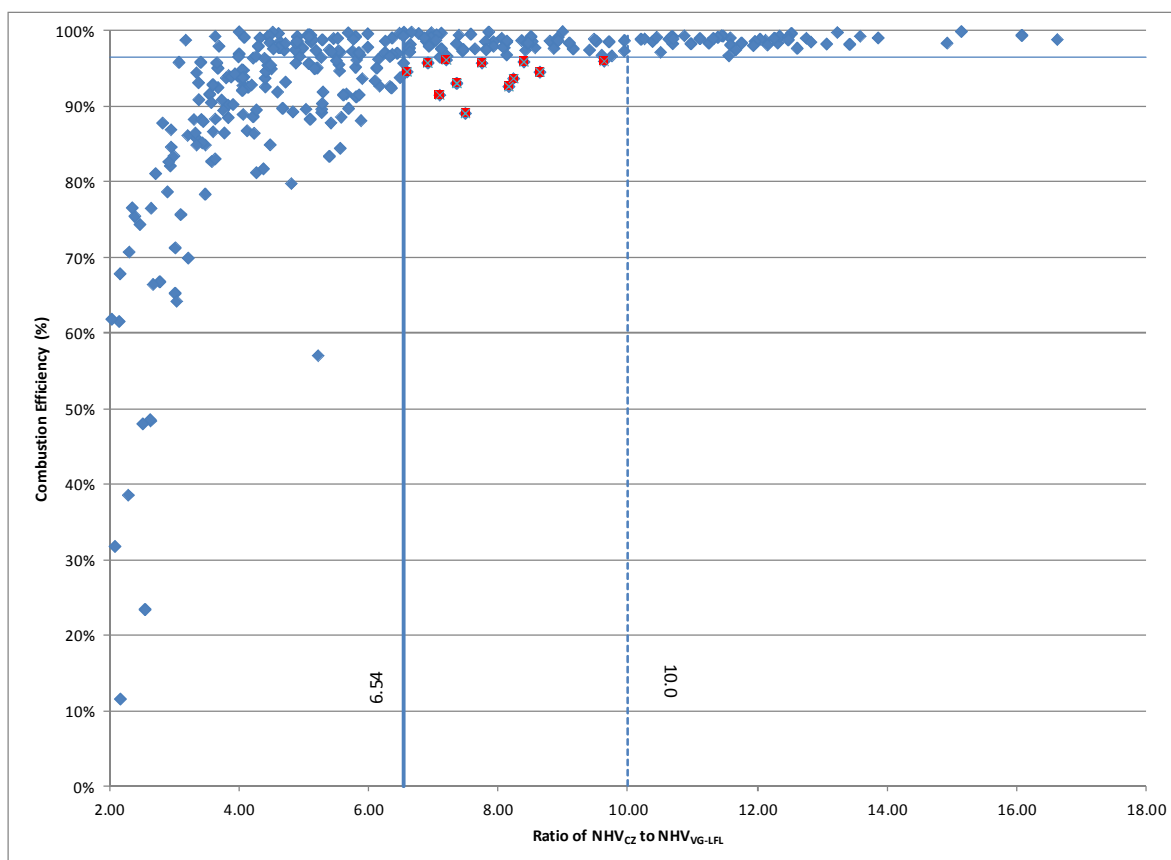


**Figure 3-10. Combustion Efficiency vs. Ratio of  $NHV_{CZ}$  to  $NHV_{VG-LFL}$**

Although the ratio of  $NHV_{CZ}$  to  $NHV_{VG-LFL}$  is mathematically equivalent to the inverse of the  $LFL_{CZ}$ , there are several test runs where differences are observed between the two parameters. Figure 3-11 is a log-log plot of  $LFL_{CZ}$  versus the ratio of  $NHV_{CZ}$  to  $NHV_{VG-LFL}$  for each of the 312 test runs. The data points marked in red have the greatest difference between the two parameters.

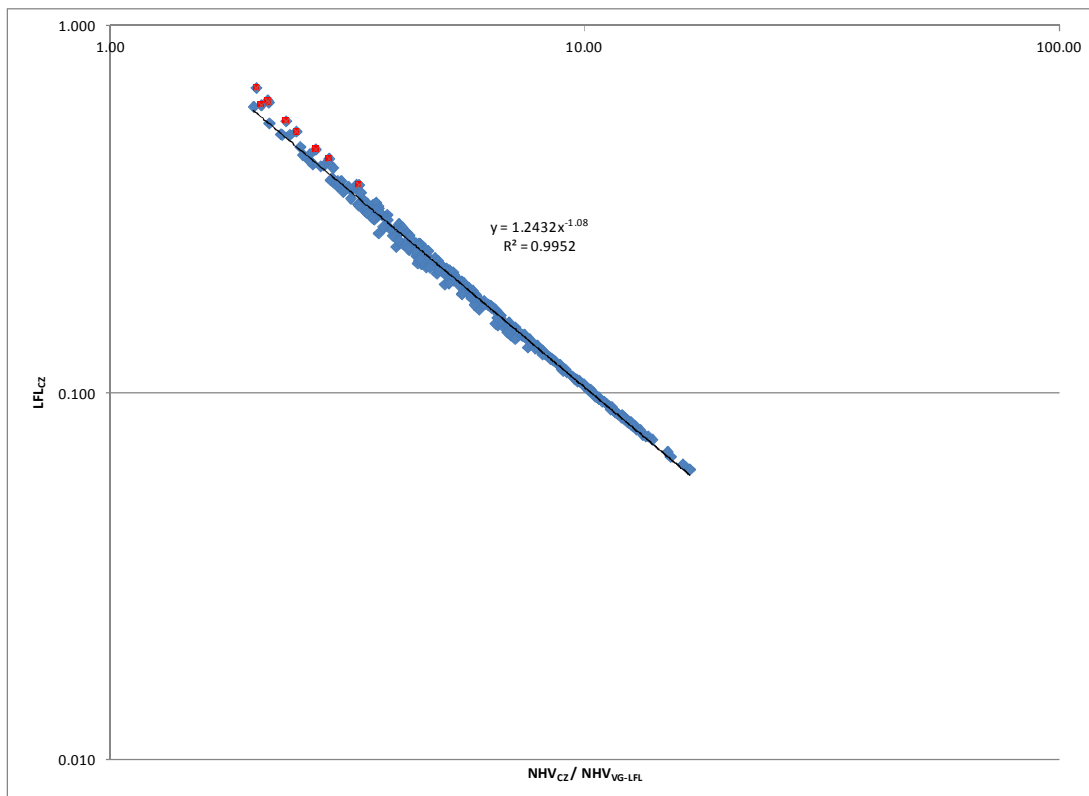


**Figure 3-11.  $LFL_{CZ}$  vs. Ratio of  $NHV_{CZ}$  to  $NHV_{VG-LFL}$**

One possible explanation for the observed differences between the two methods is the y-axis is a  $LFL_{CZ}$  value adjusted for nitrogen equivalency. A “nitrogen equivalency” adjustment was incorporated for determining the ratio of  $NHV_{CZ}$  to  $NHV_{VG-LFL}$ . However, because the procedure considers the LFL of the flare vent gas (as well as the  $NHV_{CZ}$ ) and not the actual LFL of the combustion zone gas, the adjustment is hardly noticeable. The adjustment applies to any water and carbon dioxide that is found in the flare vent gas (so it excludes the steam in the combustion zone). The data points marked in red have some of the greatest differences between the LFL not adjusted for nitrogen equivalency and the adjusted LFL. This means that these data

points had significant amounts of water and/or carbon dioxide in the combustion zone relative to nitrogen.

### **3.4 Other Operating Parameters Considered for Steam-Assisted Flares**

Numerous other operating parameters were examined to study the effects of steam on flare combustion efficiency; however, these did not prove as promising as the  $LFL_{CZ}$  operating parameter or ratio of  $NHV_{CZ}$  to  $NHV_{VG-LFL}$  when compared to the test data. A brief review of each of these parameters or concepts is provided in Sections 3.4.1 and 3.4.2.

#### **3.4.1 Net Heating Value**

The general provisions of 40 CFR 60.18(b) and 40 CFR 63.11(b) limit the net heating value of the gas being combusted in a steam-assisted flare (or air-assisted flare) to 300 Btu/scf or greater. Figure 3-12 graphs combustion efficiency versus net heating value of the flare vent gas ( $NHV_{VG}$ ) for the steam-assisted flares tested; it shows that poor combustion efficiency can occur with flare vent gases that have high heat content (greater than 300 Btu/scf — depicted by the vertical blue line) and good combustion may occur in flare vent gas with lower heat content.

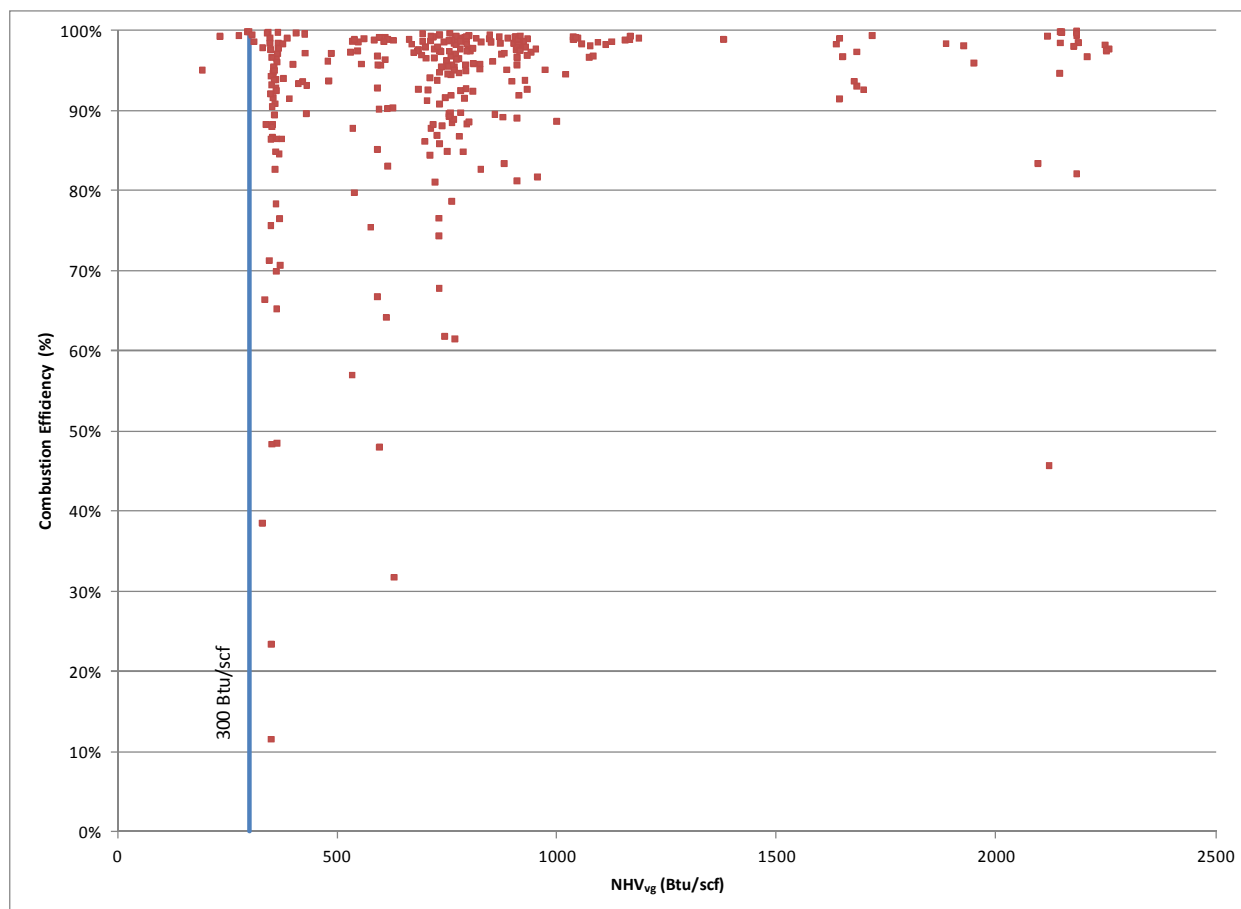


**Figure 3-12. Combustion Efficiency vs.  $NHV_{vg}$**

The figure shows a general trend, as the heat content increases, the combustion efficiency increases. However, there are a significant number of test runs with flare vent gas heat content much higher than 300 Btu/hr that do not achieve good combustion efficiency. Using the  $NHV_{vg}$  as an indicator of good combustion ignores any effect of steaming. Therefore, to incorporate steaming, a net heating value of the combustion zone gas was calculated to include the assist steam.

Figure 3-13 presents the combustion efficiency versus  $NHV_{CZ}$ . A much clearer trend forms when the steam is factored into the operating parameter; as the  $NHV_{CZ}$  increases, the combustion efficiency increases. For each test run, the  $NHV_{CZ}$  is a lower value than the  $NHV_{vg}$  shown in Figure 3-12 because the steam dilutes the gas mixture; each cubic foot of combustion zone gas has less heating value than a cubic foot of the flare vent gas.

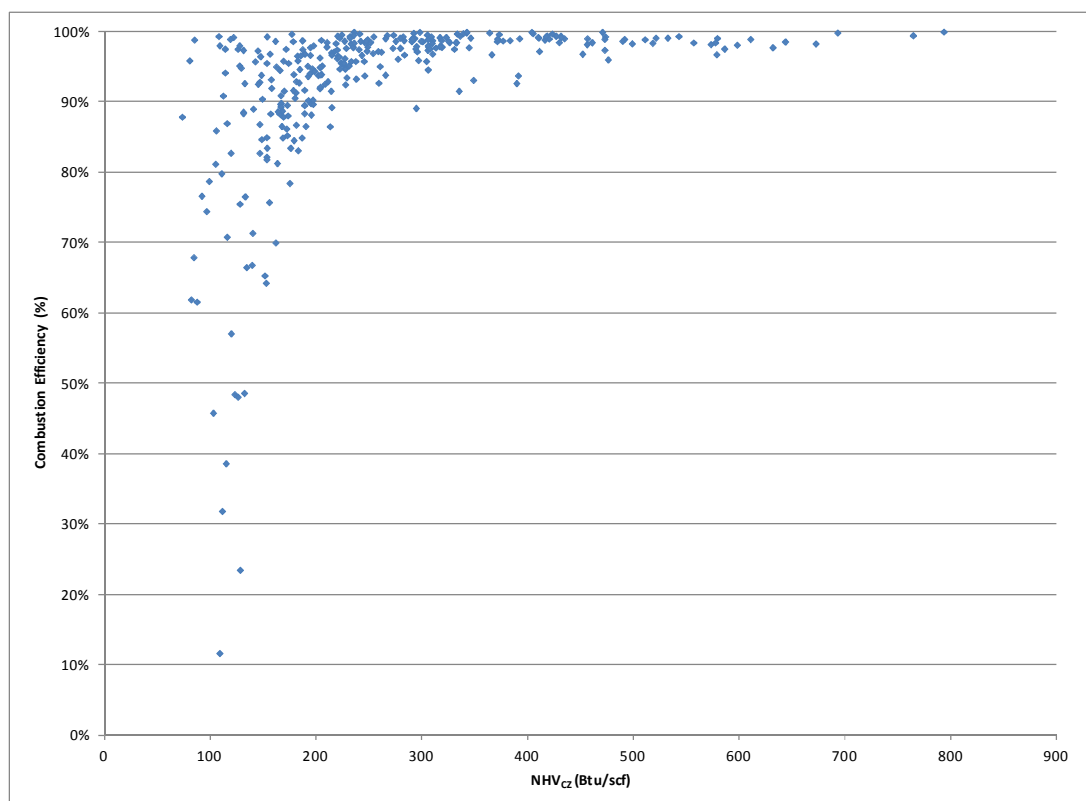


**Figure 3-13. Combustion Efficiency vs.  $NHV_{CZ}$**

If Figure 3-13 were used to determine appropriate operating conditions for flares, operators would need to maintain a  $NHV_{CZ}$  between approximately 300 and 350 Btu/scf to ensure good combustion. However, evident from Figure 3-13, there are a significant number of test runs that are showing good combustion, but have a  $NHV_{CZ}$  less than 300 Btu/scf. Out of the 312 data points available for this analysis, 164 test runs achieved a combustion efficiency of 96.5 percent or greater; 80 of these runs (or 49%) have a  $NHV_{CZ}$  less than 300 Btu/scf and achieve greater than 96.5 percent combustion efficiency.

In addition,  $NHV$  may not be the best operating parameter for determining flare performance because the net heating value of a mixture can vary significantly at certain constant lower flammability limits (and vice versa); Figure 3-14 shows this phenomenon. Figure 3-14 shows the  $NHV_{CZ}$  versus the  $LFL_{VG}$  of each test run. Based on Figure 3-14, for example, flare vent gas with a  $LFL$  of 0.04, may actually have a net heating value of anywhere between 500 Btu/scf and 2,000 Btu/scf; flare vent gas with a net heating value of 400 Btu/scf, may actually have a  $LFL$  of anywhere between 0.06 and 0.25. In fact, Azatyian, et al (2002) observes

the same relationship stating that “...in many cases, different gases, even with identical combustion heats and amounts of oxygen consumed per mole of fuel, differ essentially in concentration limits of flame propagation.” Azatyan supports this statement by providing an example of how ethylene and ethanol have similar heats of combustion (~1400 kJ/mol), but also have very different upper and lower flammability limits (ethylene: 32.0 to 3.1%; and ethanol: 19.0 to 4.3%).

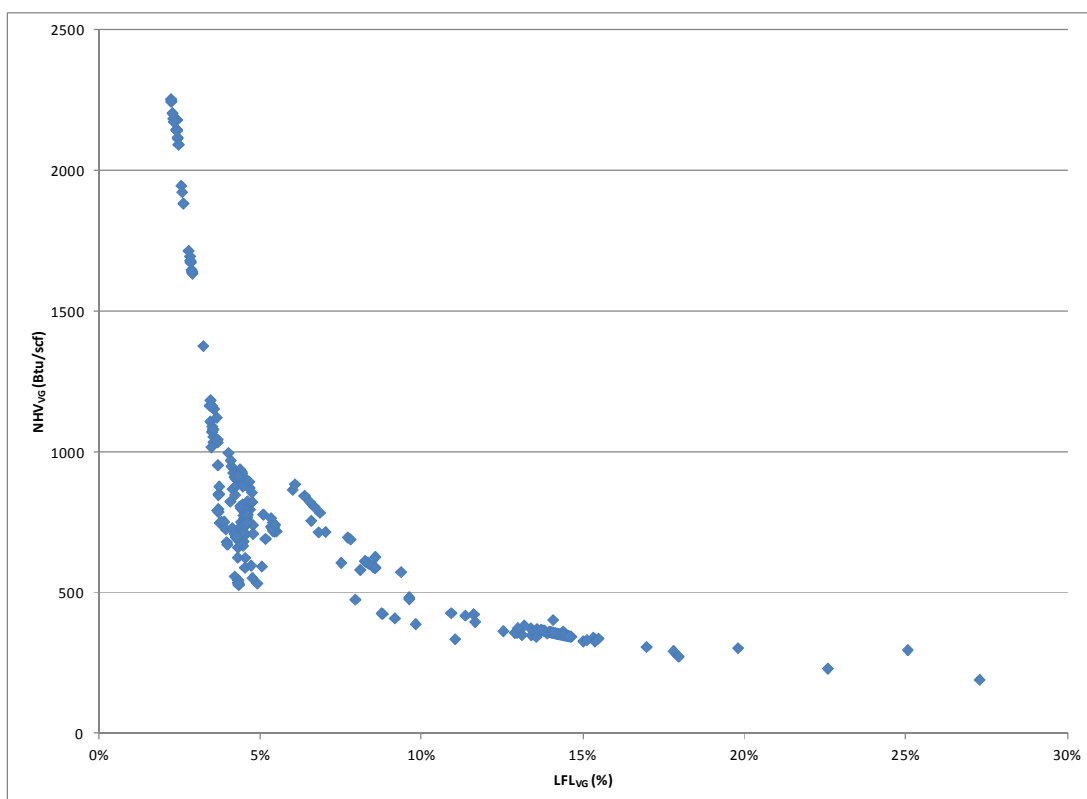
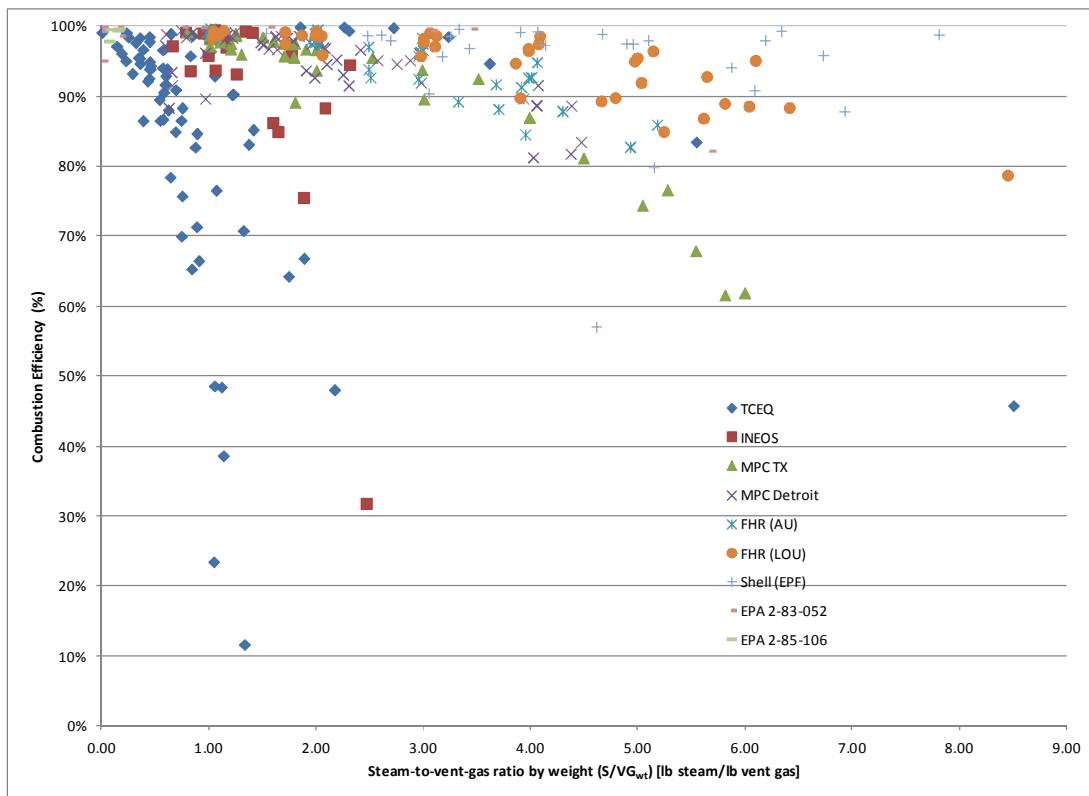


**Figure 3-14. NHV<sub>VG</sub> vs. LFL<sub>VG</sub>**

### 3.4.2 Steam Ratios

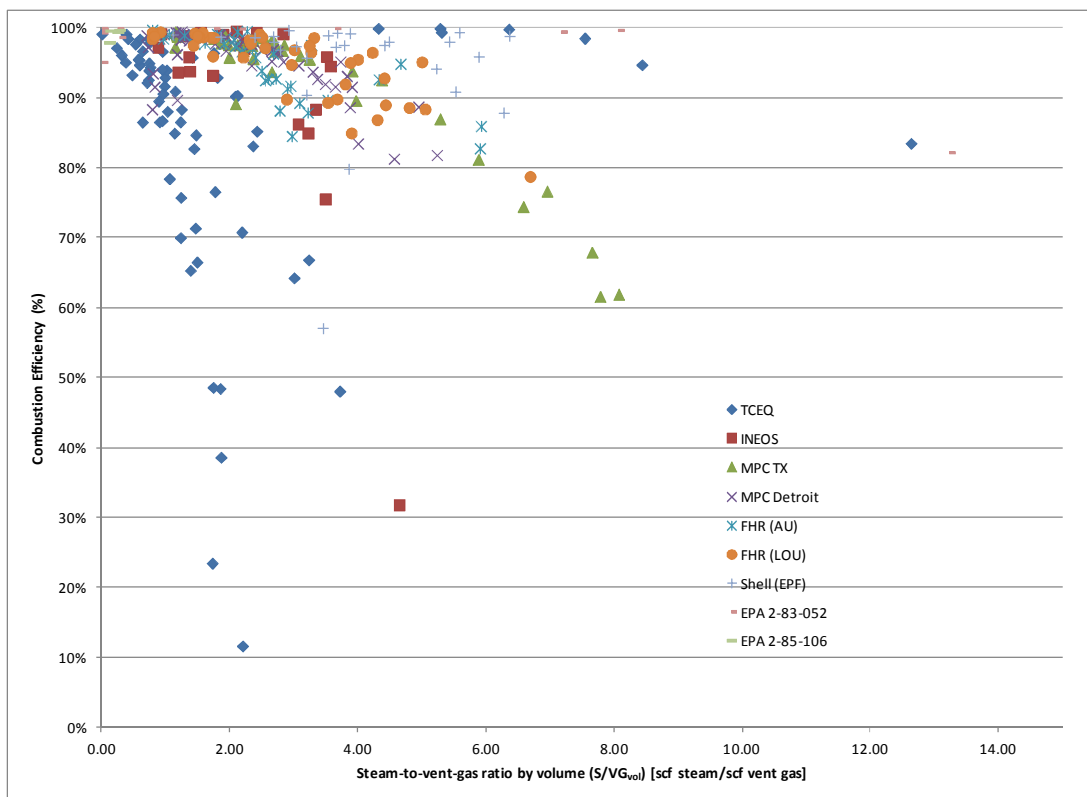
The amount of steam added to flares with respect to the amount of flare vent gas was considered as a possible flare operating condition. Figure 3-15 shows the relationship between combustion efficiency and actual steam-to-vent gas ratio (S/VG) by weight as it varied across the different data sets. In general, as the S/VG increases, the combustion efficiency deteriorates. However, there appears to be multiple trends that are defined by the different data sets and test run series within a data set. The MPC TX data show several data points above 90 percent

combustion efficiency until a S/VG of about 3 and then the combustion efficiency begins to decline more quickly with increasing S/VG. Many of the MPC-Detroit and FHR AU data points seem to follow this trend. The FHR LOU test runs seem to show an ability to accept more steam without adversely affecting the combustion efficiency, since a S/VG of 4 yields a 90 percent combustion efficiency for most test runs. The Shell, EPA, and some TCEQ data appear to follow the FHR LOU trend. Much of the TCEQ data; however, show a rapid degradation of combustion efficiency, dropping below 90 percent with S/VG greater than 0.5.



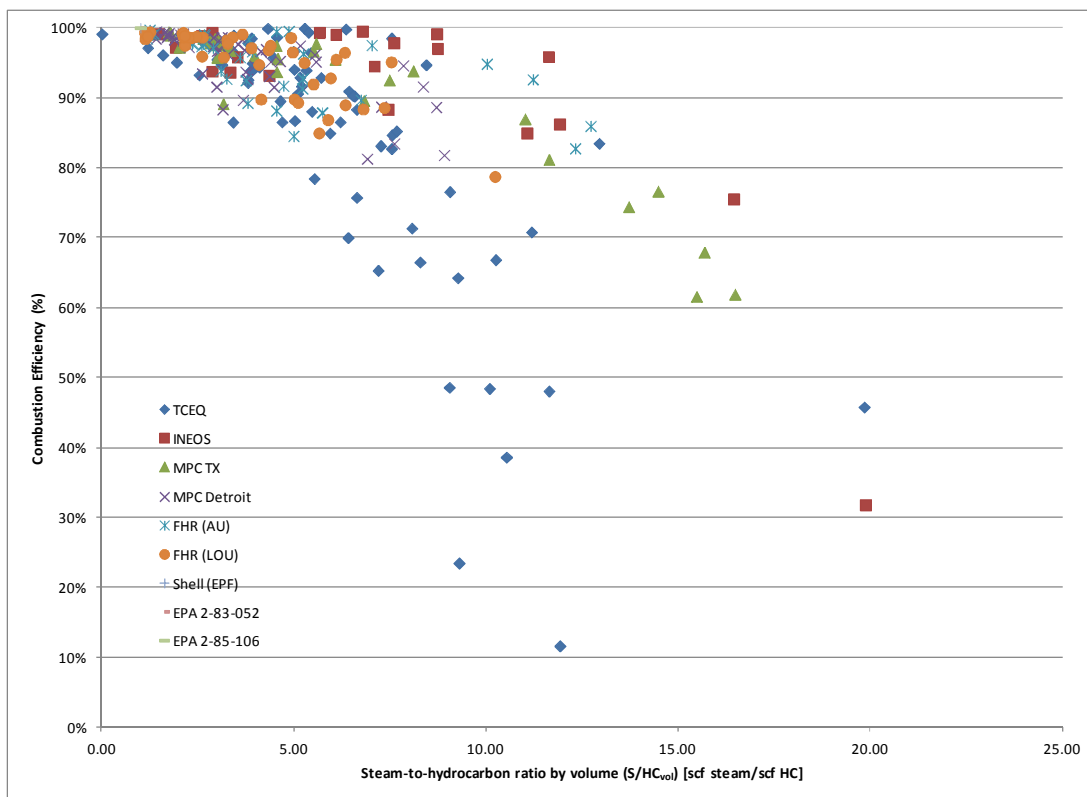
**Figure 3-15. Combustion Efficiency vs. S/VG by weight**

Figure 3-16 is a similar plot to Figure 3-15, except that it shows the S/VG by volume instead of by mass. Putting the steam ratio in units of volume consolidates the perceived trends. The MPC TX, MPC Detroit, FHR AU and FHR LOU test data seem to all follow the same general trend. The TCEQ, EPA, and some of the Shell and INEOS data points seem to define two additional trends; one of rapid decline in combustion efficiency with increasing S/VG by volume and one that is much slower.



**Figure 3-16. Combustion Efficiency vs. S/VG by volume**

Figure 3-17 presents the steam-to-hydrocarbon ratio (S/HC) by volume. This figure does seem to show further improvement in the variation between different data sets and test run series within a data set. However, this parameter does not take into account the amount of inert components in the flare vent gas.



**Figure 3-17. Combustion Efficiency vs. S/HC by volume**

The variation in trends in Figures 3-15 through 3-17 is likely due to the variation in flare vent gas components and compositions between each data set. For example, the TCEQ test data consists of flare vent gas streams of propylene or propane with nitrogen (and some natural gas used as a supplemental gas), while the INEOS tests were conducted with flare vent gas containing various mixtures of 1,3-butadiene, natural gas, and nitrogen. It appears that S/VG or S/HC alone cannot fully address over steaming because neither considers the variability of chemical properties within the flare vent gas. As discussed in Section 3.1, unlike S/VG or S/HC, the  $LFL_{CZ}$  is a good candidate for evaluating flare performance because it actually considers the variability of chemical properties.

Another parameter investigated was the ratio of actual total mass flow rate of steam to a recommended total mass flow rate of steam for a steam-assisted flare. This steam ratio parameter was based on Table 11 of the American Petroleum Institute (API) Standard 521 for pressure-relieving and depressuring systems. Table 11 of the API document suggests amounts of steam that should be injected into certain gases being flared in order to promote smokeless burning.

Because these steam recommendations in API 521 are intended for only smoke suppression, and not meant to be correlated to combustion efficiency performance, this steam ratio parameter was not investigated any further. In addition, the suggested injection steam rates are provided for only certain flared gases that are most common to petroleum and natural gas industries (they do not cover a complete list of the chemicals that may be flared).

## **4.0 AIR AND FLARE PERFORMANCE**

Similar to how steam is used (See Section 3.0 for steam discussion), air injection can promote smokeless burning in a flare. Air adds momentum and turbulence to the combustion zone, which improves mixing and reduces the possibility of smoke formation. Because the additional air is induced into the waste gas, it also provides oxygen necessary to augment smokeless capacity (Castiñeira and Edgar, 2006). However, just as in the use of steam, using too much air in a flare (excess aeration) can actually result in a flare operating outside its stable flame envelope, decreasing the combustion efficiency (Zeeco Company, 2003). Assist air can dilute the flare vent gas, making the flare vent gas too lean to burn in the combustion zone.

To identify excess aeration situations that may occur on air-assisted flares, the data suggest that the stoichiometric air ratio (SR) (the actual mass flow of assist air to the theoretical stoichiometric mass flow of air needed to combust the flare vent gas) is the most appropriate operating parameter. Specifically, the data suggest that, in order to maintain good combustion efficiency, the SR must be 7 or less for an air-assisted flare. Furthermore, the data suggest that the lower flammability limit of the flare vent gas ( $LFL_{VG}$ ) should be 15.3 percent by volume or less to ensure the flare vent gas being sent to the air-assisted flare is capable of adequately burning when introduced to enough air. This section documents the analysis supporting these observations. Note: the  $LFL_{VG}$  is different from the  $LFL_{CZ}$  described in Section 3.1.2 of this report because the  $LFL_{VG}$  does not consider any assist media; however, in general, the methodology described in Section 3.1.2 for determining LFL still applies.

### **4.1 Stoichiometric Air Ratio**

The stoichiometric air ratio (SR) is the ratio of actual mass flow of total assist air to the theoretical stoichiometric mass of air needed to combust the flare vent gas (this relationship is shown in Equation 4-1). The SR increases as more assist air is added to the flare vent gas.

$$SR = \frac{m_{Air}}{m_{Stoic}} \quad (\text{Eq. 4-1})$$

Where:

SR = Ratio of actual mass flow of total assist air to the theoretical stoichiometric mass of air needed to combust the flare vent gas, unitless.

$m_{\text{Air}}$  = Actual mass flow of total assist air, pounds per hour, lb/hr.

$m_{\text{Stoic}}$  = Theoretical stoichiometric mass of air needed to combust the flare vent gas, lb/hr.

For flares that utilize air as an assist medium, the stoichiometric amount of assist air ( $m_{\text{Stoic}}$ ) represents the theoretical amount of air needed to obtain complete combustion of a fuel gas comprised of combustible compounds. This stoichiometric amount is based on the specific chemical composition and quantity of the combustible compounds combusted in the flare. The stoichiometric amount of assist air needed is determined from only the combustible portion of the flare vent gas. While some flare vent gas streams may include non-combustible compounds, such as carbon dioxide or nitrogen, the determination of the stoichiometric air amount ignores the contributions of these compounds to the total flow and composition of the fuel gas stream.

The theoretical stoichiometric molar amount of air required for combustion varies between different combustible hydrocarbons, and can be determined by a balanced combustion reaction equation. Equations 4-2 and 4-3 below are balanced combustion reaction equations for methane and propane, respectively.



As seen in Equation 4-2, two moles of oxygen are required for the complete combustion of one mole of methane. Similarly, Equation 4-3 shows that five moles of oxygen are required to completely combust one mole of propane. Assuming ambient air contains approximately 21 percent oxygen, and using the molecular weight for methane, propane, and air, the stoichiometric ratio of air to fuel can be calculated as shown in Equation 4-4 for methane and Equation 4-5 for propane. For methane, the stoichiometric ratio of air to fuel is 17.1 pounds of air per pound of methane; and for propane, it is 15.6 pounds of air per pound of propane. These values are used with the actual amount of assist air and fuel to calculate the SR. All data sets and

the methodologies used in calculating the SR are outlined in Section 2.0, and Appendices C and D of this report.

$$\frac{2 \text{ mol } O_2}{1 \text{ mol } CH_4} \times \frac{1 \text{ mol air}}{0.21 \text{ mol } O_2} \times \frac{28.8 \text{ lb air}}{1 \text{ mol air}} \times \frac{1 \text{ mol } CH_4}{16 \text{ lb } CH_4} = \frac{17.1 \text{ lb air}}{1 \text{ lb } CH_4} \quad (\text{Eq. 4-4})$$

$$\frac{5 \text{ mol } O_2}{1 \text{ mol } C_3H_8} \times \frac{1 \text{ mol air}}{0.21 \text{ mol } O_2} \times \frac{28.8 \text{ lb air}}{1 \text{ mol air}} \times \frac{1 \text{ mol } C_3H_8}{44 \text{ lb } C_3H_8} = \frac{15.6 \text{ lb air}}{1 \text{ lb } C_3H_8} \quad (\text{Eq. 4-5})$$

## 4.2 TCEQ Test Data

The Texas Commission on Environmental Quality (TCEQ) 2010 flare study final report (Allen and Torres, 2010) examined the effects of SR on an air-assisted flare's combustion efficiency. The results of the TCEQ study show that, in general, as more assist air is added to the flare vent gas and the SR increases, the flare combustion efficiency deteriorates. Figure 4-1 plots 35 test runs from the TCEQ study that clearly shows this trend.

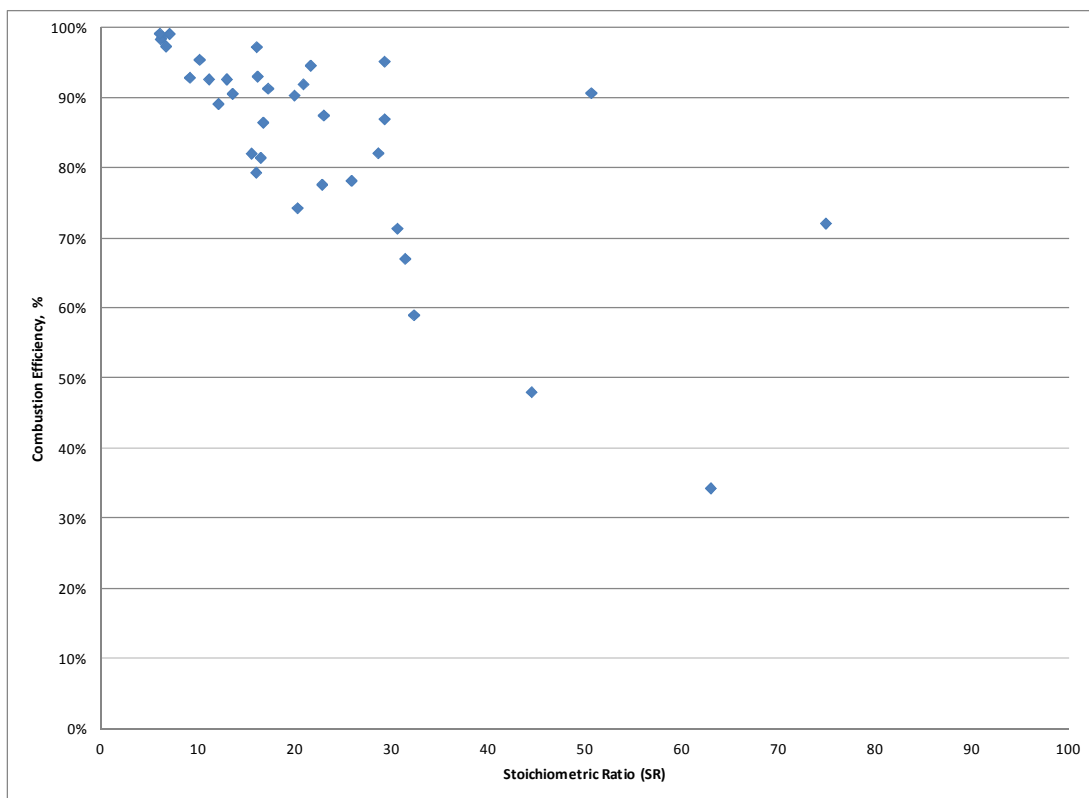
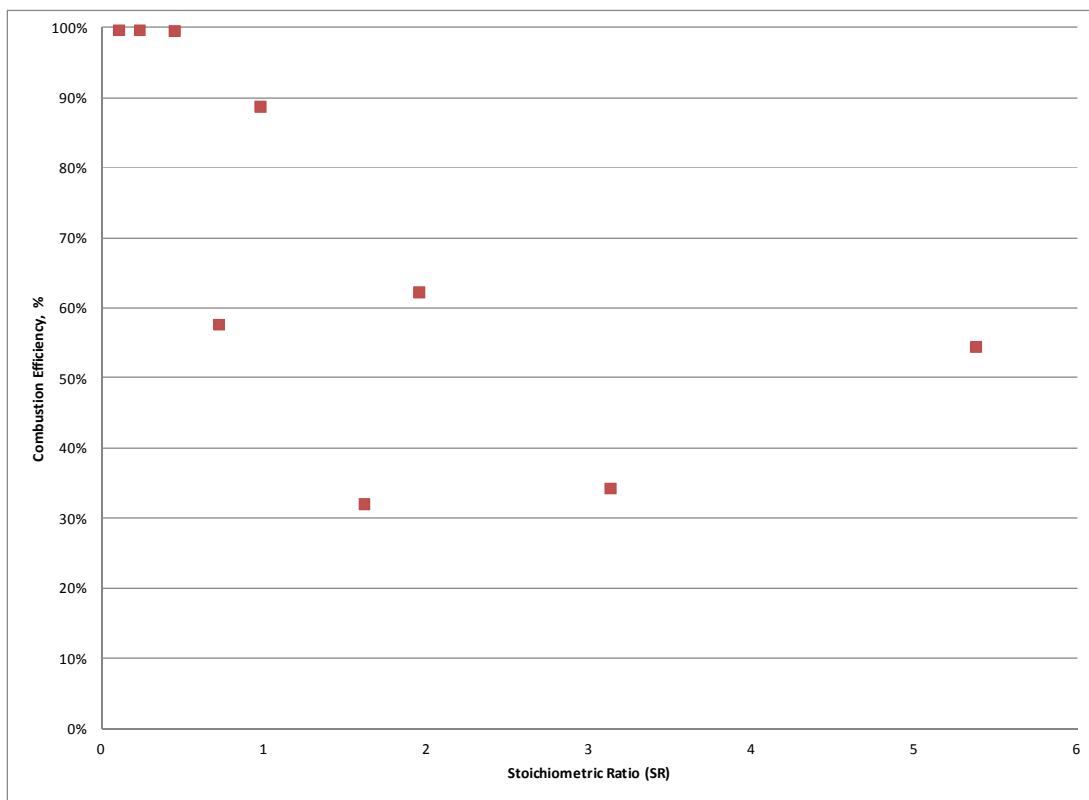


Figure 4-1. Combustion Efficiency vs. SR (using TCEQ data)

### 4.3 Other Test Data

The trend displayed in Figure 4-1 (as more assist air is added to the flare vent gas and the SR increases, the flare combustion efficiency deteriorates) also exists with the nine specific air-assist test runs extracted from the EPA-600/2-85-106 study (Pohl and Soelberg, 1985).

Figure 4-2 shows this trend. It was not possible to include, in Figure 4-2, the 13 air-assisted test runs extracted from the EPA-600/2-83-052 study (McDaniel, 1983) because the air flow and air flow velocity were considered proprietary information and not included in the test report.



**Figure 4-2. Combustion Efficiency vs. SR (using EPA-600/2-85-106 data)**

### 4.4 Analysis of Stoichiometric Air Ratio

Figure 4-3 overlays Figures 4-1 and 4-2. It shows that although the trend exists for both data sets, the threshold (or cliff) where combustion efficiency begins to deteriorate is much different between the two data sets. The two studies were reviewed carefully in an attempt to identify differences between the EPA-600/2-85-106 and TCEQ test runs. The test data from the EPA-600/2-85-106 study used mixtures of propane and nitrogen, while TCEQ used propylene or

propane with natural gas as a supplemental gas. The air-assisted flare from the EPA-600/2-85-106 study had a 1.5 inch diameter and the air-assisted flare from the TCEQ tests had a diameter of 24 inches. Most of the test runs from the EPA-600/2-85-106 study did not use a pilot during testing but the TCEQ testing did include pilots. In addition, the flare vent gas volumetric or mass flow rates for the EPA-600/2-85-106 test runs were not reported, so assumptions were made using the reported flare vent gas velocity to determine flow rates.

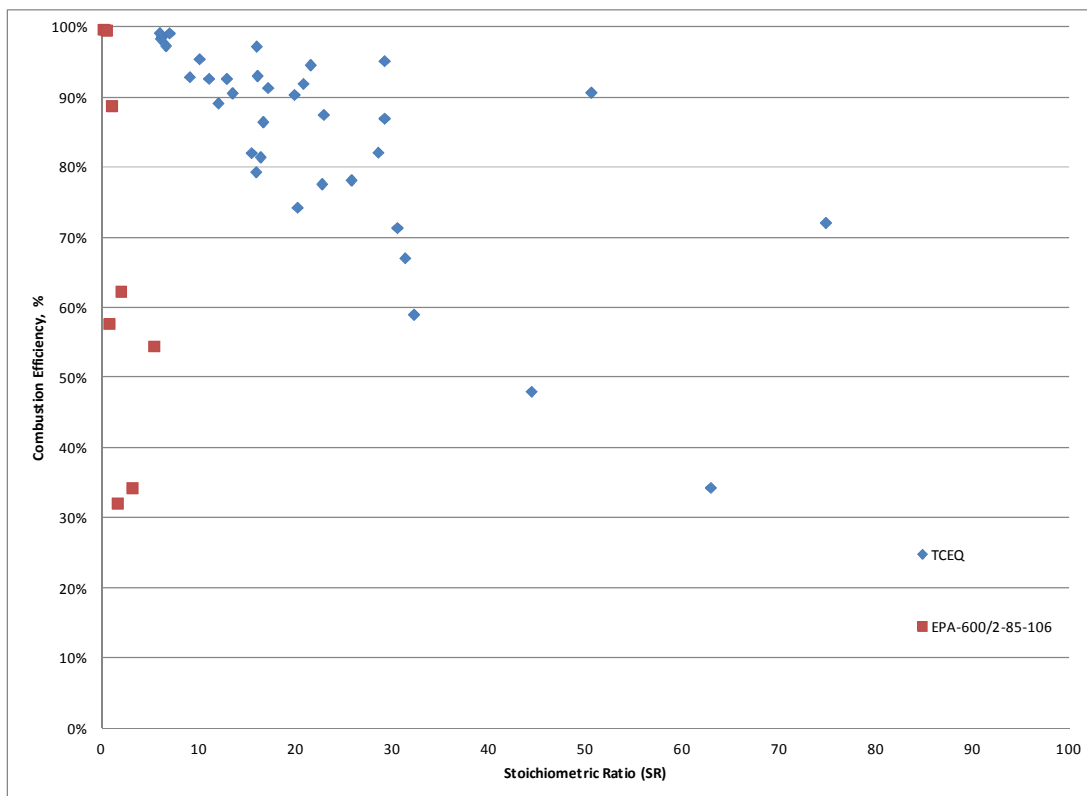


**Figure 4-3. Combustion Efficiency vs. SR (combined TCEQ and EPA-600/2-85-106 data)**

The EPA-600/2-85-106 test report noted that smaller flares did not produce data that were comparable to larger flares (greater than 3 inches). Gogolek et al. (2010b) supports this finding by concluding that results from pipe flares smaller than 3 inches are not scalable to larger diameter pipe flares (i.e., 6 to 12 inch diameter pipe flares). This conclusion seems logical with respect to all of the available air assist data, especially if the various sized flares are operated with similar SR values. There is less distance across the volumetric flare vent gas flow of a small flare at the tip exit than the distance across the volumetric flare vent gas flow of a larger flare at the tip exit; therefore, more assist air would penetrate and mix with the flare vent gas if a smaller

flare were used. Because of these differences between the EPA-600/2-85-106 and TCEQ test runs, the EPA-600/2-85-106 data were removed and only the TCEQ data were analyzed.

Figure 4-4 is the same as Figure 4-1, but with the axes narrowed to a shorter range. The vertical green line identifies the SR threshold where all test runs achieve a combustion efficiency of 96.5 percent or greater. (See Section 2.8 of this report for a discussion of why 96.5 percent was selected as a measure of good combustion efficiency for reviewing the flare test data.) This line shows a transition between good and poor combustion somewhere between a SR of 7.0 and 9.

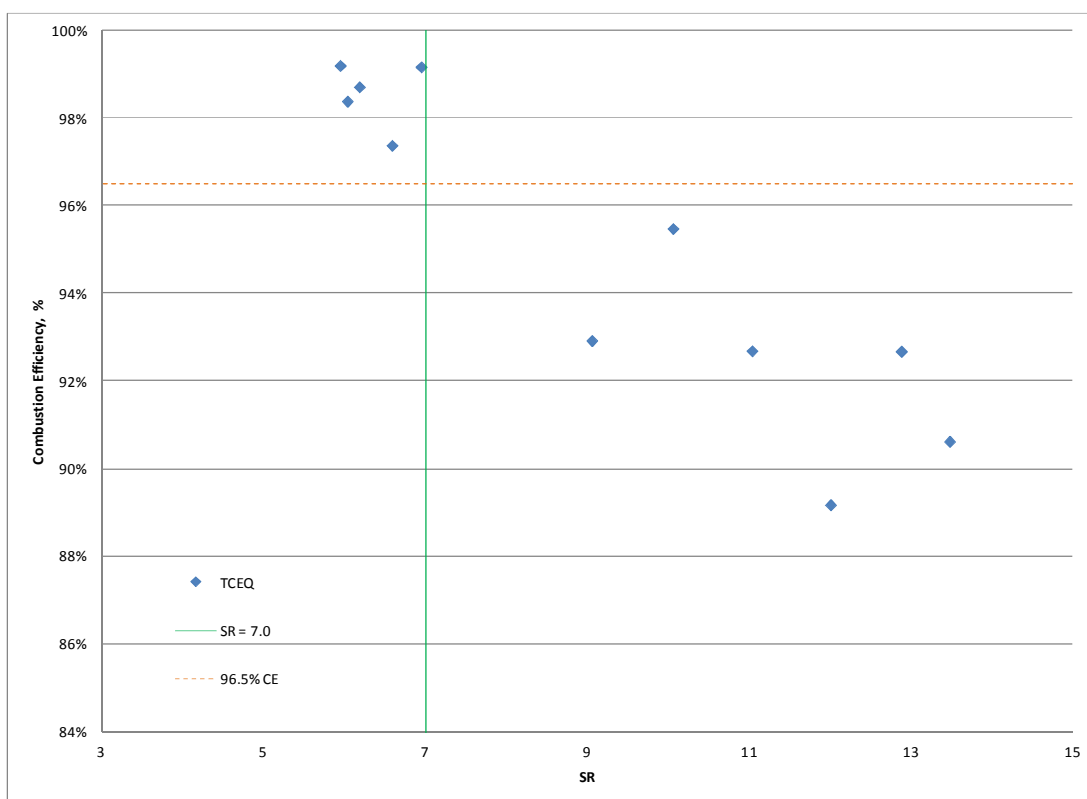


**Figure 4-4. Combustion Efficiency vs. SR, zoomed (using TCEQ data)**

Given the differences shown between the TCEQ and EPA-600/2-85-106 data sets (see Figure 4-3), we have concerns about the possible differences in SR threshold (transition between good and poor combustion) between typical commercial flare sizes. For example, is an SR value of 7.0 appropriate for a 54 inch flare? Although Gogolek et al. (2010b) concluded that results from flares smaller than 3 inches are not scalable to 6 to 12 inch diameter sized flares; the report does not determine whether 6 to 12 inch diameter sized flares are scalable to full-scale industrial

sized flares. The observed variation in SR thresholds between a 1.5 inch and 24 inch flare is not expected to be as exaggerated for typical commercial flare sizes. Given the steam-assisted flare data encompass flare tip sizes (in terms of the effective diameter of the flare tip) from 5.86 inch to 54 inches, and the apparent comparability of those results (see Section 3.0 of this report), it is likely that this issue is simply inherent with the much smaller flares (i.e., less than 3 inches).

For these reasons, the data suggest that a SR of 7.0 is the transition between good and poor combustion for air-assisted flares.

#### **4.5 Considering $LFL_{VG}$ for Air-Assisted Flares**

Operating a flare with a SR of 7.0 or less does not tell an owner or operator if there are enough combustible components in the combustion zone to burn adequately. If there are not enough combustible components in the combustion zone, then the flare vent gas will not burn, or will burn inadequately, resulting in lower combustion efficiency. Therefore, it is logical that an owner or operator should be conscious of whether the flare vent gas being sent through the air-assisted flare is capable of burning.

It seems reasonable to assume that the  $LFL_{CZ}$  analysis in Section 3.0 of this report could apply to an air-assisted flare. However, for an air-assisted flare, the “combustion zone gas” would simply reduce to the “flare vent gas” because air is the only assist media being added to the combustion zone of an air-assisted flare. As discussed in Section 3.0 of this report, for steam-assisted flares, the LFL is an indicator of how well a mixture can burn. For steam-assisted flares, the LFL in the combustion zone was used to incorporate the effect of the steam in the determination of the LFL; however for air-assisted flares, the mixture being introduced with air is contained in the flare vent gas. Although, there is air being added as an assist media, it is no different than the air in the atmosphere that the flare vent gas would be mixed with, except that the mixing is occurring much faster with air-assist. Therefore, for air-assisted flares, instead of using the term  $LFL_{CZ}$  as an indicator of how well a mixture can burn, we use the lower flammability limit of the flare vent gas ( $LFL_{VG}$ ).

An observation made regarding the EPA-600/2-85-106 and TCEQ air-assist data is that the  $LFL_{VG}$  for each of the 44 test runs (i.e., 35 TCEQ test runs and 9 EPA-600/2-85-106 test runs) is 15.0 percent by volume or less (when adjusted for nitrogen equivalency as described in Section 3.1.2 of this report), but only nine test runs achieved greater than 96.5 percent combustion efficiency. This means that each test run (using the 15.3%  $LFL_{CZ}$  threshold analysis provided in Section 3.0 of this report) had the capability of burning at high combustion efficiency, provided the mixture was not diluted with too much assist air (i.e., the SR was 7.0 or less). More details regarding the LFL are presented in Section 3.0 of this report; however, there is simply not enough air-assisted test data to determine whether a new  $LFL_{CZ}$  threshold would be warranted for air-assisted flares (i.e., a  $LFL_{VG}$  threshold different than 15.3 percent).

For these reasons, the data seem to suggest that, for an air-assisted flare, a  $LFL_{VG}$  (adjusted for nitrogen equivalency as described in Section 3.1.2 of this report) of 15.3 percent by volume or less also indicates that a mixture can combust and maintain a good combustion efficiency, assuming that the air-assist flow is not too high to deteriorate efficiency.

## **5.0 WIND AND FLARE PERFORMANCE**

The EPA Air Pollution Control Cost Manual - Sixth Edition (U.S. EPA, 2002) states that in most flares, combustion occurs by means of a diffusion flame. A diffusion flame is one in which air diffuses across the boundary of the fuel/combustion product stream toward the center of the fuel flow, forming an envelope of combustible gas mixture around a core of fuel gas. On ignition, this combustible gas mixture establishes a stable flame zone around the gas core above the flare tip. The inner gas core is heated by diffusion from the hot combustion products produced in the flame zone. Leahey et al. (2001) suggest that predicting the size (length, diameter, area, and volume) of a diffusion flame could be useful in estimating its combustion efficiency because as a flame size is reduced, less oxygen entrains into the flame. Leahey et al. (2001) also point out that if a flame's dimensions are dependent on meteorological variables (e.g., wind), a flame's combustion efficiency would also be dependent on meteorological variables (e.g., wind).

A high crosswind velocity can have a strong effect on the flare flame dimensions and shape. When the flame is bent over on the downwind side of a flare and is imbedded in the wake of the flare tip, it is said to be in a wake-dominated regime. Many experts believe a wake-dominated flame can lead to poor flare performance. The data suggest that flare performance is not significantly affected by crosswind velocities up to 22 miles per hour (mph). There are limited data for flares in winds greater than 22 mph. However, a wake-dominated flame in winds greater than 22 mph may affect flare performance. The data available indicate that the wake-dominated region begins at a momentum flux ratio (MFR) of 3 or greater. The MFR considers whether there is enough flare vent gas and center steam (if applicable) exit velocity (momentum) to offset crosswind velocity. Because wake-dominated flames can be identified visually, observations could be conducted to identify wake-dominated flames during crosswind velocities greater than 22 mph at the flare tip. This section documents the analysis supporting these observations.

## 5.1 Introduction

Smoot et al. (2009), who examined operating and design issues for pipe flares, provide an illustration on how flare performance is affected by crosswinds that shear the combustion zone. These researchers state that wind shortens the flame, causing soot formation on the downwind side of the flame. They also warn that high crosswinds can result in air egress into the flare tip, which creates internal burning and potential explosive conditions (Figure 5-1).

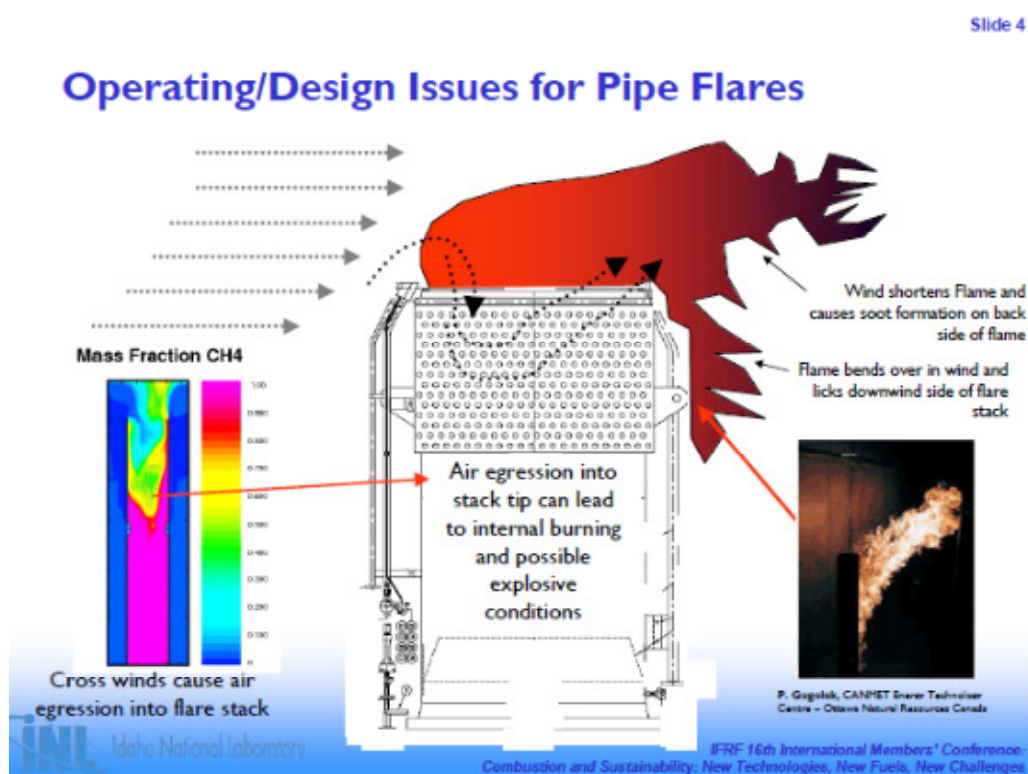


**Figure 5-1. Air Egression Into Flare Stack**  
Source: (Smoot et al., 2009)

## 5.2 Flare Flow Mixing Regimes

Depending on crosswind and flare tip velocity, the appearance of a flare flame can be quite different. In a report from a Joint International Combustion Symposium (Seebold et al., 2004), the authors summarize and provide images (Figure 5-2) of three flare flow mixing regimes: “wake-dominated”, “buoyancy-dominated”, or “inertia-dominated”. At low crosswind velocity and high flare tip velocity, the flare flame is generally inertia-dominated, with the flame

positioned directly above the jet stack and the flame curling straight upwards. In this case, the strength of the jet momentum flux in relation to the strength of the wind ensures a stable combustion zone and combustion efficiencies are invariably higher (Seebold et al., 2004).

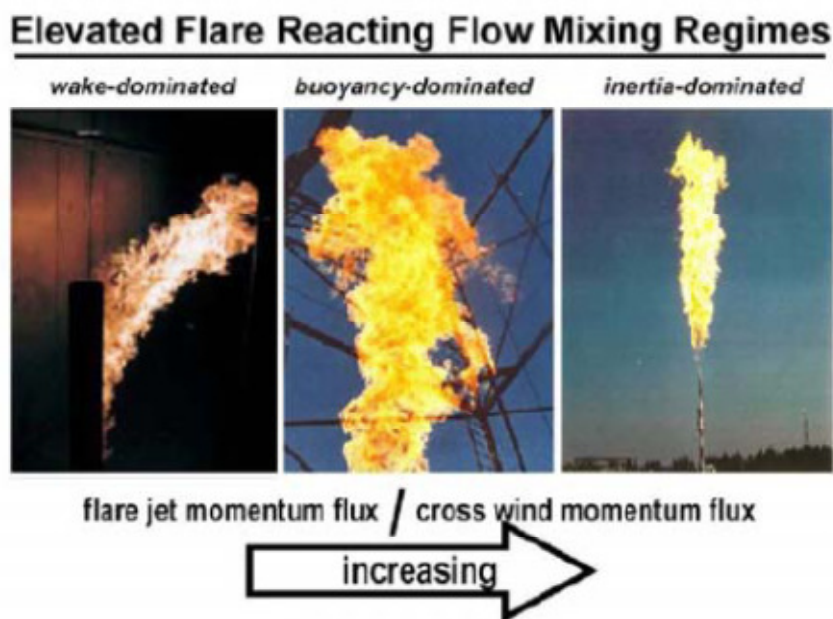


**Figure 5-2. Images of Flow Mixing Regimes**  
Source: (Seebold et al., 2004)

As crosswind velocities increase, “downwash” occurs as the flame lengthens horizontally and a portion of the combustion gases are drawn into the low pressure region on the downwind side of the stack (Johnson and Kostiuk, 2000). The flame zone diminishes into detached pockets of combustion interspersed beneath a non-reacting mixing layer containing unburned fuel (Johnson and Kostiuk, 2000; Johnson et al., 2001). In these high crosswind (and low flare vent gas velocity) situations, the flare flame is referred to as wake-dominated, which means the flame is bent over on the downwind side of a flare pipe and is imbedded in the wake of the flare tip (Figure 5-2), protected from the crosswind (Johnson et al., 2001). Under these conditions, the main tail of the flame may be extinguished, and the primary combustion zone occurs as a standing vortex on the downwind side of the stack (Johnson et al., 2001; Johnson and Kostiuk, 1999, 2000).

### 5.3 Efficiency Studies

Seebold et al. (2004) state that the wake-dominated mixing regime may lead to low combustion efficiency eddies. Several efficiency studies conducted at high crosswind velocities suggest that poor combustion efficiencies in wake-dominated flare flames result from fuel stripping where a portion of unburned fuel is stripped from the flame stream prior to reaching a flame zone (Johnson et al., 1999; Johnson and Kostiuk, 2000; Johnson et al., 2001; and Castiñeira and Edgar, 2006). The unburned fuel is primarily ejected into the underside of the flame. Johnston et al. (2001) provide a sketch of the unburned hydrocarbons detected downwind in a wake-dominated flare with a crosswind velocity of 8 meters/second (m/s) or about 18 mph (Figure 5-3).

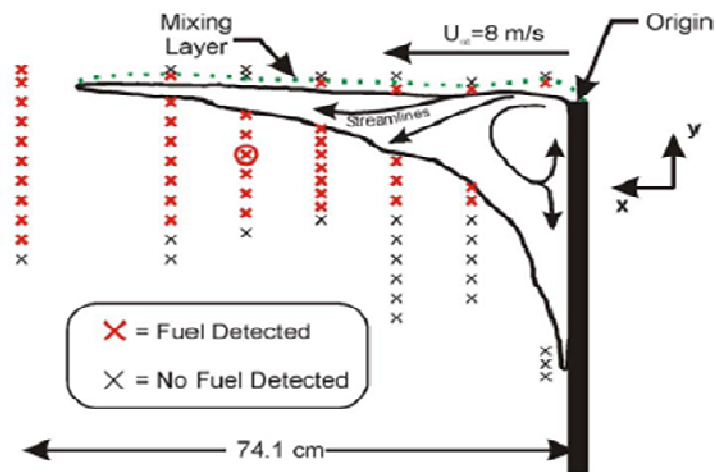


**Figure 5-3. Fuel Detection Downwind of Wake-Dominated Flare**  
Source: (Johnston et. al, 2001)

Researchers from the University of Alberta have published a series of studies that describe their investigations on the significance of wind on the fluid mechanics of a flare flame at low MFR (Bourguignon et al., 1999; Johnson et al., 1998, 1999a, 1999b, 2001; and Johnson and Kostiuk, 1999, 2000). The MFR is a measure of momentum strength of the flare vent gas relative to the crosswind (the product of flare vent gas density and velocity squared divided by the product of air density and crosswind velocity squared). The MFR at the flare tip can be calculated using Equation 5-1.

$$MFR = \frac{(\rho_{vgcs})(V_{tip})^2}{(\rho_{air})(V_{wind})^2} \quad (\text{Eq. 5-1})$$

Where:

MFR = Momentum flux ratio, unitless.

$\rho_{vgcs}$  = Density of flare vent gas including center steam if applicable, lb/scf.

$V_{tip}$  = Actual flare tip velocity (i.e., actual flare vent gas velocity plus center steam velocity, if applicable), ft/s. The flare tip velocity is dependent on how the unobstructed cross sectional area of the flare tip is calculated. John Zink provided details for determining the unobstructed cross sectional area of several flare tip designs (see Appendix I).

$\rho_{air}$  = Density of ambient air, lb/scf.

$V_{wind}$  = Crosswind velocity, ft/s.

The experiments in these studies were conducted on about a one-inch diameter simple pipe flare using a wind tunnel. The maximum crosswind velocity during these experiments was 31 mph. These studies concluded that increased crosswind velocity can adversely affect the combustion efficiency of a flare; while increased flare tip velocity makes the flame less susceptible to the effects of crosswind. One report (Johnson and Kostiuk, 2000) provides images (Figure 5-4) of the flame, showing that as MFR decreases, the combustion efficiency of the flame also decreases. Mathematical models presented by Castiñeira and Edgar (2006) determined similar results for about 0.5-inch diameter simple pipe flares. Further modeling (Castiñeira and Edgar, 2008) showed a simulated flame almost completely extinguished at crosswind velocities of 22 mph.

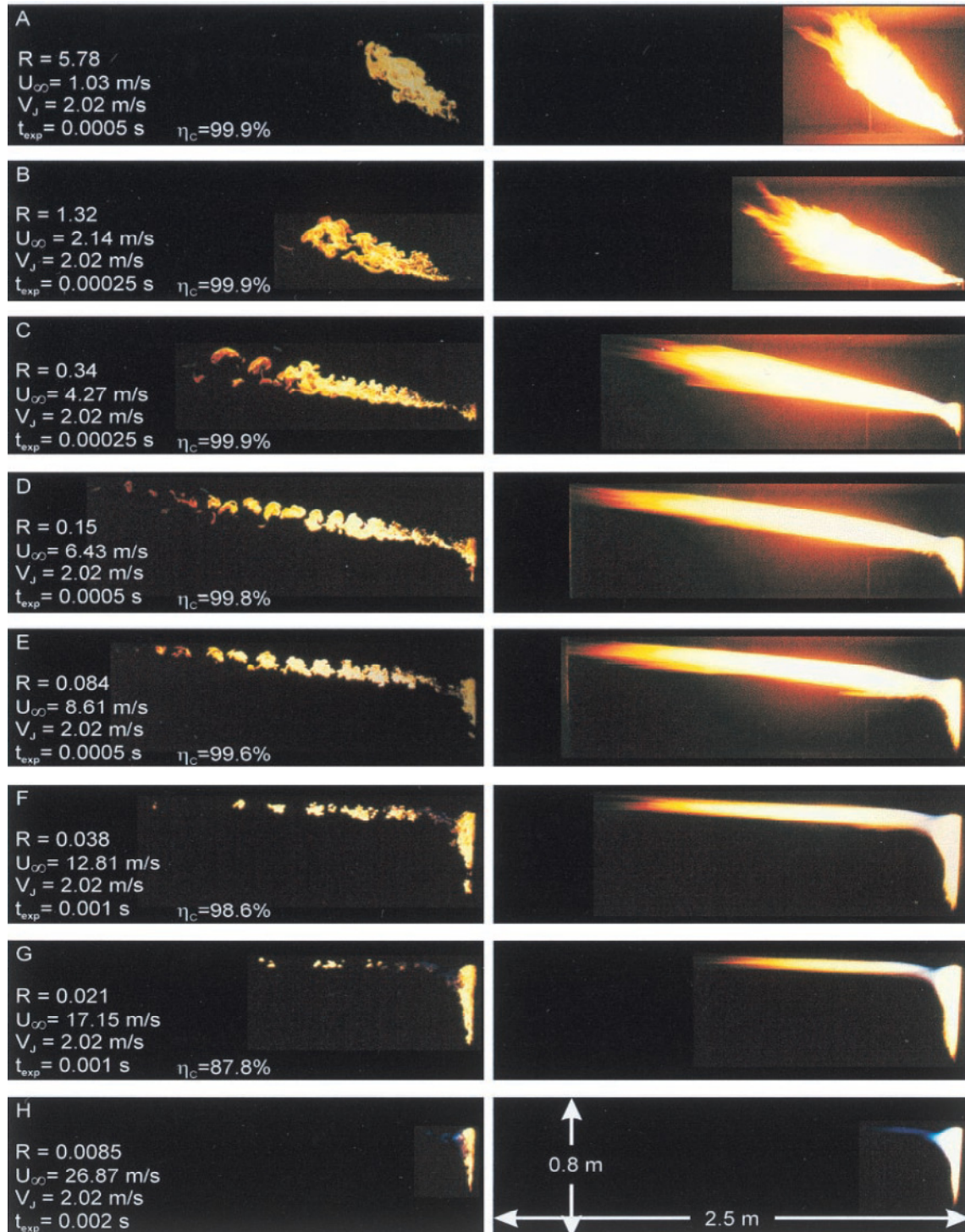


**Figure 5-4. Flame Images Relating to Momentum Flux Ratio and Combustion Efficiency**  
**Source: (Johnson and Kostiuik, 2000)<sup>1</sup>**

<sup>1</sup> Images from a one-inch diameter simple pipe flare using a wind tunnel. The “R” term is MFR, the “ $\eta_c$ ” term is the combustion efficiency of the flame, the “U” term is crosswind velocity, and the “V<sub>j</sub>” term is flare tip velocity.

Seebold et al. (2004) present a graph (Figure 5-5) that shows a potentially strong correlation between combustion efficiency and MFR, revealing that as the MFR falls below 0.1, the combustion efficiency decreases significantly (for some data). However, we are not able to confirm the source of this data or anything about these test runs. Because the reference that Seebold et al. (2004) provide (shown in the reproduced Figure 5-5 as “Reaction Efficiency of Industrial Flares – The Perspective of the Past.” September 2003) does not contain details about how Figure 5-5 was created, we have not used Figure 5-5 in our analysis.

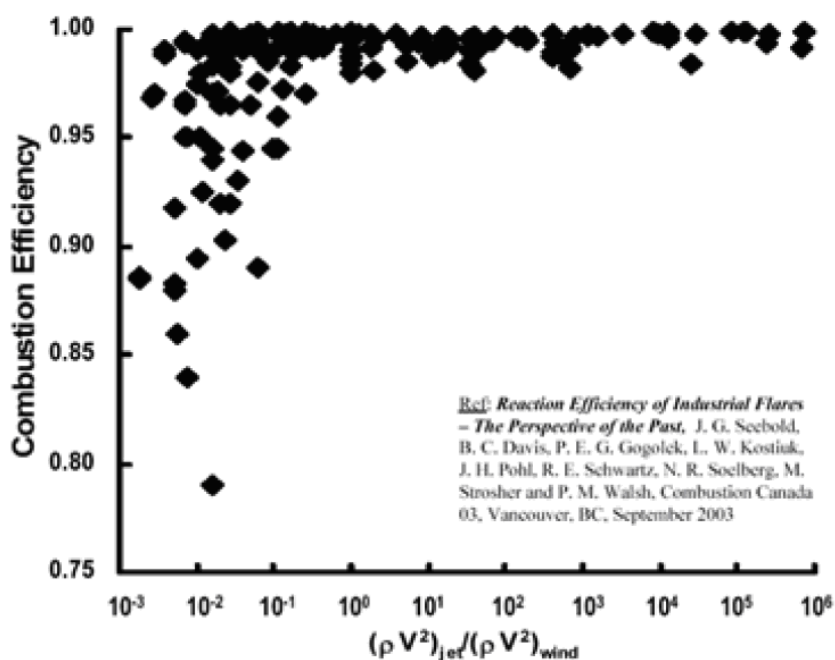


**Figure 5-5. Combustion Efficiency vs. Momentum Flux Ratio, Seebold Data**  
**Source: (Seebold et al., 2004)**

Gogolek et al. (2010b) investigated the transition from a vertical jet flame to a wake-dominated flame by performing tests on a 2 inch and 3 inch flare tip (and also on a 3 inch flare tip that had a flame retention ring). Gogolek et al. (2010b) determined visually that the transition to a wake-dominated flame occurred at a MFR of around 3 for all three pipes tested. However, the study also revealed that there is no sharp change in flare performance with the establishment of the wake-dominated flame. Additionally, Gogolek et al. (2010b) found that two sets of operating conditions with the same MFR produce drastically different flare performance (one with high crosswind and moderate flare tip velocity, and another with moderate crosswind

and low flare tip velocity), indicating that MFR may have limitations for correlating the performance of flares. The study concluded that a decrease in combustion efficiency is more likely to occur when the transition to a wake-dominated flame is caused by an increase in crosswind velocity rather than by a reduction in flare tip velocity.

In lieu of the MFR, other parameters such as a plume buoyancy factor or a power factor may be considered. It was through the research performed by the University of Alberta (Bourguignon et al., 1999; Johnson et al., 1998, 1999a, 1999b, 2001; and Johnson and Kostiuk, 1999, 2000) that these parameters were developed. Gogolek et al. (2010a) summarize the methodologies for determining a plume buoyancy factor or power factor. The plume buoyancy factor is calculated using Equation 5-2; and it considers crosswind velocity and actual flare vent gas velocity plus center steam velocity. The power factor is calculated using Equation 5-3; it is the ratio of the power of the crosswind to the power of combustion of the flare vent gas. (See Gogolek et al. (2010a) for further detail on these two parameters.) Center steam should be incorporated into the flare vent gas properties because center steam adds momentum (i.e., center steam exits the flare tip in the same direction as the flare vent gas).

$$BP = \frac{V_{wind}}{(g * D_p * V_{tip})^{1/3}} \quad (\text{Eq. 5-2})$$

Where:

- BP = Plume buoyancy factor, unitless.
- $V_{wind}$  = Average cross-sectional wind velocity, ft/s.
- g = Acceleration due to gravity, ft/s<sup>2</sup>.
- $D_p$  = Effective diameter of flare pipe, ft.
- $V_{tip}$  = Actual flare tip velocity (i.e., actual flare vent gas velocity plus center steam velocity, if applicable), ft/s. The flare tip velocity is dependent on how the unobstructed cross sectional area of the flare tip is calculated. John Zink provided details for determining the unobstructed cross sectional area of several flare tip designs (see Appendix I).

$$PF = \left( \frac{\rho_a * V_{wind} * D_p^2}{\rho_f * A_p * V_{tip} * LHV_m} \right)^{1/3} \quad (\text{Eq. 5-3})$$

Where:

- PF = Power factor, unitless.
- $\rho_a$  = Density of air, lb/scf.
- $V_{wind}$  = Average cross-sectional wind velocity, ft/s.
- $D_p$  = Effective diameter of flare pipe, ft.
- $\rho_f$  = Density of flare vent gas including center steam, lb/scf.
- $A_p$  = Unobstructed cross sectional area of the flare tip, ft<sup>2</sup>. John Zink provided details for determining the unobstructed cross sectional area of some of several flare tip designs (see Appendix I).
- $V_{tip}$  = Actual flare tip velocity (i.e., actual flare vent gas velocity plus center steam velocity, if applicable), ft/s. The flare tip velocity is dependent on how the unobstructed cross sectional area of the flare tip is calculated (See Appendix I).
- $LHV_m$  = Lower heating value (mass basis) of flare vent gas including center steam, Btu/scf.

Gogolek et al. (2010b) tested the power factor using natural gas on 3, 4, and 6 inch flare tips, and concluded that the power factor appears to be a useful dimensionless parameter for correlating flare performance data. However, Gogolek et al. (2010b) conclude that the power factor would have to be augmented to correlate performance of different flare vent gas mixtures. Gogolek et al. (2010b) also indicates that crosswind velocity thresholds for indicating good combustion efficiency may differ depending on the composition of the flare vent gas. The study concluded (based on tests using 3" flare retention ring flare tips) that destruction efficiency remains better than 98 percent for ethylene at crosswind velocities tested up to 24.6 mph; but fall below 98 percent at crosswind velocities of 17.9 mph for propylene. The study also reports that destruction efficiency remained above 97 percent for all crosswind velocities tested for propylene. These tests using 3" flare retention ring flare tips produced results similar to the 2" pipe flare, which are not scalable to industrial sized flares. All tests conducted by Gogolek et al. (2010b) on the flares found to be scalable to industrial sized flares (i.e., 3", 4", and 6" pipe flares, and 6" with flame retention rings) showed combustion efficiencies greater than 96.5 percent for all fuels tested for winds of 22 mph and less.

Gogolek et al. (2010b) incorporate a "fuel factor" into their analysis as an attempt to incorporate the effects of flare gas combustion properties, wind speed, and flare vent gas flow

rate; however, the “fuel factor” uses the upper flammability limit (UFL), which is difficult to calculate for mixtures, especially ones with inert. Also, Gogolek et al. (2010b) report that the “fuel factor” did not correlate well when flaring natural gas; and provide an explanation that the “fuel factor” does not consider the reaction kinetics of combustible mixtures.

Excluding the data shown in Figure 5-5 (because flare size is unknown for this data) as well as Gogolek’s et al. (2010b) power factor analysis, all of the studies mentioned in this section (i.e., Section 5.3 of this report) were conducted on 3 inch flare tips and smaller, which are not of typical size for an industrial flare. Gogolek et al. (2010b) states that results of pipes smaller than 3 inch do not scale-up to larger pipes; and it has not been determined whether results for 3 inch to 6 inch pipes can successfully be applied to full-scale industrial flares. However, it does appear crosswind velocity influences the size of a diffusion flame (e.g., length, diameter, area, and volume) and should be considered in flare performance no matter the size of a flare tip. It seems reasonable to assume that combustion efficiency of an industrial sized flare will also likely be sensitive to crosswind velocity.

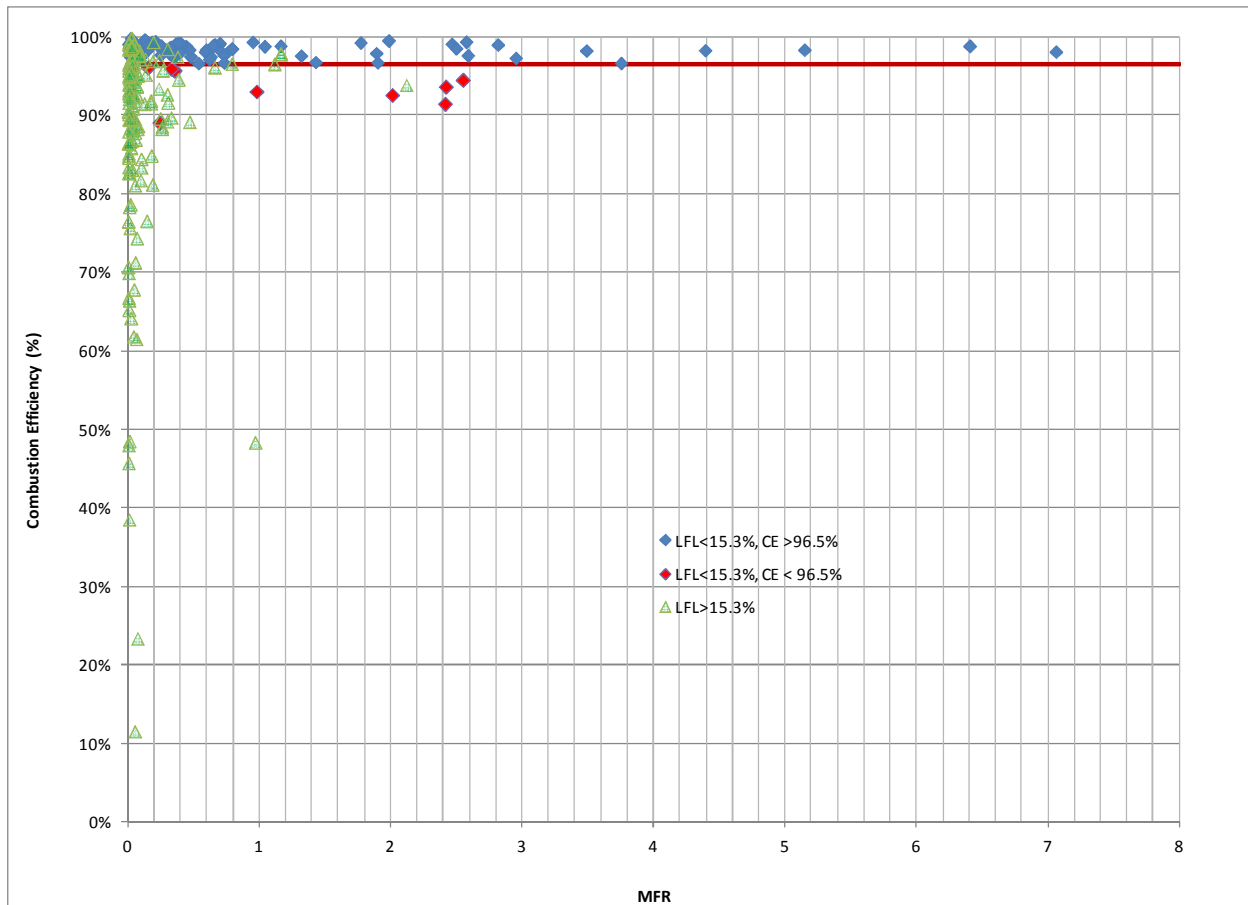
#### **5.4 Test Data Analysis**

Although Gogolek et al. (2010b) indicates that MFR may have limitations for correlating the performance of flares, we reviewed available MFR data as provided in raw test data spreadsheets for 245 steam-assisted flare test runs from five of the eight studies discussed in Section 2 of this report (i.e., TCEQ, MPC TX City, MPC Detroit, FHR AU, and FHR LOU). Unfortunately, the data provided in these reports were not used consistently to calculate MFR (i.e., some reports incorporated total assist steam, while others only center steam when using an actual flare tip velocity in their MFR methodology). Therefore, we recalculated MFR for all available test runs to incorporate only the center steam volume into the flare vent gas exit velocity because it exits the flare tip in the same direction as the flare vent gas. Steam and/or air nozzles associated with the upper and lower ring locations were not incorporated into the flare vent gas exit velocity when calculating MFR because it is less clear whether steam contribution from these nozzles should be included. Steam velocity and nozzle angle for upper and lower ring locations was not available for all of the test reports. Upper and lower ring nozzles are generally

directed up at about 30 to 45 degrees from horizontal (jetting into but also in the direction of the flare vent gas momentum), so only a portion of steam from upper and lower ring nozzles could enhance the momentum of the flare vent gas flow.

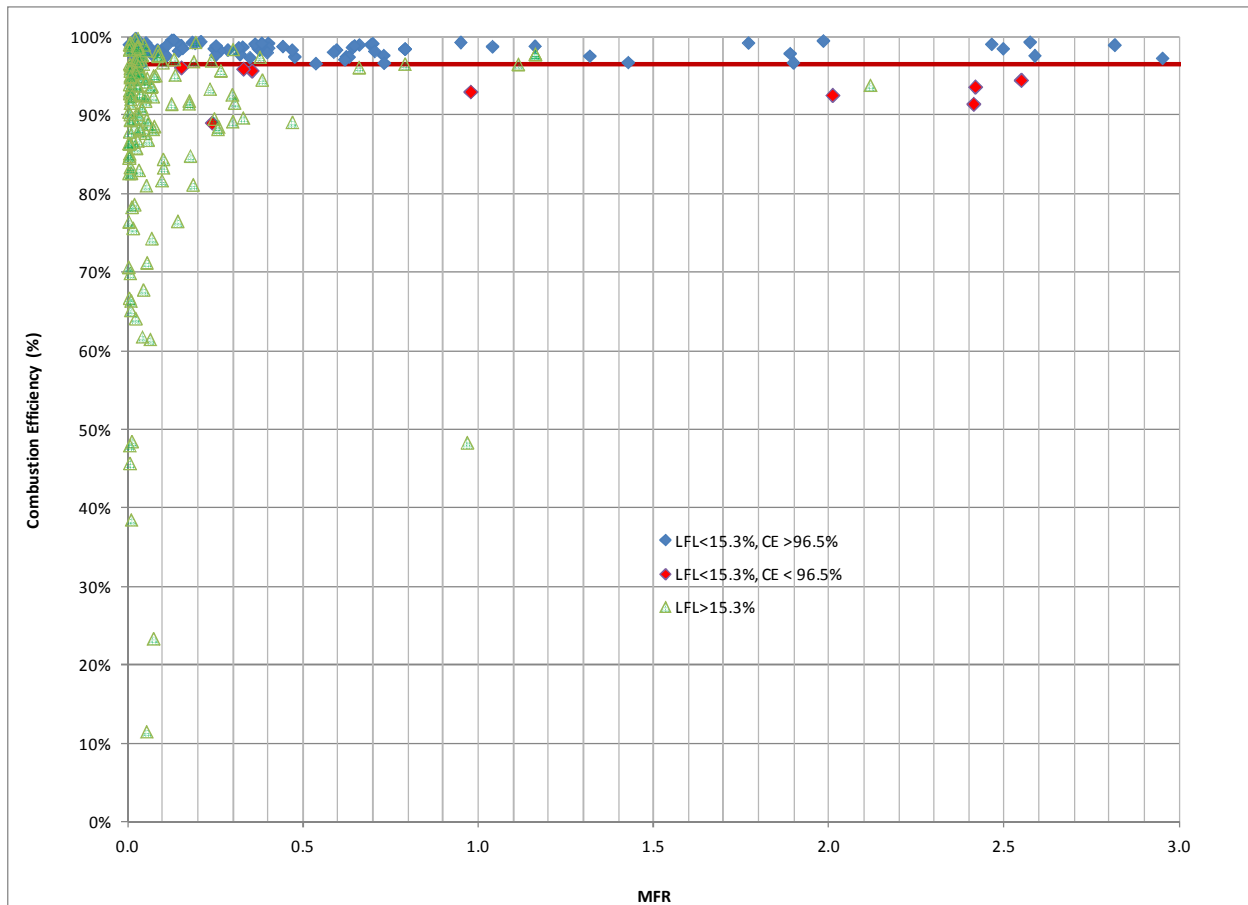
These test data represent 245 test runs with flare tip velocities (including center steam velocity) of less than 9 feet per second (ft/s) and wind speeds typically below 12 mph (approximately 20% of the test runs were performed in wind speeds above 12 mph; and no test runs were performed in winds any higher than 22 mph). Most of these test runs inevitably have low MFR values because the runs were performed at relatively low flare tip velocities. Nevertheless, the MFR from these test runs was plotted against the combustion efficiency to investigate whether a trend was discernable (Figures 5-6 and 5-7).

In general, Figure 5-6 shows that all runs were tested at a MFR less than about 7.0. However, it is assumed that most of these data (149 steam-assisted test runs) had poor flammability characteristics because the  $LFL_{CZ}$  for these test runs was greater than 15.3 percent by volume (see Section 3.0 of this report for an explanation of this  $LFL_{CZ}$  level). Also, there are 10 test runs highlighted in red in Figure 5-6 that had a  $LFL_{CZ}$  less than 15.3 percent by volume and did not achieve a combustion efficiency of 96.5 percent or greater. The poor combustion efficiency reported for these 10 test runs are discussed in Section 3.1.3 of this report.



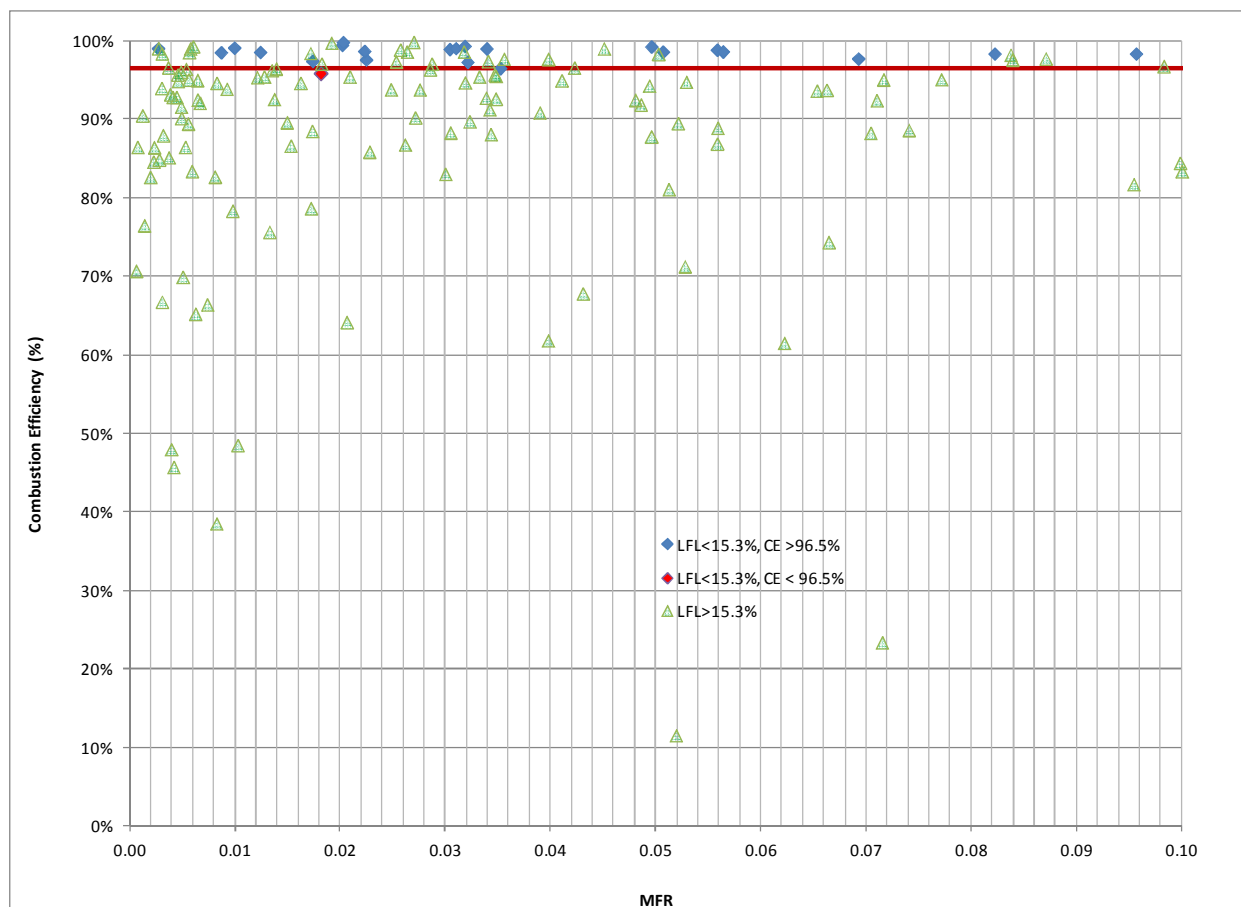
**Figure 5-6. Combustion Efficiency vs. Momentum Flux Ratio**

Figure 5-7 presents a subset of the data in Figure 5-6—those with MFR values less than 3.0—because Gogolek et al. (2010b) suggests that a MFR of 3.0 is the observed boundary for the transition to the wake-dominated mixing regime.



**Figure 5-7. Combustion Efficiency vs. Momentum Flux Ratio, zoomed (MFR < 3.0; wake-dominated mixing regime)**

These plots indicate that good flare performance can exist in a wake-dominated mixing regime. However, it is difficult to establish a MFR limit to define a wake-dominated regime with good combustion efficiency because it is not clear from these plots whether low MFR, high  $LFL_{CZ}$ , or some combination of both contribute to poor flare performance. Also, the available test data represent only a narrow range of wind and flare vent gas velocities (primarily <12 mph and <8 ft/s, respectively). For example, although the test data show that good flare performance can occur at a MFR as low as 0.003 (identified on Figure 5-8 with solid blue vertical line), this conclusion is based on only a single data point.



**Figure 5-8. Combustion Efficiency vs. Momentum Flux Ratio, further zoomed (MFR < 0.1)**

The test runs shown in Figures 5-6 through 5-8 are of moderate crosswind and low flare tip velocity. It appears that the data confirms what Gogolek et al. (2010b) observed which was that low MFRs created because of the low flare tip velocity (and less so because of higher crosswind) do not have the degraded combustion efficiency that low MFRs created by high crosswind (and less so because of low flare tip velocity) show. In other words, in the absence of higher crosswind velocities, a lower MFR does not necessarily indicate poor flare performance. Because we do not have test data of crosswind speeds greater than 22 mph, we are unable to investigate this hypothesis further using the industrial flare test data. It should be noted that Gogolek et al. (2010b) performed tests as high as about 27 mph; no test runs from that study that were performed below 22 mph reflected poor flare performance.

For these reasons, it seems reasonable to conclude that the momentum flux ratio (MFR) should be 3 or greater in crosswinds that are greater than 22 miles per hour (mph) at the flare tip. As an alternative to monitoring the MFR, flare operators could perform observations to identify wake-dominated flames during crosswind velocities greater than 22 mph at the flare tip and flare vent gas velocity could be increased if a wake-dominated flame is observed. Observation monitoring for wake-dominated flames could be established similarly to the current visible emissions monitoring requirements for flares. For example, the length of the observation period as well as the frequency could be triggered by different wind speed thresholds or categories. There are two main concerns with relying on observations: (1) that some flames may simply be too difficult to see, and (2) it may be difficult to recognize when a flame is wake-dominated.

We also reviewed the power factor for the same 245 steam-assisted flare test runs that were analyzed for MFR. Figure 5-9 is a plot of combustion efficiency versus power factor. The same could be said about power factor as was said about MFR; it is assumed that most of these data (149 steam-assisted test runs) had poor flammability characteristics because the  $LFL_{CZ}$  for these test runs was greater than 15.3 percent by volume (see Section 3.0 of this report for an explanation of this  $LFL_{CZ}$  threshold). Also, there are 10 test runs highlighted in red in Figure 5-9 that had a  $LFL_{CZ}$  less than 15.3 percent by volume and did not achieve a combustion efficiency of 96.5 percent or greater. The poor combustion efficiency reported for these 10 test runs are discussed in Section 3.1.3 of this report. Although it appears that a power factor of 0.15 or less could be used as a level for indicating good combustion efficiency, it is less clear whether this level (i.e., 0.15 or less) would be appropriate for all flare vent gas mixtures. In addition, we did not attempt to incorporate a “fuel factor” as Gogolek et al. (2010b) did with their data, because the UFL is difficult to calculate for mixtures, especially ones with inert.

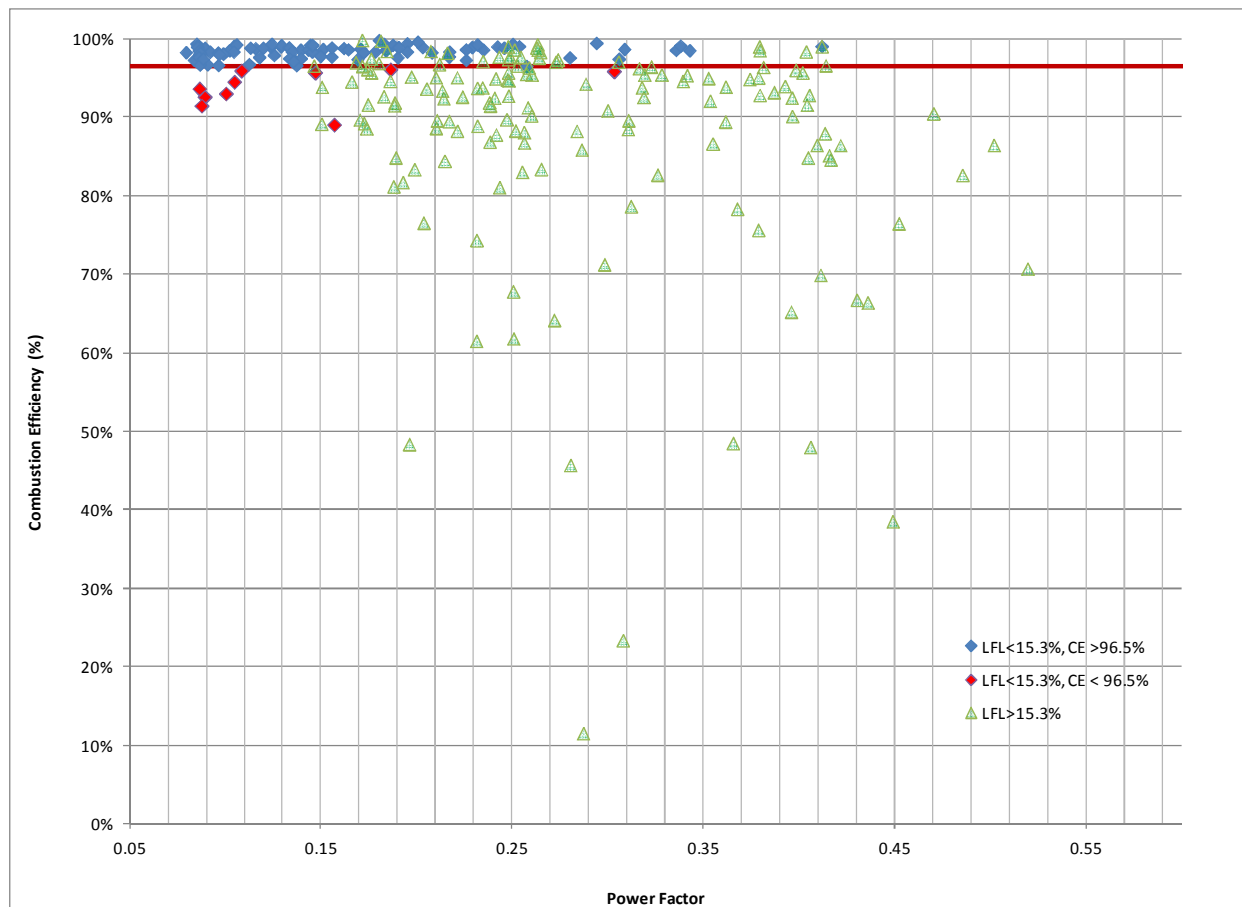


**Figure 5-9. Combustion Efficiency vs. Power Factor**

## **6.0 FLARE FLAME LIFT OFF**

Flare flame lift off can cause a flame to become unstable, which can negatively affect the combustion efficiency of a flare. To avoid flame lift off, the data suggest that the actual flare tip velocity (i.e., actual flare vent gas velocity plus center steam velocity, if applicable) should be less than an established maximum allowable flare tip velocity calculated using an equation that is dependent on combustion zone gas composition, the flare tip diameter, density of the flare vent gas, and density of air. This section documents the analysis supporting this observation.

### **6.1 Literature Review and $V_{\max}$ Calculation**

Flare flame lift off is a condition where a flame separates from the tip of the flare and there is space between the flare tip and the bottom of the flame due to excessive air induction as a result of the flare gas and center steam exit velocities (Gogolek et al., 2010a describes this situation as flame “blow-off”). Flame stability can exist when flame lift off occurs; however, as flame stability decreases (which can be caused by a variety of reasons, such as changes in flare tip velocity, combustion zone gas composition, or wind direction and speed), a flare operating at flame lift off can progress to a condition where the flame is extinguished; at a minimum, the flame will be inconsistent (Kalghatgi, 1981a; and Shore, 2007). Therefore, flame lift off should be monitored and avoided. A primary contributor to flame lift off is flare tip velocity, especially its relationship to the flame speed of the constituents in the flare vent gas (Shore, 2007).

Gogolek et al., 2010a provide three different equations that correlate flame lift off and flare tip velocity. Each of the equations presented by Gogolek et al. use a different combination of variables. However, this section primarily focuses on an equation presented by Shore (2007). Shore’s equation was one of the equations presented by Gogolek et al. (2010a). This equation was selected because it considers lower flammability limit, which would already be known by a source if the recommendation of Section 3.0 of this report were followed. Also, other equations presented by Gogolek et al. (2010a) use parameters that are not readily available for mixtures (i.e., flame speed and upper flammability limit).

In order to calculate the boundary velocity between an unstable and stable discharge velocity (or maximum velocity) for any gas or mixture exiting the flare tip, Shore's equation (Equation 6-1) considers the flare tip diameter, lower flammability limit and density of the flare vent gas, and density of air. Center steam should be incorporated into the flare vent gas properties because center steam exits the flare tip in the same direction as the flare vent gas. Shore developed the equation using published experimental results on lift off using various mixtures from several researchers.

$$\frac{V_{max}}{2\pi\sqrt{\frac{A_u}{\pi}}} = \left( \frac{\left( \frac{100 - LFL_{vgcs}}{LFL_{vgcs}} \right) \left( \frac{\rho_{vgcs}}{\rho_{air}} \right)}{6.85} \right)^5 \quad (\text{Eq. 6-1})$$

Where:

- $V_{max}$  = Maximum flare tip velocity including, if applicable, center steam at which flame lift off is not expected to occur, ft/sec.
- $\pi$  = 3.14, constant.
- $A_u$  = Unobstructed cross sectional area of the flare tip, ft<sup>2</sup>. John Zink provided details for determining the unobstructed cross sectional area of several flare tip designs (see Appendix I).
- $LFL_{vgcs}$  = The lower flammability limit of flare vent gas including, if applicable, center steam, volume %. A methodology for calculating lower flammability limits is included in Section 3.0 of this report.
- $\rho_{vgcs}$  = Density of flare vent gas including center steam if applicable, lb/scf.
- $\rho_{air}$  = Density of ambient air, lb/scf.

## 6.2 Test Data Analysis

Test run data were evaluated against Equation 6-1 to see how well they would correspond to the equation's ability to predict a maximum flare tip velocity for flame lift off. Shore explains that at the equation's predicted maximum flare tip velocity, stream eddies from the flare tip have reached a critical vertical shedding frequency and flame lift off may occur (Shore, 2007).

Three hundred thirty (330) of the 356 steam-assisted and air-assisted flare test runs were considered for this analysis. Twenty-six (26) test runs from the Shell Deer Park East Property Flare study (Shell Global Solutions (US) Inc., 2011a) were not included in the analysis because there were limited steam information for these data points and a center steam rate could not be determined (which is necessary to calculate the “ $LFL_{vgs}$ ” term in Equation 6-1). It was assumed that most of these data (183 steam-assisted test runs) had poor flammability characteristics because the  $LFL_{CZ}$  for these test runs was greater than 15.3 percent by volume (see Section 3.0 of this report for an explanation of this  $LFL_{CZ}$  threshold). It was also assumed that 30 air-assisted test runs had too much assist air because the SR was greater than 7 (see Section 4.0 of this report for an explanation of this SR threshold). Therefore, 213 of the 330 test runs were disregarded because they were expected to have poor combustion efficiency regardless of the flare tip velocity. Finally, all nine air-assist data points from the EPA-600/2-85-106 test report (Pohl and Soelberg, 1985) were removed from the Equation 6-1 evaluation because these tests were performed on a flare with a 1.5 inch diameter, which is not expected to be scalable to larger industrial type flares (see Section 4.0 of this report for more details).

The analysis was performed on the remaining 108 test runs. Figure 6-1 is a plot of Equation 6-1 against the 108 test runs that have either a  $LFL_{CZ}$  of less than or equal to 15.3 percent by volume (for steam-assist data), or a SR of less than or equal to 7 (for air-assist data). Ten (10) steam-assist test runs with a  $LFL_{CZ}$  less than 15.3 percent by volume that did not achieve a combustion efficiency of 96.5 percent or greater, are highlighted in red in Figure 6-1. The poor combustion efficiency reported for these 10 test runs is discussed in Section 3.1.3 of this report.

The left side of the green line in Figure 6-1 marks the region where vertical stability of the flame may be compromised (the green line is the linear relationship of Equation 6-1 and represents the maximum flare tip velocity including, if applicable, center steam at which flame lift off is not expected to occur). Although actual flame lift off data were available for only two of these 108 test runs (lift off information is only provided in the EPA-600/2-85-106 study (Pohl and Soelberg, 1985)), it is reasonable to assume that all of the 108 test runs did not exhibit flame lift off because the tests were done at high turndown ratios, which means the actual flare vent gas

flow rate was much lower than what the flare is designed to handle (even when center steam is incorporated into the calculation). Therefore, all 108 test runs should fall on the right side of the green line in Figure 6-1 because one would expect all 108 test runs to not have flame lift off.

It is difficult to draw any conclusions on whether the three data points on the left side of the Equation 6-1 threshold (see Figure 6-1) should be considered outliers. Using Equation 6-1 as the indicator, it is expected that these three data points would have exhibited flame lift off during their test run. However, one of these data points came from the EPA-600/2-85-106 study (Pohl and Soelberg, 1985), which noted that no lift off occurred during this particular test run (i.e., test run 206). The other two test runs came from the EPA-600/2-83-052 study (McDaniel 1983), which does not provide any information on lift off.

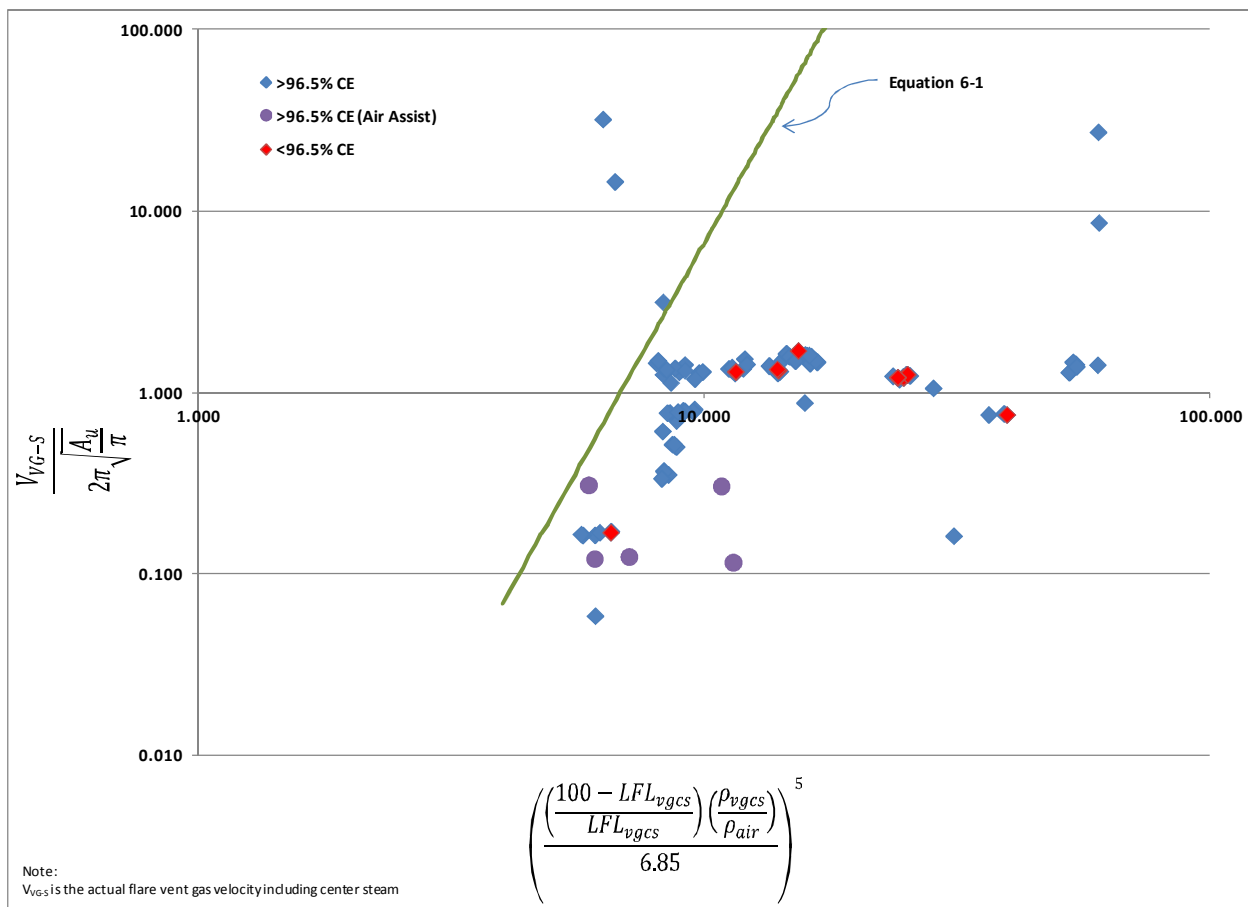


Figure 6-1. Conditions for Stable Flare Flame

Even though these three test runs fall on the left side of the Equation 6-1 threshold, they each achieved a combustion efficiency of 96.5 percent or greater. This observation is not surprising because good flare performance can still exist when flame lift off occurs. There are four other data points in Figure 6-1 that are from the 1980s EPA studies, but these test runs fall on the right side of the Equation 6-1 threshold and achieve a combustion efficiency of 96.5 percent or greater (one of these runs is from the EPA-600/2-85-106 study, which noted that no lift off occurred during the test run; and the other three runs came from the EPA-600/2-83-052 study).

The two test runs from the EPA-600/2-85-106 study did not use a pilot during testing but all other data points in Figure 6-1 had pilot operations. Also, the flare vent gas volumetric or mass flow rates for the EPA-600/2-85-106 test runs were not reported so assumptions were made using the reported steam-to-fuel ratio and fuel composition to determine flow rates. The data from the EPA-600/2-83-052 study came from tests using a steam-assisted flare that was the smallest sized flare of all test data included in Figure 6-1 (i.e., the flare tip diameter was 8.625 inches, and the effective diameter was less than 6 inches).

It appears nearly all the available test data fits Equation 6-1; all but three test runs evaluated had velocities less than the maximum velocity allowed by Equation 6-1. However, this analysis does not test Equation 6-1 over a very large range of possible flare tip velocities. All of the recent flare test data were collected during high turndown ratios and consequently have relatively low flare tip velocities. For the steam-assisted flares that were tested, the turndown ratio ranged from 504.1 to 13.8 (or 0.20 to 7.24 percent utilization); and tip velocities were less than 10 feet per second with center steam excluded. For the air-assisted flare (from the TCEQ data set), the turndown ratio ranged from 410.2 to 155.3 (or 0.24 to 0.64 percent utilization); and tip velocities were less than 2 feet per second. Maximum flare capacity design is unknown for the flares used in this analysis that are from the EPA-600/2-83-052 and EPA-600/2-85-106 studies; therefore, the turndown ratios are unknown. Flare tip velocities for these studies ranged from approximately 2 to 50 feet per second (for those test runs included in Figure 6-1).

### **6.3 Other Operating Parameters Considered for Flame Lift Off**

There are other methods studied by researchers. For example, Gogolek et al. (2010a) discuss two additional equations (other than Equation 6-1) that were developed by Nobel et al. (1984) and Kalghatgi (1981a and b); however, these two equations were not analyzed against the available flare test data. One of these equations that Gogolek et al. (2010a) discuss uses the upper flammability limit (UFL), which is difficult to calculate for mixtures, especially ones with inerts. Le Chatelier's equation could be used to determine UFLs, but it is much less accurate than calculating a LFL. The other equation Gogolek et al. (2010a) mention uses flame velocity, which is a difficult parameter to acquire, because there are relatively few flame velocities that have been tabulated and no accepted method is known for estimating flame velocities for mixtures.

## **7.0 OTHER FLARE TYPE DESIGNS TO CONSIDER**

### **7.1 Non-Assisted Flares**

A non-assisted flare does not use any auxiliary steam, air, or vent stream pressure to promote mixing at the flare tip. We are unable to verify whether any of the analyses presented in this technical report could apply to non-assisted flares because there are minimal test data available for non-assisted flares. It seems reasonable to assume that the  $LFL_{CZ}$  analysis in Section 3.0 of this report could apply to a non-assisted flare. For a non-assisted flare, the “combustion zone gas” would simply become the “flare vent gas” because no assist media is added to the combustion zone of a non-assisted flare. Therefore, a determination that  $LFL_{CZ}$  is the most appropriate operating parameter to monitor for steam-assisted flares, could also apply to non-assisted flares (i.e., the  $LFL_{CZ}$  must be 15.3 percent by volume or less when regulated material is being routed to a non-assisted flare in order to maintain good combustion efficiency). Nine of the 312 test runs that were performed on a steam-assisted flare did not use any steam during testing and could be considered a ‘non-assisted’ flare test run. Of these nine test runs, eight achieved greater than 96.5 percent combustion efficiency, but only three had a  $LFL_{CZ}$  less than 15.3 percent. The remaining test run did not achieve greater than 96.5 percent combustion efficiency and the  $LFL_{CZ}$  was greater than 15.3 percent. There is simply not enough non-assisted test data to determine whether a new  $LFL_{CZ}$  threshold would be warranted (i.e., a  $LFL_{CZ}$  threshold different than 15.3 percent); however, a  $LFL_{CZ}$  level of 15.3 percent and less appears to adequately predict good combustion for the nine non-assisted flare test runs.

It is assumed that the wind analysis in Section 5.0 of this report and the flame lift off analysis in Section 6.0 of this report apply to a non-assisted flare because these factors (wind and flame lift off) affect a diffusion flame from a non-assisted flare in the same way they would affect a diffusion flame created by a steam-assisted or air-assisted flare. The MFR and  $V_{max}$  methodologies in this report apply to non-assisted, steam-assisted, and air-assisted flares; assist media is only included in these methodologies if applicable.

## **7.2 Pressure-Assisted Flares and Other Flare Designs**

The EPA Air Pollution Control Cost Manual - Sixth Edition (U.S. EPA, 2002) states that pressure-assisted flares use the vent stream pressure to promote mixing at the burner tip. Several vendors now market proprietary, high pressure drop burner tip designs. If sufficient vent stream pressure is available, these flares can be applied to streams previously requiring steam or air assist for smokeless operation. Pressure-assisted flares generally (but not necessarily) have the burner arrangement at ground level, and consequently, must be located in a remote area of the plant where there is plenty of space available. They have multiple burner heads that are staged to operate based on the quantity of gas being released. The size, design, number, and group arrangement of the burner heads depend on the flare vent gas characteristics.

The amount of data available for pressure-assisted flares is small, especially considering the wide range in pressure-assisted flare designs. In addition, we have no data to analyze other new technologies, such as a hybrid steam-and-air-assist flare. We are aware of the Pohl and Soelberg (1985) flare study performed on pressure-assisted flares. The 1985 flare study published two curves for pressure-assisted flares illustrating a relationship between a given exit velocity and the minimum gas heat content that maintains the flame stability. We are also aware of pressure-assisted flare testing that was conducted at the John Zink test facility located in Tulsa, Oklahoma; this test program was coordinated with TCEQ and the Dow Chemical Company (Varner et al., 2007, see Docket ID No. EPA-HQ-OAR-2010-0868). The test report concluded that pressure-assisted flares can achieve performance levels at least as good as steam-assisted and air-assisted flares; however, the test program only tested two flare burner designs.

Because of lack of performance test data on pressure-assisted flare designs and other flare design technologies, and given the uniqueness in design of pressure-assisted flare designs from non-assisted, steam-assisted, and air-assisted flares (and across the population of pressure-assisted flares), it seems likely that the observations made in this report for non-assisted, steam-assisted, and air-assisted flares, cannot be applied to pressure-assisted flare designs or other flare design technologies. Also, test data are not available to form general conclusions on operating parameters that represent good combustion for these other flare designs.

## **8.0 MONITORING CONSIDERATIONS**

In order to determine if a flare is operated within the operating parameter values described in the previous sections, monitoring equipment will be needed. This section describes the types of monitoring equipment and methodologies that could be used to determine  $LFL_{CZ}$ ,  $LFL_{VG}$ ,  $LFL_{VG,C}$ , the ratio of  $NHV_{CZ}$  to  $NHV_{VG-LFL}$ ,  $C_{CZ}$ ,  $SR$ ,  $MFR$ , and  $V_{max}$  on an ongoing basis.

### **8.1 $LFL_{CZ}$ , $LFL_{VG}$ , and $LFL_{VG,C}$**

We are only aware of one viable monitoring method that could be used to continuously determine the  $LFL_{CZ}$ ,  $LFL_{VG}$ , and/or  $LFL_{VG,C}$ . These parameters (i.e.,  $LFL_{CZ}$ ,  $LFL_{VG}$ , and/or  $LFL_{VG,C}$ ) require a gas chromatograph to determine the individual component concentrations present in the flare vent gas, and flow meters to determine the volumetric flow rates of flare vent gas and total steam (if applicable). The individual component concentrations present in the flare vent gas, the pure component LFL values, and volumetric flow rates of flare vent gas and total steam (if applicable) are applied to the equations and methods described in Section 3.1.2 of this report to determine  $LFL_{CZ}$ ,  $LFL_{VG}$ , and/or  $LFL_{VG,C}$ .

There are several types of LFL monitors used for safety purposes, but we are not aware of any that provide a direct measure of the LFL of a gas mixture. Instead, these types of LFL monitors react to specific gas concentrations in air. There are personal monitoring devices available on the market that are used to detect explosive environments based on the LFL (for safety purposes); however, these devices are not meant for a continuous flow gases, can become saturated quickly if they are in continuous contact with a gas mixture, and may need a specific amount of oxygen to work properly. Other types of LFL monitoring devices that are used for safety are generally calibrated for only one type of gas, yet flare vent gas can consist of any variety of gas mixtures. The EPA is aware of one company<sup>2</sup> that makes a LFL monitor that could potentially be modified to continuously determine the  $LFL_{CZ}$ ,  $LFL_{VG}$ , and/or  $LFL_{VG,C}$ ; however, the monitor has never been used for this specific purpose. The device uses a continuous

---

<sup>2</sup> Control Instruments Corporation – PrexEx Flammability Analyzer

hydrogen flame inside a small chamber. Flammable vapors are drawn from the sample point into the chamber, where they are incinerated by the flame. A temperature detector measures the resulting change in flame temperature and provides an output reading in percent of the LFL of the gas mixture (not actual LFL). This LFL monitor provides a response time of less than 1 second, and can be accessed remotely. By combining this LFL monitor with metered air injection and a feedback control signal to adjust the air until the meter reads a preset percent of LFL, it seems possible that the meter could be used to measure the LFL. Some integrated programming to calculate the LFL from the flow rates and percent of LFL reading would also be needed, but this type of set up could potentially provide a LFL monitor without the expense of a gas chromatograph.

## **8.2 Ratio of $NHV_{CZ}$ to $NHV_{VG-LFL}$**

Because the ratio of  $NHV_{CZ}$  to  $NHV_{VG-LFL}$  requires the  $LFL_{VG}$  to be known as part of the calculation (see Equation D.22 of Appendix D of this report), this parameter (i.e., the ratio of  $NHV_{CZ}$  to  $NHV_{VG-LFL}$ ) requires a gas chromatograph. The gas chromatograph is used to determine the individual component concentrations present in the flare vent gas. Flow meters are also required to determine the volumetric flow rates of flare vent gas and total steam (if applicable). If there were a LFL monitor that could determine  $LFL_{VG}$  as discussed in Section 8.1 of this report, a calorimeter (or BTU analyzer) could be used in lieu of a gas chromatograph to determine the ratio of  $NHV_{CZ}$  to  $NHV_{VG-LFL}$ .

## **8.3 $C_{CZ}$**

Flares being used to control vent streams that have a consistently high combustible concentration can benefit from monitoring  $C_{CZ}$  in lieu of either  $LFL_{CZ}$ , or the ratio of  $NHV_{CZ}$  to  $NHV_{VG-LFL}$  (see Sections 3.2 and 3.3 of this report). The  $C_{CZ}$  parameter requires either a gas chromatograph or hydrocarbon analyzer to determine the total combustible constituents in the flare vent gas, and flow meters to determine the volumetric flow rates of flare vent gas and total steam (if applicable). The total combustible constituents in the flare vent gas, and volumetric

flow rates of flare vent gas and total steam (if applicable) are applied to Equation D.26 of Appendix D of this report to determine  $C_{CZ}$ .

#### **8.4 SR**

Flow meters measuring mass flow rates of flare vent gas and assist air (includes air controls for manifold and valve instrumentation) would be required to determine the SR parameter using the equation and methods described in Section 4.1 and Appendix D of this report. For purposes of calculating the denominator of the SR parameter, a gas chromatograph would also be needed so as to determine the individual component concentrations present in the flare vent gas.

#### **8.5 MFR**

A meteorological station or anemometer (to measure cross-sectional wind velocity at the flare tip and the density of the ambient air) and flow meters (to determine the volumetric flow rates, velocity, and density of flare vent gas and total steam (if applicable)) would be required to determine the MFR parameter using Equation D.41 of Appendix D of this report.

## **8.6** $V_{\max}$

The  $LFL_{\text{vgcs}}$  parameter that is used in the Shore equation methodology discussed in Section 6.0 of this report requires a gas chromatograph to determine the individual component concentrations present in the flare vent gas, and flow meters to determine the volumetric flow rates of flare vent gas and total steam (if applicable). The individual component concentrations present in the flare vent gas, the pure component LFL values, and volumetric flow rates of flare vent gas and total steam (if applicable) are applied to Equation D.43 of Appendix D of this report to determine  $LFL_{\text{vgcs}}$ . The  $LFL_{\text{vgcs}}$  and Equation D.45 of Appendix D are then used to determine  $V_{\max}$ . The flow meters would also be required to determine the velocity and density of flare vent gas and total steam (if applicable).

## 9.0 REFERENCES

- Allen, D. T., and V. M. Torres. 2011. 2010 Flare study final report. Prepared for the Texas Commission on Environmental Quality, Tracking No. 2008-81.  
<<http://www.tceq.texas.gov/assets/public/implementation/air/rules/Flare/2010flarestudy/2010-flare-study-final-report.pdf>>. September 20.
- API 521. 2007. Pressure-relieving and depressuring systems. 5th Edition. American Petroleum Institute.
- Avetisyan, A.A., V.V. Azatyan, V. I. Kalachev, V.V. Masalova, and A. A. Piloyan. 2007. Effect of the molecular structure of olefin admixtures on the combustion and explosion of hydrogen-air mixtures. *Kinetics and Catalysis*. 48:1, 8-16.
- Azatyan, V. V, A.A. Borisov, A.G. Merzhanov, V.I. Kalachev, V.V Masalova, A.E. Mailkov, and K.Y Troshin. 2005. Inhibition of various hydrogen combustion regimes in air by Propylene and Isopropanol. *Combustion, Explosion, and Shock Waves*. 41:1, 1-11.
- Azatyan, V., and I.A. Bolodyan. 2002. The predominant role of competition between the chain-branching and chain-terminating reactions in the formulation of concentration limits of flame propagation. *Russian Journal of Physical Chemistry*. 76:5, 775-784.
- Azatyan, V. V., V.A. Pavlov, and O.P. Shatalov. 2005. Inhibition of the combustion and detonation of hydrogen-air mixtures behind the shock front. *Kinetics and Catalysis*. 46:6, 789-799.
- Baukal, C. E. 2001. *The John Zink Combustion Handbook*. Boca Raton, Florida. CRC Press.
- Besnard, S. 1996. Fuel flammability test of gases and gas mixtures in air. Centre European Recherche Nucleaire.
- Bourguignon, E., M.R. Johnson, and L.W. Kostiuk. 1999. The use of a closed-loop wind tunnel for measuring the combustion efficiency of flames in a cross flow. *Combustion and Flame*. 119:319-334.
- Castiñeira, D., and T. F. Edgar. 2006. CFD for simulation of steam assisted and air assisted flare combustion systems. *Energy and Fuels*. 20:1044-1056.
- Castiñeira, D., and T. F. Edgar. 2008. CFD for simulation of crosswind on the efficiency of high momentum jet turbulent combustion flames. *Journal of Environmental Engineering*. 134:7:561-571.
- Choudhuri, Ahsan R. and Mahesh Subramanya 2006. *Investigation of H<sub>2</sub> Concentration and Combustion Instability Effects on the Kinetics of Strained Syngas Flames*. Final Technical Report for Department of Energy Grant DE-FG26-05NT42495.

Choudhuri, A. R. 2005. Investigation on the flame extinction limit of fuel blends. Final Technical Report. U.S. Department of Energy Grant DE-FG26-03NT41917.

Clean Air Engineering, Inc. 2010a. Performance test of a steam-assisted elevated flare with passive FTIR. Prepared by Marathon Petroleum Company, LLC, Findlay, OH and Clean Air Engineering, Inc., Palatine, IL.

Clean Air Engineering, Inc. 2010b. Performance test of a steam-assisted elevated flare with passive FTIR - Detroit. Prepared by Marathon Petroleum Company, LLC Findlay, OH and Clean Air Engineering, Inc., Palatine, IL.

Clean Air Engineering, Inc. 2010c. Steam contribution to combustion zone gas in variable wind conditions. Prepared by Marathon Petroleum Company, LLC, Findlay, OH and Clean Air Engineering, Inc., Palatine, IL.

Clean Air Engineering, Inc. 2011. PFTIR test of steam-assisted elevated flares – Port Arthur. Prepared for Flint Hills Resources Port Arthur, LLC.

Coward, H. F., and G. W Jones 1952. Limits of flammability of gases and vapors. Bureau of Mines, Bulletin 503.

Coward, H. F., C. W. Carpenter, and W. Payman. 1919. The dilution limits of inflammability of gaseous mixtures. Air. J. Chem. Soc. 115:119, 27–36.

Degges, M. J., J.E. Boyer, K.K. Kuo, and L. Basini. 2010. Influence of steam on the flammability limits of premixed natural gas/oxygen/steam mixtures. Chemical Engineering Journal. 165:2, 633-638.

Dickens, B. 2011. Personal communication from B. Dickens at U.S. EPA to J. Renzaglia, Eastern Research Group, Inc. (November).

Evans, S., and D. Roseler. 2011. Establishing a dynamic indicator of flare performance using lower flammability limits. Prepared for Marathon Petroleum Company, LLC (March).

Gogolek, P., A. Caverly, R. Schwartz, J. Seebold, and J. Pohl. 2010a. Emissions from elevated flares - A survey of the literature. Prepared for the International Flaring Consortium, CanmetENERGY (April).

Gogolek, P., A. Caverly, C. Balderson, R. Schwartz, J. Seebold, and J. Pohl. 2010b. Flare Test Facility - Results. Prepared for the International Flaring Consortium, CanmetENERGY (October).

Heffington, W. M., and W. R. Gaines. 1981. Flammability calculations for gas mixtures. Oil & Gas Journal.

Hu, E., Z. Huang, J. He, C. Jin, and J. Zheng. 2009. Experimental and numerical study on laminar burning characteristics of premixed methane–hydrogen–air flames. *International Journal of Hydrogen Energy*. 34:11, 4876-4888.

INEOS ABS (USA) Corporation. 2010. Passive Fourier transform infrared technology (FTIR) evaluation of P001 process control device at the INEOS ABS (USA) Corporation. Addyston, OH.

Johnson, M., A. Majeski, D. Wilson, and L.W. Kostiuk. 1998. The combustion efficiency of a propane jet diffusion flame in cross flow. Presented at The Combustion Institute, Western States Section, Seattle, WA (October).

Johnson, M., O. Zastavniuk, J. Dale, and L.W. Kostiuk. 1999a. The combustion efficiency of jet diffusion flames in cross-flow. Presented at The Combustion Institute, Joint Meeting of the United States Sections, Washington, D.C. (March).

Johnson, M., O.Zastavniuk, D.Wilson, and L.W. Kostiuk. 1999b. Efficiency measurements of flares in a cross flow. Presented at Combustion Canada, Calgary, Alberta (May).

Johnson, M., and L.W. Kostiuk. 1999. Effects of a fuel diluent on the efficiencies of jet diffusions flames in a crosswind. Presented at The Combustion Institute, Canadian Section, Edmonton, Alberta (May).

Johnson, M., and L.W. Kostiuk. 2000. Efficiencies of low-momentum jet diffusion flames in crosswinds. *Combustion and Flame*. 23:189-200

Johnson, M., D. Wilson, and L.W. Kostiuk. 2001. A fuel stripping mechanism for wake-stabilized jet diffusion flames in crossflow. *Combustion Science and Technology*. 169:155-174.

Jones, G. W. 1929. Inflammability of mixed gases. U.S. Department of the Interior, Bureau of Mines. Technical Paper 450.

Jones, G. W., and R. E. Kennedy. 1932. Inflammability of mixed gases: mixtures of methane, ethane, hydrogen, and nitrogen. U.S. Department of the Interior, Bureau of Mines, Report of Investigations 3172.

Jones, G. W., and R. Kennedy. 1933. Limits of inflammability of natural gases containing high percentages of carbon dioxide and nitrogen. U.S. Department of the Interior, Bureau of Mines. Report of Investigation 3216.

Jones, G. W., and R. E. Kennedy. 1938. Extinction of propylene flames by diluting with nitrogen and carbon dioxide and some observations of the explosive properties of propylene. U.S. Department of the Interior, Bureau of Mines. Report of Investigation 3395.

- Jones, G. W., and R. E. Kennedy. 1943. Prevention of butadiene-air explosions by addition of nitrogen and carbon dioxide. U.S. Department of the Interior, Bureau of Mines. Report of Investigation 3691.
- Kalghatgi, G.T. 1981a. Blow-out stability of gaseous jet diffusion flames, Part I: In still air. *Combustion Science and Technology*. 26:233-239.
- Kalghatgi, G.T. 1981b. Blow-out stability of gaseous jet diffusion flames, Part II: Effect of cross wind. *Combustion Science and Technology*. 26:241-244.
- Karim, G, Wierzba, I., & Boon, S. 1985. Some considerations of the lean flammability limits of mixtures involving hydrogen. *International Journal of Hydrogen Energy*, 10(2), 117-123.
- Karim, G. A., I. Wierzba, and Y. Al-Alousi. 1996. Methane -- Hydrogen mixtures as fuels. *International Journal of Hydrogen Energy*. 21:7, 625-631.
- Kondo, S., K. Takizawa, A. Takahashi, and K. Tokuhashi. 2006a. Extended Le Chatelier's formula and nitrogen dilution effect on the flammability limits. *Fire Safety Journal*. 41:5, 406-417.
- Kondo, S., K. Takizawa, A. Takahashi, and K. Tokuhashi. 2006b. Extended Le Chatelier's formula for carbon dioxide dilution effect on flammability limits. *Journal of Hazardous Materials*. 138:1, 1-8.
- Kondo, Shigeo, Takizawa, Kenji, Takahashi, A., Tokuhashi, Kazuaki, & Sekiya, A. 2008. A study on flammability limits of fuel mixtures. *Journal of hazardous materials*, 155(3), 440-8.
- Laskin, A., H. Wang, and C.K. Law. 2000. Detailed kinetic modeling of 1,3-butadiene oxidation at high temperatures. *International Journal of Chemical Kinetics*. 32:10, 589-614.
- Leahey, D., and K. Preston. 2001. Theoretical and observational assessments of flare efficiencies. *Journal of the Air & Waste Management Association*. 51:1610-1616.
- Loehr, C., Djordjevic, S., & Liekhus, K. 1997. Flammability assessment methodology program phase I: final report.  
<http://scholar.google.com/scholar?hl=en&btnG=Search&q=intitle:FLAMMABILITY+ASSESSMENT+METHODOLOGY+PROGRAM+PHASE+I+:+FINAL+REPORT#1>
- Mashuga, C. V., and D.A. Crowl. 1999. Flammability zone prediction using calculated adiabatic flame temperatures. *Process Safety Progress*. 18:3, 127-134.
- McDaniel, M. 1983. Flare efficiency study. Prepared for U.S. EPA Office of Research and Development EPA-600/2-83-052 by Engineering Science, Inc. (July).
- Molnarne, M., P. Mizsey, and V. Schröder. 2005. Flammability of gas mixtures. Part 2: influence of inert gases. *Journal of Hazardous Materials*. 121:1-3, 45-9.

Noble, R.K., M.R. Keller, and R.E. Schwartz. 1984. An experimental analysis of flame stability of open air diffusion flames. American Flame Research Committee International Symposium on Alternate Fuels and Hazardous Wastes. Tulsa, OK.

Peterson, J., N. Tuttle, H. Cooper, and C. Baukal. 2007. Minimize facility flaring. Hydrocarbon Processing. pp. 111–115.

Pohl, J., R. Payne, and J. Lee. 1984. Evaluation of the efficiency of industrial flares: Test Results. EPA-600/2-84-095. Prepared for U.S. EPA Office of Research and Development by Energy and Environmental Research Corporation (May).

Pohl, J. and N. Soelberg. 1985. Evaluation of the efficiency of industrial flares: Flare head design and gas composition. EPA-600/2-85-106. Prepared for U.S. EPA Office of Air Quality Planning and Standards. (September).

Schröder, V., and M. Molnarne. 2005. Flammability of gas mixtures. Part 1: Fire potential. Journal of Hazardous Materials. 121:1-3, 37-44.

Seebold, J., B. Davis, P. Gogolek, L.W. Kostiuk, J. Pohl, R. Schwartz, N. Soelberg, M. Strosher, and P. Walsh. 2003. Reaction efficiency of industrial flares: The perspective of the past. American Flame Research Committee Symposium.

Seebold, J., P. Gogolek, J. Pohl, and R. Schwartz. 2004. Practical implications of prior research on today's outstanding flare emissions questions and a research program to answer them, Environmental Control of Combustion Processes: Innovative Technology For the 21st Century. Presented at the Joint International Combustion Symposium, Maui, HI (October).

Shell Global Solutions (US) Inc. 2011a. Shell Deer Park Refining LP Deer Park Refinery East Property Flare Test Report. Prepared by Shell Global Solutions (US) Inc., Houston, TX (April).

Shell Global Solutions (US) Inc. 2011b. Shell Deer Park Site Deer Park Chemical Plant OP-3 Ground Flare Performance Test Report. Prepared by Shell Global Solutions (US) Inc., Houston, TX (May).

Shore, D. 2007. Improving flare design, a transition from art-form to engineering science. Presented at AFRC-JFRC 2007 Joint Meeting, Waikoloa, HI (October).

Smith, S. 2003. Flare system emissions control. Presented at the Texas Technology Conference by the Zeeco Company (March).

Smoot, D. L., J.D. Smith, and R.E. Jackson. 2009. Technical foundations to establish new criteria for efficient operation of industrial steam-assisted gas flares. Presented at the International Flame Research Foundation 16<sup>th</sup> International Members Conference, Boston, MA (June).

U.S. EPA. 2002. Air pollution control cost manual, 6<sup>th</sup> ed. EPA/452/B-02-001.

Van den Schoor, F., R.T.E. Hermanns, J.A. van Oijen, F. Verplaetsen, and L.P.H. de Goey. 2008. Comparison and evaluation of methods for the determination of flammability limits, applied to methane/hydrogen/air mixtures. *Journal of Hazardous Materials*. 150:3, 573-81.

Vidal, M., W. Wong, W.J. Rogers, M.S. Mannan. 2006. Evaluation of lower flammability limits of fuel-air-diluent mixtures using calculated adiabatic flame temperatures. *Journal of Hazardous Materials*. 130:1-2, 21-7.

Wang, J., Z. Huang, C. Tang, H. Miao, and X. Wang. 2009. Numerical study of the effect of hydrogen addition on methane-air mixtures combustion. *International Journal of Hydrogen Energy*. 34:2, 1084-1096.

Wang, T., Chen, C., & Chen, H. 2010. Nitrogen and carbon dioxide dilution effect on upper flammability limits for organic compound containing carbon, hydrogen and oxygen atoms. *Journal of the Taiwan Institute of Chemical Engineers*, 41(4), 453-464. Taiwan Institute of Chemical Engineers.

White, A. G. 1925. Limits for the propagation of flame in inflammable gas/air mixtures, Part II: Mixtures of more than one gas and air. *Journal of the Chemical Society, Transactions*. 127:48, 48.

Wierzba, I., and V. Kilchyk. 2001. Flammability limits of hydrogen-carbon monoxide mixtures at moderately elevated temperatures. *International Journal of Hydrogen Energy*. 26:6, 639-643.

Zabetakis, M.G. 1965. *Flammability Characteristics of Combustible Gases and Vapors*. U.S. Bureau of Mines, Bulletin 627.

*This information is distributed solely for the purpose of pre-dissemination peer review under applicable information quality guidelines. It has not been formally disseminated by EPA. It does not represent and should not be construed to represent any Agency determination or policy.*

## **APPENDIX A**

### **Appendix A. Brief Review Summary of Each Flare Performance Study and Test Report**

## **A.1 Data Set A: EPA-600/2-83-052 (McDaniel, 1983)**

Tests from data set A were conducted on pilot-scale test flares in June 1982 at the John Zink Company flare demonstration facility in Tulsa, Oklahoma. The gases used in this study included mixtures of propylene diluted with nitrogen (chemical composition for each test run, by test report, used in the steam data analysis described in this section 3.0 of this report is provided in Appendix E). The primary objectives for these tests were to determine the combustion efficiency and hydrocarbon destruction efficiency for both air- and steam-assisted flares under a wide range of operating conditions. The test methodology involved a special 27-foot sample probe suspended by a crane over the flare flame. The sample extracted by the probe was analyzed by continuous emission monitors to determine concentrations of carbon dioxide, carbon monoxide, total hydrocarbon, sulfur dioxide, nitrogen oxides, and oxygen.

The report generally concluded that when flares operate under conditions representing good industrial operating practice, combustion efficiencies at the sampling probe were greater than 98 percent. Combustion efficiencies declined under conditions of excessive steam and high exit velocities of low heat content gases.

There are 14 non-assisted, 15 steam-assisted, and 13 air-assisted test runs from this test report. The 14 non-assisted data points came from tests performed on the steam-assisted flare, but no steam was used during the test. The steam-assisted flare was a John Zink Standard STF-S-8 flare tip (effective flare tip diameter of 5.86 inches). The recommended steam flow for this flare is approximately 0.4 pounds of steam per pound of propylene. The air-assisted flare was a John Zink STF-LH-457-5 flare (flare tip diameter unknown). The mass or volumetric flow rate of assist air as well as the assist air velocity were considered proprietary information and not included in the test report; therefore, the test data associated with this particular air-assisted flare were not used in any analysis that is discussed in this report. Both flares had two constant ignition pilots designed to burn a total of 300 standard cubic feet per hour of natural gas.

## **A.2 Data Set B: EPA-600/2-84-095 (Pohl et al., 1984)**

Tests from data set B were conducted at the Energy and Environmental Research Corporation's El Toro, California test site. This study was limited to measuring the combustion efficiencies of 3-, 6-, and 12-inch pipe flares burning mixtures of propane diluted with nitrogen at steady operating conditions with and without steam injection, in the absence of wind. All steam injection was introduced as upper steam.

## **A.3 Data Set C: EPA-600/2-85-106 (Pohl and Soelberg, 1985)**

Tests from data set C were conducted at the Energy and Environmental Research Corporation's El Toro, California test site as a continuation of the tests conducted under EPA-600/2-84-095. The gases used in this study included mixtures of propane diluted with nitrogen (chemical composition for each test run, by test report, used in the steam data analysis described in this section 3.0 of this report is provided in Appendix E). The primary objective of these tests was to determine the influence of flare head design on flare combustion efficiency. The study held proprietary the design of the different flare heads; however, some information was provided. A "coanda" steam-injected flare head was tested at gas exit velocities ranging from 0.2 to 9.9 feet per second based on a 12 inch diameter opening. Steam was injected into the flare waste stream through nozzles located above the main flare tip opening (upper steam). All measurements on this flare were made with a constant upper steam flow rate of 140 pounds per hour. All steam-assisted test runs were performed without pilots. Also, an air-assisted flare head was tested at gas exit velocities ranging from 8.5 to 428 feet per second based on a 1.5 inch diameter opening. The assist air flow rate was varied. Some air-assisted test runs were performed with pilots, but the majority were not.

There are six steam-assisted and nine air-assisted test runs from this test report. This report also includes 16 pressure-assisted test runs (nine runs came from a 1.5 inch diameter pressure-assisted flare head and the other seven from a 3.8 inch diameter pressure-assisted flare head).

#### **A.4 Data Set D: MPC TX (Clean Air Engineering, Inc., 2010a)**

PFTIR performance testing was conducted from September 15, 2009 to September 24, 2009 on Marathon's Texas City (MPC TX) refinery's main flare in response to an EPA Office of Enforcement request pursuant to section 114 of the Clean Air Act. Industrial Monitor and Control Corporation (IMACC) performed the testing, and Clean Engineering, Inc. wrote the test report. Tests were conducted while flare vent gas contained saturates, olefins, nitrogen, and hydrogen mixtures (chemical composition for each test run, by test report, used in the steam data analysis described in this section 3.0 of this report is provided in Appendix E). For each test series, steam was increased from the manufacturer's recommended minimum cooling steam rate to the point of snuffing the flare. For the majority of tests conducted, combustion efficiency declined with increasing steam at constant flare vent gas mass loading and constant composition.

The Marathon Texas City main flare is an elevated steam-assisted flare. The flare has an effective tip diameter of 23.25 inches, was manufactured by Callidus Technologies (model BTZ-IS3/US-24-C), and was installed in December 2000. The tip has three points of steam addition: center steam, a lower steam ring, and an upper steam ring. Although the flare tip is equipped with upper steam, it was not used during any test runs; and all measurements on this flare were made with a constant center steam flow rate of 500 pounds per hour (Dickens 2011) and variable lower ring steam addition. The lower steam ring manifold piping has a connection to a small sweep gas ring used for shaping the flare at the tip. The flare has a manufacturer minimum total steam requirement of 1,250 pounds per hour in order to protect the flare tip. The flare operated with approximately 100 standard cubic feet per hour of pilot gas during the test runs. The typical base load for flare operation is approximately 1,100 to 2,000 pounds per hour of waste gas flow, or less than 0.25 percent of the hydraulic capacity of the flare (approximately a 250:1 turndown factor).

Raw test data (in the form of an Excel worksheet) was available for this data set. There are 138 steam-assisted test runs from the raw test data. However, 56 of these test runs were noted in the test report as having a relatively low video score indicating that the PFTIR camera was lacking aiming accuracy during the test run (see Table A.1).

**Table A.1 Test Runs Explicitly Removed From Consideration**

Condition	Run Number	Reason for Omission
<b>Data Set D</b>		
A19	1-2	Relatively low “video score” indicating that the PFTIR camera was lacking aiming accuracy during the test run.
	1-3	
	3-2	
	4-2	
	5-1	
	6-1	
	7-2	
A8	1-1	Relatively low “video score” indicating that the PFTIR camera was lacking aiming accuracy during the test run.
	2-1	
	2-2	
	2-3	
	3-1	
	3-2	
	4-1	
	5-1	
	5-2	
	6-1	
	7-1	
	7-2	
	8-1	
	8-2	
9-1		
10-1		
B	1-3	Relatively low “video score” indicating that the PFTIR camera was lacking aiming accuracy during the test run.
	2-3	
	3-3	
	4-3	
	6-3	
	7-3	
	10-1	
C	1-3	Relatively low “video score” indicating that the PFTIR camera was lacking aiming accuracy during the test run.
	2-3	
	3-3	
	4-1	
	5-1	
D	7-1	Relatively low “video score” indicating that the PFTIR camera was lacking aiming accuracy during the test run.
	9-1	

**Table A.1 (Continued)**

<b>Condition</b>	<b>Run Number</b>	<b>Reason for Omission</b>
<b>Data Set D</b>		
E	1-2	Relatively low “video score” indicating that the PFTIR camera was lacking aiming accuracy during the test run.
	2-2	
	3-2	
	4-2	
	6-1	
F	1-1	Relatively low “video score” indicating that the PFTIR camera was lacking aiming accuracy during the test run.
	2-1	
	3-1	
	4-1	
	5-1	
	6-1	
G	1-1	Relatively low “video score” indicating that the PFTIR camera was lacking aiming accuracy during the test run.
	2-1	
	3-1	
	4-1	
	5-1	
	6-1	
LTS	2-7	Relatively low “video score” indicating that the PFTIR camera was lacking aiming accuracy during the test run.
	2-8	

**A.5 Data Set E: INEOS (INEOS ABS (USA) Corporation, 2010)**

Pursuant to the consent decree (Civil Action No. 1:09-CV-545), PFTIR performance testing was conducted from November 3, 2009 to November 5, 2009 on INEOS ABS (USA) Corporation’s flare controlling their P001 process in Addyston, Ohio. IMACC performed the testing. The purpose of the evaluation was to determine the appropriate net heating value of flare vent gas necessary to assure the flare achieves 99 percent control efficiency. Tests were conducted while flaring gases containing various mixtures of 1,3-butadiene, natural gas, and nitrogen (chemical composition for each test run, by test report, used in the steam data analysis described in this section 3.0 of this report is provided in Appendix E).

The flare tested is an elevated steam-assisted flare. The flare tip has an effective diameter of 16 inches and is manufactured by John Zink (model no. EEF-QS-16). Steam is injected into

the flare waste stream through nozzles located above the main flare tip opening (upper steam). The manufacturer minimum total steam requirement to the flare tip was not provided in the test report. The flare operated with ~150 standard cubic feet per hour of pilot gas during the test runs. There are 21 steam-assisted test runs from this test report.

#### **A.6 Data Set F: MPC Detroit (Clean Air Engineering, Inc., 2010b)**

PFTIR performance testing was conducted from July 8, 2010 to July 20, 2010 on Marathon's Detroit (MPC Detroit) refinery's Complex 3 and 4 flare in response to an EPA Office of Enforcement request pursuant to section 114 of the Clean Air Act. IMACC performed the testing. The main objective of the test was to better understand the effects of steam on the overall performance of the flare in terms of combustion efficiency. Tests were conducted while flaring gases containing refinery fuel gas, propylene, hydrogen, and nitrogen mixtures (chemical composition for each test run, by test report, used in the steam data analysis described in this section 3.0 of this report is provided in Appendix E). For each test series, steam was increased from the manufacturer's recommended minimum cooling steam rate to the point of snuffing the flare. For the majority of tests conducted, combustion efficiency declined with increasing steam at constant flare vent gas mass loading and constant composition.

Marathon's Detroit refinery's Complex 3 and 4 flare is an elevated steam-assisted flare. The flare tip has an effective diameter of 16 inches and is manufactured by NAO, Inc. (model no. 20" NFF-RC) and was constructed in 1961 to 1962. The flare tip was replaced in October 2005. The flare has two points of steam addition: center steam and ring steam. The center and ring steam each have a manufacturer minimum steam requirement of 300 pounds per hour. All measurements on this flare were made with a constant center steam flow rate of 300 pounds per hour (and varying ring steam rates from 300 pounds per hour and up). The ring steam has alternating high and low points of injection around the flare tip exit. The flare operated with ~135 standard cubic feet per hour of pilot gas during the test runs. The typical base load for typical flare operation is approximately 500 to 600 pounds per hour, or less than 0.25 percent of the hydraulic capacity (approximately a 400:1 turndown factor).

Raw test data (in the form of an Excel worksheet) were available for this data set. There are 62 steam-assisted test runs from the raw test data. However, six of these test runs were noted in the test report as invalid runs (see Table A.2).

**Table A.2 Test Runs Explicitly Removed From Consideration**

Condition	Run Number	Reason for Omission
<b>Data Set F</b>		
A	6-1	Invalid run, secondary (road location) PFTIR only, no combustion efficiency data.
	8-2	Invalid run, only 4 combustion efficiency readings.
	9-2	Invalid run, only 1 combustion efficiency reading.
B	1-2	Invalid run, secondary (road location) PFTIR only, no combustion efficiency data.
D	1-1	Invalid due to run instability.
E	4-1	Combustion efficiency for the E4-1 (N <sub>2</sub> ≈66%) was measured with the secondary PFTIR at the road location. Because of hardware issues with this instrument the data is not reported and the run was marked invalid.

**A.7 Data Set G: Flint Hills Resources Aromatics Unit (FHR AU) and Light Olefins Unit (FHR LOU) (Clean Air Engineering, Inc., 2011)**

PFTIR performance testing was conducted in October and November of 2010 at Flint Hills Resources, LLC in Port Arthur, TX on their Aromatics Unit and Light Olefins Unit flares in response to an EPA Office of Enforcement request pursuant to section 114 of the Clean Air Act. IMACC performed the testing. The main objective of the tests was to better understand the effects of steam on the overall performance of each flare in terms of combustion efficiency. Two additional operating parameters were also examined during this test program. The effect of hydrogen on combustion efficiency was studied on the FHR AU flare. The effect of flare vent gas flow rate on combustion efficiency was studied on the FHR LOU flare.

The FHR AU flare is an elevated steam-assisted flare. The current tip has an effective diameter of 20 inches and was installed in 1996. This tip was manufactured by Callidus (model

no. BTZ-US-16/20-C) and has two points of steam addition: center steam and ring steam. The center steam is injected in the flare vent gas stack prior to reaching the flare tip, and the ring steam is injected with nozzles around the flare tip rim. The center steam has a manufacturer minimum steam requirement of 500 pounds per hour. All measurements on this flare were made with a constant center steam flow rate of 500 pounds per hour (and varying ring steam rates). The flare operated with approximately 100 standard cubic feet per hour of pilot gas during the test runs. The typical FHR AU flare vent gas flow rate during normal operation is approximately 800 pounds per hour, or less than 0.4 percent of the hydraulic capacity (approximately a 250:1 turndown factor).

The FHR LOU flare is an elevated steam-assisted flare. The current tip has an effective diameter of 54 inches and was installed in June 2010. This tip was manufactured by Callidus (model no. BTZ-1S3-54C) and has two points of steam addition: center steam and lower steam. The center steam is injected in the flare vent gas stack prior to reaching the flare tip, and the lower steam is injected through internal tubes interspersed throughout the flare tip. The center steam has a manufacturer minimum steam requirement of 2,890 pounds per hour; the lower steam has a manufacturer minimum steam requirement of 500 pounds per hour. All measurements on this flare were made with a constant center steam flow rate of 2,890 pounds per hour (and varying lower steam rates from 500 pounds per hour and greater). The flare operated with approximately 200 standard cubic feet per hour of pilot gas during the test runs. The typical FHR LOU flare vent gas flow rate during normal operation is approximately 3,000 pounds per hour, or less than 0.3 percent of the hydraulic capacity (approximately a 333:1 turndown factor).

Raw test data (in the form of an Excel worksheet) were available for this data set. There are 45 steam-assisted test runs from the FHR AU flare raw test data. There are 46 steam-assisted test runs from the FHR LOU flare raw test data. Chemical composition for each test run, by test report, used in the steam data analysis described in this section 3.0 of this report is provided in Appendix E.

#### **A.8 Data Set H: Shell Deer Park East Property Flare (SDP EPF) (Shell Global Solutions (US) Inc., 2011a)**

PFTIR performance testing was conducted in March and April of 2010 on the Shell Deer Park refinery's East Property Flare in response to an EPA Office of Enforcement request pursuant to section 114 of the Clean Air Act. IMACC performed the testing. The primary objective of the SDP EPF testing was to obtain a better understanding of how the ratio of steam to vent gas at the flare combustion zone and the hydrogen content of the flare vent gas affect the combustion efficiency. The composition of the flare vent gas during testing was consistent with normal operation of the SDP EPF; flare vent gas constituents consisted of hydrogen, nitrogen, and methane, with minor contributions from other low-molecular weight paraffinic, olefinic, and aromatic hydrocarbons (chemical composition for each test run, by test report, used in the steam data analysis described in this section 3.0 of this report is provided in Appendix E).

The SDP EPF is an elevated steam-assisted flare. The current tip has an effective diameter of 36 inches and was installed in May 1990. This tip was manufactured by John Zink (model no. EEF-QA-36-C) and has two points of steam addition: center steam and upper steam. The center steam has a manufacturer minimum steam requirement of 1,500 pounds per hour; the upper steam has a manufacturer minimum steam requirement of 500 pounds per hour. The flare operated with 150 standard cubic feet per hour of pilot gas during the test runs. Typical flows at the SDP EPF are approximately 4 percent of the smokeless capacity of the flare and 1 percent of the maximum relief capacity.

Raw test data (in the form of an Excel worksheet) were available for this data set. There are 53 steam-assisted test runs from the raw test data. However, 11 of these test runs were noted in the test report as being part of an experiment for comparing PFTIR detectors and were removed from consideration (see Table A.3).

**Table A.3 Test Runs Explicitly Removed From Consideration**

Condition	Run Number	Reason for Omission
<b>Data Set H</b>		
[EP-D-2.0(MCT1)]		“Without a beam splitter IMACC could not use a MCT detector and an InSb detector at the same time. Since SDP has very limited means to control the composition of the SDP EPF vent gas, it was also impractical to recreate test conditions identical to those that occurred when SDP collected data with the InSb detector. Given these constraints, the only way to compare the MCT detector to the InSb detector was to gather as many data points as practical with the MCT detector at similar, but not identical, conditions as occurred when data were gathered with the InSb detector, and then compare the two data sets.” <sup>1</sup>
[EP-D-3.0(MCT1)]		
[EP-D-4.0(MCT1)]		
[EP-D-5.0(MCT1)]		
[EP-D-4.0(MCT2)]		
[EP-D-5.0(MCT2)]		
[EP-D-2.0(MCT2)]		
[EP-D-3.0(MCT2)]		
[EP-D-4.0(MCT3)]		
[EP-D-5.0(MCT3)]		
[EP-D-4.5(MCT)]		

<sup>1</sup> See page 19 of Section 2.1.4 of Shell Global Solutions (US) Inc., 2011a.

**2.9 Data Set I: Shell Deer Park Ground Flare (SDP GF) (Shell Global Solutions (US) Inc., 2011b)**

AFTIR performance testing was conducted in March and April of 2010 on the Shell Deer Park refinery’s Olefin Plant 3 Ground Flare in response to an EPA Office of Enforcement request pursuant to section 114 of the Clean Air Act. These tests were conducted with assistance from both Shell Global Solutions (US) Inc. and IMACC personnel. The primary objective of the SDP GF testing was to obtain a better understanding of how the ratio of steam to vent gas at the flare combustion zone and the hydrogen content of the flare vent gas affect combustion efficiency. The primary components of the SDP GF flare vent gas are hydrogen, nitrogen, methane, ethylene, propylene, and small quantities of higher molecular weight olefins, di-olefins, and aromatics.

The SDP GF is a multistage steam-assisted enclosed ground flare with three different stages, which become active at successively higher flows. The SDP GF was installed in 1978 and has 92 burners (basically a refractory lined steel shell into which 92 raw flare vent gas burners discharge). The flare has three stages. The first stage has eight, horizontally-mounted burners and eight pilots. The second stage has 24 horizontally-mounted burners and 24 pilots, while the last

stage has 60, horizontally-mounted burners and 30 pilots. The enclosed ground flare has eight faces. The horizontally-mounted burners are arranged in identical vertical drops, with four burners to a drop. The flare operated with a total of 150 standard cubic feet per hour pilot gas during the test runs.

Each of the 92 burners is manufactured by John Zink (model no. ZTOF SM-10 burners) and equipped with a steam injection system to inject high-pressure steam for cooling, to aid combustion, and to reduce smoke formation. A small amount of cooling steam is always routed to each of the SDP GF's 92 burners whether each burner has flare vent gas going to it or not. Steam enters the center of each burner via a "1" steam tip. The cooling steam is controlled by a restriction orifice in a by-pass line around the steam valve to each stage. This results in approximately 870 pounds per hour of cooling steam to the 92 burners, or approximately 9.46 pounds per hour per burner. At the time of testing, typical flow at the SDP GF was approximately 5,000 pounds per hour, or 5 percent of the maximum smokeless capacity. The flare vent gas flows used for the test runs required only the eight first stage burners.

Raw test data (in the form of an Excel worksheet) were available for this data set. There are 21 steam-assisted test runs from the raw test data.

## **2.10 Data Set J: TCEQ (Allen and Torres, 2011)**

In May 2009, the TCEQ contracted with The University of Texas at Austin to conduct a comprehensive flare study project on full-scale steam- and air-assist flares at the John Zink Company flare demonstration facility in Tulsa, Oklahoma. The gas used in this study included mixtures of propylene or propane supplemented with natural gas and diluted with nitrogen (chemical composition for each test run, by test report, used in the steam data analysis described in this section 3.0 of this report is provided in Appendix E). The purpose of the project was to conduct field tests to measure flare emissions and collect process and operational data in a semi-controlled environment to determine the relationship between flare design, operation, flare vent gas lower heating value and flow rate, destruction efficiency, and combustion efficiency.

Aerodyne Research, Inc., (ARI) was contracted to directly measure flare emissions at the end of the flare plume using extractive techniques, and calculate destruction and combustion efficiency based on those measurements. The study also evaluated the performance of remote sensing technologies against the extractive technique. These remote sensing technologies included Infrared Hyper-Spectral Imaging Technology (Contractor: Telops Inc.), PFTIR and AFTIR (Contractor: IMACC), and Forward Looking Infrared (FLIR) GasFindIR Passive Infrared (IR) Cameras (Contractor: Leak Surveys Inc.). The test report for data set J concludes that the mean difference and standard deviation of the reported AFTIR and PFTIR combustion efficiency values increase as the reported extractive combustion efficiency values decrease; however, both the AFTIR and PFTIR methods actually compare very well to the extractive test results for combustion efficiencies reported as 90 percent or greater. For combustion efficiencies reported as 90 percent or greater, the test report for data set J states that the mean difference of combustion efficiency values is less than 3.2 percent between extractive and AFTIR, and less than 3.5 percent between extractive and PFTIR.

The steam-assisted flare used in this study was a John Zink model EE-QSC-36" flare tip (flare tip effective diameter of 36 inches) with three EEP-503 pilots, and a maximum capacity of 937,000 pounds per hour. The center steam has a manufacturer minimum steam requirement of 300 pounds per hour; the upper steam has a manufacturer minimum steam requirement of 525 pounds per hour. The air-assisted flare was a John Zink model LHST-24/60 flare tip (flare tip effective diameter of 24 inches) with three pilots, and a maximum capacity of 144,000 pounds of propylene per hour. Both flares operated with 225 standard cubic feet per hour of pilot gas during the test runs.

Raw test data (in the form of an Excel worksheet) were available for this data set. There are 131 steam-assisted test runs and 89 air-assisted test runs from the raw test data.

*This information is distributed solely for the purpose of pre-dissemination peer review under applicable information quality guidelines. It has not been formally disseminated by EPA. It does not represent and should not be construed to represent any Agency determination or policy.*

## **APPENDIX B**

**Appendix B is an Excel workbook that combines all data sets. The Excel workbook identifies each specific test run by the exact test condition and run identification used in each individual report. Appendices C and D provide explanation and methodologies for how certain data fields in the workbook were determined.**

*This information is distributed solely for the purpose of pre-dissemination peer review under applicable information quality guidelines. It has not been formally disseminated by EPA. It does not represent and should not be construed to represent any Agency determination or policy.*

## **APPENDIX C**

### **Test Report Nomenclature Matrix**

**Table C-1. Test Report Nomenclature Matrix**

**KEY:**

“N/A” – not applicable. The specific parameter was not considered in the data set; or the specific parameter was not calculated.

“Unknown” –unable to calculate the specific parameter because there was not enough information provided in the test report and associated data set.

“Eq. D.##” –details from the test report and associated data set used to calculate the specific parameter. See Appendix D for detailed methodology; refer to the specific Equation identified in the matrix.

Data Set ID		A: EPA 2-83-052	B: EPA 2-84-095	C: EPA 2-85-106	D: MPC TX	E: INEOS	F: MPC Detroit	G1: FHR AU	G2: FHR LOU	H: SDP EPF	I: SDP GF	J: TCEQ
Basic Run Info	Reported Combustion Efficiency (CE) [%]	"Combustion Efficiency (%)"	"Combustion Efficiency (Percent)"	"Comb Eff. (%)"	"CE"	Run Avg. Relative Efficiency using Carbon Count	"CE (weighted) %"	"CE (weighted) %"	"CE (weighted) %"	"CE"	"Comb. Eff. Calculated ND@0 %"	"IMACC - PFTIR Avg. CE (%)"
	Flare Vent Gas Net Heating Value (NHV <sub>VG</sub> ) [Btu/scf]	"Lower Heating Value (Btu/SCF)"	"Low Heating Value (Btu/ft3)"	"Low Htg Val (Btu/ft3)"	"Vent Gas HV"	Eq. D.1	"Flare Gas NHV BTU/scf"	"VG NHV (calc) BTU/scf"	"VG NHV (calc) BTU/scf"	"East Property Flare Gas Net Heating Value (BTU/SCF)"	"OP3 Ground Flare Gas Net Heating Value BTU/SCF"	"Actual Vent Gas LHV Btu/scf"
General Flare Vent Gas Data	Flare Vent Gas Flow Rate (m <sub>vg</sub> ) [lb/hr]	Eq. D.2	N/A	Eq. D.3	"Vent Gas Flow Rate (lb/h)"	"Total Panametrics Flow in lbs/hr"	"Flare Gas Flow lb/hr"	"Flare Gas Flow (DCS) lb/hr"	"Flare Gas Flow (DCS) lb/hr"	"East Property Flare- Calculated Mass Flow (lb/hr)"	"Mass Flow OP3 Ground Flare Inst LB/HR"	"Actual Vent Gas (VG) Flow Rates--Total lb/hr"
	Flare Vent Gas Flow Rate (Q <sub>vg</sub> ) [scf/hr]	Eq. D.4	N/A	Eq. D.5	"Vent Gas Flow Rate (scfh)"	Eq. D.6	"Std Flare Gas Flow scf/hr"	Eq. D.7	"Std VG Flow (calc) scf/hr"	Eq. D.6	"OP3 Ground Flare Flow SCF/HR"	Eq. D.6
	Flare Vent Gas Velocity (V <sub>vg</sub> ) [ft/s]	Eq. D.8A	"Actual Exit Velocity (ft/sec)"	"Actual Exit Velocity (ft/sec)"	"Flare Tip Velocity"	Eq. D.8A	"Flare Tip Velocity ft/s"	"VG Exit Velocity (calc) ft/s"	"Tip Velocity (no steam) (calc) ft/s"	Vent gas velocity report in test report	"OP3 Ground Flare Exit Velocity FT/SEC"	Eq. D.8B

This information is distributed solely for the purpose of pre-dissemination peer review under applicable information quality guidelines. It has not been formally disseminated by EPA. It does not represent and should not be construed to represent any Agency determination or policy.

**Table C-1. Test Report Nomenclature Matrix (Continued)**

Data Set ID		A: EPA 2-83-052	B: EPA 2-84-095	C: EPA 2-85-106	D: MPC TX	E: INEOS	F: MPC Detroit	G1: FHR AU	G2: FHR LOU	H: SDP EPF	I: SDP GF	J: TCEQ
General Flare Vent Gas Data	Flare Vent Gas Velocity w/ Center Steam ( $V_{vg-s}$ ) [ft/s]	Eq. D.8C	Eq. D.8C	Eq. D.8C	Eq. D.8C	Eq. D.8C	Eq. D.8C	Eq. D.8C	Eq. D.8C	Eq. D.8C	Eq. D.8C	"Actual Vent Gas Exit Velocity fps"
	Flare Vent Gas Molecular Weight ( $MW_{vg}$ ) [lb/lb-mol]	Eq. D.9	N/A	Eq. D.9	"MWvg"	"Panametrics Measured MW"	"MWvg (GC calc) lb/lbmol"	"MWvg (calc) lb/lb-mol"	"MWvg (calc) lb/lb-mol"	"Vent Gas MW (lb/lb-mole)"	"OP3 Ground Flare MW LB/LB-MOL"	"Actual Vent Gas Mol Wt lb/lb-mole"
	Reported Pilot Gas Flow Rate ( $Q_{pg}$ ) [scf/hr]	Reported as 26.3 lb/hr in Test Report	No pilot gas	Reported as 2.1 scf/min for some runs in Test Report	Reported as 100 scf/hr in Test Report	Reported as 150 scf/hr in Test Report	Reported as 135 scf/hr in Test Report	"Pilot Gas Flow Rate (scf/hr)"	"Pilot Gas Flow Rate (scf/hr)"	No pilot gas	No pilot gas	Reported as 225 scf/hr in Test Report
Molar Percentage of Components in Flare Vent Gas [mol %]	1-Butene [mol %]	N/A	N/A	N/A	"Butenes mol%"	N/A	"i-Butene, Butene-1 mol %"	"Butene-1 (bag)"	N/A	"HRVOC EP FLARE_Butene1&Isobutane"	"OP3 GND Flare_Butene 1&Isobutane"	N/A
	1,2-Butadiene [mol %]	N/A	N/A	N/A	N/A	N/A	N/A	"1,2-Butadiene (bag)"	N/A	N/A	N/A	N/A
	1,3-Butadiene (% <sub>1,3-B</sub> ) [mol %]	N/A	N/A	N/A	"Butadiene mol%"	Eq. D.10	"1,3-Butadiene mol %"	"1,3-Butadiene (bag)"	"Butadiene (GC) mol%"	"HRVOC EP FLARE_13BD"	"OP3 GND Flare_13BD"	N/A
	Acetylene [mol %]	N/A	N/A	N/A	"Acetylene mol%"	N/A	"Acetylene mol %"	"Acetylene (bag)"	N/A	"HRVOC EP FLARE_Acetylene"	"OP3 GND Flare_Acetylene"	N/A
	Benzene [mol %]	N/A	N/A	N/A	N/A	N/A	N/A	"Benzene (bag)"	"Benzene (GC) mol%"	N/A	"Benzene"	N/A
	Carbon Dioxide [mol %]	N/A	N/A	N/A	"CO2 mol%"	N/A	"Carbon Dioxide mol %"	"Carbon Dioxide (bag)"	"Carbon Dioxide (GC) mol%"	"HRVOC EP FLARE_Carbon Dioxide"	"OP3 GND Flare_Carbon Dioxide"	N/A
	Carbon Monoxide [mol %]	N/A	N/A	N/A	"CO mol%"	N/A	"Carbon Monoxide mol %"	N/A	"Carbon Monoxide (GC) mol%"	"HRVOC EP FLARE_Carbon Monoxide"	"OP3 GND Flare_Carbon Monoxide"	N/A

This information is distributed solely for the purpose of pre-dissemination peer review under applicable information quality guidelines. It has not been formally disseminated by EPA. It does not represent and should not be construed to represent any Agency determination or policy.

**Table C-1. Test Report Nomenclature Matrix (Continued)**

Data Set ID		A: EPA 2-83-052	B: EPA 2-84-095	C: EPA 2-85-106	D: MPC TX	E: INEOS	F: MPC Detroit	G1: FHR AU	G2: FHR LOU	H: SDP EPF	I: SDP GF	J: TCEQ
Molar Percentage of Components in Flare Vent Gas [mol %]	Cis-2-Butene [mol %]	N/A	N/A	N/A	"Cis-2-Butene mol%"	N/A	"Cis-Butene-2 mol%"	"Cis-Butene-2 (bag)"	"2-Butene (GC) mol%"	"HRVOC EP FLARE_Cis2Butene"	"OP3 GND Flare_Cis2Butene"	N/A
	Cyclopropane [mol %]	N/A	N/A	N/A	N/A	N/A	N/A	"Cyclopropane (bag)"	N/A	N/A	N/A	N/A
	Ethane [mol %]	N/A	N/A	N/A	"Ethane mol%"	N/A	"Ethane mol %"	"Ethane (bag)"	"Ethane (GC) mol%"	"HRVOC EP FLARE_Ethane"	"OP3 GND Flare_Ethane"	N/A
	Ethyl Benzene [mol %]	N/A	N/A	N/A	N/A	N/A	N/A	N/A	"Ethylbenzene (GC) mol%"	N/A	"Ethylbenzene"	N/A
	Ethylene [mol %]	N/A	N/A	N/A	"Ethylene mol%"	N/A	"Ethylene mol %"	"Ethylene (bag)"	"Ethylene (GC) mol%"	"HRVOC EP FLARE_Ethylene"	"OP3 GND Flare_Ethylene"	N/A
	Hydrogen [mol %]	N/A	N/A	N/A	"H2 mol%"	N/A	"Hydrogen mol %"	"Hydrogen (bag)"	"Hydrogen (GC) mol%"	"HRVOC EP FLARE_Hydrogen"	"OP3 GND Flare_Hydrogen"	N/A
	Hydrogen Sulfide [mol %]	N/A	N/A	N/A	N/A	N/A	N/A	N/A	N/A	"HRVOC EP FLARE_Hydrogen Sulfide"	"OP3 GND Flare_Hydrogen Sulfide"	N/A
	Iso-Butane [mol %]	N/A	N/A	N/A	"Iso-Butane mol%"	N/A	"Iso-Butane mol %"	"Isobutane (bag)"	"i-Butane (GC) mol%"	"HRVOC EP FLARE_IsoButane"	"OP3 GND Flare_IsoButane"	N/A
	Iso-Butylene [mol %]	N/A	N/A	N/A	N/A	N/A	N/A	"Isobutylene (bag)"	"iso-butylene (GC) mol%"	N/A	N/A	N/A
	Methane [mol %]	N/A	N/A	N/A	"CH4 mol%"	Eq. D.11	"Methane mol %"	"Methane (bag)"	"Methane (GC) mol%"	"HRVOC EP FLARE_Methane"	"OP3 GND Flare_Methane"	"Methane [mol %]"
	Methyl Acetylene [mol %]	N/A	N/A	N/A	N/A	N/A	N/A	"Methyl Acetylene (bag)"	N/A	N/A	N/A	N/A
n-Butane [mol %]	N/A	N/A	N/A	"N-Butane mol%"	N/A	"Normal Butane mol %"	"N-Butane (bag)"	"n-Butane (GC) mol%"	"HRVOC EP FLARE_Butane"	"OP3 GND Flare_Butane"	N/A	

This information is distributed solely for the purpose of pre-dissemination peer review under applicable information quality guidelines. It has not been formally disseminated by EPA. It does not represent and should not be construed to represent any Agency determination or policy.

**Table C-1. Test Report Nomenclature Matrix (Continued)**

Data Set ID	A: EPA 2-83-052	B: EPA 2-84-095	C: EPA 2-85-106	D: MPC TX	E: INEOS	F: MPC Detroit	G1: FHR AU	G2: FHR LOU	H: SDP EPF	I: SDP GF	J: TCEQ	
Molar Percentage of Components in Flare Vent Gas [mol %]	Nitrogen (% <sub>N</sub> ) [mol %]	Eq. D.14	N/A	Eq. D.13	"N2 mol%"	Eq. D.12	"Nitrogen mol %"	"Nitrogen (bag)"	"Nitrogen (GC) mol%"	"HRVOC EP FLARE_Nitrogen"	"OP3 GND Flare_Nitrogen"	"Nitrogen [mol %]"
	Oxygen [mol %]	N/A	N/A	N/A	"O2 mol%"	N/A	"Oxygen mol %"	"Oxygen (bag)"	"Oxygen (GC) mol%"	"HRVOC EP FLARE_Oxygen"	"OP3 GND Flare_Oxygen"	N/A
	Pentane Plus (C5+) [mol %]	N/A	N/A	N/A	"C5+ mol%"	N/A	"Pentane-Plus (C5+) mol %"	"C5 & Heavier Hydrocarbons (bag)"	"Pentane 5+ (GC) mol%"	"HRVOC EP FLARE_C5+"	"OP3 GND Flare_C5+"	N/A
	Propadiene [mol %]	N/A	N/A	N/A	N/A	N/A	N/A	"Propadiene (bag)"	N/A	N/A	N/A	N/A
	Propane (% <sub>p</sub> ) [mol %]	N/A	N/A	"% Propane in Nitrogen"	"Propane mol%"	N/A	"Propane mol %"	"Propane (bag)"	"Propane (GC) mol%"	"HRVOC EP FLARE_Propane"	"OP3 GND Flare_Propane"	"Propane [mol %]"
	Propylene [mol %]	Eq. D.14	N/A	N/A	"Propylene mol%"	N/A	"Propylene mol %"	"Propylene (bag)"	"Propylene (GC) mol%"	"HRVOC EP FLARE_Propylene"	"OP3 GND Flare_Propylene"	"Propylene [mol %]"
	Toluene [mol %]	N/A	N/A	N/A	N/A	N/A	N/A	N/A	"Toluene (GC) mol%"	N/A	"Toluene"	N/A
	Trans-2-Butene [mol %]	N/A	N/A	N/A	"Trans-2-Butene mol%"	N/A	"Trans-Butene-2 mol %"	"Trans-Butene-2 (bag)"	N/A	"HRVOC EP FLARE_Trans2Butene"	"OP3 GND Flare_Trans2 Butene"	N/A
	Water [mol %]	N/A	N/A	N/A	"Water mol%"	N/A	N/A	N/A	N/A	"HRVOC EP FLARE_Water"	"OP3 GND Flare_Water"	N/A
	Xylenes [mol %]	N/A	N/A	N/A	N/A	N/A	N/A	N/A	N/A	N/A	"Xylene's"	N/A

This information is distributed solely for the purpose of pre-dissemination peer review under applicable information quality guidelines. It has not been formally disseminated by EPA. It does not represent and should not be construed to represent any Agency determination or policy.

**Table C-1. Test Report Nomenclature Matrix (Continued)**

Data Set ID		A: EPA 2-83-052	B: EPA 2-84-095	C: EPA 2-85-106	D: MPC TX	E: INEOS	F: MPC Detroit	G1: FHR AU	G2: FHR LOU	H: SDP EPF	I: SDP GF	J: TCEQ
Steam Data	TOTAL Volumetric Steam Rate (Q <sub>s</sub> ) [scf/hr]	Eq. D.18	N/A	Eq. D.18	Eq. D.18	Eq. D.18	Eq. D.18	"Std Steam Flow (calc) scf/hr"	"Std Steam Flow (calc) scf/hr"	Eq. D.18	N/A	Eq. D.18
	TOTAL Mass Steam Rate (m <sub>s</sub> ) [lb/hr]	"Steam Flow (lbs/hr)"	N/A	140 lb/hr Constant	"Steam Flow (lb/h)"	Eq. D.19	"Steam Flow lb/hr"	"Steam Flow (DCS) lb/hr"	Eq. D.17	Eq. D.17	N/A	"Actual Steam Flow Rates-- Total lb/hr"
	Lower Volumetric Steam Rate (Q <sub>l</sub> ) [scf/hr]	N/A	N/A	N/A	Unknown	N/A	N/A	N/A	Eq. D.20	N/A	N/A	N/A
	Lower Mass Steam Rate (m <sub>l</sub> ) [lb/hr]	N/A	N/A	N/A	Unknown	N/A	N/A	N/A	Eq. D.19	N/A	N/A	N/A
	Center Volumetric Steam Rate (Q <sub>c</sub> ) [scf/hr]	N/A	N/A	N/A	Unknown	N/A	Eq. D.18	Eq. D.18	Eq. D.18	Unknown	Unknown	Eq. D.18
	Center Mass Steam Rate (m <sub>c</sub> ) [lb/hr]	N/A	N/A	N/A	Unknown	N/A	300 lb/hr Constant	500 lb/hr Constant	2,890 lb/hr Constant	Unknown	Unknown	"Actual Steam Flow Rates-- Center lb/hr"
	Ring Volumetric Steam Rate (Q <sub>r</sub> ) [scf/hr]	N/A	N/A	N/A	N/A	N/A	Eq. D.20	Eq. D.20	N/A	N/A	N/A	N/A
	Ring Mass Steam Rate (m <sub>r</sub> ) [lb/hr]	N/A	N/A	N/A	N/A	N/A	Eq. D.19	Eq. D.19	N/A	N/A	N/A	N/A
	Upper Volumetric Steam Rate (Q <sub>u</sub> ) [scf/hr]	Eq. D.20	N/A	Eq. D.18	N/A	Eq. D.18	N/A	N/A	N/A	Unknown	N/A	Eq. D.18

This information is distributed solely for the purpose of pre-dissemination peer review under applicable information quality guidelines. It has not been formally disseminated by EPA. It does not represent and should not be construed to represent any Agency determination or policy.

**Table C-1. Test Report Nomenclature Matrix (Continued)**

Data Set ID		A: EPA 2-83-052	B: EPA 2-84-095	C: EPA 2-85-106	D: MPC TX	E: INEOS	F: MPC Detroit	G1: FHR AU	G2: FHR LOU	H: SDP EPF	I: SDP GF	J: TCEQ
Steam Data	Upper Mass Steam Rate ( $m_i$ ) [lb/hr]	"Steam Flow (lbs/hr)"	N/A	140 lb/hr Constant	N/A	"Steam flow in lbs/hr primer"	N/A	N/A	N/A	Unknown	N/A	"Actual Steam Flow Rates-- Upper lb/hr"
	Steam-to-vent-gas ratio by weight ( $S/V_{G_{wt}}$ ) [lb steam/lb vent gas]	Eq. D.21A	N/A	Eq. D.21A	Eq. D.21A	Eq. D.21A	Eq. D.21A	Eq. D.21A	Eq. D.21A	Eq. D.21A	N/A	"Assist Ratio Steam / VG Flow Rate"
	Steam-to-vent-gas ratio by volume ( $S/V_{G_{vol}}$ ) [scf steam/scf vent gas]	Eq. D.21B	N/A	Eq. D.21B	Eq. D.21B	Eq. D.21B	Eq. D.21B	Eq. D.21B	Eq. D.21B	Eq. D.21B	Eq. D.21B	Eq. D.21B
	Steam-to-hydrocarbon ratio by volume ( $S/HC_{vol}$ ) [scf steam/scf HC]	Eq. D.21C	N/A	Eq. D.21C	Eq. D.21C	Eq. D.21C	Eq. D.21C	Eq. D.21C	Eq. D.21C	Eq. D.21C	Eq. D.21C	Eq. D.21C
Air Data	Air Assist Flow Rate ( $m_{Air}$ ) [lb/hr]	N/A	N/A	N/A	N/A	N/A	N/A	N/A	N/A	N/A	N/A	"Air Assist Flow Rate lb/hr"
	Air Assist Flow Rate ( $Q_{Air}$ ) [scf/hr]	N/A	N/A	"Air Assist Flow Rate SCFH"	N/A	N/A	N/A	N/A	N/A	N/A	N/A	"Air Assist Flow Rate SCFH"
Volumetric Flow Rates For Each Flare Vent Gas Component In The Combustion Zone ( $Q_{CZ,i}$ ) [scf/hr]		Eq. D.15B	N/A	Eq. D.15A	Eq. D.15A	Eq. D.15C and Eq. D.15D	Eq. D.15A	Eq. D.15A	Eq. D.15A	Eq. D.15A	N/A	Eq. D.15A
Concentration Of Each Flare Vent Gas Component In The Combustion Zone ( $X_{CZ,i}$ ) [volume fraction]		Eq. D.16A	N/A	Eq. D.16A	Eq. D.16A	Eq. D.16A	Eq. D.16A	Eq. D.16A	Eq. D.16A	Eq. D.16A	N/A	Eq. D.16A

**Table C-1. Test Report Nomenclature Matrix (Continued)**

Data Set ID		A: EPA 2-83-052	B: EPA 2-84-095	C: EPA 2-85-106	D: MPC TX	E: INEOS	F: MPC Detroit	G1: FHR AU	G2: FHR LOU	H: SDP EPF	I: SDP GF	J: TCEQ
Concentration of Each Flare Vent Gas Combustible Component (VGe) [volume fraction]		Eq. 16B	Eq. 16B	Eq. 16B	Eq. 16B	Eq. 16B	Eq. 16B	Eq. 16B	Eq. 16B	Eq. 16B	Eq. 16B	Eq. 16B
Concentration of Each Flare Vent Gas and Center Steam Only Component (X <sub>vgcs</sub> ) [volume fraction]		Eq.16C	Eq.16C	Eq.16C	Eq.16C	Eq.16C	Eq.16C	Eq.16C	Eq.16C	Eq.16C	Eq.16C	Eq.16C
Dynamic NHV <sub>CZ</sub> Calculation	Ratio of NHV <sub>CZ</sub> to NHVLFL-VG (NHV <sub>ratio</sub> ) [unitless]	Eq. D.22	N/A	Eq. D.22	Eq. D.22	Eq. D.22	Eq. D.22	Eq. D.22	Eq. D.22	Eq. D.22	N/A	Eq. D.22
	Net Heating Value of Combustion Zone Gas (NHV <sub>CZ</sub> ) [BTU/scf]	Eq. D.23	N/A	Eq. D.23	Eq. D.23	Eq. D.23	Eq. D.23	Eq. D.23	Eq. D.23	Eq. D.23	N/A	Eq. D.23
	Net Heating Value of Vent Gas if Diluted to Lower Flammability Limit (NHV <sub>VG-LFL</sub> ) [BTU/scf]	Eq. D.24	N/A	Eq. D.24	Eq. D.24	Eq. D.24	Eq. D.24	Eq. D.24	Eq. D.24	Eq. D.24	N/A	Eq. D.24
	Lower Flammability Limit of Vent Gas Adjusted for Nitrogen Equivalency (LFL <sub>VG</sub> ) [vol frac]	Eq. D.25	N/A	Eq. D.25	Eq. D.25	Eq. D.25	Eq. D.25	Eq. D.25	Eq. D.25	Eq. D.25	N/A	Eq. D.25

**Table C-1. Test Report Nomenclature Matrix (Continued)**

Data Set ID		A: EPA 2-83-052	B: EPA 2-84-095	C: EPA 2-85-106	D: MPC TX	E: INEOS	F: MPC Detroit	G1: FHR AU	G2: FHR LOU	H: SDP EPF	I: SDP GF	J: TCEQ
LFL <sub>CZG</sub> calculation	Combustible Components in the Combustion Zone (C <sub>CZ</sub> ) [vol frac]	<i>Eq. D.26</i>	<i>N/A</i>	<i>Eq. D.26</i>	<i>Eq. D.26</i>	<i>Eq. D.26</i>	<i>Eq. D.26</i>	<i>Eq. D.26</i>	<i>Eq. D.26</i>	<i>Eq. D.26</i>	<i>N/A</i>	<i>Eq. D.26</i>
	Coefficient of Nitrogen Equivalency of Water Relative to Nitrogen (N <sub>e,H2O</sub> )	<i>Eq. D.29</i>	<i>N/A</i>	<i>Eq. D.29</i>	<i>Eq. D.29</i>	<i>Eq. D.29</i>	<i>Eq. D.29</i>	<i>Eq. D.29</i>	<i>Eq. D.29</i>	<i>Eq. D.29</i>	<i>N/A</i>	<i>Eq. D.29</i>
	Coefficient of Nitrogen Equivalency of Carbon Dioxide Relative to Nitrogen (N <sub>e,CO2</sub> )	<i>Eq. D.29</i>	<i>N/A</i>	<i>Eq. D.29</i>	<i>Eq. D.29</i>	<i>Eq. D.29</i>	<i>Eq. D.29</i>	<i>Eq. D.29</i>	<i>Eq. D.29</i>	<i>Eq. D.29</i>	<i>N/A</i>	<i>Eq. D.29</i>
	Lower Flammability Limit of Combustion Zone Gas Adjusted for Nitrogen Equivalency (LFL <sub>CZ</sub> ) [vol frac]	<i>Eq. D.27</i>	<i>N/A</i>	<i>Eq. D.27</i>	<i>Eq. D.27</i>	<i>Eq. D.27</i>	<i>Eq. D.27</i>	<i>Eq. D.27</i>	<i>Eq. D.27</i>	<i>Eq. D.27</i>	<i>N/A</i>	<i>Eq. D.27</i>

This information is distributed solely for the purpose of pre-dissemination peer review under applicable information quality guidelines. It has not been formally disseminated by EPA. It does not represent and should not be construed to represent any Agency determination or policy.

**Table C-1. Test Report Nomenclature Matrix (Continued)**

Data Set ID		A: EPA 2-83-052	B: EPA 2-84-095	C: EPA 2-85-106	D: MPC TX	E: INEOS	F: MPC Detroit	G1: FHR AU	G2: FHR LOU	H: SDP EPF	I: SDP GF	J: TCEQ
Stoichiometric Air Ratio Calculation	Theoretical Stoichiometric Mass of Air Needed to Combust the Flare Vent Gas ( $m_{Stoic}$ ) [lb/hr]	N/A	N/A	Eq. D.31 through Eq. 37	N/A	N/A	N/A	N/A	N/A	N/A	N/A	Eq. D.31 through Eq. 33
	Calculated Ratio of Actual Mass Flow of Total Assist Air to the Theoretical Stoichiometric Mass of Air Needed to Combust the Flare Vent Gas ( $m_{Air} / m_{Stoic}$ ) (SR)	N/A	N/A	Eq. D.30	N/A	N/A	N/A	N/A	N/A	N/A	N/A	Eq. D.30
	Reported ( $m_{Air} / m_{Stoic}$ ) (SR)	N/A	N/A	"Air-Assist SR"	N/A	N/A	N/A	N/A	N/A	N/A	N/A	"Excess Air SR"

**Table C-1. Test Report Nomenclature Matrix (Continued)**

Data Set ID		A: EPA 2-83-052	B: EPA 2-84-095	C: EPA 2-85-106	D: MPC TX	E: INEOS	F: MPC Detroit	G1: FHR AU	G2: FHR LOU	H: SDP EPF	I: SDP GF	J: TCEQ
MFR Calculation	Reported MFR [unitless]	N/A	N/A	N/A	"MFR"	N/A	"Momentum Flux Ratio"	"Momentum Flux Ratio (calc)"	"Momentum Flux Ratio (calc)"	N/A	N/A	"Momentum Flux Ratio"
	Flare Vent Gas Flow Rate Including Center Steam ( $m_{vg-s}$ ) [lb/hr]	Eq. D.38	N/A	N/A	Eq. D.38	Eq. D.38	Eq. D.38	Eq. D.38	Eq. D.38	N/A	N/A	Eq. D.38
	Density of Flare Vent Gas Including Center Steam ( $p_{vg-s}$ ) [lb/scf]	Eq. D.39	N/A	N/A	Eq. D.39	Eq. D.39	Eq. D.39	Eq. D.39	Eq. D.39	N/A	N/A	Eq. D.39
	Wind Velocity ( $V_{wind}$ ) [ft/s]	N/A	N/A	N/A	Eq. D.40	N/A	Eq. D.40	Eq. D.40	Eq. D.40	N/A	N/A	Eq. D.40
	Calculated MFR [unitless]	N/A	N/A	N/A	Eq. D.41	N/A	Eq. D.41	Eq. D.41	Eq. D.41	N/A	N/A	Eq. D.41

**Table C-1. Test Report Nomenclature Matrix (Continued)**

Data Set ID		A: EPA 2-83-052	B: EPA 2-84-095	C: EPA 2-85-106	D: MPC TX	E: INEOS	F: MPC Detroit	G1: FHR AU	G2: FHR LOU	H: SDP EPF	I: SDP GF	J: TCEQ
Shore Equation Analysis	Shore Equation Velocity-Jet Periphery ( $U_o/[D_o]$ ) [sec <sup>-1</sup> ]	Eq. D.42	N/A	Eq. D.42	Eq. D.42	Eq. D.42	Eq. D.42	Eq. D.42	Eq. D.42	N/A	N/A	Eq. D.42
	Lower Flammability Limit of Flare Vent Gas Including Center Steam Adjusted for Nitrogen Equivalency ( $LFL_{vrgcs}$ ) [vol frac]	Eq. D.43	N/A	Eq. D.43	Eq. D.43	Eq. D.43	Eq. D.43	Eq. D.43	Eq. D.43	N/A	N/A	Eq. D.43
	Shore Equation ( $R_{AM}$ ) [lb flare vent gas including center steam / lb of air]	Eq. D.44	N/A	Eq. D.44	Eq. D.44	Eq. D.44	Eq. D.44	Eq. D.44	Eq. D.44	N/A	N/A	Eq. D.44
	Maximum Allowable Flare Vent Gas Velocity Including Center Steam ( $V_{max}$ ) [ft/s]	Eq. D.45	N/A	Eq. D.45	Eq. D.45	Eq. D.45	Eq. D.45	Eq. D.45	Eq. D.45	N/A	N/A	Eq. D.45

*This information is distributed solely for the purpose of pre-dissemination peer review under applicable information quality guidelines. It has not been formally disseminated by EPA. It does not represent and should not be construed to represent any Agency determination or policy.*

## **APPENDIX D**

**Appendix D is a detailed list of all equations used in the Excel file.**

## **APPENDIX D – CALCULATIONS**

### **INTRODUCTION**

Appendix D provides detailed calculation methodologies for the specific parameters identified in the Appendix C matrix. If a cell is labeled as “Eq. D.##” in the Appendix C matrix, the specific calculation methodology can be found here in Appendix D. As such, the equations presented in Appendix D were used only for the indicated data sets. See Table 1 in Section 2.0 of the memo to identify the test report associated with each data set. If a particular data set is not identified in the equation in this appendix, it means that the corresponding parameter was included in the test report (and no calculation was necessary).

### Equation D.1

**The flare vent gas net heating value ( $NHV_{VG}$ ), in Btu/scf, was calculated using Equation D.1.**

*This equation was only used for data set E. The reported  $NHV_{VG}$  from the associated test report was used for all other data sets. It was assumed that the reported values used this equation as a basis. The net heating value of the flare vent gas is the sum of the net heat of combustion of each individual combustible component.*

$$NHV_{VG} = \sum_{i=1}^n \left( \frac{\%_{vg,i}}{100} \right) NHV_i$$

Where:

- $NHV_{VG}$  = Flare vent gas net heating value, BTU/scf.
- $i$  = Individual combustible component in flare vent gas.
- $n$  = Number of individual combustible components in flare vent gas.
- $\%_{vg,i}$  = Percentage of combustible component  $i$  in flare vent gas (i.e., 1,3-Butadiene and Natural Gas), volumetric percentage. (See Equations D.10 through D.12).
- 100 = Constant, percentage.
- $NHV_i$  = Reported net heating value of combustible component  $i$ , BTU/scf.

### Equations D.2 and D.3

**If not reported, the flare vent gas flow rate ( $m_{vg}$ ), in lb/hr, was calculated using either Equation D.2 or D.3.**

Equation D.2:

*This equation was used for data set A.*

$$m_{vg} = m_p + m_{N2}$$

Where:

$m_{vg}$  = Flare vent gas flow rate, lb/hr.

$m_p$  = Reported mass flow rate of combustible components (i.e., Propylene Flow) in flare vent gas, lb/hr.

$m_{N2}$  = Reported mass flow rate of nitrogen (i.e., Nitrogen Flow) in flare vent gas, lb/hr.

Equation D.3:

*This equation was used for data set C.*

$$m_{vg} = MW_{vg} * \left( \frac{Q_{vg}}{379.48} \right)$$

Where:

$m_{vg}$  = Flare vent gas flow rate, lb/hr.

$MW_{vg}$  = Molecular weight of flare vent gas, lb/lb-mole. (See Equation D.9).

$Q_{vg}$  = Flare vent gas flow rate, scf/hr. (See Equation D.4).

379.48 = Constant, lb-mole/scf at dry standard conditions.

### Equations D.4 through D.7

**If not reported, the flare vent gas flow rate ( $Q_{vg}$ ), in scf/hr, was calculated using one of the Equations D.4 through D.7.**

Equation D.4:

*This equation was used for data set A.*

$$Q_{vg} = 60 * (Q_p + Q_{N2})$$

Where:

- $Q_{vg}$  = Flare vent gas flow rate, scf/hr.
- 60 = Constant, min/hr.
- $Q_p$  = Reported volumetric flow rate of propylene (i.e., Propylene Flow), scf/min.
- $Q_{N2}$  = Reported volumetric flow rate of nitrogen (i.e., Nitrogen Flow), scf/min.

Equation D.5:

*This equation was used for data set C.*

$$Q_{vg} = 379.48 * \left[ \frac{\left( \frac{m_s}{SF} \right)}{\left( \frac{\%_p}{100} \right) + \left( \frac{\%_N}{100} \right)} \right]$$

Where:

- $Q_{vg}$  = Flare vent gas flowrate, scf/hr.
- 379.48 = Constant, lb-mole/scf at dry standard conditions.
- $m_s$  = Reported total steam rate (i.e., Steam Flowrate), lb/hr.
- SF = Reported steam ratio (i.e., Steam Ratio), lb steam / lb fuel.
- $\%_p$  = Reported percentage of propane in flare vent gas (i.e., %Propane in Nitrogen), molar percentage.
- $\%_N$  = Percentage of nitrogen in flare vent gas, molar percentage. (See Equation D.13).
- 100 = Constant, molar percentage.

### Equations D.4 through D.7 (Continued)

#### Equation D.6:

*This equation was used for data sets E, H, and J.*

$$Q_{vg} = 379.48 * \left( \frac{m_{vg}}{MW_{vg}} \right)$$

Where:

- $Q_{vg}$  = Flare vent gas flow rate, scf/hr.  
 $379.48$  = Constant, lb-mole/scf at dry standard conditions.  
 $m_{vg}$  = Reported flare vent gas flow rate, lb/hr.  
*Reported for data set E as "Total Panametrics Flow in lbs/hr."*  
*Reported for data set H as "East Property Flare – Calculated Mass Flow (lb/hr)."*  
*Reported for data set J as "Actual Vent Gas (VG) Flow Rates, Total (lb/hr)."*  
 $MW_{vg}$  = Reported molecular weight of flare vent gas, lb/lb-mole.  
*Reported for data set E as "Panametrics Measured MW."*  
*Reported for data set H as "East Property Flare Gas Molecular Weight (lb/lbmole)."*  
*Reported for data set J as "Actual Vent Gas Mol Wt (lb/lb-mole)."*

#### Equation D.7:

*This equation was used for data set G1.*

$$Q_{vg} = Q_{vg,reported} * 1,000$$

Where:

- $Q_{vg}$  = Flare vent gas flow rate, scf/hr.  
 $Q_{vg,reported}$  = Reported flare vent gas flow rate (i.e., Vol Flare Gas Flow (DCS)), kscf/hr.  
 $1,000$  = Constant, scf/kscf.

### Equation D.8A and D.8B

**If not reported, the flare vent gas velocity ( $V_{vg}$ ), in ft/s, was calculated using Equation D.8A or Equation D.8B.**

Equation D.8A:

*This equation was used for data sets A and E.*

$$V_{vg} = \frac{V_{vg,reported}}{60}$$

Where:

- $V_{vg}$  = Flare vent gas velocity, ft/s.
- $V_{vg,reported}$  = Reported flare vent gas velocity, ft/min.  
Reported for data set A as "Relief Gas Flow (SCFM)."  
Reported for data set E as "Exit Velocity in ft/min."
- 60 = Constant, s/min.

Equation D.8B:

*This equation was used for data set J.*

$$V_{vg} = V_{vg-s} - \left( \frac{Q_c}{\left(\frac{\pi}{4}\right) * \left(\frac{d_{ft}}{12}\right)^2 * 60 * 60} \right)$$

Where:

- $V_{vg}$  = Flare vent gas velocity, ft/s.
- $V_{vg-s}$  = Reported flare vent gas velocity with center steam (i.e., Actual Vent Gas Exit Velocity (fps), Includes Center Steam), ft/s.
- $Q_c$  = Center steam rate, scf/hr. (See Equation D.18 for data sets F, G1 and G2).
- $\pi/4$  = Constant, used to calculate area of flare tip.
- $d_{ft}$  = Reported effective diameter of flare tip, in. (See tip sizes identified in Section 2.0 of report).
- 12 = Constant, in/ft.
- 60 = Constant, s/min.
- 60 = Constant, min/hr.

### Equation D.8C

**If not reported, the flare vent gas velocity with center steam ( $V_{vg-s}$ ), in ft/s, was calculated using Equation D.8C. For data sets A, B, C, E, and I that are without a center steam rate ( $Q_c$ ) or for data set H that has an unknown center steam rate ( $Q_c$ ), the flare vent gas velocity with center steam ( $V_{vg-s}$ ) is equal to flare vent gas velocity ( $V_{vg}$ ).**

#### Equation D.8C:

*This equation was used for data sets A, B, C, D, E, F, G1, G2, H and I.*

$$V_{vg-s} = V_{vg} + \left( \frac{Q_c}{\left(\frac{\pi}{4}\right) * \left(\frac{d_{ft}}{12}\right)^2 * 60 * 60} \right)$$

#### Where:

- $V_{vg-s}$  = Flare vent gas velocity with center steam, ft/s.
- $V_{vg}$  = Flare vent gas velocity, ft/s. (See Equation D.8A for data sets A and E).
- $Q_c$  = Center steam rate, scf/hr. (See Equation D.18 for data sets F, G1 and G2).
- $\pi/4$  = Constant, used to calculate area of flare tip.
- $d_{ft}$  = Reported effective diameter of flare tip, in. (See tip sizes identified in Section 2.0 of report).
- 12 = Constant, in/ft.
- 60 = Constant, s/min.
- 60 = Constant, min/hr.

### Equation D.9

**If not reported, the flare vent gas molecular weight ( $MW_{vg}$ ), in lb/lb-mol, was calculated using Equation D.9.**

*This equation was used for data sets A and C.*

$$MW_{vg} = \sum_{j=1}^n \left( \frac{\%_{vg,j}}{100} \right) MW_j$$

Where:

- $MW_{vg}$  = Flare vent gas molecular weight, lb/lb-mole.
- $j$  = Individual combustible or inert component in flare vent gas.
- $n$  = Number of individual components in flare vent gas.
- $\%_{vg,i}$  = Percentage of component  $j$  in flare vent gas, molar percentage.  
(See Equation D.14 for data set A and Equation D.13 for data set C).
- 100 = Constant, percentage.
- $MW_j$  = Molecular weight of component  $j$ , lb/lb-mole.

### Equations D.10 through D.12

**For data set E, the percentages of 1,3-butadiene ( $\%_{1,3-B}$ ), natural gas ( $\%_{NG}$ ), and nitrogen ( $\%_N$ ) in the flare vent gas, in volumetric percentage, were calculated using Equations D.10 through D.12, respectively.**

Equation D.10:

$$\%_{1,3-B} = 100 \left( \frac{Q_{1,3-B}}{Q_{1,3-B} + Q_N + Q_{NG}} \right)$$

Where:

- $\%_{1,3-B}$  = Percentage of 1,3-Butadiene in flare vent gas, volumetric percentage.
- 100 = Constant, percentage.
- $Q_{1,3-B}$  = Volumetric flow rate of 1,3-Butadiene, scf/hr. (See Equation D.15C).
- $Q_N$  = Volumetric flow rate of nitrogen, scf/hr. (See Equation D.15D).
- $Q_{NG}$  = Reported volumetric flow rate of supplemental natural gas (i.e., Nat Gas flow in SCFH), scf/hr.

Equation D.11:

$$\%_{NG} = 100 \left( \frac{Q_{NG}}{Q_{1,3-B} + Q_N + Q_{NG}} \right)$$

Where:

- $\%_{NG}$  = Percentage of natural gas in flare vent gas, volumetric percentage.
- 100 = Constant, percentage.
- $Q_{1,3-B}$  = Volumetric flow rate of 1,3-Butadiene, scf/hr. (See Equation D.15C).
- $Q_N$  = Volumetric flow rate of nitrogen, scf/hr. (See Equation D.15D).
- $Q_{NG}$  = Reported volumetric flow rate of supplemental natural gas (i.e., Nat Gas flow in SCFH), scf/hr.

Equation D.12:

$$\%_N = 100 \left( \frac{Q_N}{Q_{1,3-B} + Q_N + Q_{NG}} \right)$$

Where:

- $\%_N$  = Percentage of nitrogen in flare vent gas, volumetric percentage.
- 100 = Constant, percentage.
- $Q_{1,3-B}$  = Volumetric flow rate of 1,3-Butadiene, scf/hr. (See Equation D.15C).
- $Q_N$  = Volumetric flow rate of nitrogen, scf/hr. (See Equation D.15D).
- $Q_{NG}$  = Reported volumetric flow rate of supplemental natural gas (i.e., Nat Gas flow in SCFH), scf/hr.

### **Equation D.13**

**For data set C, the percentage of nitrogen in the flare vent gas ( $\%_N$ ), in molar percentage, was calculated using Equation D.13.**

$$\%_N = 100 - \%_P$$

Where:

$\%_N$  = Percentage of nitrogen in flare vent gas, molar percentage.

100 = Constant, percentage.

$\%_P$  = Reported percentage of propane in flare vent gas (i.e., %Propane in Nitrogen), molar percentage.

### Equation D.14

**For data set A, the percentage of component (propylene or nitrogen) in the flare vent gas (%<sub>j</sub>), in molar percentage, was calculated using Equation D.14.**

$$\%_{j1} = 100 \left( \frac{m_{j1}}{m_{j1} + m_{j2}} \right)$$

Where:

- $\%_j$  = Percentage of component in flare vent gas, molar percentage.
- $j$  = Individual component in flare vent gas (i.e., propylene or nitrogen).
- 100 = Constant, percentage.
- $m_{j1}$  = Reported mass flow rate of component 1 (i.e., Propylene Flow or Nitrogen Flow), lb/hr.
- $m_{j2}$  = Reported mass flow rate of component 2 (i.e., Propylene Flow or Nitrogen Flow), lb/hr.

### Equation D.15A and D.15B

The volumetric flow rate for each flare vent gas component in the combustion zone ( $Q_{CZ,i}$ ), in scf/hr, was calculated using Equation D.15A and Equation D.15B.

#### Equation D.15A:

This equation was used for data sets C, D, F, G1, G2, H, and J.

$$Q_{CZ,i} = Q_{vg} \left( \frac{\%_{vg,i}}{100} \right)$$

Where:

- $Q_{CZ,i}$  = Volumetric flow rate of each flare vent gas component  $i$  in combustion zone, scf/hr.  
 $i$  = Individual flare vent gas component in combustion zone.  
 $Q_{vg}$  = Flare vent gas flow rate, scf/hr. (If not reported, see Equations D.4 through D.7).  
 $\%_{vg,i}$  = Percentage of component  $i$  in flare vent gas, molar percentage.  
 $100$  = Constant, percentage.

#### Equation D.15B:

This equation was used for data set A.

$$Q_{CZ,i} = Q_{CZ,i \text{ reported}} * 60$$

Where:

- $Q_{CZ,i}$  = Volumetric flow rate of each flare vent gas component  $i$  in combustion zone, scf/hr.  
 $i$  = Individual flare vent gas component in combustion zone.  
 $Q_{CZ,i \text{ ,reported}}$  = Reported volumetric flow rate of each flare vent gas component  $i$  in combustion zone (i.e., Propylene Flow or Nitrogen Flow), scf/min.  
 $60$  = Constant, s/min.

### Equation D.15C and D.15D

**For data set E, the volumetric flow rates of 1,3-butadiene ( $Q_{1,3-B}$ ) and nitrogen ( $Q_N$ ) in the flare vent gas, in scf/hr, were calculated using Equations D.15C and D.15D, respectively.**

Equation D.15C:

$$Q_{1,3-B} = \left( \frac{m_{1,3-B,reported}}{0.159} \right)$$

Where:

- $Q_{1,3-B}$  = Volumetric flow rate of 1,3-Butadiene, scf/hr.  
 $m_{1,3-B,reported}$  = Reported mass flow rate of 1,3-Butadiene (i.e., BD flow in lb/hr), lb/hr.  
 $0.159$  = Constant, density of 1,3-Butadiene, lb/scf.

Equation D.15D:

$$Q_N = Q_{vg} - Q_{1,3-B} - Q_{NG}$$

Where:

- $Q_N$  = Volumetric flow rate of nitrogen, scf/hr.  
 $Q_{vg}$  = Flare vent gas flow rate, scf/hr. (See Equations D.6).  
 $Q_{1,3-B}$  = Volumetric flow rate of 1,3-Butadiene, scf/hr. (See Equation D.15C).  
 $Q_{NG}$  = Reported volumetric flow rate of supplemental natural gas (i.e., Nat Gas flow in SCFH), scf/hr.

### Equation D.16A

**The concentration of each flare vent gas component in the combustion zone ( $X_{CZ,i}$ ) was calculated using Equation D.16.**

*This equation was used for data sets A, C, D, E, F, G1, G2, H, and J.*

$$X_{CZ,i} = \frac{Q_{CZ,i}}{\sum Q_{CZ,i}}$$

Where:

- $X_{CZ,i}$  = Concentration of component  $i$  in combustion zone gas, volume fraction.
- $i$  = Individual flare vent gas component in combustion zone.
- $Q_{CZ,i}$  = Volumetric flow rate of component  $i$  in combustion zone gas, scf/hr. (See Equation D.15A or D.15B).

### **Equation D.16B**

**The concentration of each flare vent gas combustible component ( $VG_c$ ) was calculated using Equation D.16B.**

*This equation was used for all data sets.*

$$VG_c = \frac{Q_{CZ,c}}{\sum Q_{CZ,c}}$$

Where:

- $VG_c$  = Concentration of combustible component  $c$  in the flare vent gas, volume fraction.
- $c$  = Individual combustible component in the flare vent gas.
- $Q_{CZ,c}$  = Volumetric flow rate of combustible component  $c$  in the flare vent gas, scf/hr.

### Equation D.16C

**The concentration of each flare vent gas and center steam only component ( $X_{vgcs}$ ) was calculated using Equation D.16C.**

*This equation was used for all data sets.*

$$X_{vgcs} = \frac{Q_{CZ,c}}{\sum Q_{CZ,c}}$$

Where:

- $X_{vgcs}$  = Concentration of combustible component  $c$  in the flare vent gas and center steam mixture, volume fraction.
- $c$  = Individual combustible component in the flare vent gas and center steam mixture.
- $Q_{CZ,c}$  = Volumetric flow rate of combustible component  $c$  in the flare vent gas and center steam mixture, scf/hr.

### Equation D.17

**If not reported, the total mass steam rate ( $m_s$ ), in lb/hr, was calculated using Equation D.17.**

*This equation was used for data sets G2 and H.*

$$m_s = m_{s,reported} * 1,000$$

Where:

$m_s$  = Total steam rate, lb/hr.

$m_{s,reported}$  = Reported total steam rate, klb/hr.  
*Reported for data set G2 as "Steam Flow (DCS)."*  
*Reported for data set H as "EPF Steam."*

1,000 = Constant, lb/klb.

### **Equation D.18**

**The volumetric steam rate ( $Q_x$ ), in scf/hr, was calculated using Equation D.18.**

*This equation was used for data sets A, C, D, E, F, G1, G2, H, and J.*

$$Q_x = 379.48 \left( \frac{m_x}{MW_s} \right)$$

Where:

- $Q_x$  = Type x steam rate, scf/hr.
- x = Type of steam rate (i.e., Total, Lower, Center, Ring, or Upper).
- 379.48 = Constant, lb-mole/scf at dry standard conditions.
- $m_x$  = Type x steam rate, lb/hr. (See Equation D.19).
- $MW_s$  = Molecular weight of steam, 18 lb/lb-mole.

### Equation D.19

**The total mass steam rate ( $m_s$ ), lower mass steam rate ( $m_l$ ), and ring mass steam rate ( $m_r$ ), in lb/hr, were calculated using Equation D.19.**

*This equation was used for data sets E, F, G1, and G2.*

$$m_s = m_l + m_c + m_r + m_u$$

Where:

- $m_s$  = Total steam rate, lb/hr. (See Equation D.17 for data sets G2 and H).  
*Total steam rate was a reported value for data sets R and G1.*
- $m_l$  = Lower steam rate, lb/hr.
- $m_c$  = Center steam rate, lb/hr.  
*Center steam rate was a reported constant value for data sets F, G1 and G2.*
- $m_r$  = Ring steam rate, lb/hr.
- $m_u$  = Upper steam rate, lb/hr.  
*Upper steam rate was a reported value for data set E.*

### Equation D.20

**The ring volumetric steam rate ( $Q_r$ ) and lower volumetric steam rate ( $Q_l$ ), in scf/hr, were calculated using Equation D.20.**

*This equation was used for data sets F, G1, and G2.*

$$Q_s = Q_l + Q_c + Q_r + Q_u$$

Where:

- $Q_s$  = Total steam rate, scf/hr.
- $Q_l$  = Lower steam rate, scf/hr.
- $Q_c$  = Center steam rate, scf/hr. (See Equation D.18 for data sets F, G1 and G2).
- $Q_r$  = Ring steam rate, scf/hr.
- $Q_u$  = Upper steam rate, scf/hr.

### **Equation D.21A**

**The steam-to-vent-gas ratio by weight ( $S/VG_{wt}$ ), in lb steam/lb vent gas, was calculated using Equation D.21A.**

*This equation was used for data sets A, C, D, E, F, G1, G2, and H.*

$$S/VG_{wt} = \frac{m_s}{m_{vg}}$$

Where:

- |             |   |  |
|-------------|---|--|
| $S/VG_{wt}$ | = | The steam-to-vent-gas ratio by weight, lb steam/lb vent gas.   |
| $m_s$       | = | Total steam rate, lb/hr. (See Equation D.17 for data sets G2 and H. See Equation D.19 for data set E). |
| $m_{vg}$    | = | Flare vent gas flow rate, lb/hr. (See Equation D.2 for data set A. See Equation D.3 for data set C).   |

### **Equation D.21B**

**The steam-to-vent-gas ratio by volume (S/VG<sub>vol</sub>), in scf steam/scf vent gas, was calculated using Equation D.21B.**

*This equation was used for data sets A, C, D, E, F, G1, G2, H, I and J.*

$$S/VG_{vol} = \frac{Q_s}{Q_{vg}}$$

Where:

- |              |   |  |
|--------------|---|--|
| $S/VG_{vol}$ | = | The steam-to-vent-gas ratio by volume, scf steam/scf vent gas.   |
| $Q_s$        | = | Total steam rate, scf/hr. (See Equation D.18 for data sets A, C, D, E, F, and H).                              |
| $Q_{vg}$     | = | Flare vent gas flow rate, scf/hr. (See Equation D.8A for data sets A and E. See Equation D.8B for data set J). |

### Equation D.21C

**The steam-to-vent-hydrocarbon ratio by volume ( $S/HC_{vol}$ ), in scf steam/scf hydrocarbon, was calculated using Equation D.21C.**

*This equation was used for data sets A, C, D, E, F, G1, G2, H, I and J.*

$$S/HC_{vol} = \frac{Q_s}{\sum Q_{CZ,HCi}}$$

Where:

- $S/HC_{vol}$  = The steam-to-vent-gas ratio by weight, lb steam/lb vent gas.  
 $Q_s$  = Total steam rate, scf/hr. (See Equation D.18 for data sets A, C, D, E, F, and H).  
 $Q_{CZ,HCi}$  = Volumetric flow rate of component  $i$  in combustion zone gas that is a hydrocarbon, scf/hr. (See Equation D.15A or D.15B).

### Equations D.22 through D.25

**The ratio of the net heating value of the combustion zone gas to the net heating value of the flare vent gas if diluted to the lower flammability limit ( $NHV_{ratio}$ ), was calculated using Equations D.22 through D.25.**

*Equations D.22 through D.25 were used for data sets A, C, D, E, F, G1, G2, H and J.*

Equation D.22:

$$NHV_{ratio} = \frac{NHV_{CZ}}{NHV_{LFL-VG}}$$

Where:

- $NHV_{ratio}$  = The ratio of the net heating value of the combustion zone gas to the net heating value of the flare vent gas if diluted to the lower flammability limit.
- $NHV_{CZ}$  = The net heating value of the combustion zone gas, BTU/scf (See Equation D.23).
- $NHV_{LFL-VG}$  = The net heating value of the flare vent gas if diluted to the lower flammability limit, BTU/scf (See Equation D.24).

Equation D.23:

*The net heating value of the combustion zone gas is calculated by correcting the net heating value of the vent gas for the inclusion of steam in the combustion zone gas, as shown below.*

$$NHV_{CZ} = \frac{Q_{vg}NHV_{VG}}{(Q_{vg} + Q_s)}$$

Where:

- $NHV_{CZ}$  = The net heating value of the combustion zone gas, BTU/scf.
- $Q_{vg}$  = Flare vent gas flow rate, scf/hr. (See Equation D.4 for data set A. See Equation D.5 for data set C. See Equation D.6 for data sets E, H and J. See Equation D.7 for data set G1).
- $NHV_{VG}$  = Flare vent gas net heating value, BTU/scf (See Equation D.1 for data set E).
- $Q_s$  = Total steam rate, scf/hr. (See Equation D.18 for data sets A, C, D, E, F, H and J).

### Equations D.22 through D.25 (Continued)

*Equations D.22 through D.25 were used for data sets A, C, D, E, F, G1, G2, H and J.*

**Equation D.24:**

*The net heating value of the flare vent gas if diluted to its lower flammability limit is calculated by multiplying the actual net heating value of the flare vent gas by its lower flammability limit, as shown below.*

$$NHV_{LFL-VG} = NHV_{vg} * LFL_{vg}$$

Where:

- $NHV_{LFL-VG}$  = The net heating value of the flare vent gas if diluted to the lower flammability limit, BTU/scf.
- $NHV_{VG}$  = Flare vent gas net heating value, BTU/scf. (See Equation D. 1 for data set E).
- $LFL_{vg}$  = Lower flammability limit of the flare vent gas adjusted for nitrogen equivalency, volume fraction (See Equation D.25).

**Equation D.25:**

*This equation uses the Le Chatelier Principle with a nitrogen equivalency adjustment; it allows you to estimate the lower flammability limit of any mixture. For this particular analysis, the lower flammability limit of the flare vent gas is of interest. The calculation uses the weighted average of the LFLs of the individual compounds (combustible and inert) weighted by their volume percent of the flare vent gas. All inerts, including nitrogen, are assumed to have an infinite lower flammability limit (e.g.,  $LFL_{N_2} = \infty$ ).*

$$LFL_{vg} = \frac{1}{\sum_{i=1}^n \left( \frac{\%_i}{LFL_i} \right) - (N_{e,H_2O} - 1)(x_{H_2O}) - (N_{e,CO_2} - 1)(x_{CO_2})}$$

Where:

- $LFL_{vg}$  = Lower flammability limit of the flare vent gas adjusted for nitrogen equivalency, volume fraction
- $n$  = Number of individual combustible components in flare vent gas.
- $i$  = Individual combustible component in flare vent gas.
- $\%_i$  = Percentage of combustible component  $i$  in flare vent gas, molar percent. (See Table C-1 in Appendix C, most values are reported.)
- $LFL_i$  = Lower flammability limit of combustible component  $i$  in flare vent gas, volume percent. Zabetakis M.G. "Flammability Characteristics of Combustible Gases and Vapors", U.S. Bureau of Mines, Bulletin 627, 1965 was used to determine the lower flammability limit for each component in each test run. Table D.1 lists these values.
- $N_{e,H_2O}$  = Coefficient of nitrogen equivalency for water relative to nitrogen, unitless (See Equation D.29).
- $x_{H_2O}$  = Reported concentration of water in flare vent gas, volume fraction.
- $N_{e,CO_2}$  = Coefficient of nitrogen equivalency for carbon dioxide relative to nitrogen, unitless (See Equation D.29).
- $x_{CO_2}$  = Reported concentration of carbon dioxide in flare vent gas, volume fraction.

**Table D.1 – Lower Flammability Limit of Select Compounds ( $LFL_i$ ) – Flare Vent Gas**

Compound	$LFL_i$ (vol %)	Compound	$LFL_i$ (vol %)
1-Butene	1.8	Iso-Butylene	1.8
1,2-Butadiene	2	Methane	5
1,3-Butadiene	2	Methyl Acetylene	1.7
Acetylene	2.5	n-Butane	1.8
Benzene	1.3	Nitrogen	$\infty$
Carbon Dioxide	$\infty$	Oxygen	$\infty$
Carbon Monoxide	12.5	Pentane Plus ( $C_5+$ )	1.4
Cis-2-Butene	1.7	Propadiene	2.16
Cyclopropane	2.4	Propane	2.1
Ethane	3	Propylene	2.4
Ethyl Benzene	1	Toluene	1.2
Ethylene	2.7	Trans-2-Butene	1.7
Hydrogen	4	Water	$\infty$
Hydrogen Sulfide	4	Xylenes	1.1
Iso-Butane	1.8		

### Equation D.26

**The combustible components in the combustion zone ( $C_{CZ}$ ), in volume fraction, was calculated using Equation D.26.**

*This equation was used for data sets A, C, D, E, F, G1, G2, H and J.*

$$C_{CZ} = \frac{\left( \sum_{i=1}^n x_i Q_{vg} \right) + x_h Q_{vg}}{(Q_{vg} + Q_s)}$$

Where:

- $C_{CZ}$  = Combustible components in the combustion zone gas, volume fraction.
- $n$  = Number of individual combustible organic components in flare vent gas.
- $i$  = Individual combustible organic component in flare vent gas.
- $x_i$  = Concentration of combustible organic component  $i$  in flare vent gas, volume fraction.
- $x_h$  = Concentration of hydrogen in flare vent gas, volume fraction.
- $Q_{vg}$  = Flare vent gas flow rate, scf/hr. (See Equation D.4 for data set A. See Equation D.5 for data set C. See Equation D.6 for data sets E, H and J. See Equation D.7 for data set G1.).
- $Q_s$  = Total steam flow, scf/hr. (See Equation D.18 for data sets A, C, D, E, F, H and J.).

### Equations D.27 through D.29

**The lower flammability limit of combustion zone gas adjusted for nitrogen equivalency ( $LFL_{CZ}$ ), in volume fraction, was calculated using Equations D.27 through D.29.**

*Equations D.27 through D.29 were used for data sets A, C, D, E, F, G1, G2, H and J.*

Equation D.27:

*This equation uses the Le Chatelier Principle with a nitrogen equivalency adjustment; it allows you to estimate the lower flammability limit of any mixture. For this particular analysis, the lower flammability limit of the combustion zone gas is of interest. The calculation uses the weighted average of the LFLs of the individual compounds (combustible and inert) weighted by their volume percent of the combustion zone gas. All inerts, including nitrogen, are assumed to have an infinite lower flammability limit (e.g.,  $LFL_{N_2} = \infty$ ).*

$$LFL_{CZ} = \frac{1}{\sum_{i=1}^n \left( \frac{\%_i}{LFL_i} \right) - (N_{e,H_2O} - 1)(x_{H_2O}) - (N_{e,CO_2} - 1)(x_{CO_2})}$$

Where:

- $LFL_{CZ}$  = Lower flammability limit of combustion zone gas adjusted for nitrogen equivalency, volume fraction.
- $n$  = Number of components in combustion zone gas.
- $i$  = Individual component in combustion zone gas.
- $\%_i$  = Percentage of component  $j$  in combustion zone gas, volume percentage. (See Equation D.28).
- $LFL_i$  = Lower flammability limit of component  $j$ , volume percent. Zabetakis M.G. "Flammability Characteristics of Combustible Gases and Vapors", U.S. Bureau of Mines, Bulletin 627, 1965 was used to determine the lower flammability limit for each component in each test run. Table D.2 lists these values.
- $N_{e,H_2O}$  = Coefficient of nitrogen equivalency for water relative to nitrogen, unitless (See Equation D.29).
- $x_{H_2O}$  = Concentration of water in combustion zone gas, volume fraction.
- $N_{e,CO_2}$  = Coefficient of nitrogen equivalency for carbon dioxide relative to nitrogen, unitless (See Equation D.29).
- $x_{CO_2}$  = Concentration of carbon dioxide in combustion zone gas, volume fraction.

### Equations D.27 through D.29 (Continued)

**The coefficients of nitrogen equivalency of water and carbon dioxide relative to nitrogen,  $N_{e,H_2O}$  and  $N_{e,CO_2}$ , was calculated using Equation D.29.**

*Equations D.27 through D.29 were used for data sets A, C, D, E, F, G1, G2, H and J.*

Equation D.28:

$$\%_i = \left( \frac{Q_{CZ,i}}{(Q_{vg} + Q_s)} \right) * 100$$

Where:

- $\%_i$  = Percentage of component  $i$  in combustion zone gas, volume percentage.
- $Q_{CZ,i}$  = Volumetric flow rate of each flare vent gas component  $i$  in combustion zone, scf/hr. (See Equation D.15A for data sets C, D, E, F, G1, G2, H and J. See Equation D.15B for data set A).
- $Q_{vg}$  = Flare vent gas flow rate, scf/hr. (See Equation D.4 for data set A. See Equation D.5 for data set C. See Equation D.6 for data sets E, H and J. See Equation D.7 for data set G1.).
- $Q_s$  = Total steam rate, scf/hr. (See Equation D.18 for data sets A, C, D, E, F, H and J.).

Equation D.29:

$$N_{e,k} = \sum_{i=1}^n K_{k,i} \left( \frac{Q_{CZ,i}}{\sum Q_{CZ,i}} \right)$$

Where:

- $N_{e,k}$  = Coefficient of nitrogen equivalency for water or carbon dioxide relative to nitrogen, unitless.
- $k$  = Individual inert component (i.e. water and carbon dioxide).
- $n$  = Number of individual combustible components in flare vent gas.
- $i$  = Individual combustible component in flare vent gas.
- $K_{k,i}$  = Values for inert component  $k$  (i.e. water or carbon dioxide) for each combustible component  $i$  in flare vent gas. Table D.3 lists these values.
- $Q_{CZ,i}$  = Volumetric flow rate of each flare vent gas component  $i$  in combustion zone, scf/hr. (See Equation D.15A or D.15B).

**Table D.2 – Lower Flammability Limit of Select Compounds (LFL<sub>i</sub>) – Combustion Zone Gas**

Compound	LFL <sub>i</sub> (vol %)	Compound	LFL <sub>i</sub> (vol %)
1-Butene	1.8	Methane	5
1,2-Butadiene	2	Methyl Acetylene	1.7
1,3-Butadiene	2	n-Butane	1.8
Acetylene	2.5	Nitrogen	∞
Benzene	1.3	Oxygen	∞
Carbon Dioxide	∞	Pentane Plus (C <sub>5</sub> +) )	1.4
Carbon Monoxide	12.5	Propadiene	2.16
Cis-2-Butene	1.7	Propane	2.1
Cyclopropane	2.4	Propylene	2.4
Ethane	3	Toluene	1.2
Ethyl Benzene	1	Trans-2-Butene	1.7
Ethylene	2.7	Water	∞
Hydrogen	4	Xylenes	1.1
Hydrogen Sulfide	4	Steam	∞
Iso-Butane	1.8	Pilot Gas	5
Iso-Butylene	1.8		

**Table D.3 – Values for inert component k (i.e. water or carbon dioxide) for each combustible component i in flare vent gas**

Combustible Component i in Flare Vent Gas	K <sub>Water</sub>	K <sub>Carbon Dioxide</sub>
Methane	1.87	2.23
Ethane	1.40	1.87
Propane	1.51	1.93
Ethylene	1.68	1.84
Propylene	1.36	1.92
Hydrogen	1.35	1.51
All Other Combustibles	1.50	1.87

### Equations D.30 through D.37

**For air-assisted flares, the stoichiometric ratio (SR) was calculated using Equations D.30 through D.37.**

*Equations D.30 through D.32 were used for data sets C and J.*

Equation D.30:

$$SR = \frac{m_{Air}}{m_{Stoic}}$$

Where:

- $SR$  = Ratio of actual mass flow of total assist air to the theoretical stoichiometric mass of air needed to combust the flare vent gas, unitless.
- $m_{Air}$  = Actual total assist air mass flow rate, lb/hr. (See Equation D.34 for data set C).
- $m_{Stoic}$  = Theoretical stoichiometric mass of air needed to combust the flare vent gas, lb/hr (See Equation D.31).

Equation D.31:

$$m_{Stoic} = \sum_{i=1}^n (m_i) (AF_i)$$

Where:

- $m_{Stoic}$  = Theoretical stoichiometric mass of air needed to combust the flare vent gas, lb/hr.
- $n$  = Number of individual combustible components in flare vent gas.
- $i$  = Individual combustible component in flare vent gas.
- $m_i$  = Reported mass flow rate of combustible component  $i$  in the flare vent gas, lb/hr. (See Equation D.35 for data set C).
- $AF_i$  = Stoichiometric air to fuel ratio of combustible component  $i$ , lb of air/lb of combustible component  $i$  (See Equation D.32).

Equation D.32:

$$AF_i = \frac{28.84 \left( \frac{N_{O_2,i}}{0.21} \right)}{MW_i}$$

Where:

- $AF_i$  = Stoichiometric air to fuel ratio of combustible component  $i$ , lb of air/lb of combustible component  $i$ .
- $N_{O_2,i}$  = Stoichiometric amount of oxygen needed for one mole of combustible component  $i$ , moles (See Equation D.33).
- $i$  = Individual combustible component in flare vent gas.
- $MW_i$  = Molecular weight of combustible component  $i$  in the flare vent gas, lb/lb-mole.
- 28.84 = Constant, molecular weight of ambient air, lb/lb-mole.
- 0.21 = Constant, fraction of ambient air comprised of oxygen.

### Equations D.30 through D.37 (Continued)

#### Equation D.33:

*This equation was used for data sets C and J.*

$$N_{O_2,i} = N_{C,i} + \frac{N_{H,i}}{4}$$

Where:

- $N_{O_2,i}$  = Stoichiometric amount of oxygen needed for one mole of combustible component  $i$ , moles.  
 $i$  = Individual combustible component in flare vent gas.  
 $N_{C,i}$  = Number of carbon atoms per molecule of combustible hydrocarbon  $i$ .  
 $N_{H,i}$  = Number of hydrogen atoms per molecule of combustible hydrocarbon  $i$ .  
 $4$  = Constant.

#### Equation D.34:

*This equation was used for data set C.*

$$m_{air} = Q_{air\ reported} * 60 * 0.07517$$

Where:

- $m_{air}$  = Actual total assist air mass flow rate, lb/hr.  
 $Q_{air,reported}$  = Reported air assist flow rate, scf/min.  
 $60$  = Constant, min/hr.  
 $0.07517$  = Constant, assumed density of air, lb/scf.

#### Equation D.35:

*This equation was used for data set C.*

$$m_i = MW_i * \left( \frac{Q_i}{379.48} \right)$$

Where:

- $m_i$  = Mass flow rate of combustible component  $i$  in the flare vent gas, lb/hr.  
 $i$  = Individual flare vent gas component in combustion zone.  
 $MW_{vg}$  = Molecular weight of combustible component (i.e., propane) in the flare vent gas, lb/lb-mole.  
 $Q_i$  = Volumetric flow rate of each flare vent gas component  $i$ , scf/hr. (See Equation D.36).  
 $379.48$  = Constant, lb-mole/scf at dry standard conditions.

### Equations D.30 through D.37 (Continued)

#### Equation D.36:

*This equation was used for data set C.*

$$Q_i = Q_{vg} \left( \frac{\%_{vg,i}}{100} \right)$$

Where:

- $Q_i$  = Volumetric flow rate of each flare vent gas component  $i$  (i.e., propane or nitrogen), scf/hr.
- $i$  = Individual component in flare vent gas (i.e., propane or nitrogen).
- $Q_{vg}$  = Flare vent gas flow rate, scf/hr. (See Equation D.37).
- $\%_{i}$  = Percentage of component  $i$  (i.e., propane or nitrogen) in flare vent gas, molar percentage.
- $\%_p$  = Reported percentage of propane in flare vent gas (i.e., %Propane in Nitrogen), molar percentage.
- $\%_N$  = Percentage of nitrogen in flare vent gas, molar percentage. (See Equation D.13).
- 100 = Constant, percentage.

#### Equation D.37:

*This equation was used for data set C.*

$$Q_{vg} = V_{vg} * 60 * 60 \left( \frac{1.77}{144} \right)$$

Where:

- $Q_{vg}$  = Flare vent gas flow rate, scf/hr.
- $V_{vg}$  = Reported flare vent gas velocity, ft/s.
- 60 = Constant, s/min.
- 60 = Constant, min/hr.
- 1.77 = Constant, area of fuel exit port, in<sup>2</sup>.
- 144 = Constant, ft<sup>2</sup>/in<sup>2</sup>.

### Equations D.38 through D.41

**The calculated momentum flux ratio (MFR) was calculated using Equations D.38 through D.41.**

Equation D.38:

*This equation was used for data sets A, D, E, F, G1, G2, and J.*

$$m_{vg,s} = m_{vg} + m_c$$

Where:

$m_{vg,s}$  = Flare vent gas flow rate including center steam, lb/hr.

$m_{vg}$  = Flare vent gas flow rate, lb/hr. (See Equation D.2 for data set A. See Equation D.3 for data set C).

$m_c$  = Center steam rate, lb/hr.

*Center steam rate was a reported constant value for data sets F, G1 and G2.*

Equation D.39:

*This equation was used for data sets A, D, E, F, G1, G2, and J.*

$$\rho_{vg-s} = \left( \frac{m_{vg-s}}{Q_{vg} + Q_c} \right)$$

Where:

$\rho_{vg-s}$  = Density of flare vent gas including center steam, lb/scf.

$m_{vg,s}$  = Flare vent gas flow rate including center steam, lb/hr.

$Q_{vg}$  = Flare vent gas flow rate, scf/hr.

$Q_c$  = Center steam rate, scf/hr. (See Equation D.18 for data sets F, G1 and G2).

### Equations D.38 through D.41 (Continued)

#### Equation D.40:

This equation was used for data sets D, F, G1, G2, and J.

$$V_{wind} = \frac{V_{wing,reported} * 5280}{60 * 60}$$

Where:

$V_{wind}$	=	Wind velocity, ft/s.
$V_{wind, reported}$	=	Reported wind velocity, mph.
5280	=	Constant, ft/mile.
60	=	Constant, s/min.
60	=	Constant, min/hr.

#### Equation D.41:

This equation was used for data sets A, D, E, F, G1, G2, and J.

$$MFR = \left( \frac{\rho_{vg-s} * V_{vg-s}^2}{0.07492 * (V_{wind})^2} \right)$$

Where:

MRF	=	Calculated momentum flux ratio, unitless.
$\rho_{vg-s}$	=	Density of flare vent gas including center steam, lb/scf. (See Equation D.39).
$V_{vg-s}$	=	Flare vent gas velocity with center steam, ft/s. (If not reported, see Equation D.8C).
$V_{wind}$	=	Wind velocity, ft/s. (See Equation D.40).
0.07492	=	Constant, assumed density of air, lb/scf.

### Equations D.42 through D.45

**The shore equation analysis was performed using Equations D.42 through D.45.**

*These equations were used for data sets A, C, D, E, F, G1, G2, and J.*

Equation D.42:

$$U_o/\pi/D_o = \frac{V_{vg-s}}{\pi * \left(\frac{d}{12}\right)}$$

Where:

$U_o/\pi/D_o$	=	Shore Equation Velocity-Jet Periphery, sec <sup>-1</sup> .
$V_{vg-s}$	=	Flare vent gas velocity with center steam, ft/s. (If not reported, see Equation D.8C).
$\pi$	=	Constant pi used to calculate area of flare tip.
d	=	Reported effective diameter of flare tip, in. (See tip sizes identified in Section 2.0 of report).
12	=	Constant, in/ft.

### Equations D.42 through D.45 (Continued)

#### Equation D.43:

This equation uses the Le Chatelier Principle with a nitrogen equivalency adjustment; it allows you to estimate the lower flammability limit of any mixture. For this particular analysis, the lower flammability limit of the flare vent gas including center steam is of interest. The calculation uses the weighted average of the LFLs of the individual compounds (combustible and inert) weighted by their volume percent of the flare vent gas plus center steam. All inerts, including nitrogen, are assumed to have an infinite lower flammability limit (e.g.,  $LFL_{N_2} = \infty$ ).

$$LFL_{vgcs} = \frac{1}{\sum_{i=1}^n \left( \frac{X_{vgcs,i}}{LFL_i} \right) - (N_{e,H_2O} - 1)(x_{H_2O}) - (N_{e,CO_2} - 1)(x_{CO_2})}$$

Where:

- $LFL_{vgcs}$  = Lower flammability limit of the flare vent gas including center steam adjusted for nitrogen equivalency, volume fraction.
- $n$  = Number of individual combustible components in flare vent gas.
- $i$  = Individual combustible component in flare vent gas.
- $X_{vgcs,i}$  = Concentration of combustible component  $i$  in the flare vent gas and center steam mixture, volume fraction. (See Equation D.16C).
- $LFL_i$  = Lower flammability limit of combustible component  $i$  in flare vent gas, volume percent. Zabetakis M.G. "Flammability Characteristics of Combustible Gases and Vapors", U.S. Bureau of Mines, Bulletin 627, 1965 was used to determine the lower flammability limit for each component in each test run. Table D.4 lists these values.
- $N_{e,H_2O}$  = Coefficient of nitrogen equivalency for water relative to nitrogen, unitless. (See Equation D.29).
- $x_{H_2O}$  = Reported concentration of water in flare vent gas, volume fraction.
- $N_{e,CO_2}$  = Coefficient of nitrogen equivalency for carbon dioxide relative to nitrogen, unitless. (See Equation D.29).
- $x_{CO_2}$  = Reported concentration of carbon dioxide in flare vent gas, volume fraction.

**Table D.4 – Lower Flammability Limit of Select Compounds ( $LFL_i$ ) – Flare Vent Gas**

<b>Compound</b>	<b><math>LFL_i</math> (vol %)</b>	<b>Compound</b>	<b><math>LFL_i</math> (vol %)</b>
1-Butene	1.8	Iso-Butylene	1.8
1,2-Butadiene	2	Methane	5
1,3-Butadiene	2	Methyl Acetylene	1.7
Acetylene	2.5	n-Butane	1.8
Benzene	1.3	Nitrogen	$\infty$
Carbon Dioxide	$\infty$	Oxygen	$\infty$
Carbon Monoxide	12.5	Pentane Plus ( $C_5+$ )	1.4
Cis-2-Butene	1.7	Propadiene	2.16
Cyclopropane	2.4	Propane	2.1
Ethane	3	Propylene	2.4
Ethyl Benzene	1	Toluene	1.2
Ethylene	2.7	Trans-2-Butene	1.7
Hydrogen	4	Water	$\infty$
Hydrogen Sulfide	4	Xylenes	1.1
Iso-Butane	1.8		

### Equations D.42 through D.45 (Continued)

The shore equation analysis was performed using Equations D.42 through D.45.

These equations were used for data sets A, C, D, E, F, G1, G2, and J.

Equation D.44:

$$R_{AM} = \left( \frac{100 - (LFL_{vgcs} * 100)}{LFL_{vgcs} * 100} \right) \left( \frac{\rho_{vgcs}}{0.07492} \right)$$

Where:

- $R_{AM}$  = Shore Equation, lb flare vent gas including center steam / lb of air.  
 $LFL_{vgcs}$  = Lower flammability limit of the flare vent gas including center steam adjusted for nitrogen equivalency, volume fraction. (See Equation D.43).  
 100 = Constant, percentage.  
 $\rho_{vgcs}$  = Density of flare vent gas including center steam, lb/scf. (See Equation D.39).  
 0.07492 = Constant, assumed density of air, lb/scf.

Equation D.45:

$$V_{MAX} = \left( 2\pi * \sqrt{\frac{\frac{\pi}{4} * \left(\frac{d}{12}\right)^2}{\pi}} \right) * \left(\frac{R_{AM}}{6.85}\right)^5$$

Where:

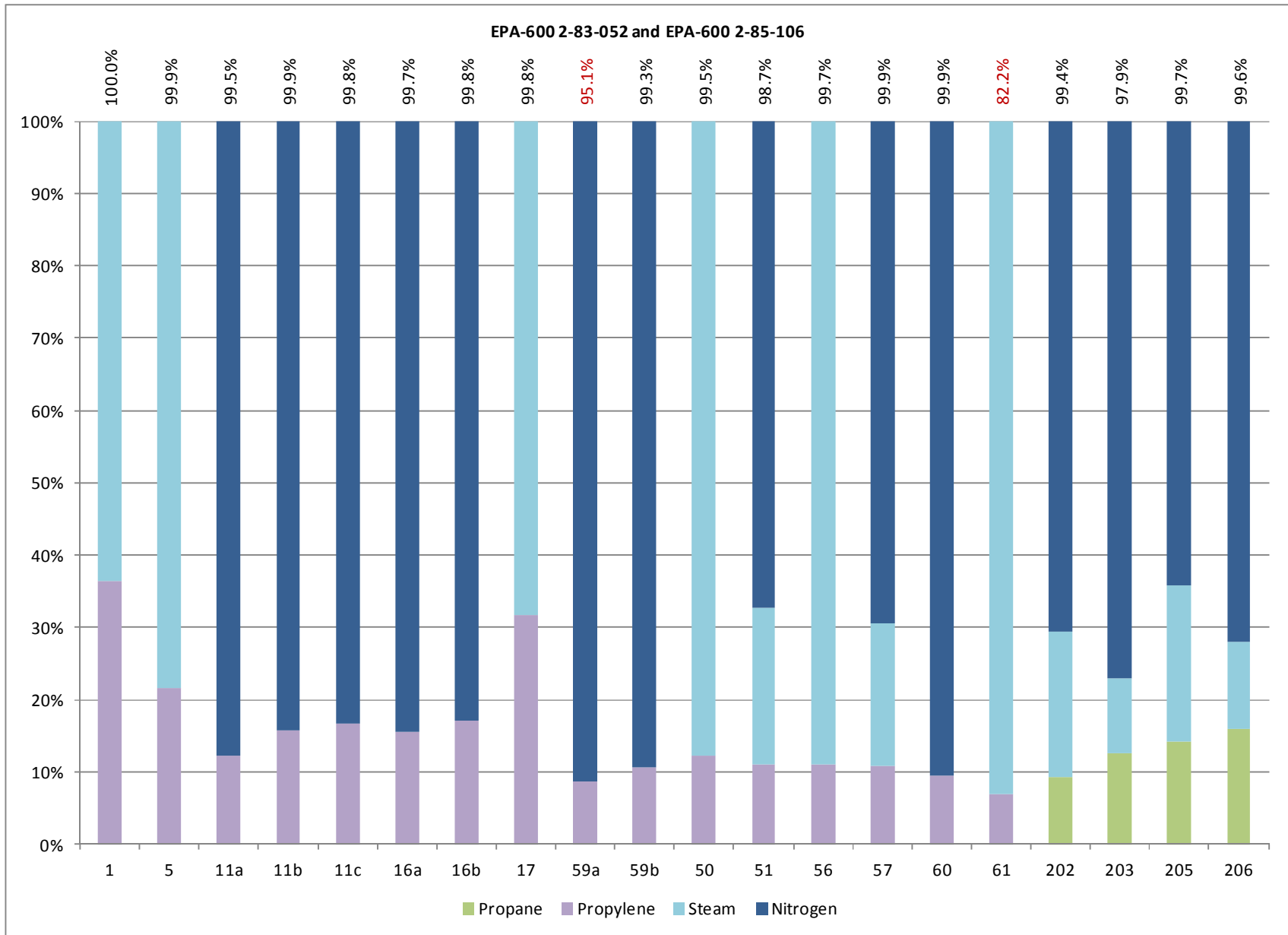
- $V_{MAX}$  = Maximum allowable flare vent gas velocity including center steam, ft/s.  
 $R_{AM}$  = Shore Equation, lb flare vent gas including center steam / lb of air. (See Equation D.44).  
 $\pi$  = Constant pi used to calculate area of flare tip.  
 $d$  = Reported effective diameter of flare tip, in (See tip sizes identified in Section 2.0 of report).  
 12 = Constant, in/ft.  
 6.85 = Empirical constant, may contain elements of viscosity and other transport properties of the gas and air.

*This information is distributed solely for the purpose of pre-dissemination peer review under applicable information quality guidelines. It has not been formally disseminated by EPA. It does not represent and should not be construed to represent any Agency determination or policy.*

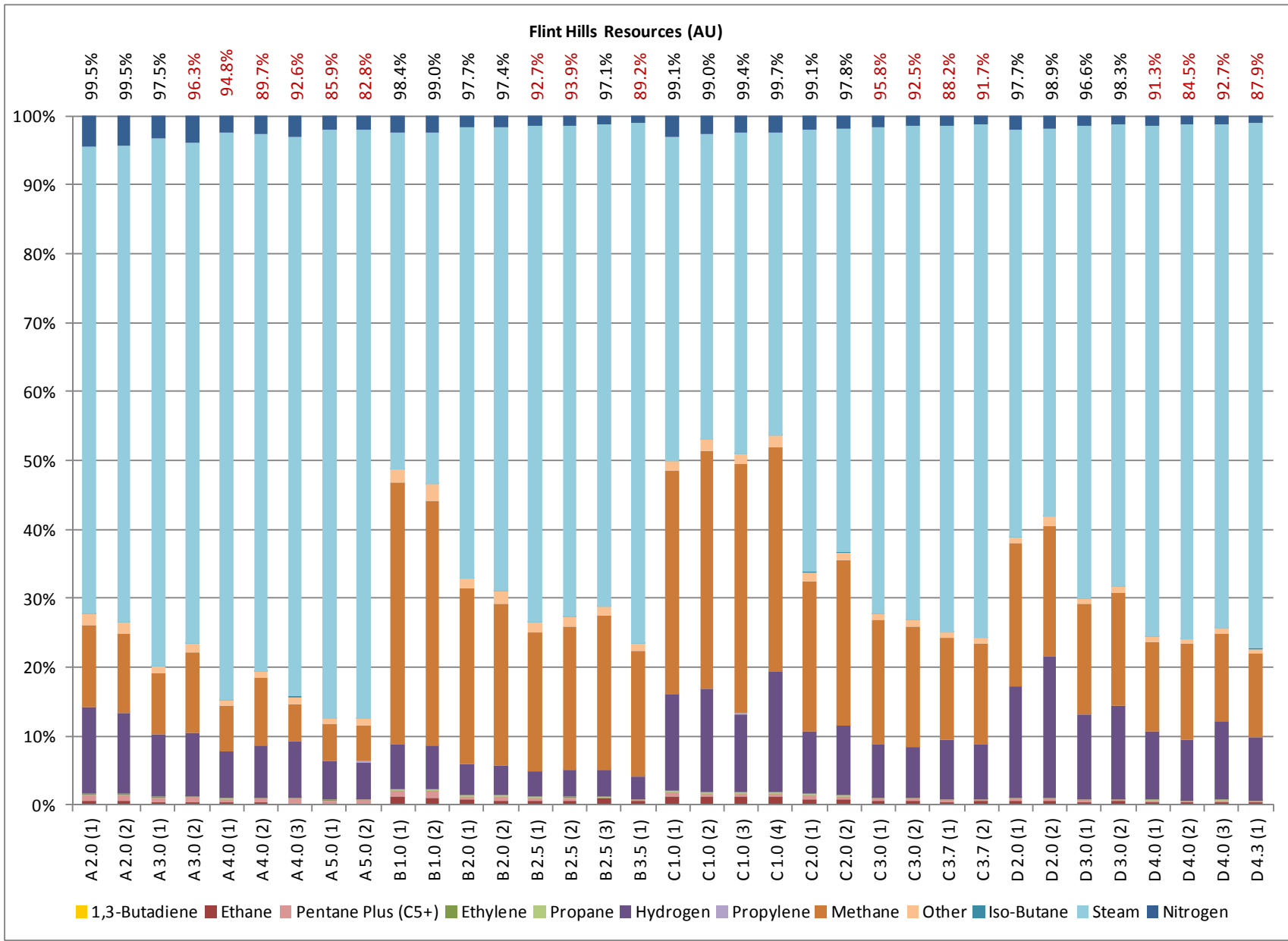
## **Appendix E**

### **Type And Amount Of Components In Each Test Run By Test Report.**

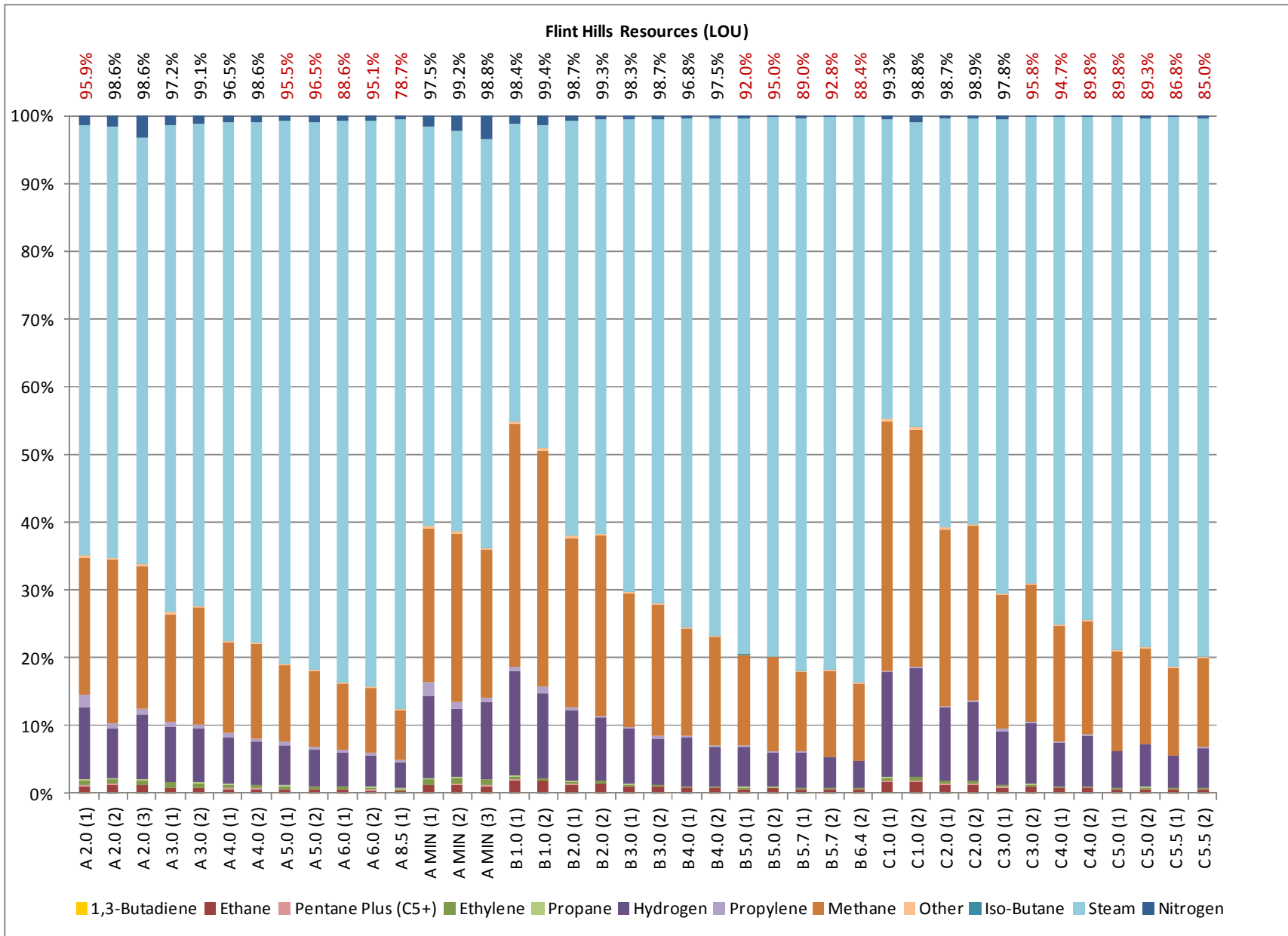
This information is distributed solely for the purpose of pre-dissemination peer review under applicable information quality guidelines. It has not been formally disseminated by EPA. It does not represent and should not be construed to represent any Agency determination or policy.



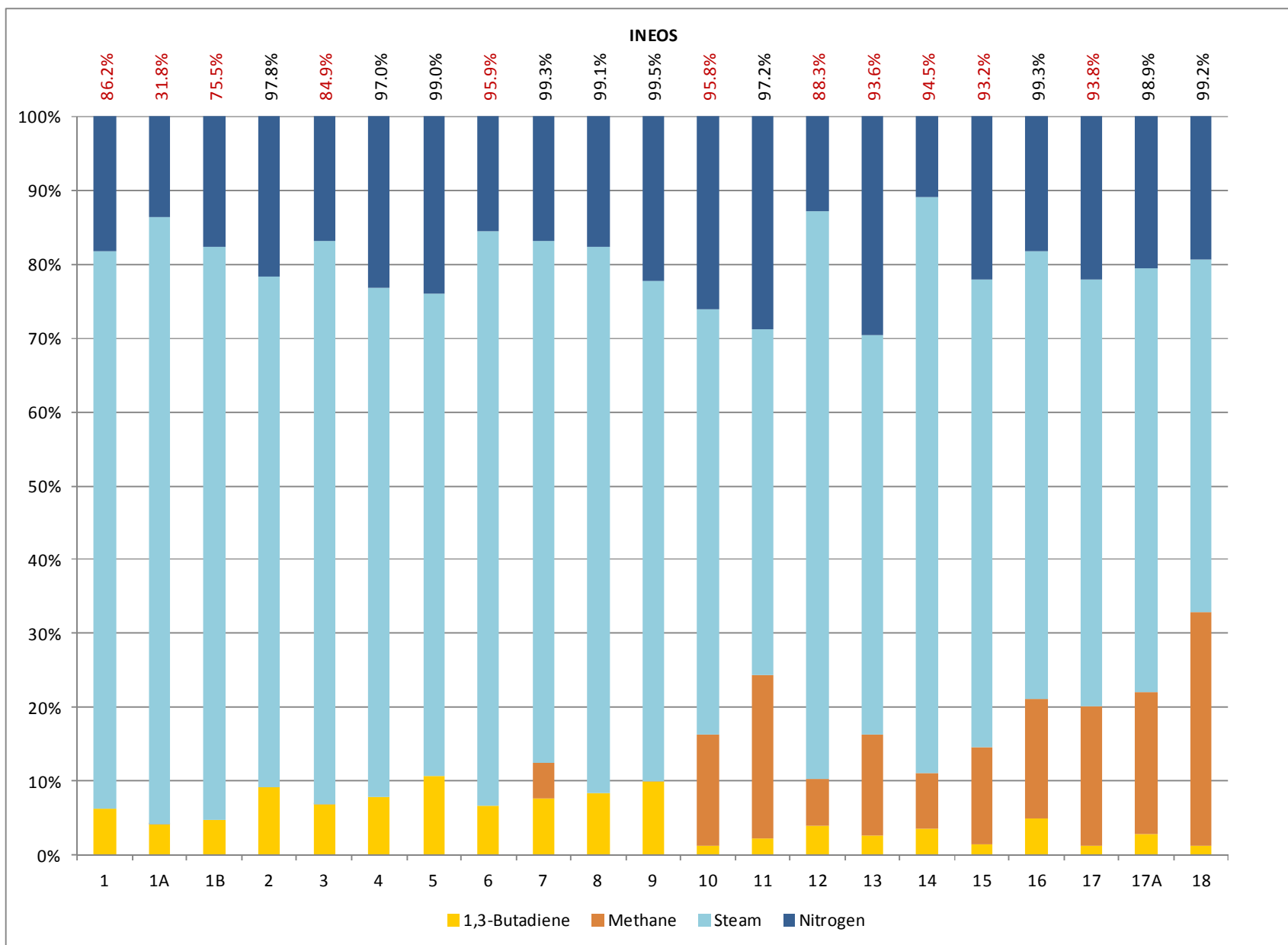
This information is distributed solely for the purpose of pre-dissemination peer review under applicable information quality guidelines. It has not been formally disseminated by EPA. It does not represent and should not be construed to represent any Agency determination or policy.



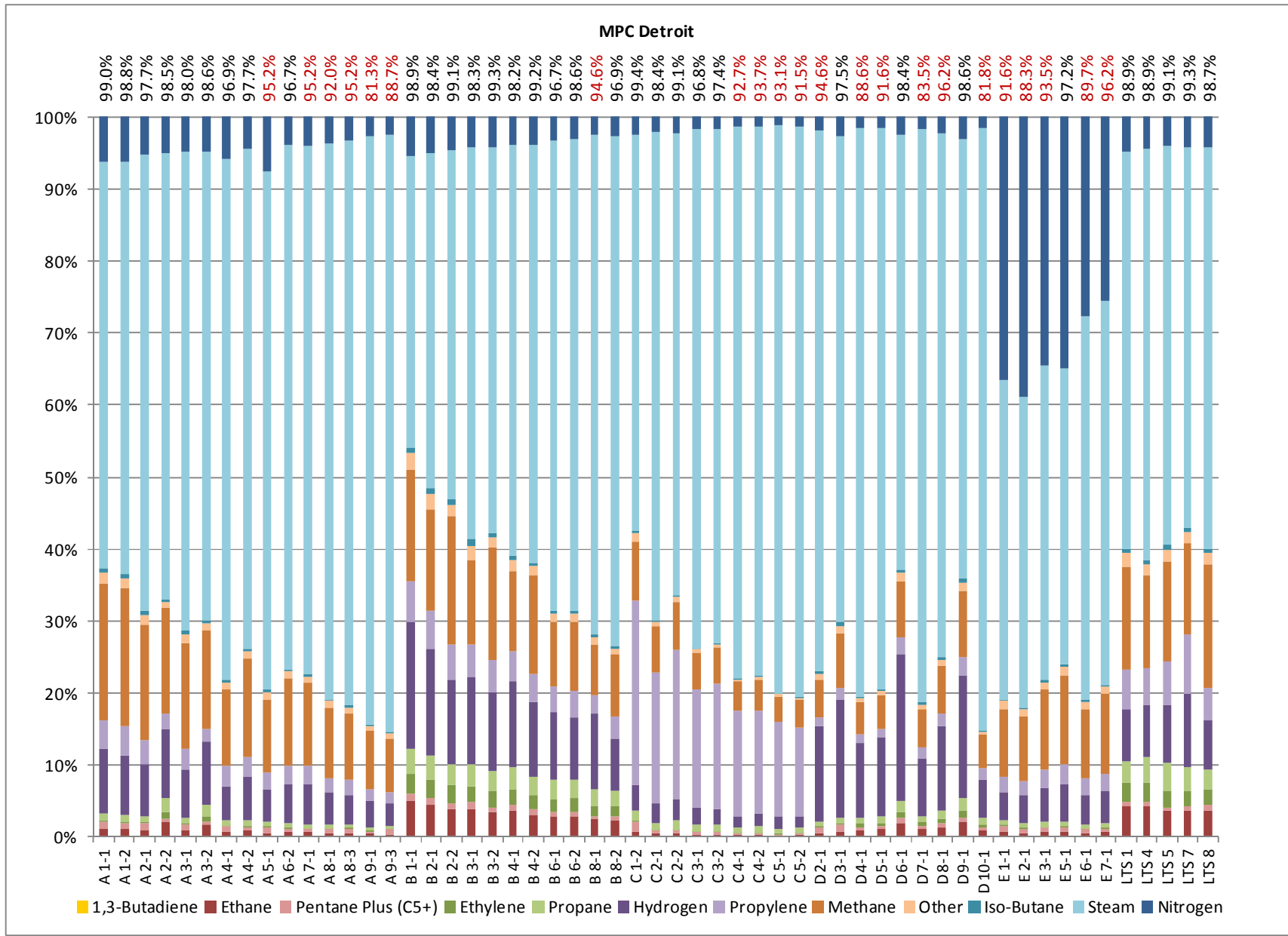
This information is distributed solely for the purpose of pre-dissemination peer review under applicable information quality guidelines. It has not been formally disseminated by EPA. It does not represent and should not be construed to represent any Agency determination or policy.



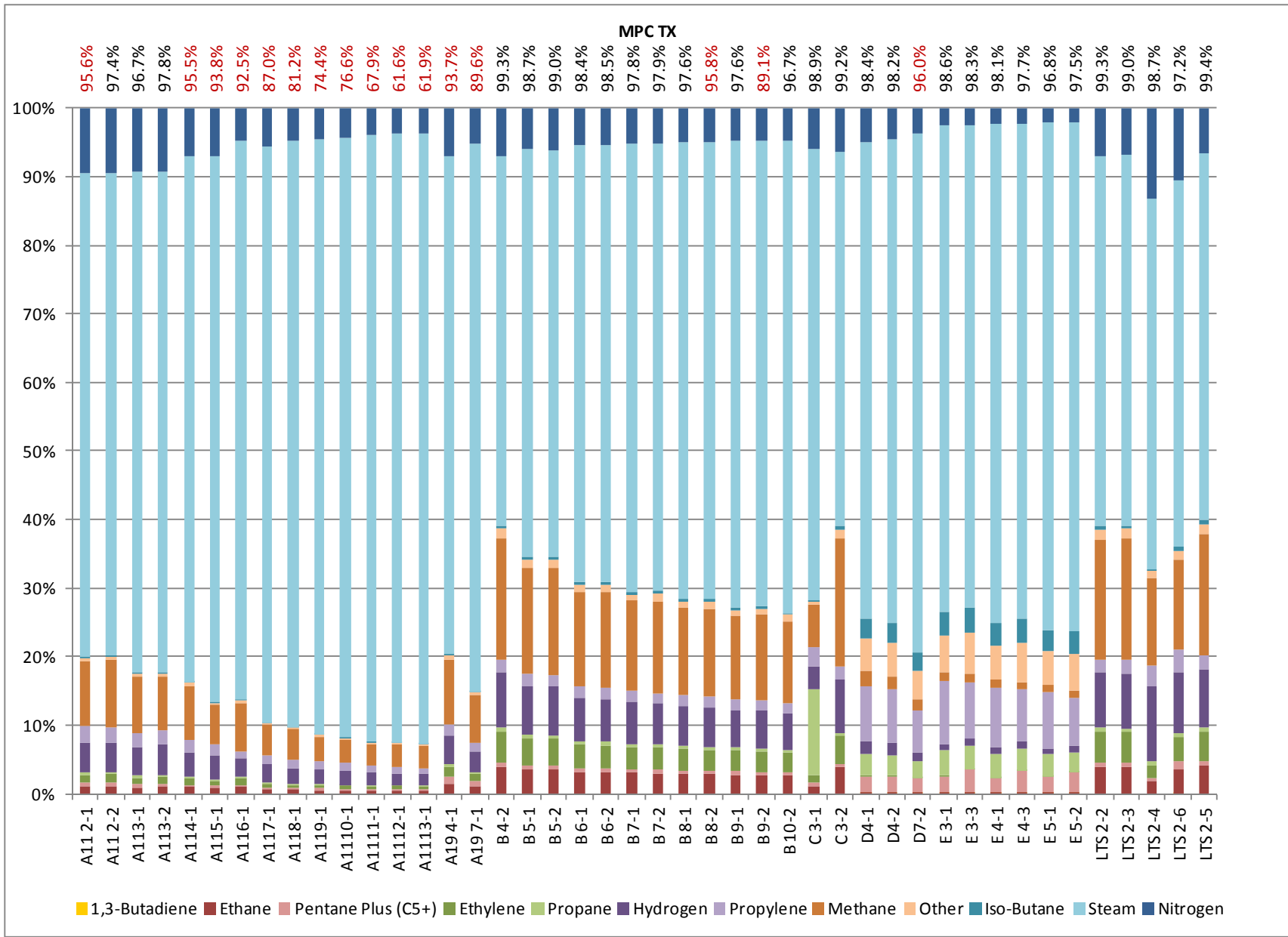
This information is distributed solely for the purpose of pre-dissemination peer review under applicable information quality guidelines. It has not been formally disseminated by EPA. It does not represent and should not be construed to represent any Agency determination or policy.



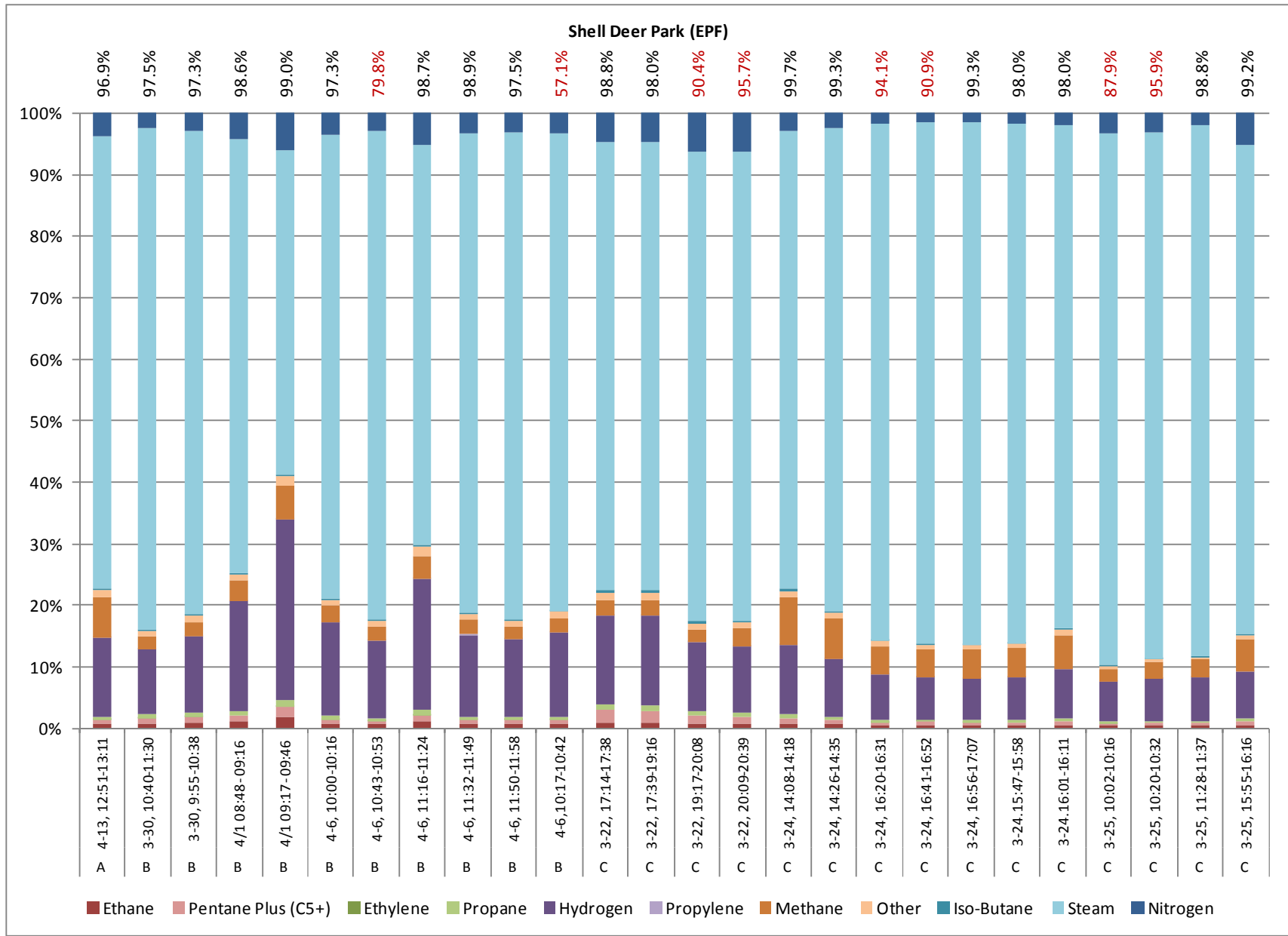
This information is distributed solely for the purpose of pre-dissemination peer review under applicable information quality guidelines. It has not been formally disseminated by EPA. It does not represent and should not be construed to represent any Agency determination or policy.



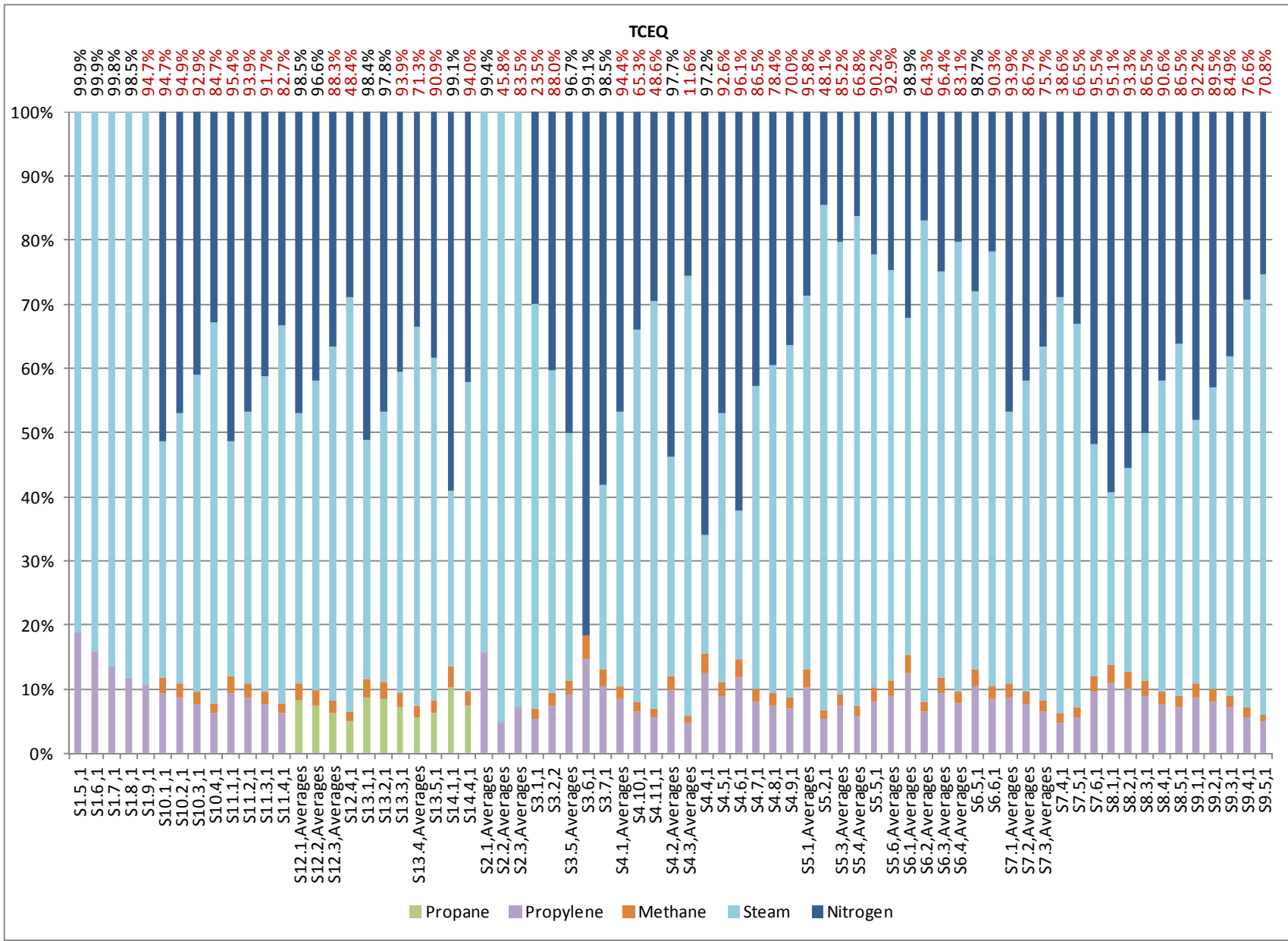
This information is distributed solely for the purpose of pre-dissemination peer review under applicable information quality guidelines. It has not been formally disseminated by EPA. It does not represent and should not be construed to represent any Agency determination or policy.



This information is distributed solely for the purpose of pre-dissemination peer review under applicable information quality guidelines. It has not been formally disseminated by EPA. It does not represent and should not be construed to represent any Agency determination or policy.



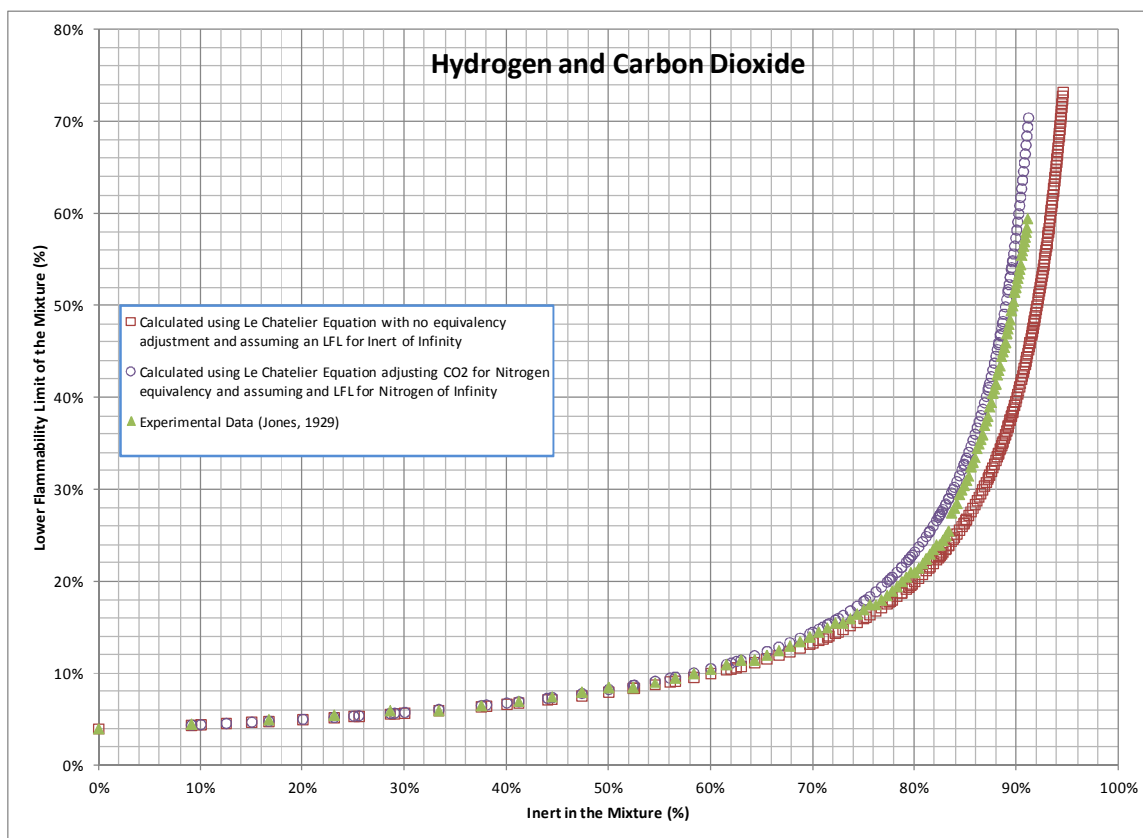
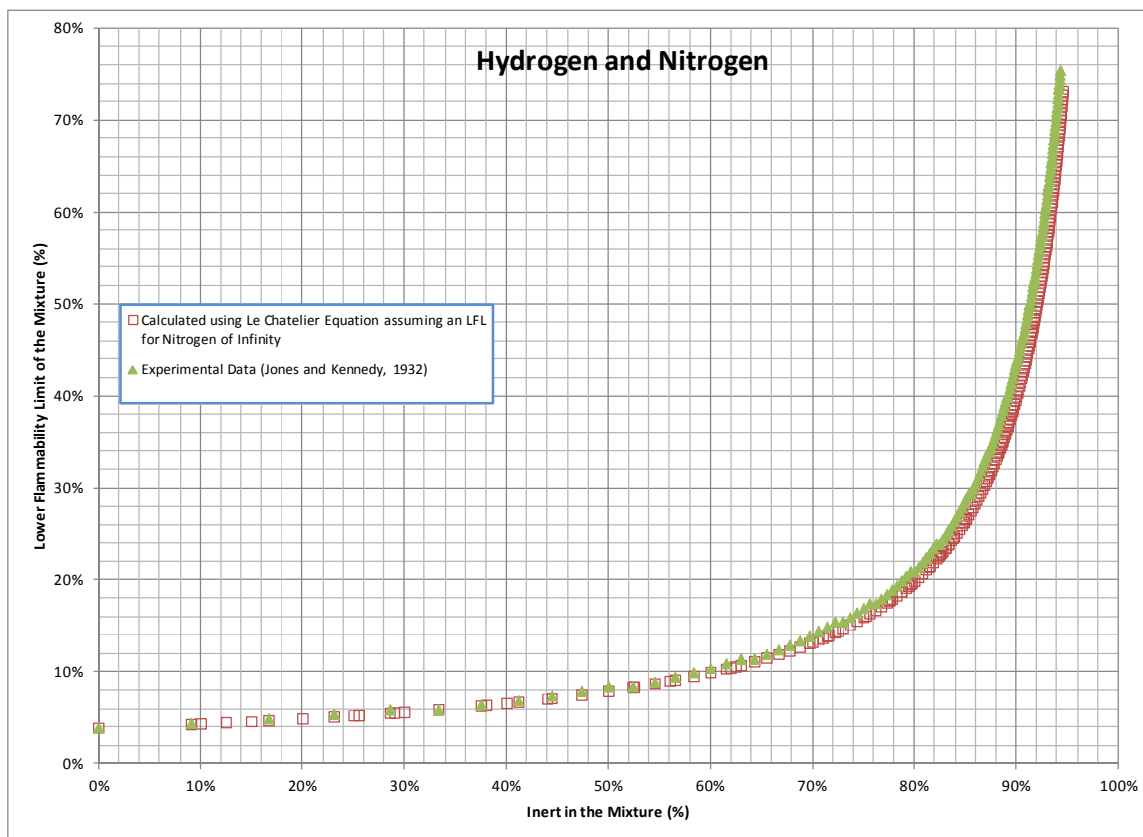
This information is distributed solely for the purpose of pre-dissemination peer review under applicable information quality guidelines. It has not been formally disseminated by EPA. It does not represent and should not be construed to represent any Agency determination or policy.

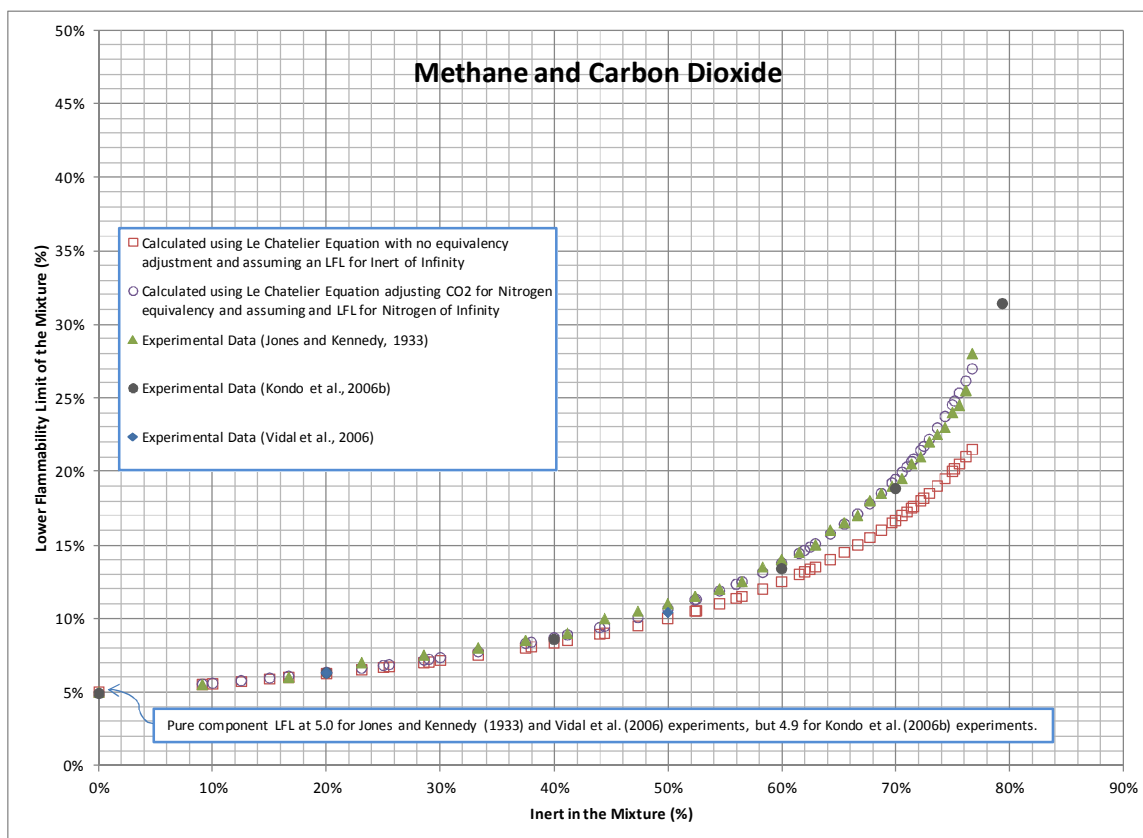
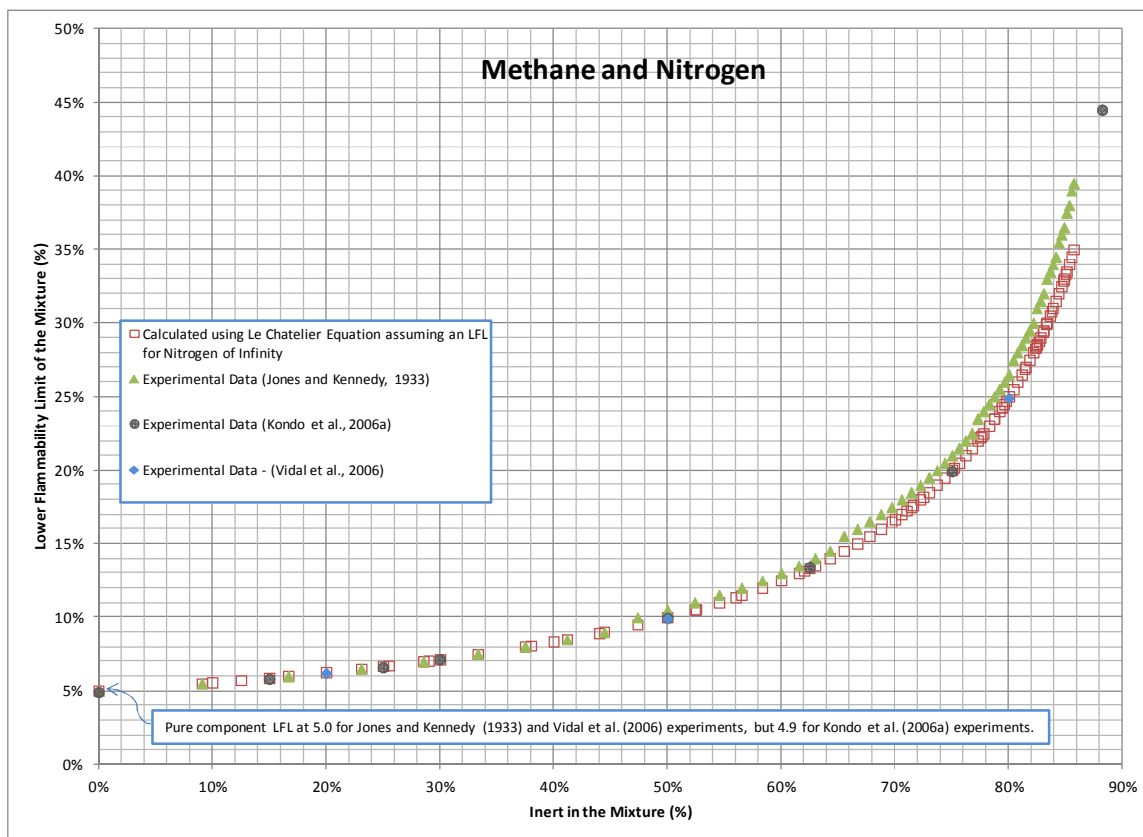


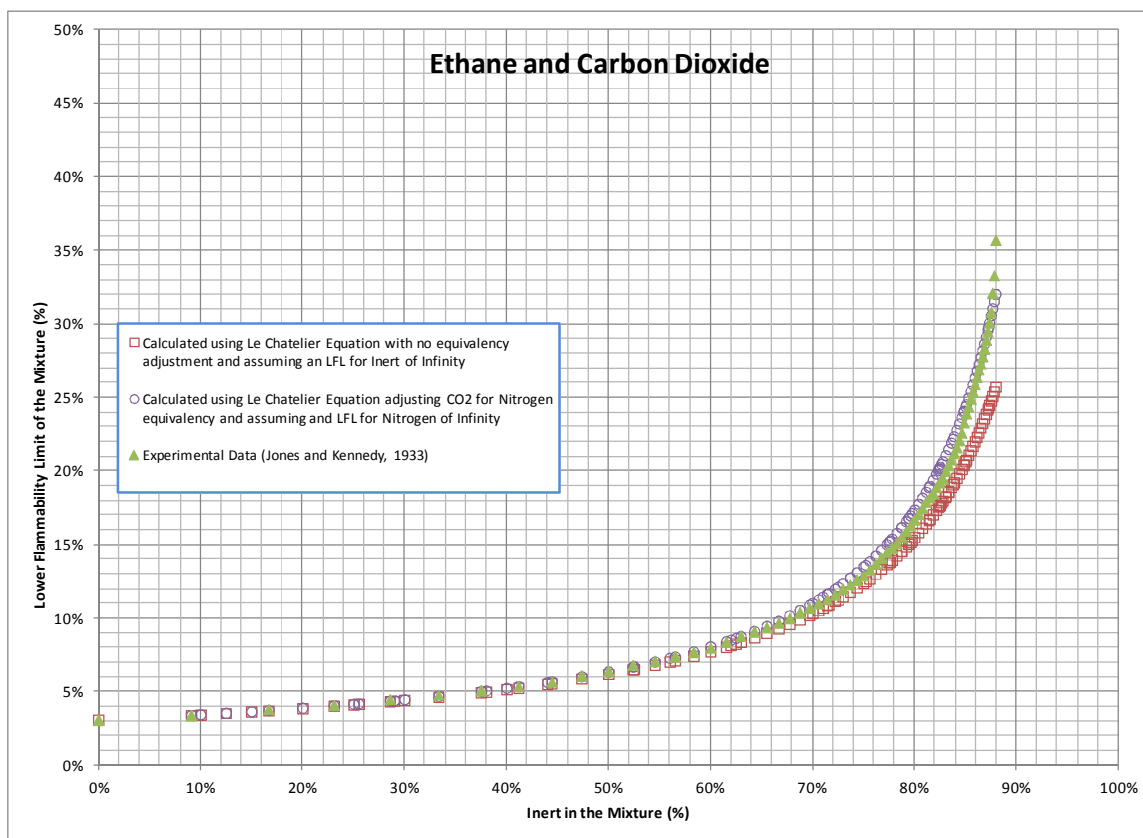
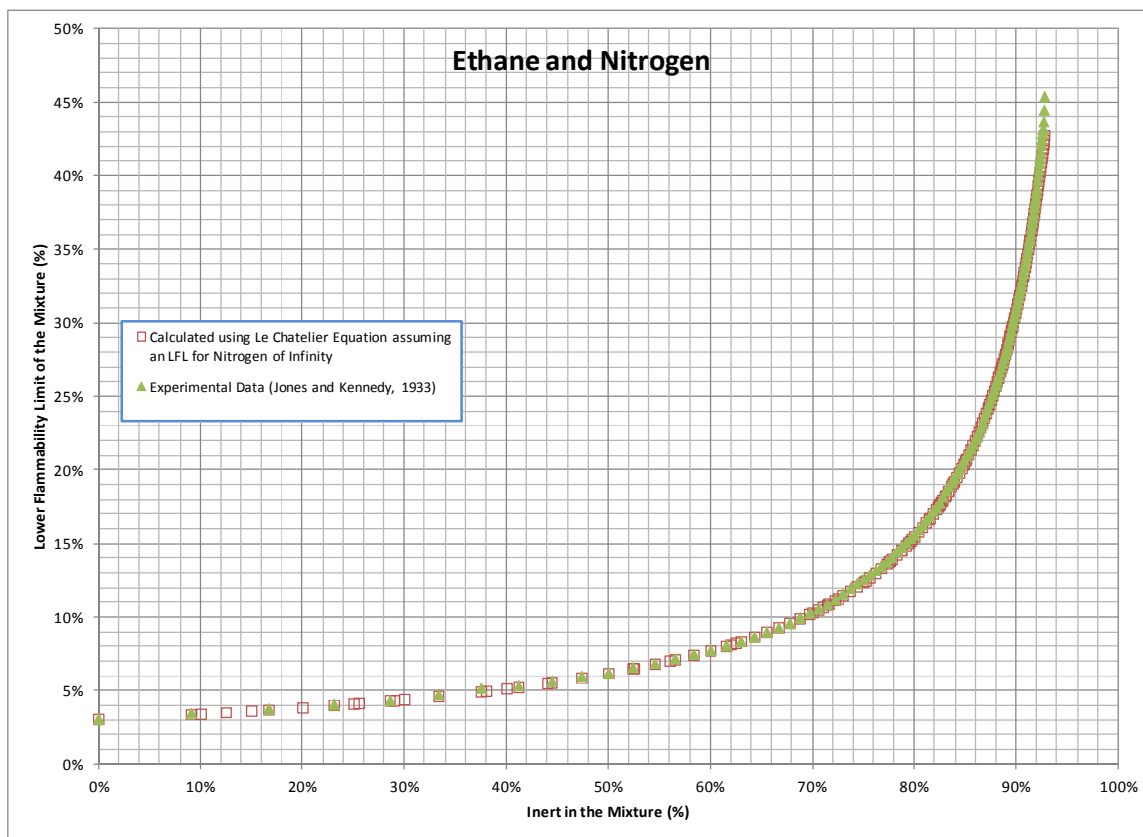
*This information is distributed solely for the purpose of pre-dissemination peer review under applicable information quality guidelines. It has not been formally disseminated by EPA. It does not represent and should not be construed to represent any Agency determination or policy.*

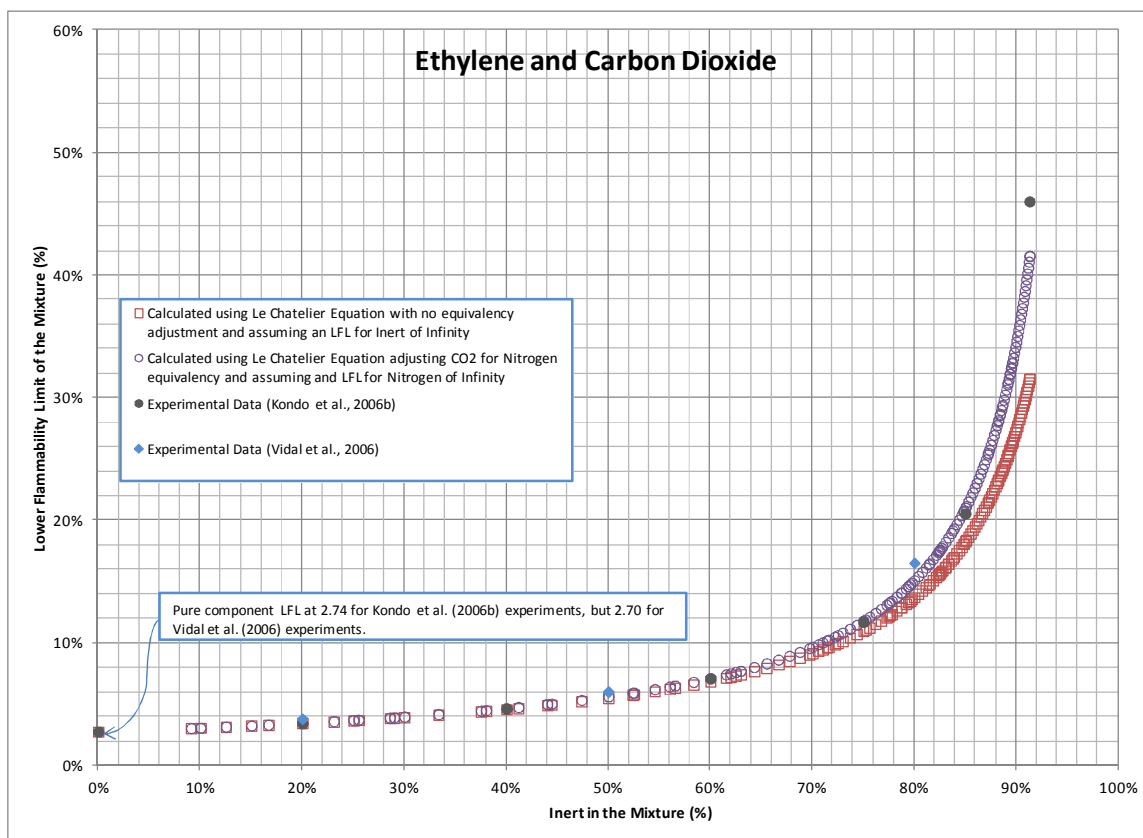
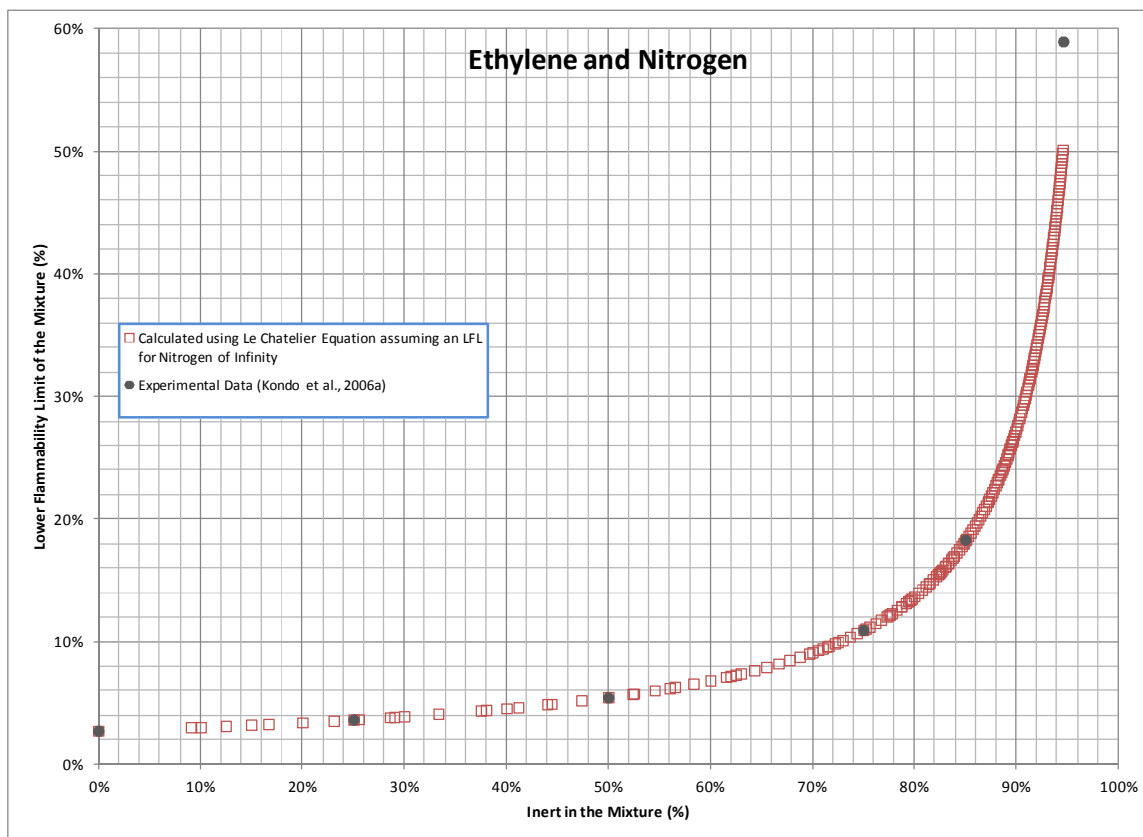
## **Appendix F**

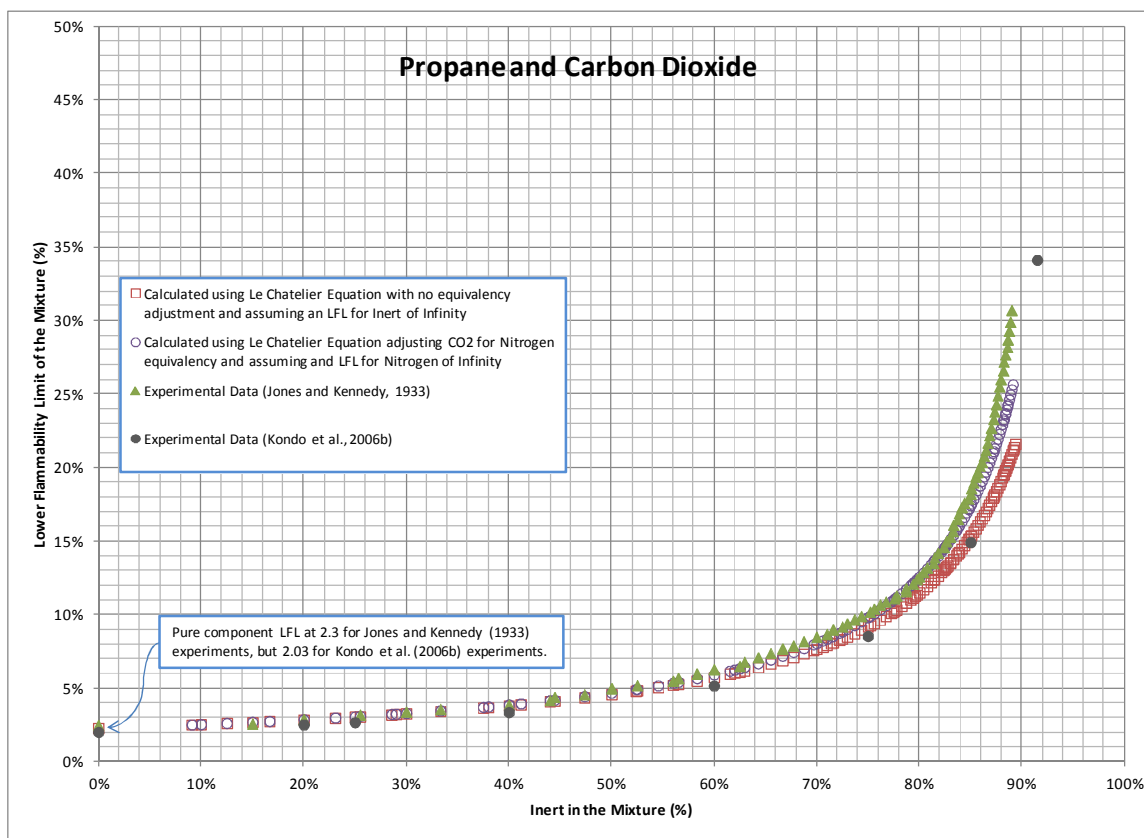
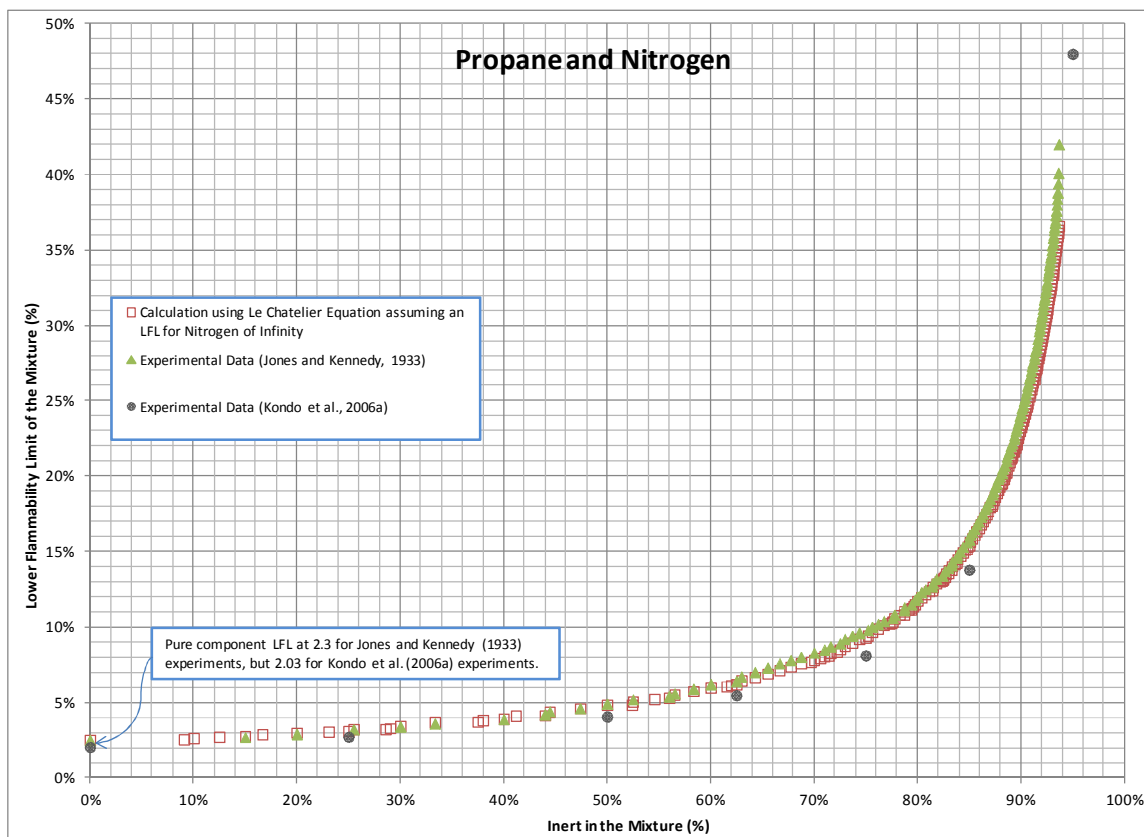
### **Charts Of Calculated And Measured LFL For Various Combustible Gases In Nitrogen And Carbon Dioxide**

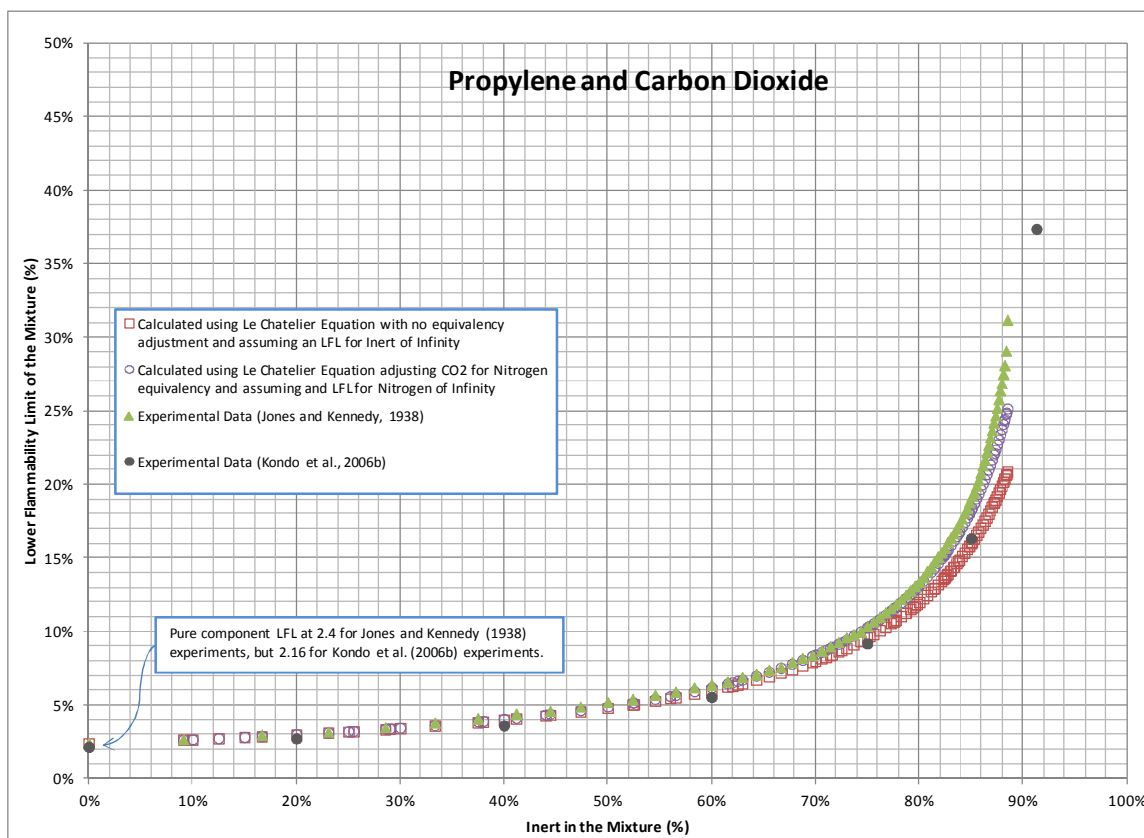
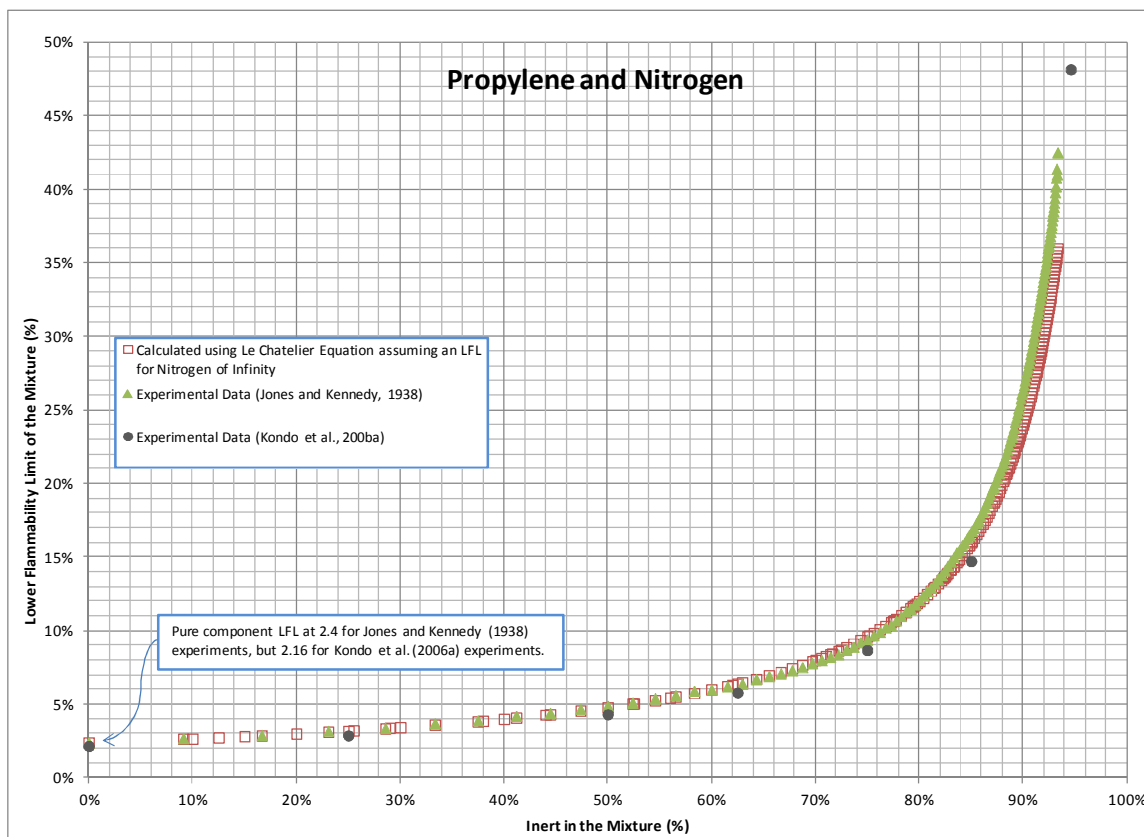


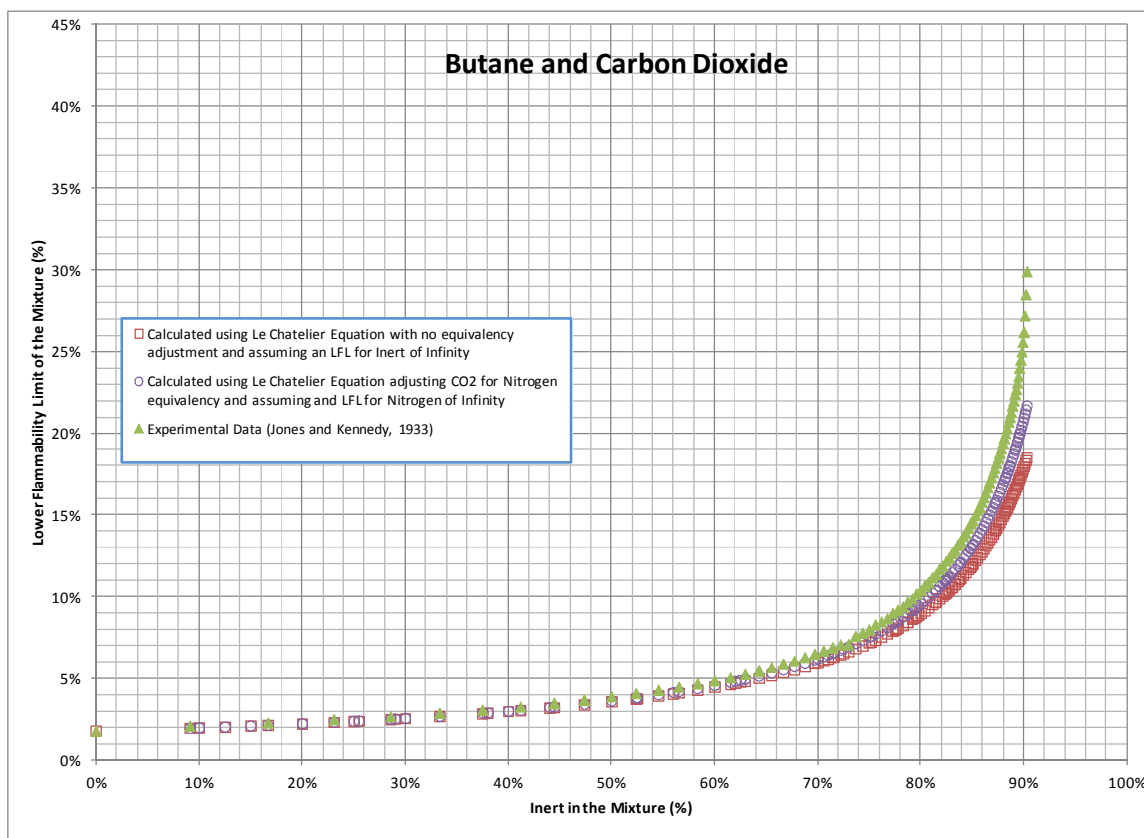
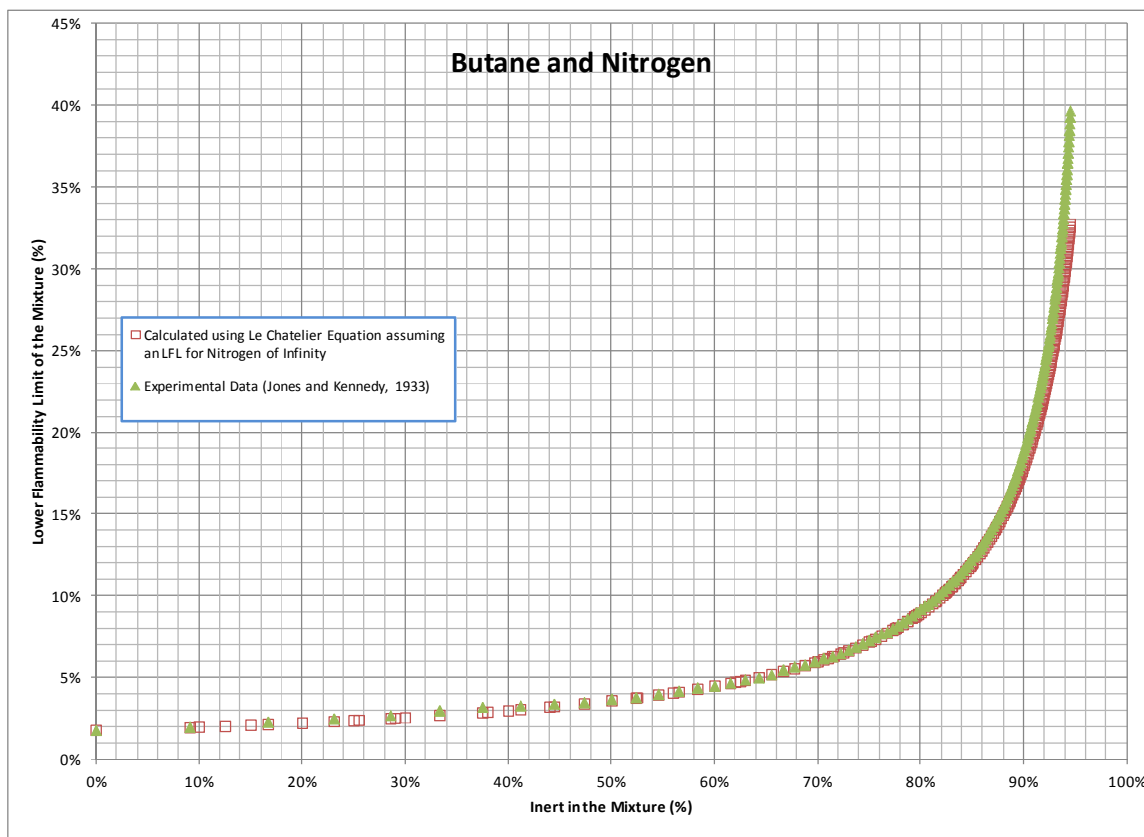


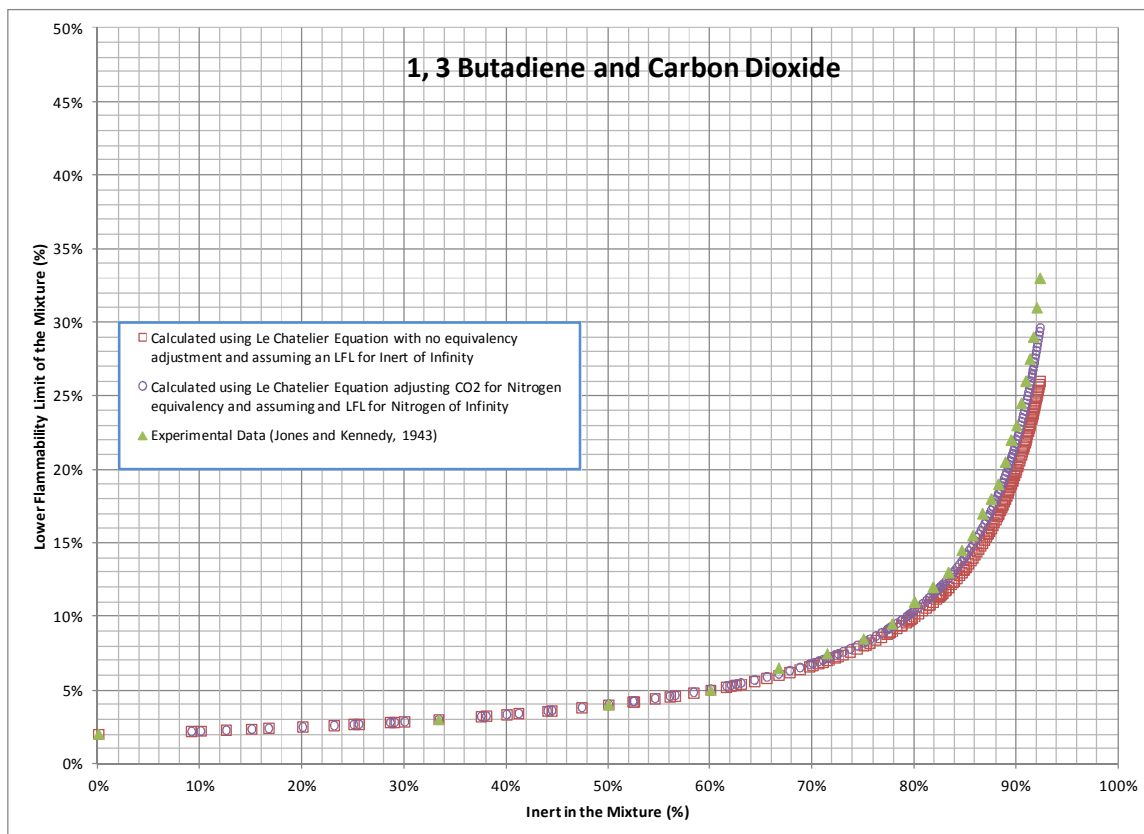
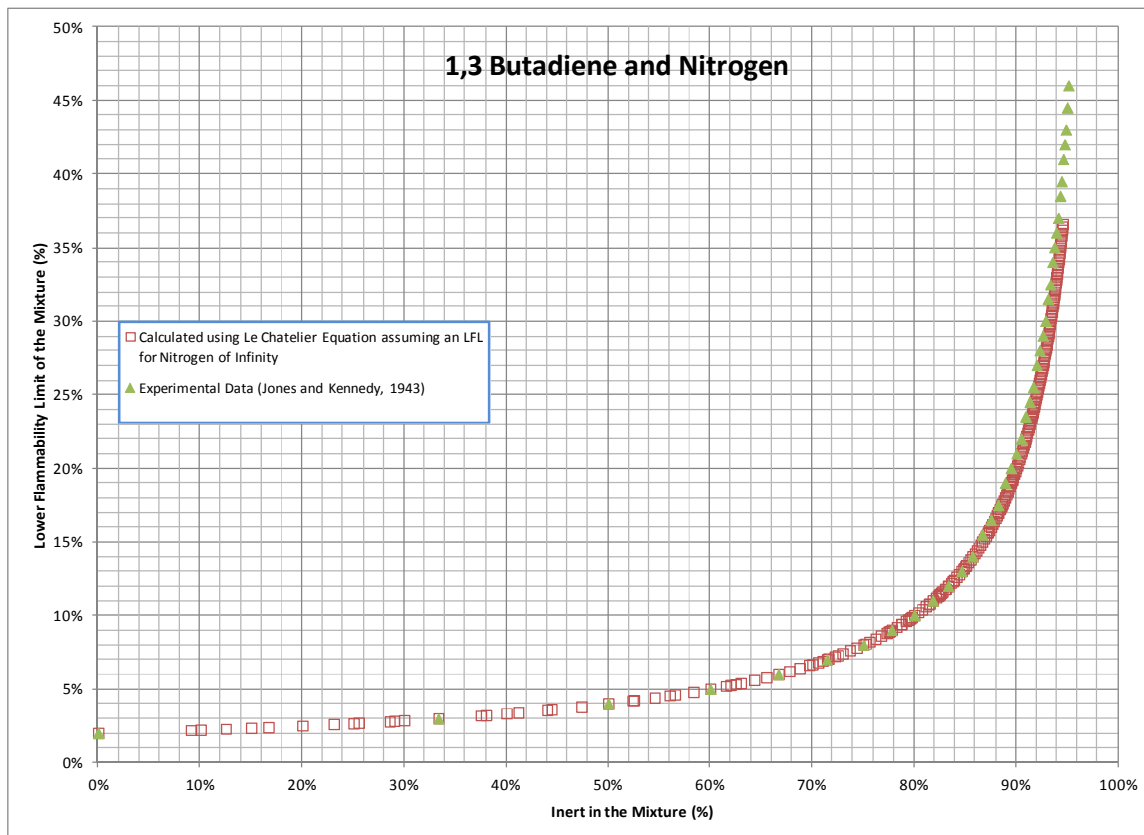


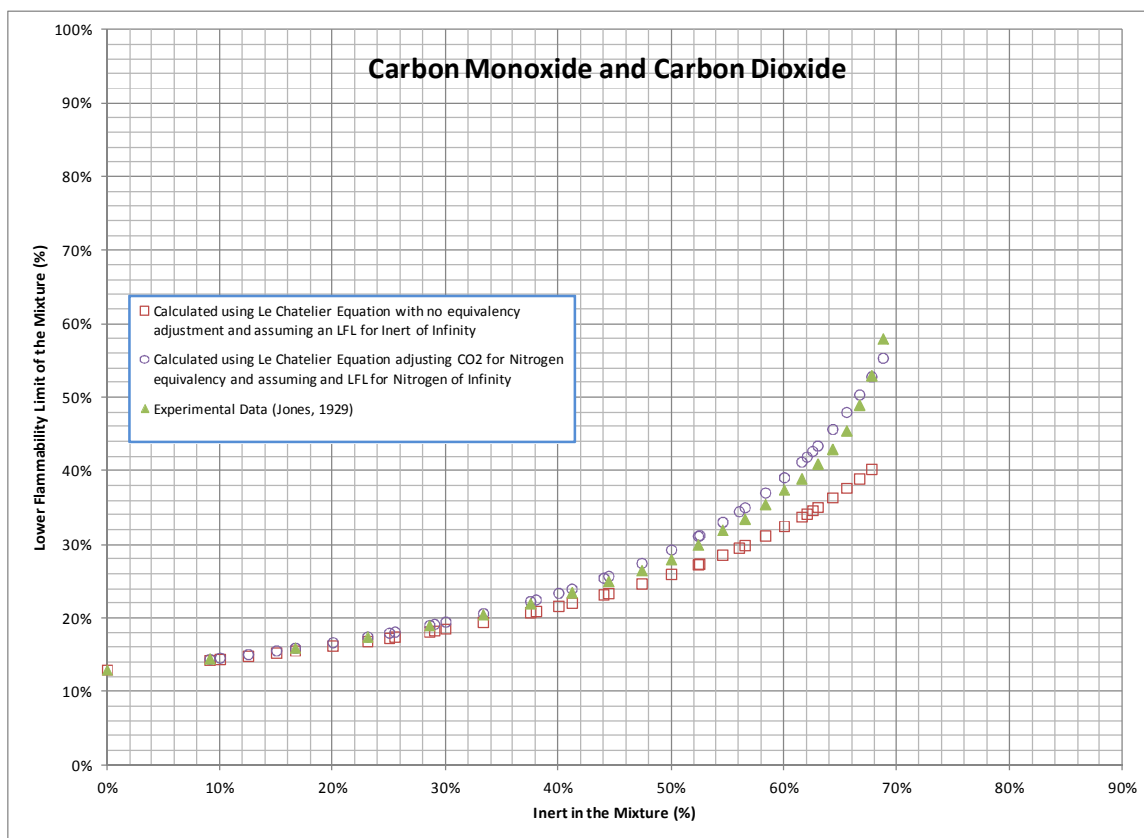
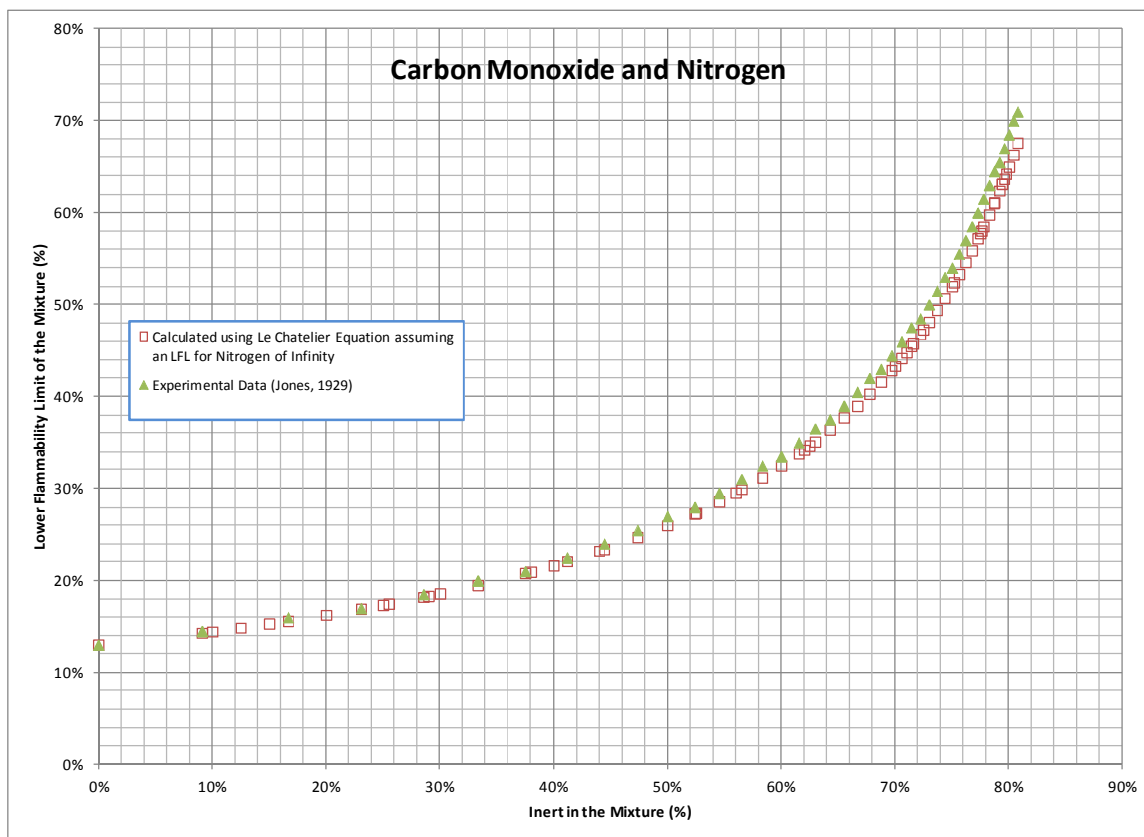


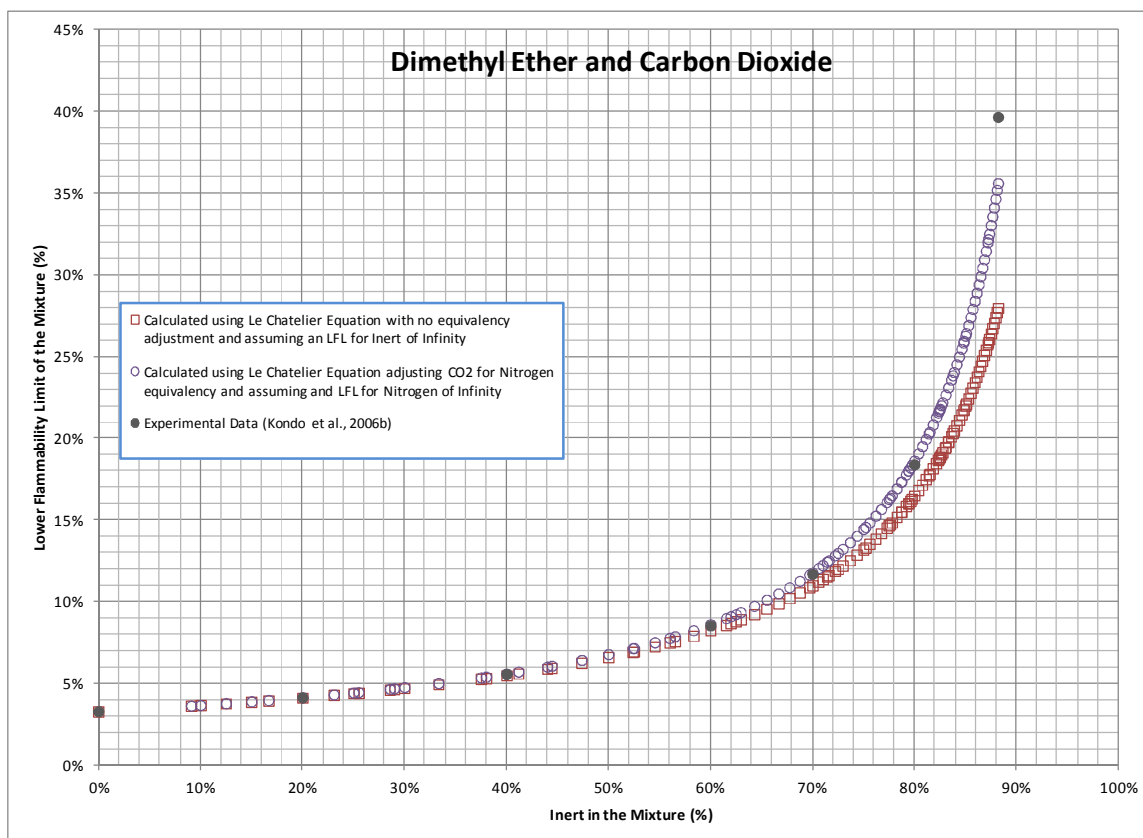
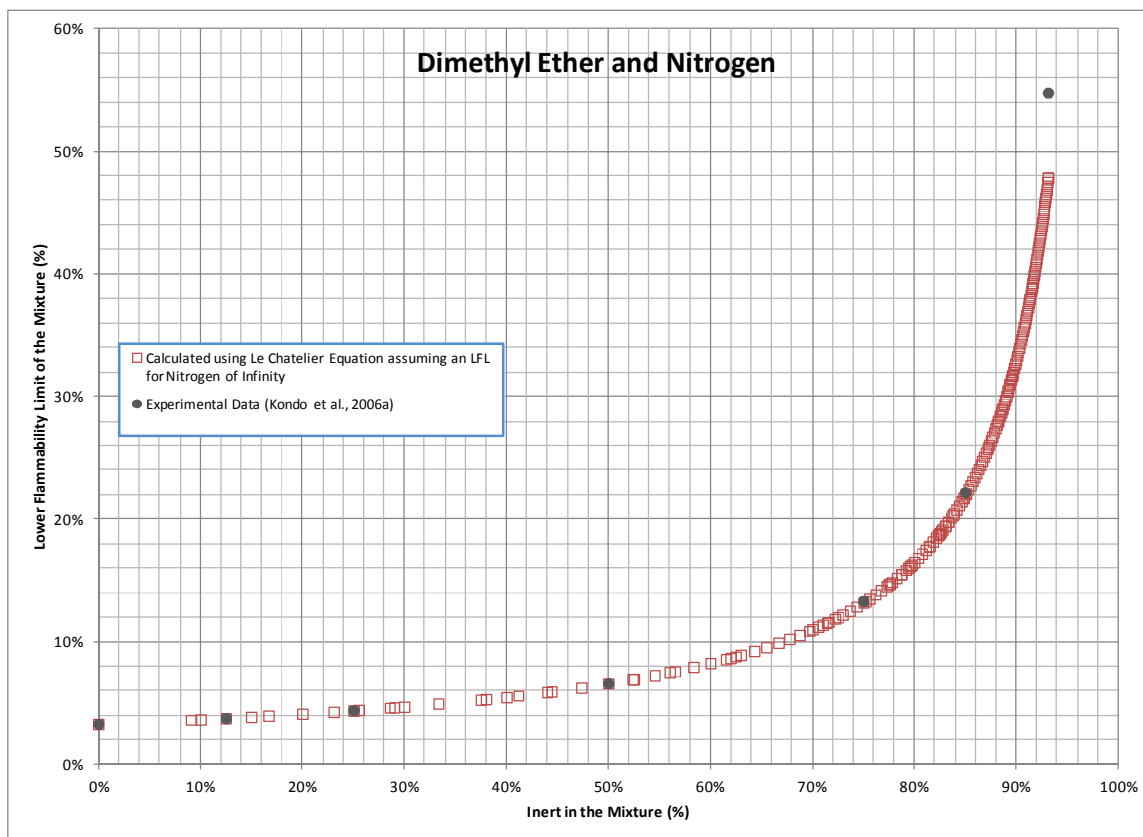


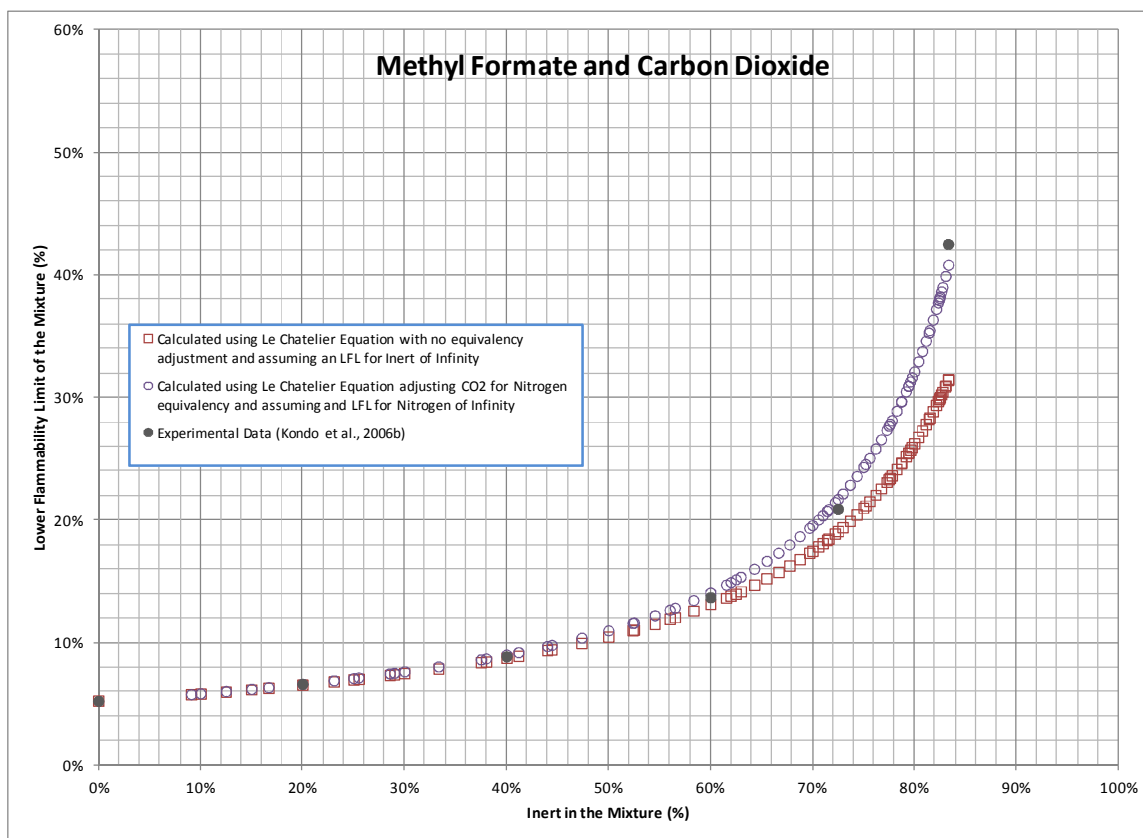
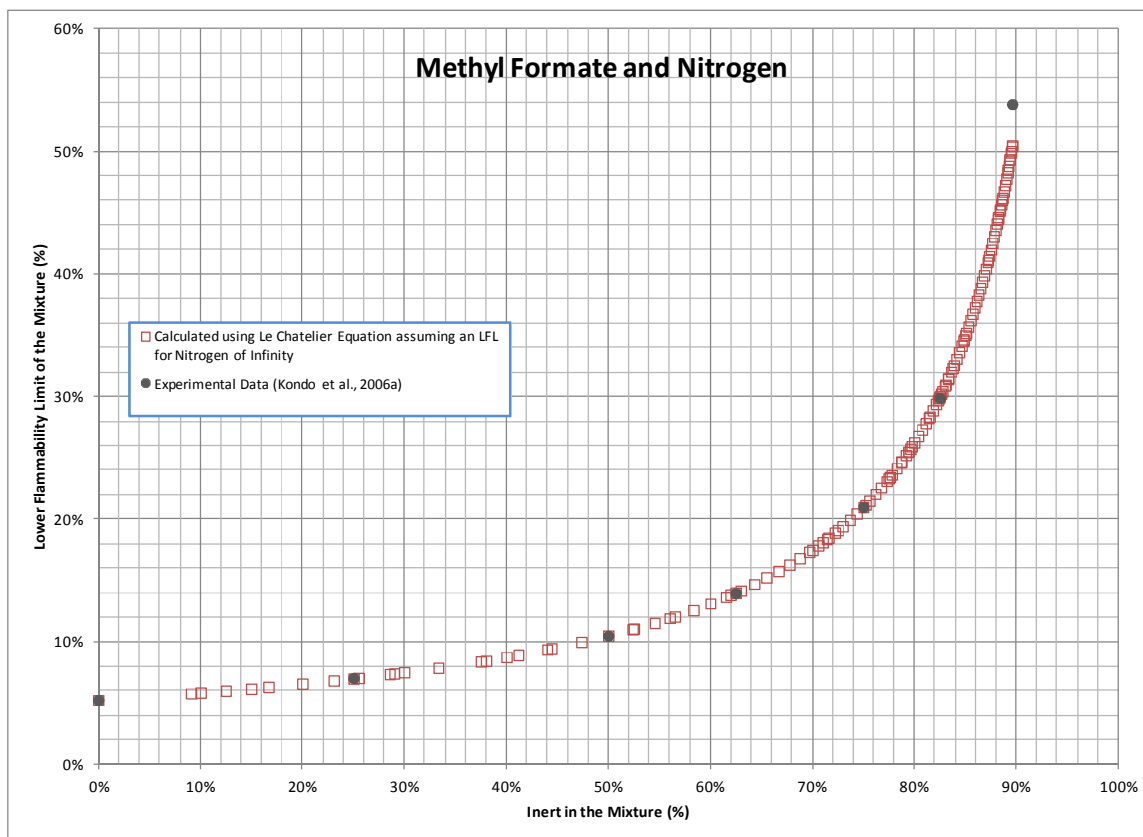


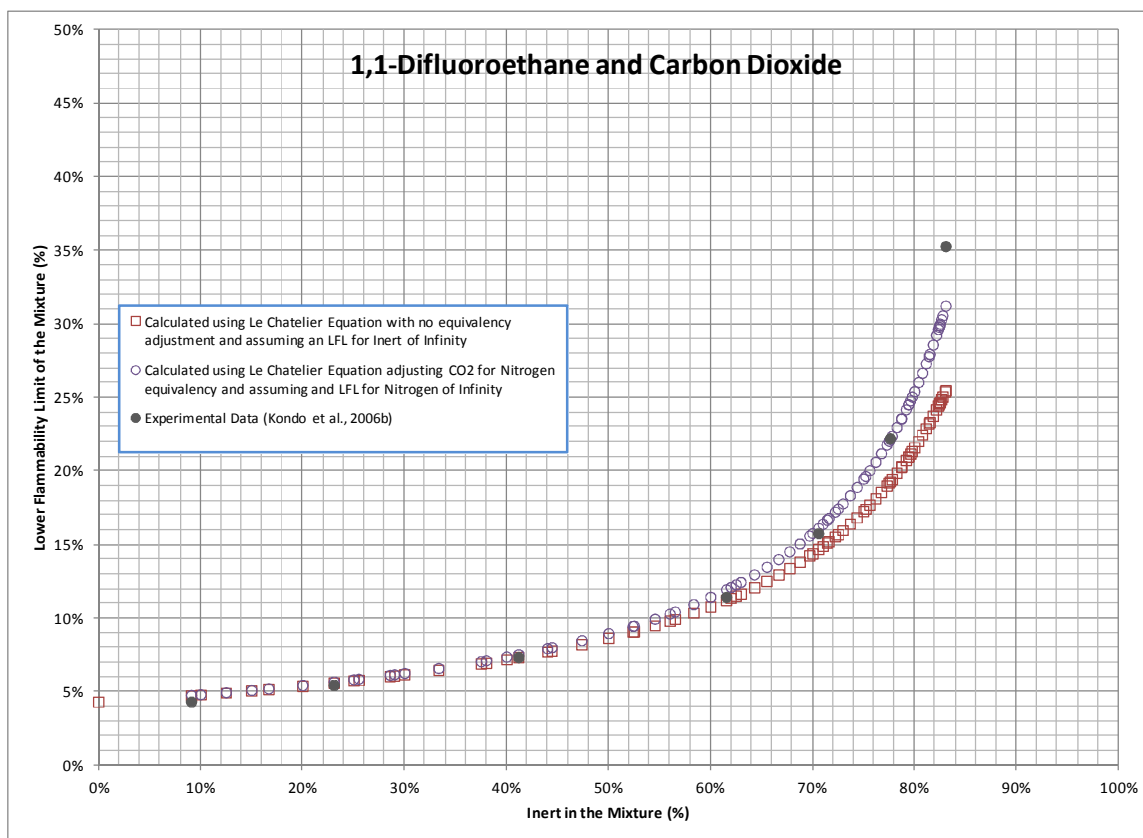
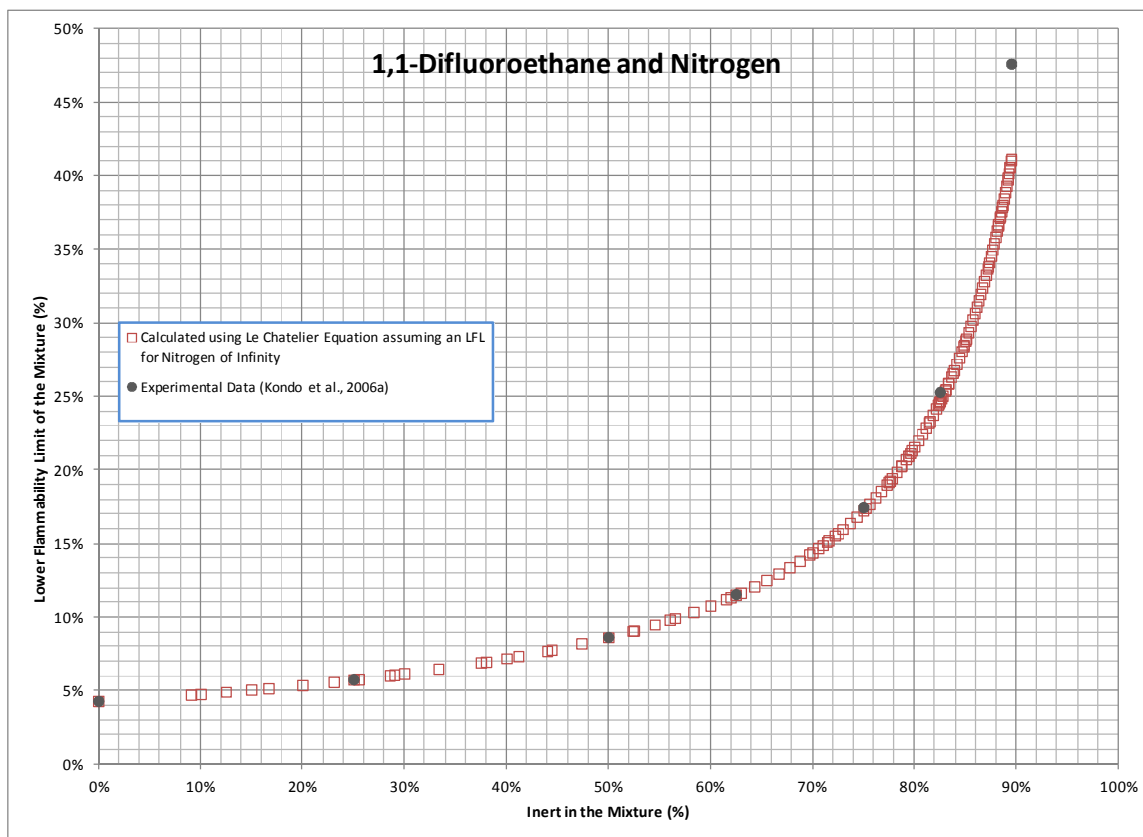


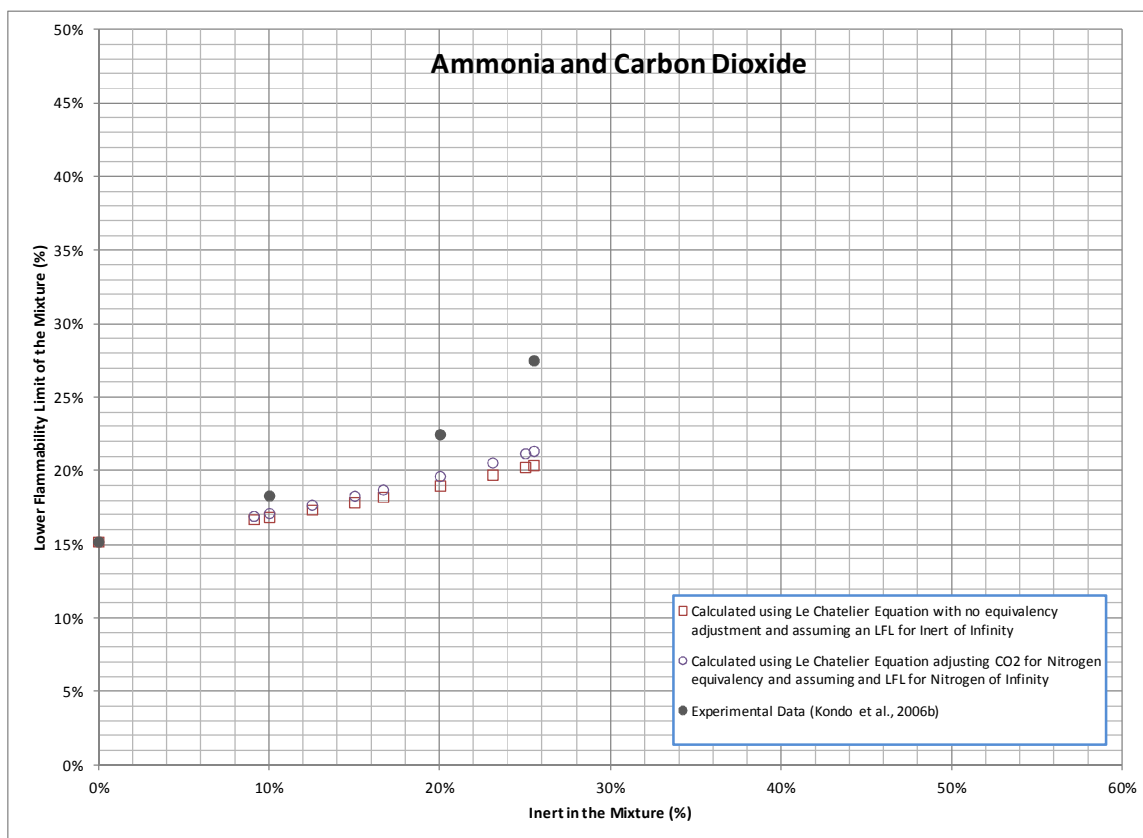
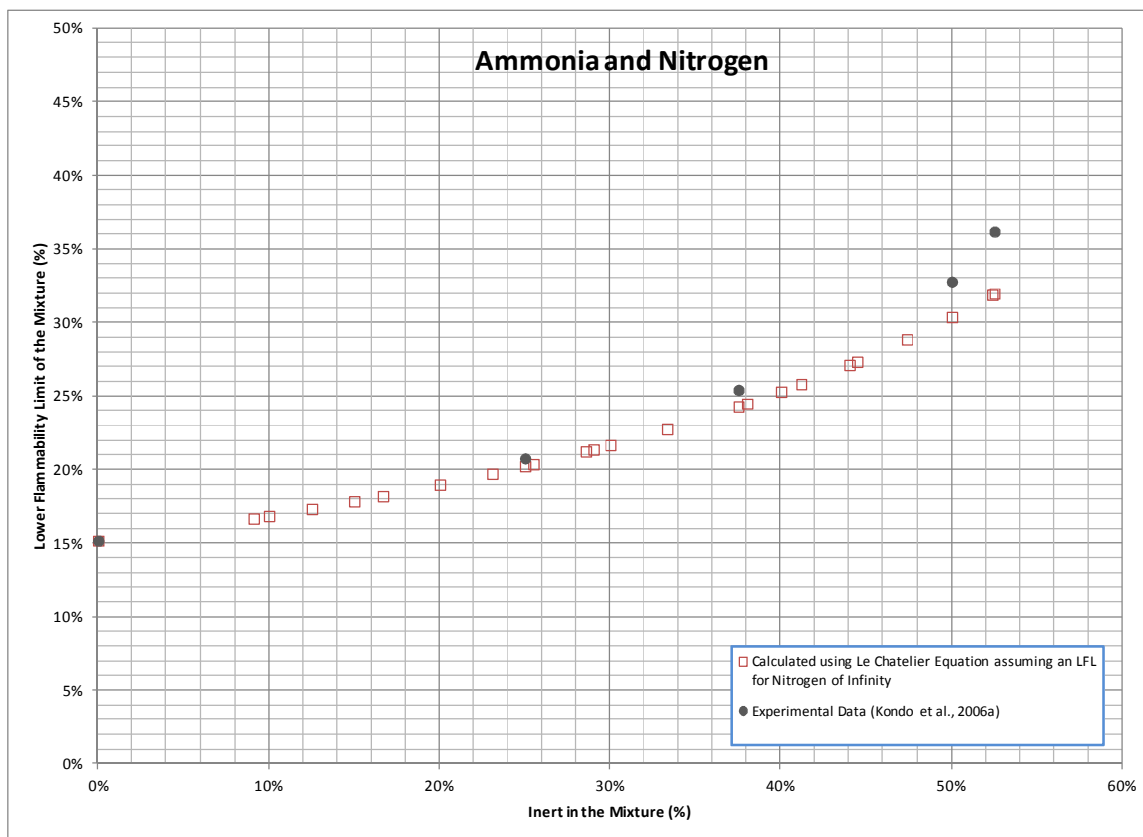












## **Appendix G**

**The following Appendix contains details about inerts and further explanation for including an equivalency adjustment to correct for different inert behavior. Section G.1 explores the accuracy of Le Chatelier with varying chemical composition in the mixture. Section G.2 presents research on nitrogen composition and its effect on calculated LFL with respect to measured LFL; and Section G.3 discusses the effect of other types of inerts. There are additional uncertainties associated with the calculation of UFL; however, these are not discussed in this report because UFL is not presented as an operating parameter to indicate adequate combustion in flares.**

## **G.1 LFL Calculation Accuracy Associated with No-inert in Gas Mixture**

### *Researcher's Observations of Measured and Calculated LFL*

Some researchers have observed that certain mixtures do not obey the Le Chatelier principle and Le Chatelier's equation does not accurately predict the LFL for these mixtures. Heffington and Gaines (1981) noted that large amounts of hydrogen sulfide can cause deviations between calculated and experimental LFLs, and White (1925) specifically identified hydrogen sulfide and methane mixtures as not following the rule. White (1925) also found that hydrogen and ethylene, acetylene and hydrogen, and mixtures containing carbon disulfide do not follow Le Chatelier. Coward and Jones (1952) specifically noted that the LFL calculated using Le Chatelier's equation for mixtures containing at least 2 of the compounds methane, hydrogen, or carbon monoxide are "approximately accurate". Choudhuri (2005) described variations in the measured and calculated LFLs (using Le Chatelier's equation) for methane and propane, and methane and ethane mixtures; and for hydrogen and carbon monoxide mixtures (Choudhuri and Subramanya, 2006).

Coward and Jones (1952) provided a qualitative discussion of the variation in accuracy of the LFL calculated for mixtures using Le Chatelier's equation with different chemical composition of the combustible gases. Table G.1 provides a summary of the researcher's observations and of other researchers' findings on the differences in LFLs determined through measurement and calculations using Le Chatelier's equation. Although it is difficult to judge the extent of deviations shown in Table G.1 from the researcher's qualitative remarks (e.g., "Agreed Closely" versus "Deviated Somewhat") between measured and calculated LFLs, it would appear that mixtures containing carbon disulfide, acetylene, and paraffin-hydrocarbon halides give the largest deviations. Carbon disulfide and paraffin-hydrocarbon halides seem to effect a broader group of mixtures, while it is less clear whether acetylene mixed with non-hydrogen combustibles will cause calculated LFL values to vary significantly from the measured values. Some variation was seen with methane and acetylene mixtures, but only slight; and carbon monoxide and acetylene mixtures had measured and calculated LFLs that were in close agreement.

Coward and Jones (1952) provide graphs (Figures 56 and 57 of Coward and Jones) for the LFL of different mixtures of hydrogen sulfide and methane, and hydrogen sulfide and

hydrogen. Both figures indicate a variation of the calculated LFL up to 1 percentage point below the measured value for these mixtures. For hydrogen sulfide and hydrogen mixtures the variation does not occur until there is about 22 percent H<sub>2</sub>S in the mixture. For hydrogen sulfide and methane the variation occurs in almost all mixtures, but is less significant for mixtures with 2 percent or less H<sub>2</sub>S.

Paraffin-hydrocarbon halides cause variations of the measured LFL from the calculated value; however, current regulations do not allow flaring of fuel gases with significant amounts of halides, so these compounds should not affect the calculation of LFL<sub>CZ</sub> or its effectiveness as a parameter to indicate flare combustion performance. It is assumed that the amount of hydrogen sulfide and carbon disulfide that is burned in regulated flares is also small because of the emission limits of previous rules, such as the NSPS for petroleum refineries (40 CFR 60, subparts J and Ja), Onshore Natural Gas Processing (40 CFR 60, subpart LLL), and New Source Review permit limits, although this may require further investigation. Therefore, hydrogen sulfide and carbon disulfide are also not expected to be present in large enough quantities to affect the accuracy of the calculated LFL<sub>CZ</sub>.

**Table G.1. Le Chatelier Accuracy Observations by Coward and Jones (1952)**

Mixture Constituents	Differences Between Measured LFL and Values Calculated Using Le Chatelier's Equation <sup>1</sup>
Hydrogen and carbon monoxide	Just exceeded experimental error
Hydrogen and hydrogen sulfide	Diverged widely; calculated LFL lower than measured
Hydrogen, carbon monoxide, and methane	Approximately accurate
Hydrogen, methane, and ethane	Approximately accurate
Hydrogen and ethylene	Calculated LFL slightly lower than measured
Hydrogen and acetylene	Calculated LFL lower than measured by a significant amount for some mixtures. <sup>2</sup>
Hydrogen sulfide and methane	Calculated LFL lower than measured
Hydrogen sulfide and acetylene	Deviated by maximum of 0.3%
Carbon disulfide and ether, benzene, acetone, or acetaldehyde	No agreement
Carbon monoxide and methane	Fair agreement
Carbon monoxide and acetylene	Close agreement
Any two of: methane, ethane, propane, and butane	Close agreement
Methane and pentane in air	Close agreement
Natural gas	Fair agreement
Methane and ethylene	Calculated LFL slightly lower than measured
Methane and acetylene	Calculated LFL slightly lower than measured
Two or more of: cyclohexane, benzene, ethanol	Fair agreement at temperatures of 100 to 250°C
Two or more of: toluene, ethanol, ethyl acetate	Fair agreement
Two or more of: methyl cyclohexane, alcohol, ether	Fair agreement
Ethanol and gasoline; ethanol, gasoline and ether	Fair agreement
Isopropanol and gasoline	Nearly agreed
Benzene and toluene	Close agreement
Benzene and ethanol	Deviated somewhat <sup>3</sup>
Benzole, methanol, ethanol	Agreed within 11% at temperatures of 100 to 250°C
Methanol and ethanol	Agreed (at 75°C)
Methanol and ether; methanol and acetone; ethyl acetate and benzene; acetaldehyde and toluene; ethyl nitrite and ether	Close agreement
Ethanol and ether; acetone and ether	Good agreement
Ethanol and furfural	Deviated somewhat
Ethanol and acetone	Nearly agreed
Ether and acetaldehyde	Good agreement
Acetone and methyl ethyl ketone	Close agreement <sup>4</sup>
Paraffin-hydrocarbon halides: methyl chloride and ethyl chloride; methyl chloride and methyl bromide; methyl bromide and ethyl chloride	Differed appreciably

<sup>1</sup> As observed by Coward and Jones (1952)

<sup>2</sup> For mixtures up to 43% acetylene calculated values significantly lower than measured values. Between 43 to 50% acetylene, the difference between calculated and measured LFL decreased and greater than 50% acetylene the mixtures follow Le Chatelier's equations.

<sup>3</sup> However, at temperatures from 100 to 250 °C the values agreed fairly well.

<sup>4</sup> However, the LFL measured using an upward propagation method were slightly higher than calculated.

Table G.1 also indicates that several of the alcohol mixtures had some deviation between calculated and measured LFLs, indicating that mixtures of benzene and ethanol, and furfural and ethanol deviated “somewhat;” and measured LFL values for ethanol and acetone, and isopropanol and gasoline mixtures “nearly agreed” with the calculated values.

The researchers (Coward and Jones 1952) also noted small differences in calculated and measured LFL values of various mixtures of hydrogen, carbon monoxide, methane, ethane, and ethylene. The qualitative observations in Table G.1 do not provide enough specific information to judge the accuracy of using Le Chatelier’s equation for these mixtures, but they do raise some questions regarding how effective the  $LFL_{CZ}$  can be as an indicator of good combustion for a wide variety of flare gas compositions.

#### *Research on Reaction Kinetics and the Effect in LFL*

Several other researchers (Azatyan et al., 2002, 2005a, 2005b, and 2007; Degges et al. 2010; Laskin et al., 2000; Wang et al., 2009) have investigated the reaction kinetics of burning gases, which is a possible explanation for these observations. In the flame of a flare, numerous chemical reactions are taking place with the reaction priority dependent on the temperature and chemical composition in the burning mixture. Changes in composition can shift the reaction kinetics to other primary pathways that can have consequences on the ability to achieve good combustion. The LFL does a reasonable job of “summarizing” (in one number) the reactions going on during combustion of a specific chemical or mixture. However, LFL of mixtures calculated using Le Chatelier’s equation is only as accurate as how closely the individual component’s LFL represent the combustion pathways the chemical follows when it is part of a mixture. This is because pure component LFLs used in the Le Chatelier’s equation to estimate LFL for the mixture are based on the combustion pathways when the chemical is burned alone. If mixture components follow reaction pathways that are different from their pure components, the calculated  $LFL_{CZ}$  will vary from the actual. However, if the mixture’s reaction pathways result in similar heats of combustion, the variation in the calculated LFL and the actual may not be meaningful with respect to the  $LFL_{CZ}$  of 15.3 percent. Also, other factors may effect the accuracy of the calculated LFL which could mitigate or exacerbate the error, either making the deviation between calculated and actual LFL more, or less, of a concern.

The reaction kinetic researchers describe reactions that are considered “chain branching” and “chain terminating.” The chain terminating reactions are ones that lead to products that are less active or that participate in reaction chains that recreate the original chemical and may not result in complete combustion. Degges et al. (2010) describes the addition of steam and its chemical influence on the kinetics of a flame including the effect of the steam cooling the flame. Azatyan et al. (2002) provides an analysis on the reactions taking place with hydrogen and methane combustion (pure gases not a mixture). Wang et al., (2009) analyzes the combustion reactions when hydrogen is added to methane in small amounts. The researcher shows an enhancement of combustion with the addition of hydrogen to methane and found that in mixtures with hydrogen concentrations lower than 20 percent, hydrogen participates predominately in intermediate reactions. Azatyan et al. (2005a, 2005b, and 2007) describes the reaction kinetics of hydrogen combustion with the addition of small amounts of propylene or isopropanol and shows that these compounds can inhibit the combustion reactions of hydrogen to some degree. Laskin et al. (2000) investigates the reaction kinetics of 1,3-butadiene combustion.

#### *Compiled Measured and Calculated LFL*

To judge whether the differences between measured and calculated LFLs are significant, experimental LFL values for mixtures were collected and compared to calculated LFL values. Experimental LFL values were collected from eight previous studies. These studies were identified from the numerous research papers collected for the investigation of flare operating parameters that indicate performance level. An exhaustive search for every measured mixture LFL was not conducted, but using a targeted search of papers describing calculational or modeled methods of determining LFL, a large group of measured values was collected. (Papers presenting analytical methods for determining LFL often have experimental values of LFL to compare against the computational method.)

From the eight studies, 221 measured LFL values for mixtures were identified. The values were limited to mixtures that had at least two combustible compounds. (Mixtures with one combustible and an inert are discussed in Sections G.2 and G.3). Values were found for mixtures containing two or more of 16 combustible constituents (hydrogen, methane, ethane, ethylene, propane, propylene, butane, methyl ethyl ketone, toluene, dimethyl ether, methyl

formate, 1,1-difluoroethane, 1,2-dichloroethane, hydrogen sulfide, ammonia, and carbon monoxide). Some mixtures also had inert compounds including nitrogen, carbon dioxide and carbon tetrachloride.

Of the 221 measured values, 146 did not have inert compounds and 65 were mixtures with inert compounds (mixtures with inerts are discussed in Section G.3). In calculating the LFL for the mixture, the pure component LFL values used in Le Chatelier's equation were taken from the research paper that presented the measured values. This was done so the pure component LFL was consistent with the same measurement method, technique, apparatus, and environment that the mixture LFL was measured. Therefore, any significant variation in measured and calculated LFL that was identified was more likely due to the chemical constituents not following Le Chatelier's equation and not a variation due to the test method. LFL was also calculated using pure component LFLs from Zabetakis (1965) for comparison.

Appendix H provides the list of pure component LFL values used in the LFL calculations for each research report and the measured LFLs collected, the mixture composition, the calculated LFL using Zabetakis referenced pure component LFLs, the calculated LFL using the specific researcher's pure component LFLs, the source of each measured value, and the difference between the measured and calculated values. The mixtures with and without inerts are presented in two different tables in Appendix H.

The variation between measured and calculated LFL values is small for those mixtures without inert components. The difference between measured and calculated values was between -0.30 and 0.88 percentage points and the average deviation for the 146 measured and calculated pairs was 0.04 percentage points. Averaging the absolute value of the difference gave an average deviation just above this of 0.08 percentage points. There were only six measured LFL values that varied from the calculated LFL by  $\pm 0.3$  percentage points or greater. These are shown in Table G.2.

Table G.2 does not reveal an obvious trend for the six measured LFL values with the largest deviation from the Le Chatelier calculated values. One could speculate on what these six points imply; however, the overall trend is that for most of the data for mixtures without inerts,

the Le Chatelier’s equation does a good job of predicting the LFL. With all but six data points showing agreement within a third of a percentage point of the measured value, it would be difficult to parse out experimental error from any situations where the components do not obey Le Chatelier’s principal. Even the mixtures with higher deviations (Table G.2) are very close, all but one having a deviation less than 10 percent of the experimental value.

Furthermore, very few, and possibly none, of the variations between measured and experimental LFL values that could occur in gas mixtures containing only combustion gases (with no steam or air added) are important from the perspective of flare vent gas. In using the LeChatelier equation to estimate the  $LFL_{CZ}$ , all mixtures will have a  $LFL_{CZ}$  of less than the maximum pure component LFL of any component in the mixture. For example, ammonia has the highest LFL (15%) of any compound in the Zabetakis (1965) LFL reference list; any mixture of a combustible gas with ammonia (and no inert added) will have a  $LFL_{CZ}$  less than 15 percent. This is dictated by the use of Le Chatelier’s equation. A value greater than 15 percent is not mathematically possible. Consequently all mixtures of 100 percent combustible gases, including mixtures with ammonia, will have a  $LFL_{CZ}$  less than 15.3 percent. Therefore, any flare vent stream with no added assist air or steam containing no inerts will have a LFL that meets 15.3 percent and any variations between calculated and measured are likely unimportant unless there are specific chemical interactions that can cause a mixture of only combustibles to have a much higher LFL than calculated. The comparison of the Le Chatelier equation to experimental LFL values shown in the Appendix H data does not indicate large variations for 100 percent combustible mixtures. However, it should be noted that none of these mixtures with measured LFLs contained acetylene, carbon disulfide, hydrogen sulfide, or alcohol, which were the chemicals specifically cited as not following Le Chatelier’s rule as closely as most chemicals.

**Table G.2. Largest Deviations Found Between Measured and Calculated LFLs for Mixtures with No Inerts**

Hydrogen (H <sub>2</sub> ) (Volume %)	Dimethyl ether (C <sub>2</sub> H <sub>6</sub> O) (Volume %)	Ammonia (NH <sub>3</sub> ) (Volume %)	Other (Volume %)	Experimental LFL (Volume %)	Researcher Pure Component LFLs		Zabetakis Pure Component LFLs		Source
					Calculated LFL (Volume %)	Difference Between Experimental and Calculated	Calculated LFL (Volume %)	Difference Between Experimental and Calculated	
50			50% methyl ethyl ketone (C <sub>4</sub> H <sub>8</sub> O)	3.15	2.75	0.40	2.58	0.57	Loehr et al. (1997)

**Table G.2. Largest Deviations Found Between Measured and Calculated LFLs for Mixtures with No Inerts (Continued)**

Hydrogen (H <sub>2</sub> ) (Volume %)	Dimethyl ether (C <sub>2</sub> H <sub>6</sub> O) (Volume %)	Ammonia (NH <sub>3</sub> ) (Volume %)	Other (Volume %)	Experimental LFL (Volume %)	Researcher Pure Component LFLs		Zabetakis Pure Component LFLs		Source
					Calculated LFL (Volume %)	Difference Between Experimental and Calculated	Calculated LFL (Volume %)	Difference Between Experimental and Calculated	
50			50% 1,2 Dichloroethane (C <sub>2</sub> H <sub>4</sub> Cl <sub>2</sub> )	5.35	4.92	0.43	4.38	0.97	Loehr et al. (1997)
		75	25% methyl formate (C <sub>2</sub> H <sub>4</sub> O <sub>2</sub> )	10.94	10.31	0.63	10.00	0.94	Kondo et al. (2008)
		75	25% Carbon Monoxide (CO)	15.2	14.32	0.88	14.29	0.91	Kondo et al. (2008)
	75	25		3.8	4.10	-0.30	4.21	-0.41	Kondo et al. (2008)
	50		50% Methane (CH <sub>4</sub> )	4.25	3.94	0.31	4.05	0.20	Kondo et al. (2008)

## G.2 Accuracy of Le Chatelier Principle for Mixtures with Nitrogen

As stated in Section 3.1.2, the calculation of LFL<sub>CZ</sub> shown in Figure 3-3 of this report includes an assumption that inerts have an infinite LFL. This can be understood for nitrogen by reviewing the same Zabetakis nose plot that is shown in Figure 3-1 of this report (for ease, refer to Figure G.1 as it is the same as Figure 3-1 of this report). The plot shows several different inerts in methane and air mixtures. Looking specifically at the LFL portion of the nitrogen curve in Figure G.1, the methane concentration stays relatively constant as nitrogen is added (moving along the line at the underside of the nose). The LFL boundary is relatively horizontal as nitrogen is added and the concentration of the combustible stays constant in the combustible-nitrogen-air mixture. Additional combustion gas (methane in Figure G.1) is not needed to offset the addition of nitrogen. The addition of nitrogen displaces air in the methane-nitrogen-air mixture. Because the chemical properties of nitrogen and air are very similar and the amount of oxygen in air displaced by the nitrogen is not significant (since oxygen is not a limiting factor at the LFL), the addition of nitrogen does not affect the measured methane concentration at the LFL.

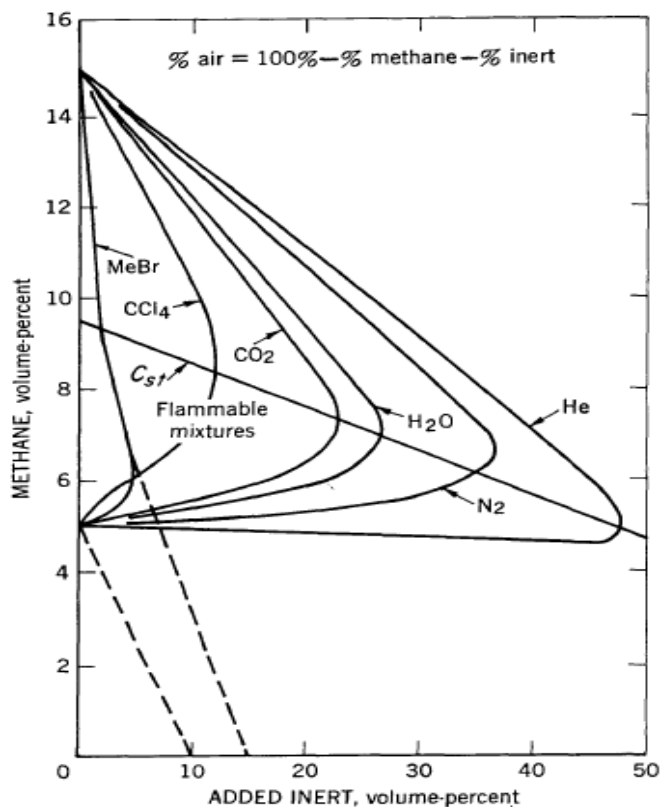


**Figure G.1. Zabetakis nose plot for methane and inert in air**

In the research conducted on calculating the LFL, mixtures with inert gases have specifically been investigated. In general, the more inert (for flares, these are generally nitrogen, carbon dioxide, and steam) added to a combustible gas, the higher the LFL will be for the mixture. Le Chatelier's principle was investigated regarding its accuracy to estimate LFL values for combustion gases and nitrogen. It was found that the LFL calculated using Le Chatelier's principle deviates somewhat from experimental values with higher concentrations of nitrogen in the fuel mixture (and as the fuel mixture's LFL approaches the UFL at the point of maximum inert – at the tip of the nose on a Zabetakis plot). In addition, the amount the calculated value deviates from the experimental value is dependent on the type of combustible compound in the fuel mixture.

Experimental LFL data for individual combustible compounds (i.e. hydrogen, methane, ethane, ethylene, propane, propylene, butane, butadiene, carbon monoxide, dimethyl ether, methyl formate, 1,1-difluoroethane, and ammonia) in nitrogen were graphed against the nitrogen volume percent used in the experiments. The experimental data were extracted from a series of

tests conducted by Jones and Kennedy (1932, 1938, and 1943), Kondo et al. (2006a and 2006b), and Vidal et al (2006). Figure G.2 shows the effect of increasing nitrogen on the LFL of methane-nitrogen mixtures. Appendix F provides these graphs for all 13 combustible gases in nitrogen.

Figure G.2 illustrates the variation that can be found between the calculated LFL and the measured LFL for methane and nitrogen mixtures. For most compounds considered (see Appendix F for graphs showing other combustible compounds with nitrogen) there is little to no variation identified between the calculated and experimental LFL values. The deviations that were found generally occur at greater than a LFL of 15.3 percent. Other than ammonia, methane showed the greatest deviation at the lowest concentration for the compounds examined. Looking at a nitrogen concentration of 66 percent on Figure G.2, which crosses the LFL lines near the LFL value of 15.3 percent shown in Figure 3-4 of this report (where combustion efficiency begins to degrade), the LFL is 15.5 percent for the experimental methane data and 14.8 percent for the calculated results.

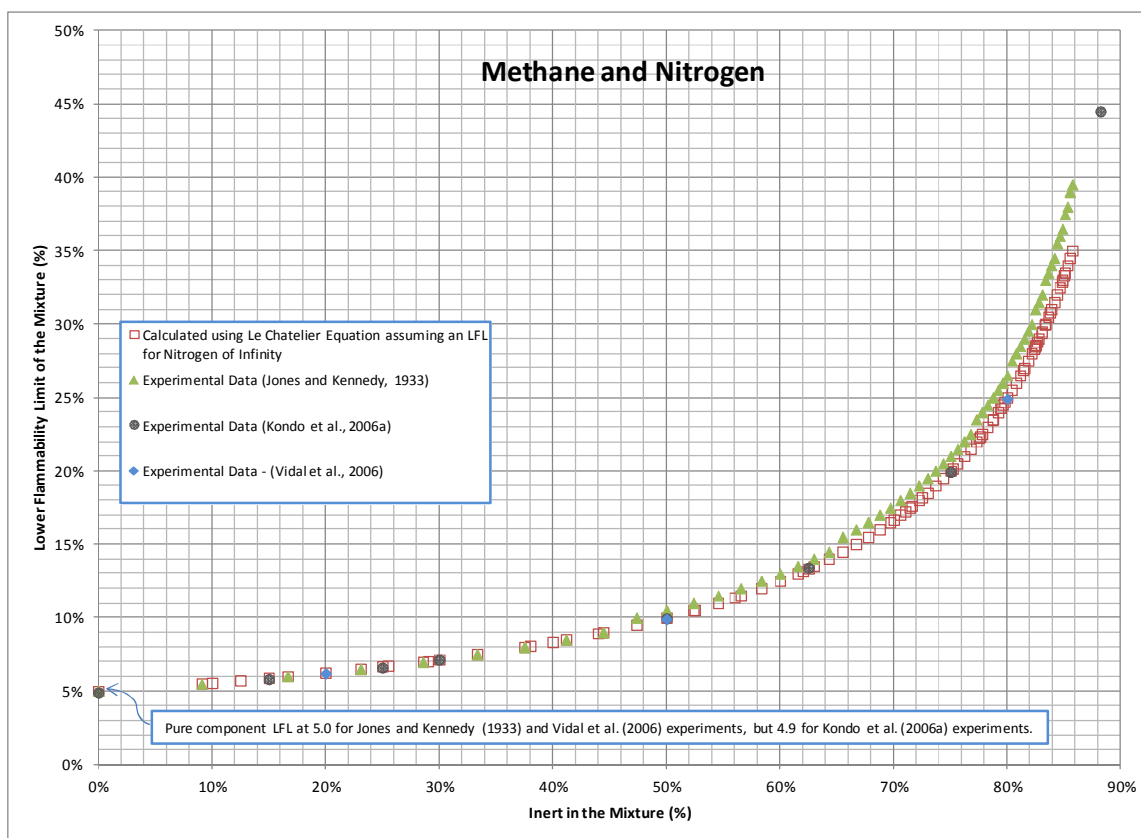


Figure G.2. Effect of Nitrogen on LFL of Methane

This example illustrates that there could be situations where a source would be in compliance with the proposed 15.3 percent LFL<sub>CZ</sub> threshold for a given gas composition in the combustion zone based on the calculated value, but a measured LFL for the mixture would not support this conclusion. However, most combustion gases showed a smaller deviation near 15.3 percent LFL (see Appendix F) between the calculated and measured LFL and the deviation for methane is relatively small and would not affect a wide range of flare gas compositions. Also the uncertainties in using Le Chatelier's equation are built into the analysis that resulted in the proposed 15.3 percent maximum LFL. The limit was established using the Le Chatelier equation and pure component LFLs from Zabetakis (1965). Therefore, the determination of compliance should occur using Le Chatelier's equation and Zabetakis pure component LFLs.

In reviewing the information in Figures G.1 and G.2 it is important to consider the differences in these graphs. Figure G.1 shows the percent of methane in a mixture of air and added nitrogen (the LFL of the methane in a "nitrogen-enriched" atmosphere); from the perspective of a flare, Figure G.1 represents the gas mixture immediately above the flare. The x-axis of Figure G.1 shows the composition of added nitrogen in the "nitrogen-enriched" atmosphere. Therefore, the quantity of air can be calculated from the figure by adding the LFL of methane and the amount of added nitrogen, and subtracting from 100 percent; or for example, for Figure G.1, added nitrogen of 20 percent shows a 5 percent concentration of methane, which means there is 75 percent air in the mixture at the LFL ( $100 - 20 - 5 = 75$ ). Figure G.2 shows the same data but gives the LFL of a mixture containing methane and nitrogen (instead of the LFL for methane in nitrogen-enriched air). The LFL value still reflects the percent of "combustible" in air ("combustible" for Figure G.2 represents the mixture of methane and added nitrogen); however, the x-axis of Figure G.2 is the composition of the nitrogen in the methane-nitrogen mixture, prior to mixing with air. Using the same example for illustration, the mixture of 5 percent methane, 20 percent added nitrogen and 75 percent air on Figure G.2 would be shown with a nitrogen content of 80 percent because the ratio of methane to added nitrogen in the air would be the same as in the mixture without air (5% methane to 20% nitrogen would be  $20/(5+20)$  or 80% nitrogen). From Figure G.2, 80 percent nitrogen in the mixture shows about a 25 percent LFL which means 25 percent of the methane-nitrogen mixture in air is the LFL for that mixture. This Figure G.2 example also indicates that there would be 75 percent air at this LFL which is consistent with the Figure G.1 Zabetakis plot.

### **G.3 Using Le Chatelier's Equation for Non-Nitrogen Inerts**

The amount of deviation between a calculated LFL (using the Le Chatelier equation and assuming infinity as the LFL for inerts) from experimental LFL values is also dependent on the type of inert in the gas mixture. For example, Figure G.1 shows the variation of the LFL for methane in different inert-air mixtures. As can be seen, it takes a concentration lower than nitrogen for some non-nitrogen inerts to render the mixture non-flammable. Also the bottom of the nose is less horizontal. For carbon dioxide, water, carbon tetrachloride, and methylene bromide, Figure G.1 shows that more methane must be added as the inert is increased to maintain a combustible gas mixture. The carbon dioxide curve has the least horizontal nose underside of the three inerts that are most often found in flare gas (steam, nitrogen, and carbon dioxide). For example, at a carbon dioxide concentration in the methane, air, and carbon dioxide mixture of 20 percent, the methane concentration (LFL) would have to increase an additional percent, up to about 6 percent, in order to maintain a flammable mixture. Based on Figure G.1, the effect of water in a mixture is greater than nitrogen, but not as great as carbon dioxide. Because of this, we have included a 'nitrogen equivalency' adjustment in the Le Chatelier's equation (see Equation 3-3 in Section 3.1.2 of this report).

Figure G.3 provides the same data for methane and carbon dioxide mixtures in Figure G.1 but in the same format as Figure G.2. The figure shows three sets of experimental data for methane and carbon dioxide mixtures and two sets of calculated values. One set of calculated LFLs (outline of red squares) is based on using Le Chatelier's equation assuming a LFL of infinity for the carbon dioxide (no adjustment) and the other set of calculated LFL values (outlines of blue circles) is the Le Chatelier's equation with values adjusted for nitrogen equivalency. The nitrogen adjusted calculated LFL values are very close to the experimental data from all three sources. Comparing the two calculated sets of values shows the effect of the nitrogen adjustment. Left unadjusted, the calculated LFL for methane in CO<sub>2</sub> would deviate a significant amount even for mixtures with a LFL less than 15 percent. Appendix F provides similar graphs to Figures G.2 and G.3 (with nitrogen and carbon dioxide) for 13 combustible gases.

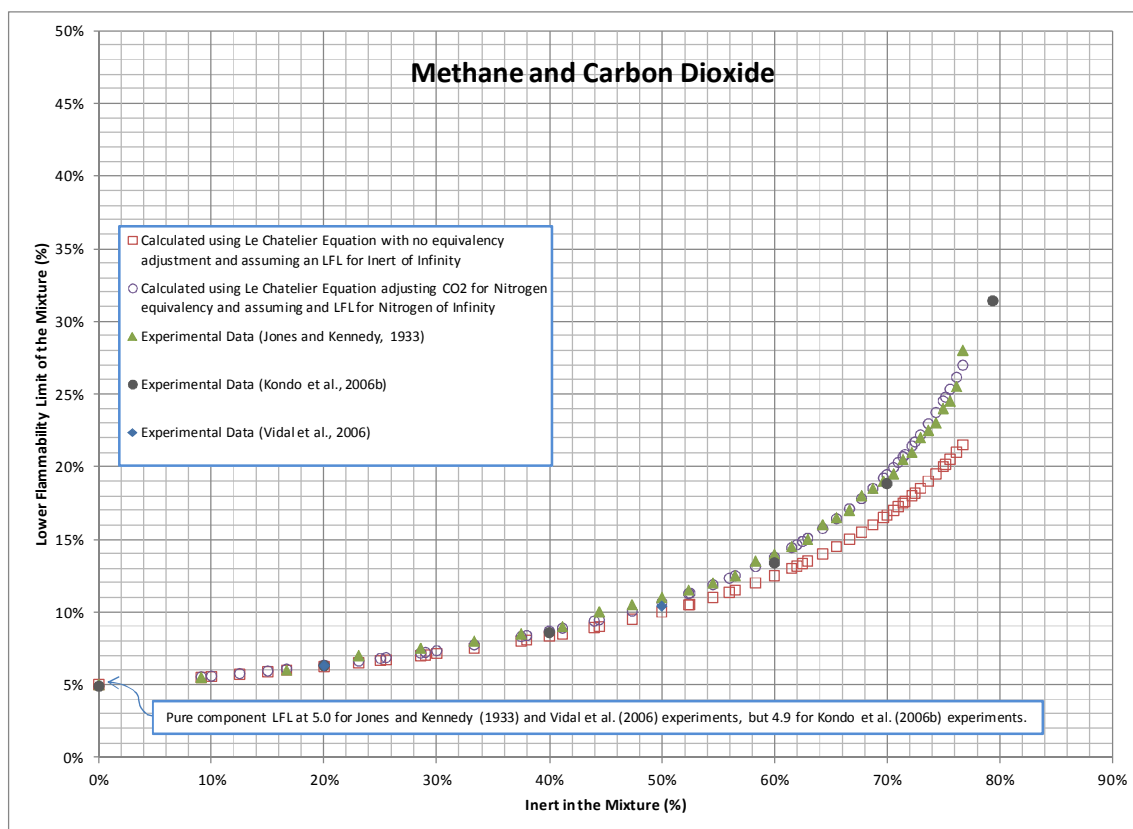


**Figure G.3. Effect of Carbon Dioxide on LFL of Methane**

As mentioned in Section 3.1.2 of this report, the nitrogen equivalency methodology is based on a method investigated by Molnarne et al. (2005) for taking into account non-nitrogen inerts which is used in ISO 10156 and described by Besnard (1996). This nitrogen equivalency adjustment is also described by Shore (2007) and Gogolek et al. (2010a). The Molnarne et al. (2005) recommended values of “nitrogen equivalency” are tabulated in Table G.3 for water (or steam) and carbon dioxide, the inerts that are likely to be included in the flare combustion zone (other than nitrogen).

**Table G.3. Recommended Values of Nitrogen Equivalency for Water and Carbon Dioxide**

Combustible Component <i>i</i> in Flare Vent Gas	$K_{\text{Water}}$	$K_{\text{Carbon Dioxide}}$
Methane	1.87	2.23
Ethane	1.40	1.87
Propane	1.51	1.93
Ethylene	1.68	1.84
Propylene	1.36	1.92
Hydrogen	1.35	1.51
All Other Combustibles	1.50	1.87

Source: Molnarne et al. (2005)

As can be seen in Figure G.2 and in Appendix F for other combustibles, the assumption that the LFL is equal to infinity works well for nitrogen, but not as well for other inerts (see Figure G.3 and Appendix F for carbon dioxide). The intent of the adjustment is to normalize the effect of non-nitrogen inerts in the gas mixture and to adjust the LFL to be on the same basis with respect to inerts. After making the adjustment, all inerts are assumed to have an infinite LFL and the Le Chatelier equation can be used. The flare data sets used in the final analysis have gas mixtures that contain various amounts of nitrogen, carbon dioxide, and water.

*Compiled Measured and Calculated LFL for Mixtures with Inerts*

As previously described, Appendix H provides measured LFLs for 65 mixtures that contain inert components. The variation between the measured and the calculated value (calculated using the specific researcher’s pure component LFL values and adjusting for nitrogen equivalency) ranged from -1.56 and 4.88 percentage points, and an average of 0.73 percentage points. The information for these mixtures is shown in Table H.3 of Appendix H. The mixtures in Table H.3 include the inerts carbon tetrachloride, nitrogen, carbon dioxide, or both nitrogen and carbon dioxide; combustibles include hydrogen, methane, ethane, methyl ethyl ketone, toluene, 1,2-dichlorethane, and carbon monoxide. Table G.4 summarizes the variation between measured and calculated LFLs for the different inerts and shows a summary for the mixtures with no inerts. Clearly the addition of inert compounds has increased the variation between calculated and measured LFLs for mixtures. The average of the absolute value of the differences between calculated and measured LFLs for mixtures with inerts is roughly ten times that seen with mixtures with no inerts.

**Table G.4. Summary of Differences Between Calculated and Measured LFLs for Mixtures**

<b>Type of Inert</b>	<b>Average Difference</b>	<b>Average of the Absolute Value of Difference</b>	<b>Maximum</b>	<b>Minimum</b>	<b>Number of Mixtures</b>
No Inert	0.04	0.08	0.88	-0.30	145
All Inerts	0.73	0.94	4.88	-1.56	65
Carbon Tetrachloride	0.74	0.74	2.52	0.08	18
Carbon Dioxide	-0.78	0.78	-0.19	-1.56	5
Nitrogen	0.71	0.91	4.88	-0.70	24
Carbon Dioxide and Nitrogen	1.16	1.21	2.97	-0.21	18
Carbon Dioxide and/or Nitrogen	0.72	1.01	4.88	-1.56	47

The differences summarized in Table G.4, as well as shown in Appendix H, are calculated as the measured minus the calculated values. Therefore, a negative value indicates that the calculated value is higher than the measured value. In less than 25% of the mixtures with inerts (15 out of 65) the difference was negative. Generally for mixtures with inert concentrations close to the maximum amount of inert possible, while still flammable, the deviation between measured and calculated LFL is at its greatest, with the measured LFL being greater than the calculated value. This can be quickly seen for mixtures with only one combustible and one inert in Figures G.2 and G.3 and in Appendix F; note the difference in acceleration of the increase in slope between the measured and calculated values as inert increases. Look at the termination of the calculated data in Figure G.2. The calculated data ends at a nitrogen content of about 86 percent and a LFL of 35 percent; the measured data from Jones and Kennedy (1933) ends at a LFL of about 39.5 percent, giving a maximum difference between measured and calculated data of 4.5 percentage points near the point of maximum inert concentration.<sup>5</sup> As previously discussed regarding Figure G.2, the difference in measured and calculated LFL at 66 percent nitrogen concentration is about 1 percentage point. Comparing this to the 4.5 percentage point difference shows that the greater difference between measured and calculated LFLs are at maximum inert concentrations. Looking at Figure G.2 also shows why the difference is expected to be a positive difference; Le Chatelier's equation does not account for the same level of increasing slope that appears to happen as mixtures approach their lower limit. Except for two data points with carbon tetrachloride as the inert and one negative difference, the difference between measured and calculated LFL is less than 1 percentage point for LFLs measured less than 25%. Therefore, the larger positive differences seen in Appendix H and Table G.4 are at least partly due to the mixture being closer to the maximum inert concentration.

Most of the experimental data found were for mixtures of hydrogen, methane, carbon monoxide, nitrogen, and/or carbon dioxide, except for mixtures with carbon tetrachloride as the inert. The calculated LFL for the carbon tetrachloride mixtures were adjusted for nitrogen equivalency, but because a k value was not available for carbon tetrachloride, the k values for carbon dioxide were used. All of the measured and calculated differences for these mixtures were less than 1 except for two mixtures that were two of the highest LFLs (9.7 and 10.1%).

---

<sup>5</sup> The Kondo, 2006a, data point in Figure G.2 at about 88 percent nitrogen and a LFL of 44.5 percent is an inconsistency between the measurement methods used by Kondo and Jones and Kennedy in determining the maximum concentration of nitrogen that will still allow flame propagation.

Although these are not high values with respect to the 15.3% that appears to be important for good flare combustion, these could be high values for carbon tetrachloride. Carbon tetrachloride is a stronger inert than either carbon dioxide or nitrogen.

The mixtures with inert other than carbon tetrachloride all have hydrogen in them except for eight with methane and ethane. The methane and ethane mixtures all have LFLs of 21% or less, and the range of differences between measured and calculated is -0.15 to 0.43 with an average of 0.14 percentage points. These appear very close differences. The second highest difference is 0.33 percentage points, so most of the differences are less than what it may appear from the range.

There are six additional mixtures containing ethane. Three of these also include hydrogen, methane, and nitrogen. All of these have high differences between measured and calculated LFL ranging from 2.47 to 4.88 percentage points. They also have very high LFLs of 37 to 42%. Therefore, the mixtures are likely close to their maximum inert concentration and any additional cause for the high differences cannot be determined given only 3 data points.

The other three mixtures containing ethane also include hydrogen and nitrogen. The range of differences between measured and calculated values is 0.15 to 2.74 percentage points. The higher difference (2.74) is for a mixture with a high LFL or 25.8, but it is difficult to form any conclusions with these three points. However, because of ethane's similarity to methane, these points could be compared to the results for hydrogen and methane.

The remainder of the mixtures (33) with inert other than carbon tetrachloride, contain methane, hydrogen and nitrogen and/or carbon dioxide, with seventeen of the mixtures also containing carbon monoxide.

Numerous researchers (for example Karim et al., 1996, Wang et al. 2009 and 2010, Hu et al. 2009, and White, 1925) have shown that hydrogen enhances the combustion of methane. For mixtures that are not premixed, this effect levels off somewhat at about 32 or 40 percent hydrogen in the fuel mixture (Wang et al., 2010). From the perspective of LFL values for mixtures of hydrogen and methane, one would expect that the LFL values would be lower than

what would be calculated using Le Chatelier's equation, because the equation does not take into account the enhancement behavior. However, for mixtures where there is more hydrogen than methane, hydrogen still enhances the methane combustion, but the primary combustible is hydrogen; and from the perspective of hydrogen, methane is inhibiting hydrogen combustion. Because, methane has a higher LFL than hydrogen, the use of Le Chatelier's equation results in a "dilution" of the hydrogen LFL by an amount proportional to methane's LFL and the concentration of methane in the mixture. This calculation may be enough to represent the inhibition of hydrogen combustion by methane or there would be positive differences between the measured and calculated LFL values.

Table G.5 shows all the mixtures with hydrogen, methane, and an inert. The values in Table G.5 are shown in order of the relative amount of hydrogen in total combustibles [hydrogen concentration/(hydrogen plus methane concentrations)]. As expected the difference between the measured and calculated LFL values is negative for mixtures where hydrogen is 33% or less showing the enhancement in combustion is likely due to the presences of hydrogen. For mixtures with a relative amount of hydrogen of 66% or greater, the difference between the measured and calculated LFLs is between -0.66 and 0.55 percent. There are four of these mixtures and two have negative difference and two with positive differences. These correspond with the inert in the mixture; carbon dioxide is part of the mixtures with negative differences, and nitrogen is the inert in the mixtures with positive differences. Gogolek et al. (2010a) recommended different k-values from those provided in Molnarne et al. (2005) and shown in Table G.3. The Gogolek et al. recommended values are shown in Table G.6. Using the Gogolek et al. recommended k values, the differences between the measured and calculated LFLs is between -0.07 to 0.55. This is closer to what one would expect for hydrogen and methane mixtures when hydrogen makes up 66 percent or more of the combustibles.

**Table G.5: Hydrogen, Methane Mixtures With Either Only Nitrogen or Carbon Dioxide as the Inert**

Hydrogen (H <sub>2</sub> ) (Volume %)	Methane (CH <sub>4</sub> ) (Volume %)	Nitrogen (N <sub>2</sub> ) (Volume %)	Carbon Dioxide (CO <sub>2</sub> ) (Volume %)	Experimental LFL (Volume %)	Calculated LFL (Volume %)	Difference Between Calculated Experimental LFL Values	% Error	Fraction of Hydrogen in Total Combustibles (volume fraction)	Source
3.6	20.6	75.8		20.85	21.55	-0.70	-3.23	0.15	Karim et al., 1985
5.6	29.7	64.7		14.37	14.75	-0.38	-2.57	0.16	Karim et al., 1985
6.9	26.5	66.7		15	15.38	-0.38	-2.48	0.21	Karim et al., 1985
5.1	18.7	76.3		21.17	21.58	-0.41	-1.88	0.21	Karim et al., 1985
7.3	23.6	69.1		16.07	16.43	-0.36	-2.20	0.24	Karim et al., 1985
10.4	29.0		60.6	13.2	13.91 <sup>a</sup>	-0.71 <sup>a</sup>	-5.13	0.26	Karim et al., 1985
10.5	21.1		68.4	15.93	17.49 <sup>b</sup>	-1.56 <sup>b</sup>	-8.94	0.33	Karim et al., 1985
16.6	16.7	66.7		14	13.58	0.42	3.06	0.50	Jones, 1929
10.9	10.9	78.2		21.5	20.74	0.76	3.65	0.50	Jones, 1929
15.1	15.1		69.8	16.41	17.20 <sup>c</sup>	-0.79 <sup>c</sup>	-4.57	0.50	Karim et al., 1985
12.8	12.8	74.5		18.55	18.46	0.09	0.51	0.50	Karim et al., 1985
25.3	25.2	49.5		9.5	8.95	0.55	6.13	0.50	Jones, 1929
14.7	7.6	77.6		20.35	20.15	0.20	0.98	0.66	Karim et al., 1985
16.5	4.4		79.1	22.75	23.41 <sup>d</sup>	-0.66 <sup>d</sup>	-2.83	0.79	Karim et al., 1985
13.5	2.8	83.7		27	26.45	0.55	2.09	0.83	Karim et al., 1985
18.3	3.6		78.1	21.59	21.78 <sup>e</sup>	-0.19 <sup>e</sup>	-0.87	0.84	Karim et al., 1985

<sup>a</sup> Using k values recommended by Gogolek et al. (2010a), the calculated LFL would be 13.39 % with a difference of -0.19 % from the experimental value.

<sup>b</sup> Using k values recommended by Gogolek et al. (2010a), the calculated LFL would be 16.65 % with a difference of -0.72 % from the experimental value.

<sup>c</sup> Using k values recommended by Gogolek et al. (2010a), the calculated LFL would be 16.56 % with a difference of -0.15 % from the experimental value.

<sup>d</sup> Using k values recommended by Gogolek et al. (2010a), the calculated LFL would be 22.82 % with a difference of -0.07 % from the experimental value.

<sup>e</sup> Using k values recommended by Gogolek et al. (2010a), the calculated LFL would be 21.37 % with a difference of +0.22 % from the experimental value.

**Table G.6. Nitrogen Equivalency Values from Molnarne et al. (2005) and Gogolek et al. (2010a)**

<b>Species</b>	<b>Molnarne et al. Nitrogen Equivalency Values for CO<sub>2</sub></b>	<b>Gogolek et al Nitrogen Equivalency Values for CO<sub>2</sub></b>
Methane	2.23	1.6
Propane	1.93	2.5
Ethylene	1.84	1.8
Ethane	1.92	2.4
Hydrogen	1.51	1.5

There are five mixtures that have 50 percent of the combustibles as hydrogen. The differences between the measured and calculated values are 0.09 to 0.76% for the mixtures with nitrogen, and -0.79% for the mixture with carbon dioxide. Using the Gogolek et al. (2010a) recommended k values, the difference for the mixture with carbon dioxide between the measured and calculated LFL is -0.15 percent. The Jones (1929) values have a much higher level of uncertainty than the newer Karim et al. (1985) data has. For the higher inert mixtures, the uncertainty is at least  $\pm 0.5$  percent for the Jones data. Also, the highest difference for hydrogen of 66% or greater for the Karim et al data set (0.55%) is for the highest inert concentration, which one would expect to result in a higher positive difference. Taking the high uncertainty in the Jones data and the high inert concentration mixture into account and using Gogolek et al. recommended k values, the mixtures with hydrogen of 66 percent and greater have close calculated and measured LFLs; the range of differences is from -0.15 and 0.20 percent.

There are 17 mixtures with hydrogen, methane, and carbon monoxide. Small amounts of hydrogen in carbon monoxide mixtures have also been found to enhance combustion (Wierzba and Kilchyk, 2001). Wierzba and Kilchyk showed that 20 percent or less hydrogen with carbon monoxide, will result in the calculated LFL values to be greater than the measured values. This behavior is not identifiable by the measured LFL found for the 17 mixtures of hydrogen, methane, and carbon monoxide. These data all came from Jones (1929) and have a large variability. Eleven of the mixtures have an inert concentration of 79 percent or greater; therefore, the mixtures are close to its LFL where the variation between measured and calculated are at their greatest. The difference between measured and calculated LFL from the 17 mixtures is

between -0.21 and 2.97 percent. Just looking at those mixtures with an inert concentration less than 79 percent the variation is -0.21 and 0.71 percent. All but two of the mixtures had carbon dioxide and nitrogen as inert; therefore, these would be affected by using the Gogolek et al. (2010a) k values. Using these k values, the range in differences for the 17 mixtures is -0.21 to 3.48 and looking only at the mixtures with inert concentration less than 79 percent, the variation would be -0.21 to 0.85 percent. In both cases the range widens between the calculated and measured differences.

The differences in the measured and calculated LFLs are relatively close when looking at mixtures that are not as close to the maximum inert concentration. For hydrogen concentrations of 33% or less of the total combustible, the data appears to show some combustion enhancement by hydrogen (although the dataset is small so this can only be considered a preliminary observation). Additional observations are less clear or not possible with the data collected. Also, it should be noted that no data was found to investigate other chemical interactions reported in literature (e.g., propylene inhibition of hydrogen combustion).

*This information is distributed solely for the purpose of pre-dissemination peer review under applicable information quality guidelines. It has not been formally disseminated by EPA. It does not represent and should not be construed to represent any Agency determination or policy.*

## **Appendix H**

### **Effect Of Nitrogen And Carbon Dioxide On The LFL Of Various Components. [comparison of Le Chatelier equation to experimental LFL values]**

**Table H.1. List of pure component LFL values used in the LFL calculations for each research report.**

Component i	LFL <sub>i</sub>								
	Zabetakis (1965)	Van den Schoor (2008)	Kondo et al. (2008)	Vidal et al. (2005)	Mashuga (1999)	Loehr et al. (1997)	Karim (1985)	Jones (1929)	Jones & Kennedy (1932) and (1933)
Hydrogen (H <sub>2</sub> )	4	-	-	-	-	5	4.13	4	4
Methane (CH <sub>4</sub> )	5	4.4	4.9	5	4.85	-	5.47	5.2	5
Ethane (C <sub>2</sub> H <sub>6</sub> )	3	-	-	-	-	-	-	-	3.1
Ethylene (C <sub>2</sub> H <sub>4</sub> )	2.7	-	2.74	2.7	2.62	-	3.22	-	-
Propylene (C <sub>3</sub> H <sub>6</sub> )	2.4	-	2.16	-	-	-	-	-	-
Propane (C <sub>3</sub> H <sub>8</sub> )	2.1	-	2.03	-	-	-	2.4	-	2.3
Butane (C <sub>4</sub> H <sub>10</sub> )	1.8	-	-	-	-	-	-	-	1.8
Methyl ethyl ketone (C <sub>4</sub> H <sub>8</sub> O)	1.9	-	-	-	-	1.95	-	-	-
Toluene (C <sub>7</sub> H <sub>8</sub> )	1.2	-	-	-	-	1.2	-	-	-
Dimethyl ether (C <sub>2</sub> H <sub>6</sub> O)	3.4	-	3.3	-	-	-	-	-	-
Methyl formate (C <sub>2</sub> H <sub>4</sub> O <sub>2</sub> )	5	-	5.25	-	-	-	-	-	-
1,1 Difluoroethane (C <sub>2</sub> H <sub>4</sub> F <sub>2</sub> )	4.32 <sup>a</sup>	-	4.32	-	-	-	-	-	-
1,2 Dichloroethane (C <sub>2</sub> H <sub>4</sub> Cl <sub>2</sub> )	4.85 <sup>b</sup>	-	-	-	-	4.85	-	-	-
Hydrogen Sulfide (H <sub>2</sub> S)	4	-	-	-	-	-	-	-	-
Carbon Monoxide (CO)	12.5	-	12.2	-	-	-	13.76	13.3	-
Ammonia (NH <sub>3</sub> )	15	-	15.2	-	-	-	-	-	-

<sup>a</sup> Zabetakis (1965) does not include a LFL for 1,1 Difluoroethane. This value is from Kondo et al. (2008).

<sup>b</sup> Zabetakis (1965) does not include a LFL for 1,2 Difluoroethane. This value is from Loehr et al. (1997).

**Table H.2. Collected measured LFLs, the mixture composition, the calculated LFL using Zabetakis referenced pure component LFLs, the calculated LFL using the specific researcher’s pure component LFLs, the source of each measured value, and the difference between the measured and calculated values. WITHOUT INERT.**

Hydrogen (H2)	Methane (CH4)	Ethane (C2H6)	Ethylene (C2H4)	Propylene (C3H6)	Propane (C3H8)	Butane (C4H10)	Methyl ethyl ketone (C4H8O)	Toluene (C7H8)	Dimethyl ether (C2H6O)	Methyl formate (C2H4O2)	1,1 Difluoroethane (C2H4F2)	1,2 Dichloroethane (C2H4Cl2)	Ammonia (NH3)	Carbon Monoxide (CO)	Experimental LFL	Using Zabetakis Pure Component LFL Values			Using Experimental Pure Component LFL Values			Source
																Calculated Le Chatelier LFL	Difference Between Calculated and Experimental	Difference On a Percent Basis (%)	Calculated Le Chatelier LFL	Difference Between Calculated and Experimental	Difference On a Percent Basis (%)	
									75				25		3.8	4.21	-0.41	-10.92	4.10	-0.30	-7.98	Kondo et al., 2008
40	60														4	4.55	-0.55	-13.64	4.23	-0.23	-5.77	Van den Schoor et al., 2008
									50						5.2	5.54	-0.34	-6.61	5.42	-0.22	-4.28	Kondo et al., 2008
	25													75	8.71	9.09	-0.38	-4.37	8.89	-0.18	-2.06	Kondo et al., 2008
33.3	33.3		33.4												3.91	3.66	0.25	6.51	4.08	-0.17	-4.29	Karim et al., 1985
60	40														4	4.35	-0.35	-8.70	4.15	-0.15	-3.77	Van den Schoor et al., 2008
							50					50			2.65	2.73	-0.08	-3.03	2.78	-0.13	-4.97	Loehr et al, 1997
20	80														4.2	4.76	-0.56	-13.38	4.31	-0.11	-2.71	Van den Schoor et al., 2008
			25											75	6.44	6.55	-0.11	-1.76	6.55	-0.11	-1.68	Kondo et al., 2008
			75										25		3.35	3.40	-0.05	-1.38	3.45	-0.10	-2.87	Kondo et al., 2008
23.1	76.9														5	4.73	0.27	5.46	5.09	-0.09	-1.78	Karim et al., 1985
							50					50			2.7	2.73	-0.03	-1.12	2.78	-0.08	-3.02	Loehr et al, 1997
50	50														4.63	4.44	0.19	4.01	4.71	-0.08	-1.65	Karim et al., 1985
3.13	3.13													93.7	12.21	11.23	0.98	8.06	12.28	-0.07	-0.58	Karim et al., 1985
40	40		20												4.25	3.94	0.31	7.39	4.31	-0.06	-1.38	Karim et al., 1985
30	40		30												4.13	3.76	0.37	9.01	4.19	-0.06	-1.34	Karim et al., 1985
			50											50	4.42	4.44	-0.02	-0.47	4.47	-0.05	-1.24	Kondo et al., 2008
					33				33					33	3.41	3.56	-0.15	-4.51	3.45	-0.04	-1.26	Kondo et al., 2008
					50								50		3.54	3.68	-0.14	-4.07	3.58	-0.04	-1.18	Kondo et al., 2008
							50	50							1.45	1.47	-0.02	-1.45	1.49	-0.04	-2.46	Loehr et al, 1997
40	30		30												4.05	3.69	0.36	8.93	4.08	-0.03	-0.84	Karim et al., 1985
					50								50		3.75	4.14	-0.39	-10.34	3.78	-0.03	-0.87	Kondo et al., 2008
33.3	33.3		33.3												4.05	3.66	0.39	9.71	4.08	-0.03	-0.71	Karim et al., 1985
			33		33									33	3.2	3.27	-0.07	-2.20	3.23	-0.03	-0.79	Kondo et al., 2008
				33						33	33				3.4	3.57	-0.17	-5.08	3.42	-0.02	-0.72	Kondo et al., 2008
					33					33	33				3.29	3.34	-0.05	-1.48	3.31	-0.02	-0.71	Kondo et al., 2008
			50										50		4.62	4.58	0.04	0.95	4.64	-0.02	-0.50	Kondo et al., 2008
83.3	8.34													8.33	4.46	4.32	0.14	3.22	4.48	-0.02	-0.51	Karim et al., 1985
					33	33						33			2.53	2.70	-0.17	-6.53	2.55	-0.02	-0.90	Kondo et al., 2008
7.15	85.7													7.15	5.56	5.13	0.43	7.76	5.58	-0.02	-0.38	Karim et al., 1985
			33						33					33	4.02	4.07	-0.05	-1.25	4.04	-0.02	-0.51	Kondo et al., 2008
					25					75					3.74	3.72	0.02	0.62	3.76	-0.02	-0.51	Kondo et al., 2008
					50					50					2.91	2.96	-0.05	-1.64	2.93	-0.02	-0.61	Kondo et al., 2008

**Table H.2. Collected measured LFLs, the mixture composition, the calculated LFL using Zabetakis referenced pure component LFLs, the calculated LFL using the specific researcher’s pure component LFLs, the source of each measured value, and the difference between the measured and calculated values. WITHOUT INERT.**

Hydrogen (H2)	Methane (CH4)	Ethane (C2H6)	Ethylene (C2H4)	Propylene (C3H6)	Propane (C3H8)	Butane (C4H10)	Methyl ethyl ketone (C4H8O)	Toluene (C7H8)	Dimethyl ether (C2H6O)	Methyl formate (C2H4O2)	1,1 Difluoroethane (C2H4F2)	1,2 Dichloroethane (C2H4Cl2)	Ammonia (NH3)	Carbon Monoxide (CO)	Experimental LFL	Using Zabetakis Pure Component LFL Values			Using Experimental Pure Component LFL Values			Source
																Calculated Le Chatelier LFL	Difference Between Calculated and Experimental	Difference On a Percent Basis (%)	Calculated Le Chatelier LFL	Difference Between Calculated and Experimental	Difference On a Percent Basis (%)	
			50	50											2.4	2.54	-0.14	-5.88	2.42	-0.02	-0.65	Kondo et al., 2008
				33	33					33					2.63	2.77	-0.14	-5.43	2.64	-0.01	-0.54	Kondo et al., 2008
				50	50										2.08	2.24	-0.16	-7.69	2.09	-0.01	-0.62	Kondo et al., 2008
30	50				20										4.03	3.70	0.33	8.18	4.04	-0.01	-0.31	Karim et al., 1985
				50										50	3.66	4.03	-0.37	-10.02	3.67	-0.01	-0.28	Kondo et al., 2008
	75												25		5.89	6.00	-0.11	-1.87	5.90	-0.01	-0.16	Kondo et al., 2008
	25		75												3.07	3.05	0.02	0.62	3.08	-0.01	-0.30	Kondo et al., 2008
25														75	8.69	8.17	0.52	6.02	8.70	-0.01	-0.08	Karim et al., 1985
	33				33						33				3.26	3.34	-0.08	-2.41	3.26	0.00	-0.15	Kondo et al., 2008
					75									25	2.56	2.65	-0.09	-3.57	2.56	0.00	-0.17	Kondo et al., 2008
					50				50						2.51	2.60	-0.09	-3.44	2.51	0.00	-0.15	Kondo et al., 2008
									50	50					4.05	4.05	0.00	0.06	4.05	0.00	-0.06	Kondo et al., 2008
	33			33							33				3.37	3.57	-0.20	-6.02	3.37	0.00	-0.07	Kondo et al., 2008
			50		50										2.33	2.36	-0.03	-1.39	2.33	0.00	-0.09	Kondo et al., 2008
							33	33				33			1.95	1.94	0.01	0.76	1.95	0.00	-0.11	Loehr et al, 1997
					50						50				2.76	2.83	-0.07	-2.40	2.76	0.00	-0.08	Kondo et al., 2008
									50	50					3.74	3.81	-0.07	-1.74	3.74	0.00	-0.05	Kondo et al., 2008
			33		33				33						2.61	2.66	-0.05	-1.78	2.61	0.00	-0.04	Kondo et al., 2008
					50									50	3.48	3.60	-0.12	-3.33	3.48	0.00	-0.02	Kondo et al., 2008
				50						50					3.06	3.24	-0.18	-5.99	3.06	0.00	-0.02	Kondo et al., 2008
				50							50	50			2.88	3.09	-0.21	-7.14	2.88	0.00	0.00	Kondo et al., 2008
										50	50				4.74	4.64	0.10	2.21	4.74	0.00	0.00	Kondo et al., 2008
					75									25	2.72	3.01	-0.29	-10.57	2.72	0.00	0.02	Kondo et al., 2008
					75						25				2.47	2.70	-0.23	-9.31	2.47	0.00	0.06	Kondo et al., 2008
			75	25											2.57	2.62	-0.05	-1.87	2.57	0.00	0.09	Kondo et al., 2008
					25					75					3.87	3.93	-0.06	-1.66	3.87	0.00	0.08	Kondo et al., 2008
					75				25						2.25	2.32	-0.07	-3.20	2.25	0.00	0.17	Kondo et al., 2008
			50						50						3	3.01	-0.01	-0.33	2.99	0.01	0.20	Kondo et al., 2008
	50													50	7	7.14	-0.14	-2.04	6.99	0.01	0.12	Kondo et al., 2008
			25		75										2.18	2.22	-0.04	-2.00	2.17	0.01	0.43	Kondo et al., 2008
									25		75				4.02	4.05	-0.03	-0.65	4.01	0.01	0.25	Kondo et al., 2008
									75	25					3.65	3.70	-0.05	-1.25	3.64	0.01	0.33	Kondo et al., 2008
				75	25										2.14	2.32	-0.18	-8.28	2.13	0.01	0.66	Kondo et al., 2008
	33				33					33					3.43	3.46	-0.03	-0.83	3.42	0.01	0.42	Kondo et al., 2008

**Table H.2. Collected measured LFLs, the mixture composition, the calculated LFL using Zabetakis referenced pure component LFLs, the calculated LFL using the specific researcher's pure component LFLs, the source of each measured value, and the difference between the measured and calculated values. WITHOUT INERT.**

Hydrogen (H2)	Methane (CH4)	Ethane (C2H6)	Ethylene (C2H4)	Propylene (C3H6)	Propane (C3H8)	Butane (C4H10)	Methyl ethyl ketone (C4H8O)	Toluene (C7H8)	Dimethyl ether (C2H6O)	Methyl formate (C2H4O2)	1,1-Difluoroethane (C2H4F2)	1,2-Dichloroethane (C2H4Cl2)	Ammonia (NH3)	Carbon Monoxide (CO)	Experimental LFL	Using Zabetakis Pure Component LFL Values			Using Experimental Pure Component LFL Values			Source
																Calculated Le Chatelier LFL	Difference Between Calculated and Experimental	Difference On a Percent Basis (%)	Calculated Le Chatelier LFL	Difference Between Calculated and Experimental	Difference On a Percent Basis (%)	
			50								50				3.37	3.32	0.05	1.39	3.35	0.02	0.50	Kondo et al., 2008
	33			33	33										2.63	2.77	-0.14	-5.43	2.61	0.02	0.64	Kondo et al., 2008
6.24														93.8	12.03	11.04	0.99	8.26	12.01	0.02	0.15	Karim et al., 1985
			75							25					3.13	3.05	0.08	2.53	3.11	0.02	0.58	Kondo et al., 2008
										75	25				5	4.81	0.19	3.79	4.98	0.02	0.36	Kondo et al., 2008
				50					50						2.63	2.81	-0.18	-6.99	2.61	0.02	0.72	Kondo et al., 2008
					75						25				2.36	2.41	-0.05	-2.10	2.34	0.02	0.84	Kondo et al., 2008
			25						75						3.16	3.19	-0.03	-1.05	3.14	0.02	0.65	Kondo et al., 2008
83.3														16.7	4.7	4.51	0.19	4.01	4.68	0.02	0.52	Karim et al., 1985
				75					25						2.39	2.59	-0.20	-8.39	2.36	0.03	1.08	Kondo et al., 2008
	33			33						33					3.56	3.71	-0.15	-4.23	3.53	0.03	0.74	Kondo et al., 2008
80	10				10										3.97	3.74	0.23	5.88	3.94	0.03	0.70	Karim et al., 1985
	25										75				4.48	4.47	0.01	0.18	4.45	0.03	0.63	Kondo et al., 2008
											75		25		5.29	5.26	0.03	0.65	5.26	0.03	0.54	Kondo et al., 2008
	50				50										2.9	2.96	-0.06	-1.99	2.87	0.03	1.01	Kondo et al., 2008
40	40				20										3.98	3.63	0.35	8.71	3.95	0.03	0.81	Karim et al., 1985
			25								75				3.81	3.76	0.05	1.40	3.78	0.03	0.90	Kondo et al., 2008
	50		50												3.55	3.51	0.04	1.23	3.51	0.04	1.00	Kondo et al., 2008
80	10		10												4.15	3.89	0.26	6.25	4.11	0.04	0.86	Karim et al., 1985
	25								75						3.63	3.70	-0.07	-1.81	3.59	0.04	1.01	Kondo et al., 2008
14.3	14.3				71.4										2.83	2.47	0.36	12.62	2.79	0.04	1.38	Karim et al., 1985
			50							50					3.64	3.51	0.13	3.67	3.60	0.04	1.08	Kondo et al., 2008
	33									33	33				4.88	4.80	0.08	1.67	4.84	0.04	0.81	Kondo et al., 2008
33							33	33							2	1.88	0.12	5.87	1.96	0.04	2.01	Loehr et al., 1997
33.3	33.3													33.3	6.07	5.66	0.41	6.74	6.03	0.04	0.67	Karim et al., 1985
									25						7.33	7.49	-0.16	-2.17	7.29	0.04	0.59	Kondo et al., 2008
64.3														35.7	5.55	5.28	0.27	4.84	5.50	0.05	0.82	Karim et al., 1985
50														50	6.4	6.06	0.34	5.30	6.35	0.05	0.73	Karim et al., 1985
7.7	84.6		7.7												5.12	4.61	0.51	9.98	5.07	0.05	0.97	Karim et al., 1985
16.7														83.3	9.96	9.23	0.73	7.33	9.91	0.05	0.52	Karim et al., 1985
8.33	83.3				8.33										4.88	4.40	0.48	9.80	4.83	0.05	1.12	Karim et al., 1985
	50			50											3.06	3.24	-0.18	-5.99	3.00	0.06	2.02	Kondo et al., 2008
50					50										3.1	2.75	0.35	11.16	3.04	0.06	2.07	Karim et al., 1985
													50	50	13.6	13.64	-0.04	-0.27	13.54	0.06	0.47	Kondo et al., 2008

**Table H.2. Collected measured LFLs, the mixture composition, the calculated LFL using Zabetakis referenced pure component LFLs, the calculated LFL using the specific researcher’s pure component LFLs, the source of each measured value, and the difference between the measured and calculated values. WITHOUT INERT.**

Hydrogen (H2)	Methane (CH4)	Ethane (C2H6)	Ethylene (C2H4)	Propylene (C3H6)	Propane (C3H8)	Butane (C4H10)	Methyl ethyl ketone (C4H8O)	Toluene (C7H8)	Dimethyl ether (C2H6O)	Methyl formate (C2H4O2)	1,1-Difluoroethane (C2H4F2)	1,2-Dichloroethane (C2H4Cl2)	Ammonia (NH3)	Carbon Monoxide (CO)	Experimental LFL	Using Zabetakis Pure Component LFL Values			Using Experimental Pure Component LFL Values			Source
																Calculated Le Chatelier LFL	Difference Between Calculated and Experimental	Difference On a Percent Basis (%)	Calculated Le Chatelier LFL	Difference Between Calculated and Experimental	Difference On a Percent Basis (%)	
								50						50	5.26	5.35	-0.09	-1.63	5.19	0.07	1.24	Kondo et al., 2008
	50										50				4.66	4.64	0.02	0.53	4.59	0.07	1.46	Kondo et al., 2008
											50				6.45	6.42	0.03	0.45	6.38	0.07	1.08	Kondo et al., 2008
28.6					71.4										2.8	2.43	0.37	13.22	2.73	0.07	2.63	Karim et al., 1985
12.5	12.5		75												3.57	2.99	0.58	16.14	3.50	0.07	2.07	Karim et al., 1985
62.5					37.5										3.33	2.99	0.34	10.31	3.25	0.08	2.37	Karim et al., 1985
	75				25										3.7	3.72	-0.02	-0.45	3.62	0.08	2.15	Kondo et al., 2008
	37.2	62.8													3.7	3.52	0.18	4.74	3.61	0.09	2.42	Jones & Kennedy, 1933
										75				25	6.22	5.88	0.34	5.43	6.12	0.10	1.58	Kondo et al., 2008
										50				50	7.44	7.14	0.30	3.99	7.34	0.10	1.33	Kondo et al., 2008
	75			25											3.82	3.93	-0.11	-3.00	3.72	0.10	2.61	Kondo et al., 2008
											25			75	8.48	8.48	0.00	-0.05	8.38	0.10	1.19	Kondo et al., 2008
33							33					33			3.4	3.08	0.32	9.29	3.30	0.10	3.02	Loehr et al, 1997
51	29.4				19.6										3.97	3.58	0.39	9.92	3.86	0.11	2.71	Karim et al., 1985
77.8					22.2										3.67	3.33	0.34	9.25	3.56	0.11	3.00	Karim et al., 1985
50								50							2.05	1.85	0.20	9.94	1.94	0.11	5.59	Loehr et al, 1997
50								50							2.05	1.85	0.20	9.94	1.94	0.11	5.59	Loehr et al, 1997
42.9					57.2										3.04	2.64	0.40	13.27	2.93	0.11	3.78	Karim et al., 1985
25							25	25				25			2.4	2.20	0.20	8.21	2.28	0.12	4.89	Loehr et al, 1997
25							25	25				25			2.4	2.20	0.20	8.21	2.28	0.12	4.89	Loehr et al, 1997
	50												50		7.53	7.50	0.03	0.40	7.41	0.12	1.58	Kondo et al., 2008
	62.8				37.2										3.6	3.30	0.30	8.25	3.48	0.12	3.33	Jones & Kennedy, 1933
								50				50			2.05	1.92	0.13	6.15	1.92	0.13	6.15	Loehr et al, 1997
											50		50		6.86	6.71	0.15	2.21	6.73	0.13	1.93	Kondo et al., 2008
										50			50		7.94	7.50	0.44	5.54	7.80	0.14	1.71	Kondo et al., 2008
		82.8				17.2									2.9	2.69	0.21	7.19	2.76	0.14	4.92	Jones & Kennedy, 1933
	50														5.22	5.00	0.22	4.21	5.07	0.15	2.89	Kondo et al., 2008
	90.5	7.1			1.6	0.8									4.8	4.61	0.19	3.87	4.64	0.16	3.24	Jones & Kennedy, 1933
	75														5.15	5.00	0.15	2.91	4.98	0.17	3.24	Kondo et al., 2008
	90.7	9.3													4.9	4.71	0.19	3.92	4.73	0.17	3.46	Jones & Kennedy, 1933
30	40				30										3.89	3.36	0.53	13.69	3.69	0.20	5.06	Karim et al., 1985
					25								75		6	5.92	0.08	1.41	5.80	0.20	3.38	Kondo et al., 2008
33								33				33			2.65	2.35	0.30	11.32	2.44	0.21	7.75	Loehr et al, 1997
	83.5	16.5													4.75	4.50	0.25	5.17	4.54	0.21	4.40	Jones & Kennedy, 1933

**Table H.2. Collected measured LFLs, the mixture composition, the calculated LFL using Zabetakis referenced pure component LFLs, the calculated LFL using the specific researcher’s pure component LFLs, the source of each measured value, and the difference between the measured and calculated values. WITHOUT INERT.**

Hydrogen (H2)	Methane (CH4)	Ethane (C2H6)	Ethylene (C2H4)	Propylene (C3H6)	Propane (C3H8)	Butane (C4H10)	Methyl ethyl ketone (C4H8O)	Toluene (C7H8)	Dimethyl ether (C2H6O)	Methyl formate (C2H4O2)	1,1 Difluoroethane (C2H4F2)	1,2 Dichloroethane (C2H4Cl2)	Ammonia (NH3)	Carbon Monoxide (CO)	Experimental LFL	Using Zabetakis Pure Component LFL Values			Using Experimental Pure Component LFL Values			Source
																Calculated Le Chatelier LFL	Difference Between Calculated and Experimental	Difference On a Percent Basis (%)	Calculated Le Chatelier LFL	Difference Between Calculated and Experimental	Difference On a Percent Basis (%)	
	74.4					25.6									3.65	3.44	0.21	5.86	3.44	0.21	5.86	Jones & Kennedy, 1933
	91.2				8.8										4.75	4.46	0.29	6.14	4.53	0.22	4.59	Jones & Kennedy, 1933
	50		50												3.65	3.51	0.14	3.93	3.40	0.25	6.79	Mashuga, 1999
				25									75		6.31	6.49	-0.18	-2.80	6.06	0.25	4.00	Kondo et al., 2008
33.4	33.3				33.3										3.83	3.24	0.59	15.41	3.57	0.26	6.92	Karim et al., 1985
	89.5					10.5									4.5	4.21	0.29	6.37	4.21	0.29	6.37	Jones & Kennedy, 1933
	50							50							4.25	4.05	0.20	4.76	3.94	0.31	7.20	Kondo et al., 2008
50							50								3.15	2.58	0.57	18.21	2.81	0.34	10.93	Loehr et al, 1997
50												50			5.35	4.38	0.97	18.05	4.92	0.43	7.97	Loehr et al, 1997
										25			75		10.94	10.00	0.94	8.59	10.31	0.63	5.73	Kondo et al., 2008
													75	25	15.2	14.29	0.91	6.02	14.32	0.88	5.79	Kondo et al., 2008

**Table H.3. Collected measured LFLs, the mixture composition, the calculated LFL using Zabetakis referenced pure component LFLs, the calculated LFL using the specific researcher’s pure component LFLs, the source of each measured value, and the difference between the measured and calculated values. WITH INERT.**

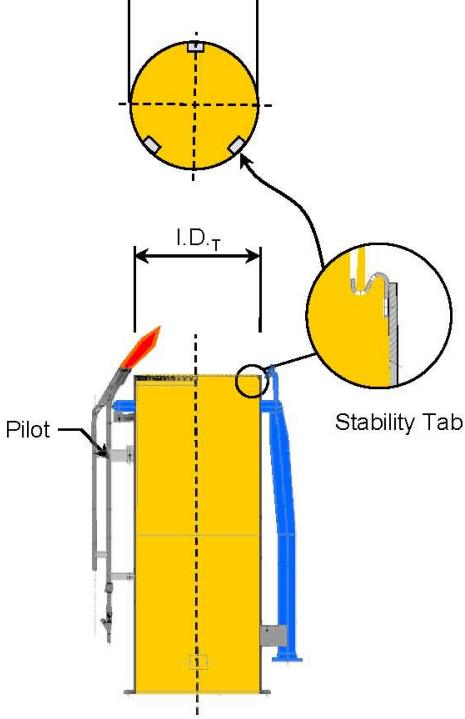
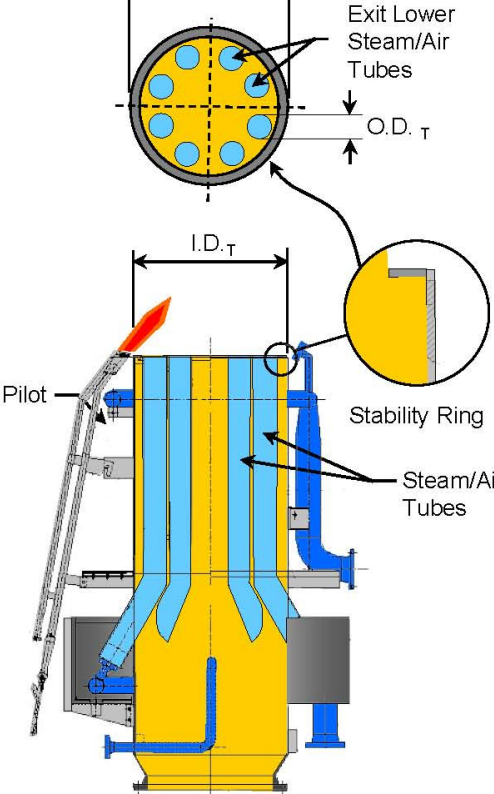
Hydrogen (H2)	Methane (CH4)	Ethane (C2H6)	Methyl ethyl ketone (C4H8O)	Toluene (C7H8)	1,2 Dichloroethane (C2H4Cl2)	Carbon Monoxide (CO)	Nitrogen (N2)	Carbon Dioxide (CO2)	Carbon Tetrachloride (CCl4)	Total Inert	Experimental LFL	Using Zabetakis Pure Component LFL Values			Using Experimental Pure Component LFL Values			Source			
												Calculated Le Chatelier LFL	Difference Between Calculated and Experimental	Difference On a Percent Basis (%)	Calculated Le Chatelier LFL	Difference Between Calculated and Experimental LFL Values	Difference On a Percent Basis (%)		Calculated LFL	Difference Between Calculated Experimental LFL Values	Difference On a Percent Basis (%)
5.2	4.95					4.6	61.6	23.65		85.25	42.5	37.62	4.88	11.48	38.49	4.01	9.43	41.78	0.72	1.72	Jones, 1929
10.48	21.09							68.42		68.42	15.93	14.62	1.31	8.21	15.64	0.29	1.83	17.49	-1.56	-9.82	Karim et al., 1985
10.9	10.9						78.2			78.20	21.5	20.39	1.11	5.18	20.74	0.76	3.53	20.74	0.76	3.65	Jones, 1929
6.3	6					5.25	72.45	10		82.45	34	31.30	2.70	7.94	32.01	1.99	5.84	32.93	1.07	3.26	Jones, 1929
9.3	10.3					9.5	70.9			70.90	20.5	19.44	1.06	5.19	19.92	0.58	2.83	19.92	0.58	2.91	Jones, 1929
15.11	15.11							69.77		69.77	16.41	14.70	1.71	10.39	15.57	0.84	5.11	17.20	-0.79	-4.79	Karim et al., 1985
10.38	29.02							60.61		60.61	13.2	11.91	1.29	9.79	12.79	0.41	3.09	13.91	-0.71	-5.41	Karim et al., 1985
3.60	20.62						75.78			75.78	20.85	19.90	0.95	4.53	21.55	-0.70	-3.34	21.55	-0.70	-3.34	Karim et al., 1985
16.48	4.40							79.12		79.12	22.75	20.00	2.75	12.09	20.86	1.89	8.32	23.41	-0.66	-2.91	Karim et al., 1985
5.05	18.66						76.29			76.29	21.17	20.02	1.15	5.44	21.58	-0.41	-1.92	21.58	-0.41	-1.92	Karim et al., 1985
6.87	26.47						66.67			66.67	15	14.27	0.73	4.90	15.38	-0.38	-2.55	15.38	-0.38	-2.55	Karim et al., 1985
5.57	29.71						64.72			64.72	14.37	13.63	0.74	5.12	14.75	-0.38	-2.64	14.75	-0.38	-2.64	Karim et al., 1985
7.28	23.65						69.07			69.07	16.07	15.27	0.80	4.99	16.43	-0.36	-2.25	16.43	-0.36	-2.25	Karim et al., 1985
4.1	1.35					7.6	79.2	7.75		86.95	58	52.55	5.45	9.40	53.88	4.12	7.11	55.73	2.27	4.08	Jones, 1929
18.30	3.57							78.14		78.14	21.59	18.91	2.68	12.40	19.68	1.91	8.86	21.78	-0.19	-0.87	Karim et al., 1985
4.3	0.2					23.7	55.9	15.9		71.80	36	33.21	2.79	7.75	34.54	1.46	4.06	36.16	-0.16	-0.45	Jones, 1929
	14.5	5.7					79.8			79.80	20.95	20.83	0.12	0.56	21.10	-0.15	-0.73	21.10	-0.15	-0.72	Jones & Kennedy, 1933
6.3	6.7					6.1	80.9			80.90	31.5	29.39	2.11	6.71	30.10	1.40	4.44	30.10	1.40	4.65	Jones, 1929
5.4	0.4					8.5	73.75	11.95		85.70	52.5	47.39	5.11	9.73	48.40	4.10	7.81	50.58	1.92	3.80	Jones, 1929
	52.6	18					0.3	29.1		29.40	6.2	6.05	0.15	2.37	6.13	0.07	1.21	6.25	-0.05	-0.83	Jones & Kennedy, 1933
	52.3	19					28.7			28.70	6	5.95	0.05	0.75	6.03	-0.03	-0.47	6.03	-0.03	-0.47	Jones & Kennedy, 1933
	69	15.8					0.4	14.8		15.20	5.4	5.24	0.16	2.87	5.29	0.11	2.00	5.34	0.06	1.11	Jones & Kennedy, 1933
			33	33					33	33.00	2.35	2.23	0.12	5.16	2.25	0.10	4.21	2.27	0.08	3.74	Loehr et al, 1997
12.75	12.75						74.50			74.50	18.55	17.43	1.12	6.04	18.46	0.09	0.50	18.46	0.09	0.50	Karim et al., 1985
20.8		4.9					74.3			74.30	14.9	14.63	0.27	1.78	14.75	0.15	1.02	14.75	0.15	1.03	Jones & Kennedy, 1932
			33	33					33	33.00	2.45	2.23	0.22	9.03	2.25	0.20	8.12	2.27	0.18	8.16	Loehr et al, 1997
9	9.7					11.3	52	18		70.00	21.5	19.63	1.87	8.69	20.14	1.36	6.32	20.80	0.70	3.35	Jones, 1929
14.74	7.62						77.64			77.64	20.35	19.20	1.15	5.66	20.15	0.20	0.97	20.15	0.20	0.97	Karim et al., 1985
			25	25	25				25	25.00	2.8	2.55	0.25	8.77	2.58	0.22	7.97	2.59	0.21	8.05	Loehr et al, 1997
	27.5	8.4					64.1			64.10	12.4	12.05	0.35	2.84	12.18	0.22	1.77	12.18	0.22	1.80	Jones & Kennedy, 1933
25.3	25.2						49.5			49.50	9.2	8.80	0.40	4.36	8.95	0.25	2.70	8.95	0.25	2.77	Jones, 1929
25			25	25					25	25.00	2.9	2.49	0.41	14.31	2.59	0.31	10.79	2.60	0.30	11.55	Loehr et al, 1997
	73.1	12.1					14.8			14.80	5.7	5.36	0.34	5.95	5.40	0.30	5.29	5.40	0.30	5.58	Jones & Kennedy, 1933
	40.6	7.6					27.6	24.2		51.80	10.05	9.39	0.66	6.60	9.46	0.59	5.88	9.72	0.33	3.39	Jones & Kennedy, 1933

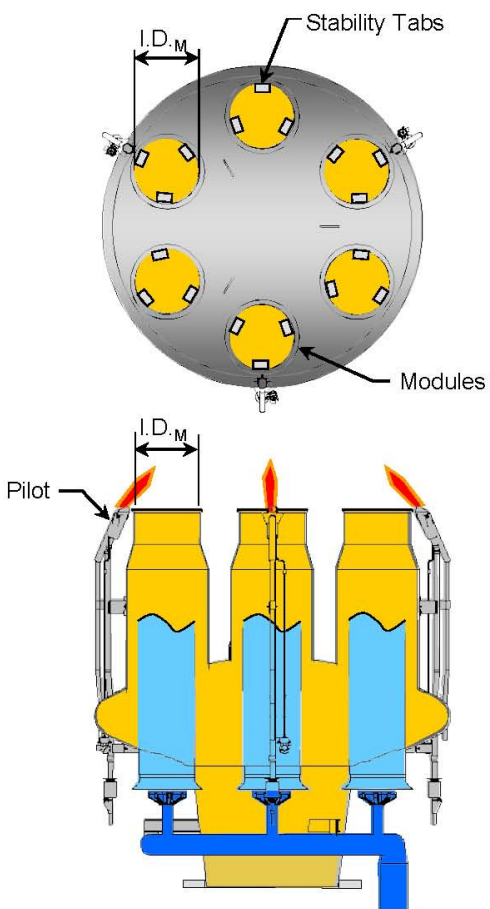
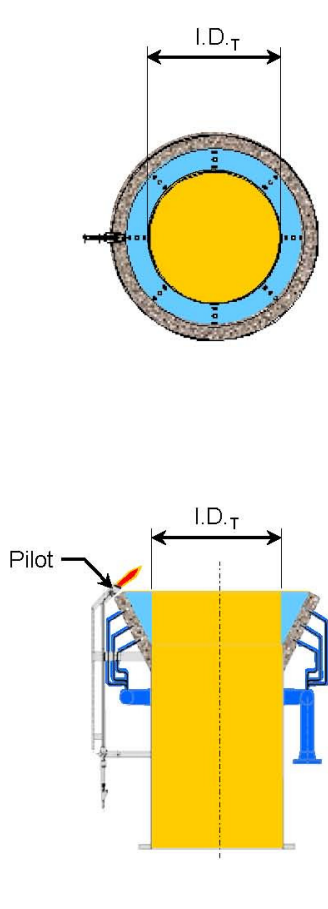
**Table H.3. Collected measured LFLs, the mixture composition, the calculated LFL using Zabetakis referenced pure component LFLs, the calculated LFL using the specific researcher’s pure component LFLs, the source of each measured value, and the difference between the measured and calculated values. WITH INERT.**

Hydrogen (H2)	Methane (CH4)	Ethane (C2H6)	Methyl ethyl ketone (C4H8O)	Toluene (C7H8)	1,2-Dichloroethane (C2H4Cl2)	Carbon Monoxide (CO)	Nitrogen (N2)	Carbon Dioxide (CO2)	Carbon Tetrachloride (CCl4)	Total Inert	Experimental LFL	Using Zabetakis Pure Component LFL Values			Using Experimental Pure Component LFL Values			Source			
												Calculated Le Chatelier LFL	Difference Between Calculated and Experimental	Difference On a Percent Basis (%)	Calculated Le Chatelier LFL	Difference Between Calculated and Experimental LFL Values	Difference On a Percent Basis (%)		Calculated LFL	Difference Between Calculated Experimental LFL Values	Difference On a Percent Basis (%)
16.6	16.7						66.7			66.70	14	13.35	0.65	4.63	13.58	0.42	2.97	13.58	0.42	3.06	Jones, 1929
	26.3	23.6					50.1			50.10	8.2	7.62	0.58	7.10	7.77	0.43	5.27	7.77	0.43	5.56	Jones & Kennedy, 1933
				50					50	50.00	2.9	2.40	0.50	17.24	2.40	0.50	17.24	2.43	0.47	19.57	Loehr et al, 1997
				33	33				33	33.00	3.45	2.92	0.53	15.50	2.92	0.53	15.50	2.94	0.51	17.39	Loehr et al, 1997
20			20	20	20				20	20.00	3.4	2.75	0.65	19.01	2.85	0.55	16.08	2.87	0.53	18.63	Loehr et al, 1997
50									50	50.00	10.8	8.00	2.80	25.93	10.00	0.80	7.41	10.26	0.54	5.25	Loehr et al, 1997
7.25	7.8					9.95	60	15		75.00	26	23.99	2.01	7.73	24.63	1.37	5.28	25.45	0.55	2.15	Jones, 1929
13.52	2.78						83.70			83.70	27	25.41	1.59	5.88	26.45	0.55	2.05	26.45	0.55	2.05	Karim et al., 1985
				33	33				33	33.00	3.5	2.92	0.58	16.71	2.92	0.58	16.71	2.94	0.56	19.09	Loehr et al, 1997
			33		33				33	33.00	4.85	4.14	0.71	14.70	4.21	0.64	13.10	4.26	0.59	13.73	Loehr et al, 1997
25.2		23.6					51.2			51.20	7.8	7.06	0.74	9.50	7.19	0.61	7.85	7.19	0.61	8.52	Jones & Kennedy, 1932
7.55	3.55					2.4	81.6	4.9		86.50	39.5	35.85	3.65	9.24	36.36	3.14	7.96	36.86	2.64	7.17	Jones, 1929
			50						50	50.00	4.65	3.80	0.85	18.28	3.90	0.75	16.13	3.97	0.68	17.21	Loehr et al, 1997
33				33					33	33.00	3.65	2.80	0.85	23.36	2.93	0.72	19.66	2.95	0.70	23.66	Loehr et al, 1997
25				25	25				25	25.00	3.95	3.10	0.85	21.47	3.23	0.72	18.30	3.25	0.70	21.66	Loehr et al, 1997
25			25		25				25	25.00	5.15	4.07	1.08	20.95	4.35	0.80	15.48	4.39	0.76	17.36	Loehr et al, 1997
0.95	36.7					3.7	58.2	0.45		58.65	13	12.70	1.30	9.28	13.20	0.80	5.68	13.21	0.79	5.95	Jones, 1929
33			33						33	33.00	5.2	3.90	1.30	24.93	4.25	0.95	18.25	4.29	0.91	21.18	Loehr et al, 1997
33			33						33	33.00	5.2	3.90	1.30	24.93	4.25	0.95	18.25	4.29	0.91	21.18	Loehr et al, 1997
3.65	3.55					9.5	67.25	16.05		83.30	48.5	41.97	6.53	13.46	43.30	5.20	10.72	46.08	2.42	5.25	Jones, 1929
3.55	1.95					13.8	78.5	2.2		80.70	46	41.99	4.01	8.72	43.48	2.52	5.49	43.83	2.17	4.95	Jones, 1929
2.1	13.75					4	73.4	6.75		80.15	30.5	27.82	2.68	8.80	28.82	1.68	5.51	29.44	1.06	3.61	Jones, 1929
3	0.1					30.65	57.95	8.3		66.25	34	31.04	2.96	8.72	32.53	1.47	4.31	33.29	0.71	2.14	Jones, 1929
6.25	2.4					12.05	73	6.3		79.30	36.5	33.26	3.24	8.87	34.13	2.37	6.50	34.73	1.77	5.10	Jones, 1929
33					33				33	33.00	9.7	6.64	3.06	31.52	7.46	2.24	23.09	7.58	2.12	27.89	Loehr et al, 1997
2.3	9.4	1.5					86.8			86.80	36.5	33.84	2.66	7.29	34.03	2.47	6.78	34.03	2.47	7.27	Jones & Kennedy, 1932
33					33				33	33.00	10.1	6.64	3.46	34.23	7.46	2.64	26.13	7.58	2.52	33.17	Loehr et al, 1997
4.7		9.8					85.5			85.50	25.8	22.51	3.29	12.74	23.06	2.74	10.62	23.06	2.74	11.88	Jones & Kennedy, 1932
2.3	8.3	2.1					87.3			87.30	37.7	34.07	3.63	9.62	34.34	3.36	8.92	34.34	3.36	9.80	Jones & Kennedy, 1932
2.4	8.95					6.65	69.95	12.05		82.00	40	34.22	5.78	14.44	35.45	4.55	11.38	37.03	2.97	8.02	Jones, 1929
2.1	9	1.1					87.8			87.80	42.2	37.15	5.05	11.96	37.32	4.88	11.57	37.32	4.88	13.09	Jones & Kennedy, 1932

## **APPENDIX I**

**Appendix I provides methodology for calculating unobstructed cross sectional area of several flare tip designs.**

Type I	Type II
	
$A_{\text{tip-unob}} = \pi(I.D.T)^2/4 - (X_T * A_{ST})$	$A_{\text{tip-unob}} = \pi(I.D.T)^2/4 - A_{ST} - N_T * \pi * (O.D.T)^2/4$
<p>Where: <math>A_{\text{tip-unob}}</math> = Unobstructed Cross Sectional Area of Flare Tip  <math>I.D.T</math> = Inside Diameter Flare Tip  <math>X_T</math> = Number of Stability Tabs  <math>A_{ST}</math> = Area of a Stability Tab</p>	<p>Where: <math>A_{\text{tip-unob}}</math> = Unobstructed Cross Sectional Area of Flare Tip  <math>I.D.T</math> = Inside Diameter Flare Tip  <math>A_{ST}</math> = Area of Stability Ring  <math>O.D.T</math> = Outside Diameter of Steam/Air Tubes  <math>N_T</math> = Number of Steam/Air Tubes</p>
<p>Example: <math>I.D.T</math> = 41.5 inches  <math>X_T</math> = 3  <math>A_{ST}</math> = 3 Sq. inches</p>	<p>Example: <math>I.D.T</math> = 47.5 inches  <math>A_{ST}</math> = 100 Sq. inches  <math>O.D.T</math> = 6.5 inches  <math>N_T</math> = 8</p>
<p><math>A_{\text{tip-unob}} = \pi(41.5)^2/4 - (3 * 3)</math>  <math>A_{\text{tip-unob}} = 1344</math> Sq. inches</p>	<p><math>A_{\text{tip-unob}} = \pi(47.5)^2/4 - 100 - 8 * \pi * (6.5)^2/4</math>  <math>A_{\text{tip-unob}} = 1322</math> Sq. inches</p>

Type III	Type IV
	
$A_{tip-unob} = N_M * (\pi * (I.D._M)^2 / 4 - X_T * A_{ST})$	$A_{tip-unob} = \pi (I.D._T)^2 / 4$
<p><b>Where:</b> <math>A_{tip-unob}</math> = Unobstructed Cross Sectional Area of Flare Tip  <math>I.D._M</math> = Inside Diameter of One Tip Module  <math>N_M</math> = Number of Modules  <math>X_T</math> = Number of Stability Tabs per Module  <math>A_{ST}</math> = Area of a Stability Tab</p>	<p><b>Where:</b> <math>A_{tip-unob}</math> = Unobstructed Cross Sectional Area of Flare Tip  <math>I.D._T</math> = Inside Diameter of Flare Tip</p>
<p><b>Example:</b> <math>I.D._M = 17</math> inches  <math>N_M = 6</math>      <math>X_T = 3</math>  <math>A_{ST} = 3</math> Sq. inches</p>	<p><b>Example:</b> <math>I.D._T = 41.5</math> inches</p>
$A_{tip-unob} = 6 * (\pi * (17)^2 / 4 - 3 * 3)$ $A_{tip-unob} = 1308 \text{ Sq. inches}$	$A_{tip-unob} = \pi (41.5)^2 / 4$ $A_{tip-unob} = 1353 \text{ Sq. inches}$